UNIVERSITY OF CALIFORNIA,
IRVINE

Genetic analysis of sRNAs in *Chlamydia trachomatis*

DISSERTATION

submitted in partial satisfaction of the requirements
for the degree of

DOCTOR OF PHILOSOPHY

in Microbiology and Molecular Genetics

by

Kevin Wang

Dissertation Committee:

Professor Ming Tan, Chair

Professor Christine Sütterlin

Professor Melissa B. Lodoen

Distinguished Professor Bert L. Semler

Professor Yongsheng Shi

2022

Table of Contents

List of Figures

List of Tables

Acknowledgments

I want to first thank my mentors, Drs. Ming Tan and Christine Sütterlin, for their guidance over the past four years and for always pushing me to think more critically. I also want to thank them for providing me with a learning environment where I can express my scientific ideas freely and grow into an independent scientist.

I want to thank Dr. Lauren M. Sheehan, a previous post-doc in the lab, who recruited me a few years back to start the chlamydial sRNA project with her and introduced me to the wonderful field of bacterial sRNA. She had helped me gain a strong foundation, both in knowledge and lab techniques, in bacterial sRNAs and has continued to guide me over the years.

I also want to thank (soon-to-be Dr.) Karissa Muñoz, a fellow Ph.D. student and a close friend in the lab. From working with her, she has taught me how to conduct research in a more systematic and logical manner. We shared so many late-night experiments, chats about our respective research projects, tears, and laughter over the years—It is safe to say that I would not have made it through this training without the support she had provided me, both outside and inside the lab.

I want to thank the post-docs, both past and present, in the lab, as they have been a great resource and provided great feedback on my project. I especially want to thank our lab technician, Cuper Ramirez, who worked with me in generating dozens of chlamydial transformants. It has also been a pleasure to work with the post-docs in the "sRNA group" (Drs. Asha Densi, Roseleen Ekka, and Janina Ehses) and I cannot wait to see where the project will go in the future.

I want to thank my committee members, Drs. Melissa Lodoen, Bert Semler, and Yongsheng Shi, for providing great suggestions on my project and for always making sure I was on track in my training. I also want to thank Dr. Clay Caswell at Virginia Tech for being a source of knowledge and expertise in the field of bacterial sRNAs.

I would also like to thank the National Institute of Allergy and Infectious Disease (NIAID), T32 training program in Microbiology and Infectious Disease at UCI for funding part of my Ph.D. training and for providing a space in which I can learn about different research areas of microbiology. I want to thank the UCI MSTP, both the students and the administration, for supporting my training throughout the years.

Lastly, I want to thank my parents, siblings, friends, partner, and my cat for providing emotional support through my Ph.D. training. Thank you for always taking the time to listen to me complain about lab work and never judging me. Thank you for being understanding and patiently waiting for me as I make a ‘quick’ stop at the lab. I appreciate you all immensely.

Vita

Kevin Wang

EDUCATION

2014	B.S. in Microbiology, Immunology, and Molecular Genetics, University of California, Los Angeles
2014-2016	Staff Research Associate I, University of California, Los Angeles
2022	Ph.D. in Microbiology and Molecular Genetics, University of California, Irvine
	M.D. (expected 2024), University of California, Irvine

PUBLICATIONS

Wang, K., Peng, E. D., Huang, A. S., Xia, D., Vermont, S. J., Lentini, G., Lebrun, M., Wastling, J. M. & Bradley, P. J. 2016. Identification of novel O-linked glycosylated Toxoplasma proteins by *Vicia villosa* lectin chromatography. *PLoS ONE*, **11**:e0150561.

Ziyad S, Riordan JD, Cavanaugh AM, Su T, Hernandez GE, Hilfenhaus G, Morselli M, Huynh K, **Wang K**, Chen JN, Dupuy AJ, Iruela-Arispe ML. A Forward Genetic Screen Targeting the Endothelium Reveals a Regulatory Role for the Lipid Kinase Pi4ka in Myelo- and Erythropoiesis. Cell Rep. 2018 Jan 30;22(5):1211-1224. doi: 10.1016/j.celrep.2018.01.017. PMID: 29386109; PMCID: PMC5828030.

Tormanen K, Ton C, Waring BM, **Wang K**, Sütterlin C. Function of Golgi-centrosome proximity in RPE-1 cells. PLoS One. 2019 Apr 15;14(4):e0215215. doi: 10.1371/journal.pone.0215215. PMID: 30986258; PMCID: PMC6464164.

Muñoz KJ, **Wang K**, Sheehan LM, Tan M, Sütterlin C. The Small Molecule H89 Inhibits *Chlamydia* Inclusion Growth and Production of Infectious Progeny. Infect Immun. 2021 Jun 16;89(7):e0072920. doi: 10.1128/IAI.00729-20. Epub 2021 Jun 16. PMID: 33820812; PMCID: PMC8373235.

Wang K, Muñoz KJ, Tan M, Sütterlin C. *Chlamydia* and HPV induce centrosome amplification in the host cell through additive mechanisms. Cell Microbiol. 2021 Dec;23(12):e13397. doi: 10.1111/cmi.13397. Epub 2021 Nov 10. PMID: 34716742; PMCID: PMC8665076.

Abstract of the Dissertation

Genetic analysis of small RNAs in *Chlamydia trachomatis*

by

Kevin Wang

Doctor of Philosophy in Microbiology and Molecular Genetics

University of California, Irvine, 2022

Professor Ming Tan, Chair

Bacterial small RNAs (sRNAs) are short transcripts that play critical roles in post-transcriptional gene regulation. In the obligate intracellular pathogen *Chlamydia trachomatis*, however, sRNAs are poorly understood because genetic tools in *Chlamydia* have only recently become available. As such, functional studies of two chlamydial sRNAs were limited to an *E. coli* heterologous system. A major issue with this approach is that *Chlamydia* lacks the important sRNA chaperone protein, Hfq, that is found in *E. coli*. The heterologous system is also not suitable for studying the function of a sRNA in the *Chlamydia* developmental cycle, which involves conversion between the infectious (EB) and the replicative (RB) forms within a eukaryotic host cell.

With recent advances in *Chlamydia* genetics, we have developed an inducible sRNA overexpression system in *C. trachomatis.* Utilizing our approach, we conducted a genetic screen and identified 4 previously uncharacterized sRNAs (i.e. CtrR3, CtrR7, CtrR0332, and CTIG684) whose individual overexpression reduced the production of infectious chlamydial progeny. We then determined that overexpression of CtrR3 and

CtrR0332 both blocked RB-to-EB conversion, whereas CtrR7 overexpression hindered RB replication. To demonstrate how our system can be used to find mRNA targets of a chlamydial sRNA, we took a multi-step approach to identify YtgB and CTL0389 as targets of CtrR3. We also showed the versatility of this genetic approach by applying it to develop a novel sRNA-mediated conditional knockdown system in *C. trachomatis*.

This is the first study to analyze sRNAs in *Chlamydia* and to experimentally demonstrate that chlamydial sRNAs can regulate gene expression. Our genetic approach for studying sRNAs and for identifying mRNA targets can be readily applied to elucidate the function of other chlamydial sRNAs. In addition, our knockdown system can be utilized to investigate the function of essential genes in *C. trachomatis*. Overall, the work described in this dissertation has significantly advanced our understanding of sRNAs and post-transcriptional gene regulation in *C. trachomatis*.

Chapter 1: General Introduction

Significance of *Chlamydia*

Chlamydiae is a phylum of gram-negative, obligate intracellular bacteria that infect protozoans, animals, and humans (Bachmann et al., 2014; Elwell et al., 2016). Three species of the phylum are pathogenic to humans, these include *Chlamydia psitacci*, *Chlamydia pneumoniae*, and *Chlamydia trachomatis*. Specifically, *C. psitacci* can be transmitted from birds to humans and causes psittacosis, a form of pneumonia (Bennett et al., 2014). *C. pneumoniae* infection accounts for ~10% of community-acquired pneumonia and has been linked to asthma and atherosclerosis (Bennett et al., 2014). *Chlamydia trachomatis* is most important clinically and is further divided into serovars that have specific tissue tropism and cause three separate clinical manifestations: 1) trachoma, 2) chlamydia, and 3) lymphogranuloma venerum (LGV) (Jordan et al., 2020).

Serovars A-C infect the eye conjunctival epithelium and cause trachoma, which ranges from self-limiting follicular conjunctivitis to blindness due to conjunctival scarring (Stocks et al., 2014). Trachoma is highly contagious and can be eliminated by clean water sources, making it the world's leading cause of preventable blindness (Jordan et al., 2020). In contrast, serovars D-K predominantly infect the urogenital tract and cause chlamydia, the most common bacterial sexually transmitted disease with >1.8 million new cases reported annually in the US alone (CDC, 2021). Most cases of chlamydia are asymptomatic (Stamm, 1999), however, chronic infection leads to severe sequelae such as pelvic inflammatory disease (PID), ectopic pregnancy, and infertility in women (Haggerty et al., 2010; Lan et al., 1995; Taylor & Haggerty, 2011). Interestingly, genital serovars have also been linked to HPV-induced cervical cancer (Appleby et al., 2007;

Fonseca-Moutinho, 2011; Silva et al., 2014). Serovars L1-L3 infect the mucosal surfaces of the anogenital tract, as well as macrophages. The latter attribute allows serovars L1-L3 to spread to regional lymph nodes and cause lymphogranuloma venerum, which is characterized by painful lymphadenopathy in the groin or pelvis (Bennett et al., 2014; Herring & Richens, 2006).

Although antibiotics are available to treat chlamydial infection, the asymptomatic nature of the infection and the lack of vaccines make *Chlamydia trachomatis* a major public health issue. For these reasons, this dissertation and the rest of this chapter will focus mainly on *C. trachomatis*.

Developmental cycle of *Chlamydia trachomatis*

Chlamydia trachomatis undergoes a unique developmental cycle within a eukaryotic host cell (Fig. 1). The *Chlamydia* developmental cycle is biphasic and requires the conversion between two specialized developmental forms. The first developmental form is called the elementary body (EB), which is smaller (~0.2 μm in diameter), has the ability to infect a host cell, but cannot replicate. EBs are also environmentally resistant due to their outer membrane complex that is composed of proteins cross-linked by disulfide bonds (Nelson, 2012). The second developmental form is called the reticulate body (RB), which is larger (~0.8 μm in diameter), non-infectious, environmentally labile, and can undergo replication.

The *Chlamydia* developmental cycle begins with an EB adhering to the host cell membrane via interaction between chlamydial outer membrane proteins (e.g. OmcB) and host cell receptors (e.g. heparin sulfate proteoglycans) (Hegemann & Moelleken, 2012; Mehlitz & Rudel, 2013; Rosmarin et al., 2012). Upon contact, EB secretes pre-loaded T3SS effectors into the host cell that facilitate the endocytosis of the bacterium into a membrane-bound inclusion (Ghosh et al., 2020; Jiwani et al., 2013; Saka et al., 2011). Within a few hours after entry, the EB differentiates into an RB, which divides to expand bacterial numbers (J. K. Lee et al., 2018; Rosario CJ, 2020). After multiple rounds of RB replication, individual RBs asynchronously convert back into an EB. The developmental cycle ends with EBs released from the host cell either through host cell lysis or inclusion extrusion (Hybiske & Stephens, 2007). The time course of the intracellular infection differs among species. For *C. trachomatis*, EB-to-RB conversion occurs around 2-8 hours post infection (hpi), RB-to-EB conversion starts at around 24

hpi, and the cycle ends at around 36-48 hpi (Belland, Zhong, et al., 2003; Rosario CJ, 2020).

If growth conditions are unfavorable, *Chlamydia* will divert from the developmental cycle and enter into a state of persistence (Fig. 1). Persistence is generally defined as a halt in the development cycle induced by stressors such as nutrient deprivation, beta-lactam antibiotics treatment, or IFN-γ treatment (Panzetta et al., 2018). Once the stress-inducing agent is removed, *Chlamydia* can exit from persistence and complete the development cycle with the formation of infectious EBs (Beatty et al., 1995; Hogan et al., 2004). The classic examples of persistence are induced by penicillin or IFN-γ treatment (Kintner et al., 2014; Schoborg, 2011). In these cases, RBs will continue genome replication but will stop cell division, resulting in an inclusion containing only a few abnormally large RBs termed the aberrant bodies (Beatty et al., 1994, 1995). However, it is important to note that not all persistence is defined by the presence of aberrant RBs (Panzetta et al., 2018; Schoborg, 2011).

A hallmark of the developmental cycle is the temporal expression of chlamydial genes in three main classes (early, midcycle, and late), which correlate with the timing of different steps in the developmental cycle (Table 1) (Rosario CJ, 2020). In *C. trachomatis*, early genes are expressed starting at 1-3 hpi and are thought to be important for establishing the inclusion (Belland, Zhong, et al., 2003; Rosario CJ, 2020). For example, CT850 is an early gene product that localizes to the inclusion membrane and interacts with host dynein (Clausen et al., 1997; S. S. Grieshaber et al., 2006; Mital et al., 2015). This interaction mediates the trafficking of the inclusion to the microtubule organizing center (MTOC) of the cell, where the inclusion is in a nutrient-rich

environment and in close proximity to various host organelles (e.g. Golgi) (Gitsels et al., 2019). Midcycle genes are first transcribed by RBs at 8-16 hpi and are involved in nutrient acquisition and metabolism to support RB growth and replication (Belland, Zhong, et al., 2003; Rosario CJ, 2020). This class of genes also encodes proteins that are important for bacterial division (e.g. MreB) and cell wall synthesis (e.g. Penicillin-binding-proteins) (Ouellette et al., 2012; Ranjit et al., 2020). Lastly, late genes are transcribed by RBs starting at 24 hpi and are important for RB-to-EB conversion. For example, the histone-like proteins, HctA (Hc1) and HctB (Hc2), are late gene products that are proposed to condense chlamydial DNA to silence transcription in EBs (Barry et al., 1992, 1993; Brickman et al., 1993a; Hackstadt et al., 1991; Pedersen et al., 1996).

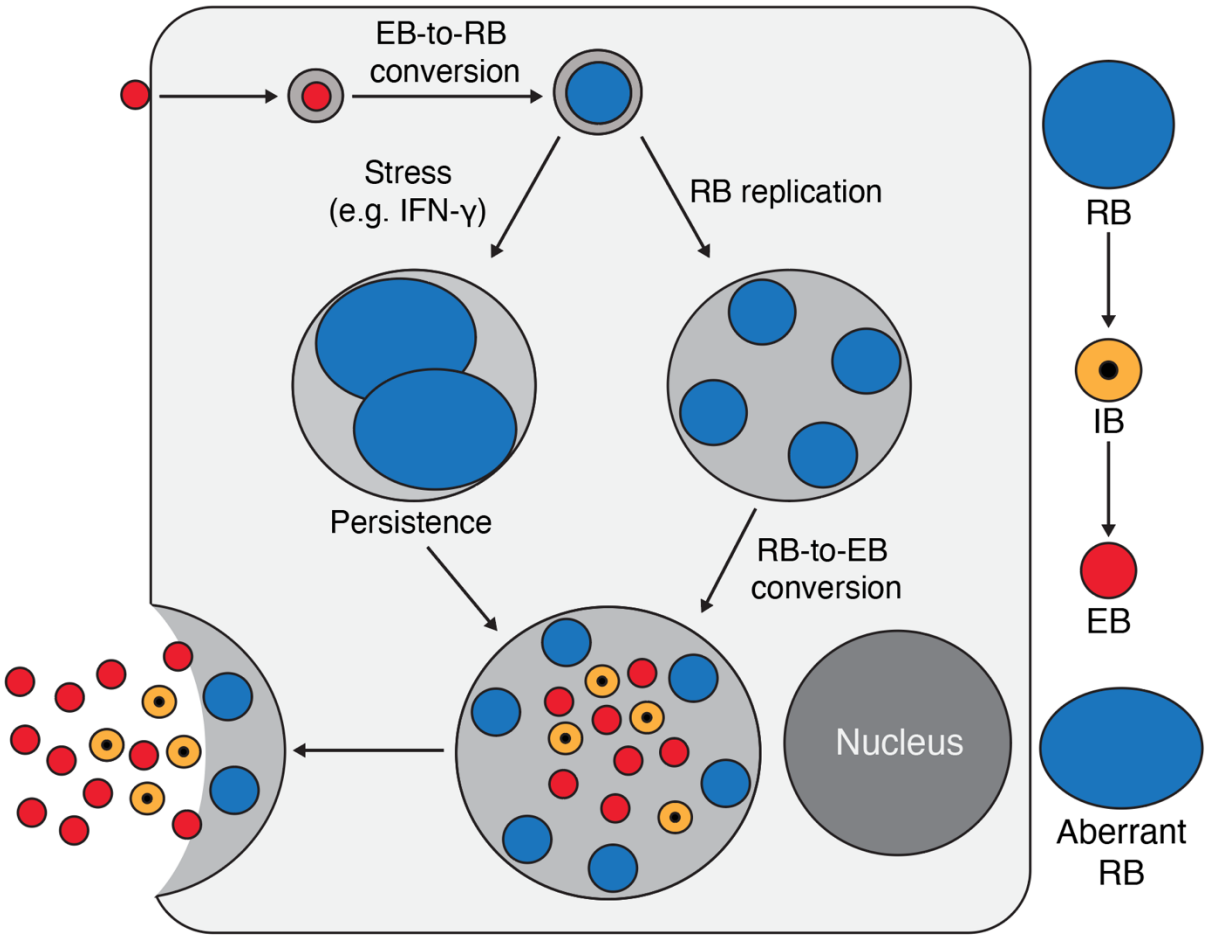

Figure 1. *Chlamydia trachomatis* has a biphasic developmental cycle.
Diagram depicts the chlamydial developmental cycle, which begins with an infectious elementary body (EB) attaching and entering a host cell. In the host cell, the EB resides in an inclusion, where it converts into a reticulate body (RB). In nutrient-rich conditions, RBs will undergo several rounds of replication. During late infection time, individual RB will start to asynchronously convert back into the infectious EB. Intermediate bodies (IB) are RBs in the process of converting into an EB. The cycle ends when EBs exit the host cell through lysis or extrusion and infect a nearby cell. During stress conditions, such as IFN-γ treatment, *Chlamydia* enters a persistence state where the RBs do not divide, resulting in the formation of large aberrant RBs. Once the stressor is removed, aberrant RBs convert into EBs to complete the developmental cycle.

Table 1. Transcriptional regulators of temporal gene expression in *C. trachomatis*

	Early genes	**Midcycle genes**	**Late genes**
Purpose	Inclusion establishment	RB replication	RB-to-EB conversion
Start of transcription	1-3 hpi	8-16 hpi	~24 hpi
Sigma factor(s)	σ^{66}	σ^{66} σ^{54} (subset)	σ^{66} σ^{28} (subset) σ^{54} (subset)
Additional regulators	Supercoiling-dependent promoters (subset)	Supercoiling-dependent promoters	Supercoiling-independent promoters EUO repressor
	HctA and HctB		

Transcriptional regulation in *Chlamydia trachomatis*

Chlamydia trachomatis uses different forms of RNA polymerase to transcriptionally regulate gene expression in a temporal manner (Table 1). A sigma factor (σ) is a subunit of RNA polymerase (RNAP) that binds the core enzyme ($\alpha_2\beta\beta'$ subunits in *Chlamydia*) and recognizes specific DNA sequences in the promoter region to initiate transcription (Toyoda et al., 2021). *Chlamydia* has three sigma factors: σ^{66}, σ^{28}, and σ^{54} (Douglas & Hatch, 2000; Rosario CJ, 2020). σ^{66} is the major chlamydial sigma factor and is a homolog of the *E. coli* major sigma factor σ^{70}. Expression of σ^{66} is detected throughout the developmental cycle and σ^{66} RNAP transcribes early and midcycle genes and the majority of late genes (Belland et al., 2003; Rosario CJ, 2020; Saka et al., 2011). In contrast, the alternative sigma factors, σ^{28} and σ^{54}, have transcripts detected starting at 8 hpi. σ^{28} RNAP transcribes a subset of late genes (e.g. *hctB*) (Yu et al., 2006; Yu & Tan, 2003), whereas σ^{54} RNAP is thought to transcribe a subset of midcycle and late genes that are involved in T3SS (Soules et al., 2020).

C. trachomatis utilizes DNA supercoiling to activate the expression of midcycle genes and a subset of early genes (Rosario CJ, 2020). Negative DNA supercoiling level can increase transcription at specific promoters in bacteria (Travers & Muskhelishvili, 2005). In the *C. trachomatis* developmental cycle, the chlamydial DNA is most negatively supercoiled during midcycle and relaxed during early and late infection times (Niehus et al., 2008). In addition, midcycle promoters and a subset of early promoters are responsive to negative supercoiling, whereas late promoters are not (Table 1) (Cheng & Tan, 2012, p. 2; Niehus et al., 2008). Thus, the current model is that expression of midcycle genes and a subset of early genes is activated when negative

supercoiling increases during midcycle infection time, which is mediated through the expression of chlamydial DNA gyrase (Orillard & Tan, 2016; Rosario CJ, 2020). It is also hypothesized that supercoiling provides a mechanism for *C. trachomatis* to coordinately upregulate transcription of hundreds of midcycle genes (~650 genes total) via their supercoiling-responsive promoters; however, further work is required to confirm this hypothesis (Belland, Zhong, et al., 2003).

Chlamydia trachomatis, like other bacteria, employs transcription factors to activate or repress transcription of specific genes. Transcriptional activators bind to DNA sequence near the target promoter and interact with RNAP, which activates transcription by recruiting the RNAP to the promoter (Seshasayee et al., 2011). In contrast, transcriptional repressors bind to a specific DNA sequence, known as an operator, near the target promoter and prevent RNAP from interacting with the promoter (Rosario CJ, 2020; Seshasayee et al., 2011). The same activator or repressor-binding sequences can be located at different promoters, allowing transcriptional activators and repressors to coordinately regulate the transcription of a set of target genes. *Chlamydia trachomatis* is predicted to have 15 transcription factors, and the majority of them are transcriptional repressors (Domman & Horn, 2015; Rosario CJ, 2020). However, few chlamydial transcription factors are proposed to regulate the developmental cycle.

One chlamydial transcriptional repressor, EUO, is proposed to regulate the developmental cycle by preventing premature late gene expression (Table 1). EUO is an early gene that is specific to and conserved within the *Chlamydiae* phylum (Belland, Zhong, et al., 2003; Domman & Horn, 2015). It represses the transcription of σ^{66} and σ^{28}-dependent late promoters via binding operators near these promoters (Rosario et

al., 2014; Rosario & Tan, 2012). Thus, during early and midcycle infection times, EUO is proposed to repress the expression of late genes while allowing transcription to occur at EUO-independent early and midcycle promoters. It is proposed that during late infection time, the activity of EUO is de-repressed, allowing for late gene expression and subsequent RB-to-EB conversion. The mechanism of EUO de-repression is unknown but it can potentially occur through EUO protein degradation or decreased translation of the EUO mRNA (Rosario CJ, 2020).

Chlamydia expresses two histone-like proteins, HctA and HctB, that are proposed to shut down transcription in EBs via DNA condensation (Table 1). HctA and HctB have amino acid sequence homology to the eukaryotic histones and are thought to bind to DNA in a nonspecific manner. This hypothesis is supported by *in vitro* experiments that demonstrated that both histone-like proteins can bind and condense DNA (Barry et al., 1992, 1993; Brickman et al., 1993a). Furthermore, the expression of HctA and HctB in *E. coli* led to the formation of nucleoids that are similar to the ones observed in EBs. As a result of nucleoid formation, HctA and HctB expression decreased both transcription and translation in *E. coli* (Barry et al., 1992; Brickman et al., 1993a; N. A. Grieshaber, Grieshaber et al., 2006; N. A. Grieshaber, Sager, et al., 2006). The two histone-like proteins are expressed at a time of RB-to-EB conversion and thus, are thought to be important for the formation of EBs by condensing chlamydial DNA and silencing transcription (Belland et al., 2003; E. I. Shaw et al., 2000). Out of the two proteins, HctA is proposed to be the primary driver of DNA condensation in EBs because only HctA is conserved in *Chlamydia*-related bacteria (Collingro et al., 2011).

Most of the work on chlamydial gene regulation has been focused on mechanisms of transcriptional regulation. In contrast, much less is known about post-transcriptional regulation in *Chlamydia*, which includes small RNAs (sRNAs) that can affect the stability or the translational efficiency of one or more mRNAs. Before I introduce chlamydial sRNAs, I will first discuss the general function of bacterial sRNAs.

Bacterial small RNAs (sRNAs)

Bacteria require tight control of gene regulation to adapt quickly to their environment. This is often achieved through the expression of sRNAs, which are transcripts that range from 50-400 nt. Bacterial sRNAs can regulate gene expression on both a transcriptional and post-transcriptional level (Storz et al., 2011). The mechanisms by which sRNAs can achieve this are diverse. Mechanisms of RNA regulation include Riboswitches, mRNA-binding RNA, protein-binding RNA (e.g. CsrB and 6S RNA), RNA mimicry of tRNAs for ribosome recycling (i.e. tmRNA), and CRISPR RNA (Storz et al., 2011; Waters & Storz, 2009). The post-transcriptional mechanism that will be the main focus of this section involves direct complementary base pairing of the sRNA to one or more mRNA targets (Dutta & Srivastava, 2018; Waters & Storz, 2009). Examples of sRNA and its mRNA target will be shown in the following sections as sRNA-mRNA target pair.

The majority of mRNA-binding sRNAs negatively regulates the target transcript. The classic mechanism of negative regulation is through sRNA binding at/or near the ribosome binding site (RBS) of the mRNA target to prevent ribosome loading or translation initiation (e.g. SymR-SymE in enterobacteria) (Dutta & Srivastava, 2018; Waters & Storz, 2009). The lack of translation or ribosomes on the mRNA target destabilizes the mRNA as the transcript is more prone to RNA cleavage by RNases, such as RNase E (Fig. 2A) (Hui et al., 2014; Vargas-Blanco & Shell, 2020). Additionally, sRNA-mRNA interactions can lead to active recruitment of RNase E to degrade the target transcript. Recruitment of RNase E is often mediated by an RNA chaperone

protein Hfq, which facilitates the sRNA-mRNA interaction (e.g. RyhB-MsrB in *E. coli*) (Dutta & Srivastava, 2018).

In addition, sRNAs can negatively regulate their mRNA targets through noncanonical mechanisms. For example, sRNAs have been shown to bind sequences upstream of the RBS (e.g, Spot42-SdhC and OmrA-CirA in *E. coli*) or in the coding region of the mRNA target (e.g. RybB-OmpN in *E. coli*) (Bouvier et al., 2008; Desnoyers & Massé, 2012; Dutta & Srivastava, 2018; Guillier & Gottesman, 2008). Some sRNAs block translation of a target transcript without destabilizing the mRNA (e.g. Spot42-GalK in *E. coli*) (Møller et al., 2002). In some instances, negative regulation of sRNA occurs on a transcriptional level by inducing the formation of a transcriptional terminator (e.g. RnaG-IcsA in *Shigella flexneri*) (Dutta & Srivastava, 2018; Georg & Hess, 2011).

Bacterial sRNAs can also activate the expression of their mRNA targets. In comparison to negative regulation, positive regulation of a sRNA on an mRNA target is less common. This positive regulation is achieved by the sRNA binding to the 5' UTR of the mRNA target and melting the intrinsic secondary structure that sequesters the RBS (e.g. RNAIII-Hla in *Staphylococcus aureus*) (Fig. 2A) (Papenfort & Vanderpool, 2015). In addition, some sRNAs mask RNase E cleavage sites in the mRNA target to prevent RNA decay (e.g. RydC-Cfa1 in *Salmonella enterica*) (Fröhlich et al., 2013; Vargas-Blanco & Shell, 2020). Binding of sRNA to an mRNA target can also direct RNase III cleavage at the interaction site, generating stable mRNA transcripts (e.g. GadY-GadX in *E. coli*) (Georg & Hess, 2011; Opdyke et al., 2011). Lastly, sRNAs have been shown to activate the expression of the mRNA target on a transcriptional level by preventing

premature Rho-dependent transcription termination (e.g. DsrA-RpoS in *E. coli*) (Sedlyarova et al., 2016).

Transcript-binding sRNAs are further divided into *cis*-encoded or *trans*-encoded sRNAs. *Cis*-encoded sRNAs are expressed as an anti-sense RNA to their mRNA target (Fig. 2B). As such, *cis*-encoded sRNAs have a single target to which they share an extended region of perfect complementary (Storz et al., 2011; Waters & Storz, 2009). Most of the *cis*-encoded sRNAs that have been studied are involved in maintaining mobile element copy numbers or acting as antitoxins to toxin mRNAs (Wagner et al., 2002; Waters & Storz, 2009). Thus, anti-sense RNAs are often expressed constitutively. In contrast to *cis*-encoded sRNA genes, *trans*-encoded sRNA genes are located separately in the genome from their target genes (Fig. 2B). These sRNA genes are typically found in the intergenic region of the genome and are under the control of their own promoters. However, it is now clear that *trans*-encoded sRNAs can also be processed from an mRNA or even a tRNA (Carrier et al., 2018; Hör et al., 2020). *Trans*-encoded sRNAs have short, limited complementary with their mRNA target(s). Due to this feature, *trans*-encoded sRNAs can have multiple mRNA targets and their interaction with mRNAs often requires the help of RNA chaperone proteins such as Hfq or ProQ (Dutta & Srivastava, 2018; Smirnov et al., 2017; Waters & Storz, 2009). The majority of *trans*-encoded sRNAs are crucial for responding to environmental stress (e.g. envelope stress, metal homeostasis) and thus, these sRNAs are often transcribed under specific growth conditions (Hör et al., 2020; Storz et al., 2011; Waters & Storz, 2009).

Canonical *trans*-encoded sRNAs are expressed under a promoter that is controlled by a specific transcription regulator that senses the environmental condition.

For example, the transcription of the *E. coli* sRNA RyhB is repressed by the Fe^{2+}-dependent transcriptional repressor, Fur, under iron abundant conditions (Hassan & Troxell, 2013). However, during iron-depleted conditions, RyhB expression is de-repressed as Fur lacks the co-repressor, Fe^{2+}. RyhB then in turn downregulates the translation of iron-containing proteins to decrease iron usage in *E. coli* (Massé & Gottesman, 2002). In contrast, noncanonical sRNAs that function as an RNA sponge are constitutively expressed. For example, $3'ETS^{leuZ}$ is an sRNA that is processed from the 3' external transcribed spacer of the *glyW-cysT-leuZ* tRNA precursor and is constitutively expressed. $3'ETS^{leuZ}$ binds to and acts as a sponge to repress the transcriptional noise of sRNAs RybB and RyhB, which are expressed under powerful promoters (Lalaouna et al., 2015).

There are advantages for bacteria to utilize *trans*-encoded sRNAs, instead of transcription factors, as a mechanism of gene regulation to respond to environmental stress. By nature, the production of sRNA, a short RNA transcript, requires less energy than the production of transcription factors, which requires the entire translation machinery (e.g. ribosomes, tRNAs, amino acids). In addition, sRNAs are less stable than transcription factors. This means that once a sRNA exerts its function and is no longer transcribed, the sRNA level will decrease and cease to regulate its mRNA targets (Storz et al., 2011). Regulation on a post-transcriptional level also allows sRNAs to quickly block the production of new protein synthesis of the target transcript, whereas transcriptional regulation cannot prevent the mRNAs that have already been synthesized from translating new proteins. It has become clear that *trans*-encoded sRNAs can largely impact gene expression by regulating multiple mRNA targets; thus,

trans-encoded sRNAs and their regulatory circuits have been the focus of bacterial sRNA research.

The characterization of a *trans*-encoded sRNA function has been largely focused on the identification of mRNA targets. One approach is to alter the levels of sRNA and then measure genome-wide changes in transcript levels by RNA-sequencing (Sharma & Vogel, 2009a; Vogel & Wagner, 2007). sRNA levels can be altered either through gene deletion, exogenous overexpression, or induction of sRNA expression (e.g. iron depletion induces RyhB expression). It is important to note that the RNA-seq approach can only detect mRNA targets that are destabilized or stabilized from the sRNA-mRNA interaction, which is not always the case (e.g. Spot42-GalK) (Møller et al., 2002). Thus, a more comprehensive approach entails coupling RNA-sequencing with proteomics or conducting Ribo-Seq, which measures the translational efficiency of individual mRNA (J. Wang et al., 2015). sRNAs can also be tagged with RNA aptamers (e.g. MS2) that can be affinity purified to identify interacting mRNA targets (Lalaouna et al., 2017, 2018; Lalaouna & Massé, 2015; Said et al., 2009). Alternatively, putative mRNA targets can be identified via bioinformatic tools (e.g. TargetRNA2, IntaRNA) that predict sRNA-mRNA interactions (Busch et al., 2008; Kery et al., 2014; Mann et al., 2017; Wright et al., 2014). More recently, interactions of different sRNAs with their respective mRNA targets have been captured on a genome-wide level by affinity purifying RNA chaperone proteins and searching for sRNA-mRNA chimeras (e.g. Hfq-CLASH, RIL-seq) (Iosub et al., 2020; Melamed et al., 2020). Unfortunately, methods that utilize Hfq as bait to identify sRNA-mRNA interaction are not applicable to bacteria that do not have any identifiable RNA chaperone proteins, including a subset of gram-positive bacteria (e.g.

Mycobacterium tuberculosis) and *Chlamydia trachomatis*. Interestingly, Zhang et al. recently demonstrated that the Hi-GRIL-seq approach, which utilizes a T4 RNA ligase to ligate sRNAs to their mRNA targets, was able to detect sRNA-mRNA pairs that are Hfq-independent (Zhang et al., 2017).

The mRNA targets identified by the aforementioned approaches must be validated experimentally. The best approach is to show that the sRNA regulates the endogenous protein level of a target. However, this requires an antibody to the protein of interest that is readably available. A good substitution for this approach is the use of translational fusions. Translational fusions are generated by fusing the 5'UTR of the putative mRNA target, where sRNAs typically bind, to a reporter gene such as *gfp* (Sharma & Vogel, 2009a). An mRNA target is considered a direct target of sRNA if altering the levels of the sRNA also alters the level of the translational fusion reporter protein. An advantage of translational fusion is that it allows for compensatory base-pair exchange experiments, which are the gold standard for validating sRNA-mRNA interactions (Sharma & Vogel, 2009a).

Bacterial sRNAs regulate various pathogenic processes in prokaryotes such as virulence, biofilm formation, quorum sensing, and antibiotic resistance, making them good therapeutic targets (Dersch et al., 2017; Papenfort & Vanderpool, 2015; Wagner & Romby, 2015). For example, the *E. coli* sRNA GcvB negatively regulates the expression of CycA, which is a serine transporter that imports the antibiotic D-cycloserine (Pulvermacher et al., 2009). As such, GcvB can be targeted to combat antibiotic resistance against D-cycloserine (Dersch et al., 2017; Parmeciano Di Noto et al., 2019). RNA-based therapies such as delivering sRNAs or short antisense oligonucleotides

(ASOs) to bacteria are also being developed to generate pathogen-specific RNA antibiotics (Parmeciano Di Noto et al., 2019; Vogel, 2020). Our understanding of bacterial sRNAs is advancing at a fast rate. However, this has not been the case for *Chlamydia trachomatis*, where the function of chlamydial sRNAs is largely unknown due to the genetic intractability of this intracellular pathogen.

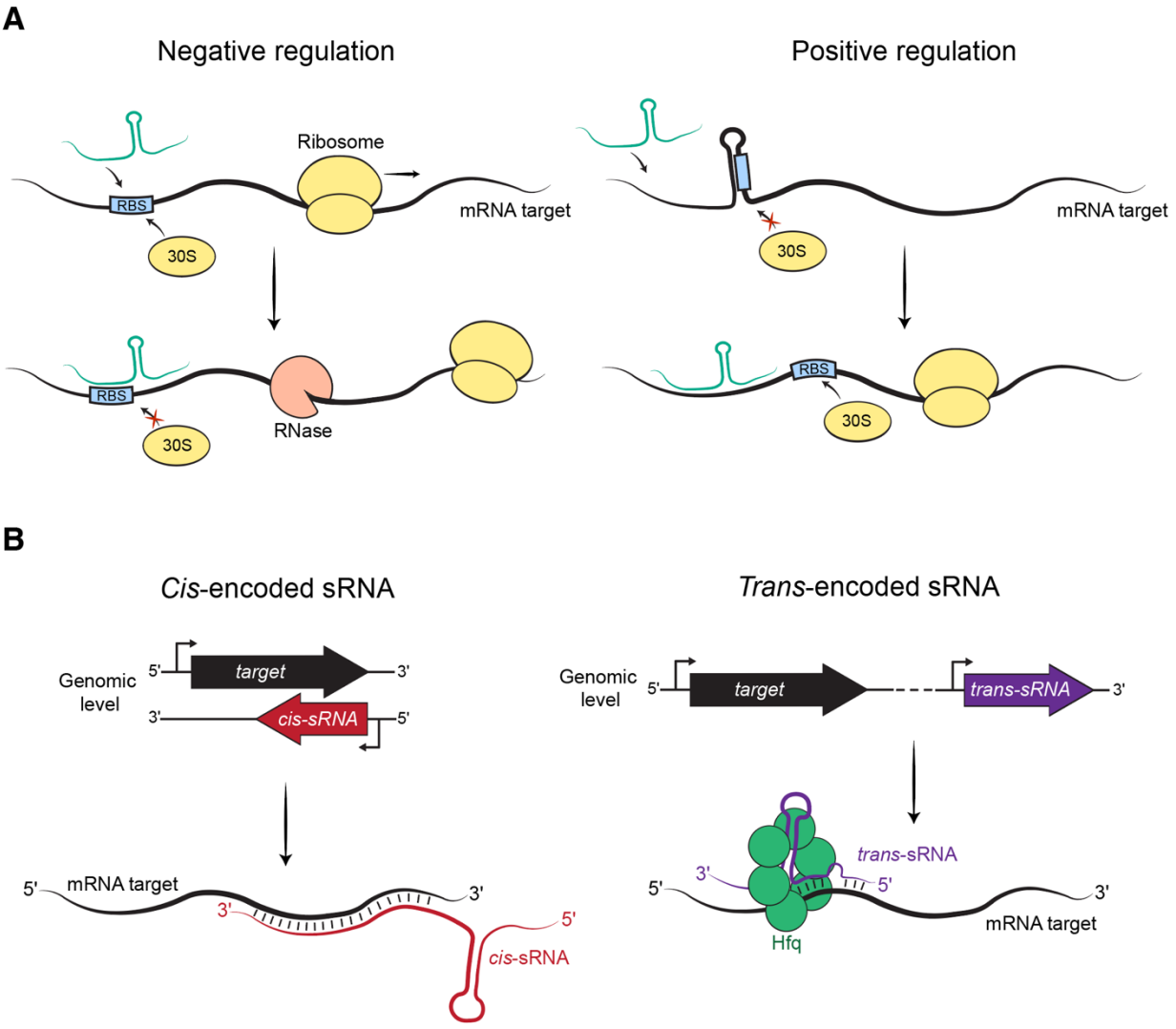

Figure 2. Modes of action and types of bacterial sRNAs.
(A) Diagram of sRNA-mediated negative and positive regulations. Negative regulation is more common and is often achieved when a sRNA base pairs with the RBS of the mRNA target to prevent ribosome loading. The lack of translation and ribosomes on the mRNA target also leads to mRNA decay facilitated by RNases (e.g. RNase E). Positive regulation can be achieved when a sRNA base pairs with the mRNA target and melts the intrinsic secondary structure, revealing the RBS for ribosome loading.
(B) Diagram of types of bacterial sRNAs. *Cis*-encoded sRNAs are anti-sense RNA against their target gene, resulting in long perfect complementarity with the mRNA target. The genes for *trans*-encoded sRNAs are found away from their target genes and form short imperfect base-pairing with the mRNA target, which usually requires the help of a sRNA chaperone protein Hfq.

Chlamydial sRNAs

To date, 66 putative *C. trachomatis* sRNAs have been identified but only 21 (4 *cis* and 17 *trans*) have been verified by northern blot analysis (AbdelRahman et al., 2011; Albrecht et al., 2010). Albrecht utilized deep RNA-sequencing to identify 41 sRNAs and verified 10 of them (3 *cis* and 7 *trans*) in *C. trachomatis* serovar L2. In contrast, AbdelRahman used intergenic microarray to identify an additional 25 sRNAs and validated 11 of them (1 *cis* and 10 *trans*) in *C. trachomatis* serovar D. None of these chlamydial sRNAs have homologs in other bacteria and only 6 have motifs that are conserved among other *Chlamydia* species (e.g. CtrR3 and CtrR0332) (Albrecht et al., 2010). The majority of these chlamydial sRNAs have their transcription start sites (TSS) mapped either through manual annotation in the deep RNA-seq study or 5' RACE in the microarray study. The secondary structures and mRNA targets have been predicted bioinformatically for some of these *C. trachomatis* sRNAs; however, their mRNA targets and functions remain unknown. Currently, only two chlamydial sRNAs have been experimentally tested in an *E. coli* system.

Although relatively little work has been done on *C. trachomatis* sRNAs, Grieshaber et al. used *E. coli* as a heterologous system to characterize one chlamydial *trans*-encoded sRNA, IhtA, and its mRNA target, HctA. Co-expression of IhtA with the histone-like protein rescued the lethal effects of HctA expression in *E. coli* (N. A. Grieshaber, Grieshaber, et al., 2006). Bioinformatic analysis further predicted IhtA binding to the sequence at the start codon of HctA mRNA, which Grieshaber et al. confirmed through compensatory base-pair exchange experiments at the predicted interaction site (N. A. Grieshaber et al., 2015). The interaction between IhtA and HctA

mRNA is thought to halt translation initiation as expression of IhtA led to a decrease in HctA protein, but not mRNA levels, in *E. coli* (N. A. Grieshaber, Grieshaber, et al., 2006). Lastly, IhtA may negatively regulate HctA translation in *C. trachomatis* because there is an inverse relationship in the expression patterns of IhtA and the HctA protein, with IhtA expressed in RBs and HctA protein found in EBs (N. A. Grieshaber, Grieshaber, et al., 2006). These findings, coupled with the function of HctA, led to the hypothesis that IhtA blocks the translation of HctA mRNA to prevent premature DNA condensation in RB.

In addition to HctA, Grieshaber and colleagues identified CTL0322 as another potential target of IhtA. The group predicted that IhtA must bind to other mRNA targets similarly to how it interacts with HctA mRNA (N. A. Grieshaber et al., 2015). Using bioinformatic prediction software (i.e. TargetRNA), the group identified CTL0322 as a putative mRNA target as it was predicted to bind the IhtA target sequence at the start codon. More importantly, IhtA negatively regulated CTL0322 translational fusion in *E. coli*, suggesting that it is a potential mRNA target of IhtA (N. A. Grieshaber et al., 2015). Based on their recent work, Grieshaber and colleagues propose that CTL0322 (DdbA), similar to HctA, is also involved in EB production (N. A. Grieshaber et al., 2021). However, it is unclear how CTL0322 is involved in EB formation since its transcript is detected starting at 8 hpi, a time earlier than the onset of RB-to-EB conversion (Belland, Zhong, et al., 2003). Additionally, like HctA, the regulation of IhtA on CTL0322 has not been validated in *C. trachomatis*.

Similar to work evaluating the function of IhtA, a *cis*-encoded sRNA was analyzed with co-expression studies in *E. coli*. AbdelRahman et al. showed that

expression of the *cis*-encoded sRNA, CTIG270, resulted in the downregulation of both protein and mRNA levels of its antisense gene *ftsI*, which encodes a peptidoglycan synthesis protein involved in RB replication (AbdelRahman et al., 2011; Ouellette et al., 2012). This regulation requires the interaction of CTIG270 with the FtsI mRNA, as the expression of CTIG270Δ, a version of the anti-sense RNA that lacks the complementary base-pairing region, did not affect FtsI protein levels in *E. coli*. AbdelRahman also observed that in *C. trachomatis*, FtsI mRNA expression starts in midcycle and drops during late infection time, whereas CTIG270 is expressed as a late gene. Thus, the authors proposed that CTIG270 could potentially act as a mechanism to turn off RB replication in *Chlamydia* during late infection time.

The use of *E. coli* as a heterologous system allowed both Grieshaber et al. and AbdelRahman et al. to hypothesize that a chlamydial sRNA represses the expression of an mRNA target on a post-transcriptional level to regulate a step in the *C. trachomatis* developmental cycle. However, no definite conclusions about *Chlamydia* sRNAs and their function can be drawn from these *E. coli* studies due to the limitations of the heterologous system. A major issue with this approach is that *Chlamydia*, in contrast to *E. coli*, has no apparent homolog of Hfq. This suggests that *C. trachomatis* could be utilizing different machinery to regulate sRNA activity and function. Another limitation is that the heterologous system does not reveal the roles of chlamydial sRNAs in the *C. trachomatis* developmental cycle. Importantly, these *E. coli* studies cannot provide direct evidence that chlamydial sRNAs post-transcriptionally regulate mRNA targets in *Chlamydia* or that they are important for the *C. trachomatis* infection. The two

aforementioned studies used *E. coli* to investigate chlamydial sRNAs because of the lack of genetic tools in *Chlamydia*.

Genetic tools in *Chlamydia trachomatis*

The inability to transform and genetically manipulate *Chlamydia* has been a roadblock to defining the molecular mechanism of *Chlamydia* pathogenesis. Historically, the investigation of a gene function relied on ectopic expression of the chlamydial protein in the host cell (e.g. studying Inc protein-host protein interaction) or in heterologous systems such as *E. coli* or *Salmonella* (e.g. studying Type-III-secretion effectors) (Agaisse & Derré, 2014; Almeida et al., 2018; Alzhanov et al., 2009; Betts-Hampikian & Fields, 2010; da Cunha et al., 2014; Dumoux et al., 2015). Importantly, the lack of *Chlamydia* transformation made it impossible to satisfy Molecular Koch's postulates, which require gene deletion followed by mutant complementation to experimentally define the molecular function of a specific gene (Falkow, 1988). The first part has been achieved in a transformation-independent approach via chemical mutagenesis coupled with whole-genome sequencing. This approach takes advantage of lateral gene transfer (LGT) in *Chlamydia* (DeMars et al., 2007; Harris et al., 2012; Suchland et al., 2009), gene linkage, and spontaneous chromosomal mutants that are resistant to a specific antibiotic (e.g. *rpoB* mutant is resistant to Rifampin) (Bastidas & Valdivia, 2016). However, mutant strains produced from chemical mutagenesis often contain several mutations in the genome, and thus require mutant complementation and more importantly, *Chlamydia* transformation, to fulfill Koch's postulates (Rahnama & Fields, 2018).

Chlamydia transformation is difficult to achieve due to the biphasic nature of this obligate intracellular bacteria. The infectious EBs are not competent because of their rigid cell wall that contains highly cross-linked proteins (Hatch, 1996). In contrast, RBs

are thought to be competent because they express DNA repair enzymes involved in homologous recombination (Skipp et al., 2005). However, RB transformation is difficult because recombinant DNA has to cross the host, inclusion, and bacterial membranes. To circumvent this issue, one group has developed an axenic culture system to isolate and potentially transform host-free RBs (Omsland et al., 2012). One main roadblock of this approach is that transformed RBs must be converted back to EBs in the axenic media to infect a host cell, which is currently not possible. In addition, selection markers used for *Chlamydia* transformation are limited to antibiotics that can cross multiple lipid bilayers to reach the bacteria (e.g. ampicillin, penicillin), further demonstrating the difficulty in transforming *Chlamydia* (Bastidas & Valdivia, 2016; O'Neill et al., 2020, p. 11; Rahnama & Fields, 2018).

In a seminal study conducted in 2011, Wang et al. utilized a $CaCl_2$-based approach to transform *C. trachomatis* serovar L2 EBs with a shuttle vector. This vector contained serovar L2 plasmid-encoded genes, an *E. coli* origin of replication, a *gfp* gene, and a *bla* gene (Y. Wang et al., 2011). More importantly, the group was able to generate transformants that stably maintained the recombinant vector. Transformation of *C. trachomatis* has also been achieved through electroporation (Tam et al., 1994) and dendrimer-enabled system (Kannan et al., 2013); however, the $CaCl_2$-based approach is the most widely used. The transformation process is long (approximately 2 months) as it requires serial passaging of transformed *Chlamydia* onto a new host cell monolayer under antibiotic selection, followed by plaque cloning to acquire a clonal population of a transformant. In addition, transformation efficiency is relatively low compared to transformation in other gram-negative bacteria. However, introducing

exogenous DNA into *Chlamydia* has opened the door for chlamydial genetic manipulation.

Chlamydia transformation made it possible to ectopically express a specific chlamydial gene from the shuttle vector in *C. trachomatis*. Genes can be expressed from their endogenous promoters to study their temporal expression during the developmental cycle (Chiarelli et al., 2020; Cortina et al., 2019). However, expressing a chlamydial protein from its endogenous promoter will increase the concentration of the protein in *Chlamydia* due to increased copy number, which in some cases (e.g. expressing transcription factors), can be toxic to the bacteria. Alternatively, ectopic gene expression can be regulated under the control of a tetracycline-inducible promoter (e.g. shuttle vectors pBOMB4 or pASK) (Bauler & Hackstadt, 2014; Wickstrum et al., 2013). This approach has been utilized to investigate the effect of transcription factors on the chlamydial transcriptome (Soules et al., 2020; Wurihan et al., 2021). In addition, inducible expression of a tagged chlamydial protein allows for investigation of its cellular localization (Bauler & Hackstadt, 2014; J. Lee et al., 2020) and its interacting partners (Dickinson et al., 2019; Y. Han & Derré, 2017). Importantly, ectopic gene expression allows for mutant complementation and for defining the functional domain that is required to rescue a phenotype (Auer et al., 2020; Ghosh et al., 2020; Weber et al., 2016; Wood et al., 2020).

The ability to introduce recombinant DNA into *C. trachomatis* has also led to the development of multiple gene knockout systems (Andersen et al., 2021; C. M. Johnson & Fisher, 2013; LaBrie et al., 2019; Mueller et al., 2016). One example is the use of TargeTron™ (Sigma) for site-directed gene inactivation (C. M. Johnson & Fisher, 2013;

J. H. Shaw et al., 2018; Weber et al., 2016). This system takes advantage of mobile group II introns and their ability to insert into target genes with the help of intron encoded protein (IEP) (Lambowitz & Zimmerly, 2004). Another gene disruption method is the use of the hyperactive *Himar* transposase, which inserts transposons non-specifically into the genome (Lampe et al., 1999, p. 19). This method has led to vector-driven transposon mutagenesis screens conducted in both *C. trachomatis* and *C. muridarum* (LaBrie et al., 2019; Y. Wang et al., 2019). In addition, site-directed gene deletion through allelic exchange has been developed by Fields and colleagues, which involves replacing the gene of interest with a cassette that expresses an antibiotic resistance marker (Mueller et al., 2016). One limitation of utilizing these knockout systems is that insertion into the chlamydial chromosome can have polar effects on upstream or downstream genes or change the overall DNA topology, which may affect the transcription of multiple genes (O'Neill et al., 2020; Rahnama & Fields, 2018). Fields et al. resolved this issue by flanking the inserted cassette with LoxP sites, which can be excised when Cre is expressed (Keb et al., 2021). An important limitation of using gene knockout approaches to study a chlamydial gene is that *Chlamydia* has a reduced genome size, in which most genes are likely to be essential. As such, roughly only 15% of the chlamydial genome has been disrupted using the aforementioned approaches (LaBrie et al., 2019; O'Neill et al., 2020).

To date, only one conditional gene knockdown system has been developed to study the function of essential genes in *C. trachomatis*. In a proof-of-principle study, Ouellette applied CRISPR interference (CRISPRi) to knockdown a non-essential gene, *incA* (Ouellette, 2018). This system utilizes an inactive Cas9 variant (dCas9) that binds

to a single guide RNA (sgRNA), which directs the complex to a target DNA sequence in the *incA* promoter region (Bikard et al., 2013; Qi et al., 2013). The target sequence must also have a downstream protospacer adjacent motif (PAM) site to be recognized by dCas9 (Mojica et al., 2009). The dCas9-sgRNA complex then blocks transcription of *incA* via steric hindrance. More importantly, the dCas9 is placed under the control of a tetracycline-inducible promoter, resulting in a conditional gene knockdown system (Ouellette, 2018; Ouellette et al., 2021). Using this approach, Ouellette and colleagues were able to knockdown the essential chlamydial genes *clpP2* and *clpX* (Wood et al., 2020). Repressing gene expression on a transcriptional level has a strong gene silencing effect, however, this also indicates that knocking down the first gene in an operon will cause a polar effect on downstream genes in an operon (Wood et al., 2020). Thus, a conditional knockdown system that can selectively target a gene in an operon would be beneficial.

Chapter concluding statement

Small RNAs (sRNAs) are a class of regulatory RNAs that play important roles in bacterial physiology and pathogenesis. However, in the intracellular bacterium *Chlamydia*, sRNAs are poorly understood, and functional studies have been limited to a heterologous system. In this study, we took advantage of the recent advances in chlamydial genetics and developed an inducible sRNA overexpression system in *C. trachomatis* (Ch 2). We applied the genetic system to a screen and identified 4 previously uncharacterized sRNAs that had a deleterious effect on the *C. trachomatis* developmental cycle when they were overexpressed (Ch 2). For 3 of the 4 sRNAs, we further determined which step in the developmental cycle was disrupted by their overexpression (Ch 2). Through a multi-step approach, we also demonstrated how our genetic system can be utilized to identify mRNA targets of a chlamydial sRNA (Ch 2). Lastly, we applied the overexpression system to develop a sRNA-mediated knockdown system in *C. trachomatis* (Ch 3). Overall, this work offers a novel and generalizable approach for investigating the role of chlamydial sRNAs in their native organism.

In Chapter 5, I will also discuss a separate study that was conducted during the early stages of my Ph.D. training. In this work, we provided biological plausibility for *C. trachomatis* as a co-factor for HPV-induced cervical cancer.

Chapter 2: A novel genetic system to study small RNAs in *Chlamydia trachomatis*

Abstract

sRNAs are non-coding transcripts that play critical roles in post-transcriptional regulation in prokaryotes. In the intracellular bacterium *Chlamydia*, sRNAs have been identified, but functional studies have been limited to an *E. coli* heterologous system. We have developed an inducible sRNA overexpression system in *Chlamydia trachomatis* and used it to screen putative sRNAs for effects on the *Chlamydia* developmental cycle, which involves conversion between replicating (RB) and infectious (EB) chlamydial forms. Overexpression of 6 of 15 *C. trachomatis* sRNAs decreased production of infectious EBs. We performed detailed characterization of CtrR3, CtrR7, and CtrR0332 the three sRNAs that caused the largest progeny defects in our screen. By quantifying chlamydial number and infectious progeny, and by visualizing chlamydial forms using electron microscopy, we showed that overexpression of CtrR3 and CtrR0332 prevented RB-to-EB conversion, whereas CtrR7 overexpression blocked bacterial replication. We also describe a workflow that allowed us to identify the mRNA targets of CtrR3 in *Chlamydia*. We first used MS2 aptamer affinity purification coupled with RNA sequencing as an unbiased approach to isolate interacting mRNAs. We then prioritized candidates based on sequence complementarity to the CtrR3 target recognition sequence, which we had identified with bioinformatic and mutational analyses. Finally, we tested putative targets with translational fusion assays in *E. coli* and *C. trachomatis*. Using this integrated approach, we provide experimental evidence that YtgB and CTL0389 are mRNA targets of CtrR3 in *Chlamydia*. These findings demonstrate how our *C. trachomatis* sRNA overexpression system can be used to investigate the functions and mRNA targets of chlamydial sRNAs.

Introduction

Chlamydia are obligate intracellular bacteria that cause a wide array of human illnesses. *Chlamydia trachomatis* is the most common cause of bacterial sexually transmitted disease, with more than 1.8 million new cases reported annually in the U.S.(CDC, 2021). *C. trachomatis* also causes an infectious blindness called trachoma, and the related species, *C. pneumoniae* and *C. psittaci*, are responsible for community-acquired pneumonia and psittacosis, respectively (Batteiger BE, Tan M., 2019).

All *Chlamydia* spp. share a developmental cycle that is marked by conversion between two specialized forms within a eukaryotic host cell (Moulder, 1991). An infectious form, called the elementary body (EB), binds and enters the host cell. Within 2-8 hours post infection (hpi), the EB differentiates into a larger, intracellular form, known as the reticulate body (RB), in a membrane-bound vacuole called the chlamydial inclusion. RBs are metabolically active and undergo multiple rounds of replication before asynchronously converting back into EBs. This conversion step is critical for transmission because only EBs can infect new host cells. The time course of the intracellular infection varies between species, but for *C. trachomatis*, RB-to-EB conversion starts at around 24 hpi, with EBs released by 48 hpi to end the developmental cycle (J. K. Lee et al., 2018).

Another hallmark of this developmental cycle is the regulated expression of chlamydial genes in three temporal groups (Belland, Zhong, et al., 2003). Early genes play important roles in establishing the inclusion, and midcycle genes are expressed during RB replication. Late genes are expressed during RB-to-EB conversion and

include genes with EB-specific functions (Rosario CJ, 2020). For example, *hctA* and *hctB* encode histone-like proteins HctA (also known as Hc1) and HctB (or Hc2), which condense the DNA in EBs, while *omcB* encodes an EB-specific outer membrane protein (Brickman et al., 1993b; Hackstadt et al., 1991). Most of the work on chlamydial gene expression has focused on the regulation of transcription by transcription factors and alternative sigma factors (Rosario CJ, 2020). In contrast, little is known about the post-transcriptional regulation of gene expression in *Chlamydia*.

Small RNAs (sRNAs) play an important role in regulating protein expression in bacteria. These sRNAs are 50 to 500-nucleotides long and form stable secondary structures that are critical for their function. Binding of a sRNA to one or more mRNA targets through complementary base pairing commonly leads to decreased expression of each target protein (Gottesman & Storz, 2011; Storz et al., 2011). sRNAs can be grouped into two classes (Waters & Storz, 2009). A *cis*-encoded sRNA is transcribed from the complementary strand of its single target gene and functions as an anti-sense RNA that binds its mRNA target to regulate its stability (Georg & Hess, 2011). In contrast, a *trans*-encoded sRNA typically has multiple mRNA targets and binds at or near their respective ribosome binding site (RBS). This association occurs via a short region of imperfect sequence complementarity that impedes ribosome binding and/or promotes mRNA degradation. Target genes of *trans*-encoded sRNAs are located at different genomic sites from the sRNA, which makes their identification more challenging (Waters & Storz, 2009).

Putative chlamydial sRNAs have been identified, but functional analysis has been limited to a heterologous system. Albrecht et al. and AbdelRahman et al. used

RNA sequencing or an intergenic tiling microarray to identify a total of 66 putative sRNAs in *C. trachomatis*, 21 of which were confirmed by northern blotting (4 *cis* and 17 *trans* sRNAs) (AbdelRahman et al., 2011; Albrecht et al., 2010). Functional studies have been performed on two *C. trachomatis* sRNAs, IhtA and CTIG270. IhtA is a *trans*-encoded sRNA that decreased protein, but not transcript levels of its target HctA when both were co-expressed in *E. coli* (N. A. Grieshaber, Grieshaber, et al., 2006). CTIG270, in contrast, is a *cis*-encoded sRNA that downregulated transcript and protein expression of the peptidoglycan synthesis gene *ftsI* in an *E. coli* co-expression assay (AbdelRahman et al., 2011; Ouellette et al., 2012). The functions and targets of these sRNAs have not been assessed in *Chlamydia* with its complex biphasic developmental cycle.

In this study, we describe a novel *C. trachomatis* sRNA overexpression system to study chlamydial sRNAs in their native environment. We used this genetic approach to screen 15 chlamydial sRNAs for deleterious effects on the infection and identified 6 whose overexpression caused a severe reduction in infectious progeny. We also applied our genetic system to identify mRNA targets of a chlamydial sRNA. By combining an unbiased screen to capture putative mRNA targets with a bioinformatics-based prioritization scheme and functional studies in *E. coli* and *Chlamydia*, we identified YtgB and CTL0389 as likely mRNA targets of the uncharacterized sRNA CtrR3.

Results

2.1 Development of a sRNA overexpression system in *Chlamydia*

To study the role of chlamydial sRNAs in the developmental cycle, we developed an inducible system to express individual sRNAs in *C. trachomatis*. This system is based on the pBOMB4 plasmid, a chlamydial shuttle vector for tetracycline-inducible protein expression in *C. trachomatis* (Bauler & Hackstadt, 2014). We modified pBOMB4 by removing the downstream Tet operator to avoid adding extra nucleotides to the 5' end of the sRNA, which might alter its secondary structure and function (Fig. 3A). The sRNA overexpression cassette was also relocated to avoid possible read-through transcription of downstream genes. We call this new plasmid pBOMB5 (Fig. 4).

We tested this overexpression system with IhtA, the best characterized chlamydial sRNA. In studies using a heterologous system, IhtA has been shown to negatively regulate translation of the histone-like protein HctA (N. A. Grieshaber, Grieshaber, et al., 2006). We generated pBOMB5-tet-IhtA, and a control plasmid, pBOMB5-tet-mCherry, and transformed each into *C. trachomatis* (Fig. 3A). Induction with anhydrotetracycline (aTc) increased IhtA expression in the IhtA transformant, as measured by northern blots (Fig. 3B) and decreased protein levels of HctA, but not for other late genes, HctB and OmcB (Fig. 3C). These effects were specific for IhtA because they were not seen when mCherry expression was induced by aTc in the control transformant (data not shown). IhtA overexpression did not change mRNA levels of HctA, HctB, or OmcB (Fig. 3D). These data show that IhtA negatively regulates protein, but not transcript, levels of HctA in *Chlamydia*. They also provide proof of

principle for our overexpression system as an approach for altering the levels of sRNA and its target in this intracellular bacterium.

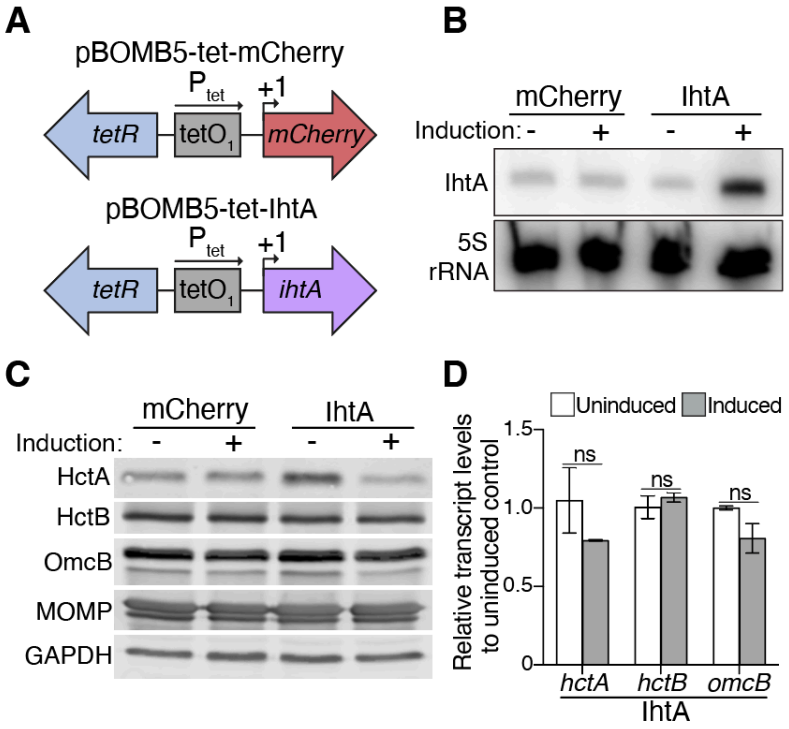

Figure 3. Development of an inducible sRNA overexpression system in *C. trachomatis*.
(A) Schematics of the overexpression cassettes for mCherry (control) and IhtA in the pBOMB5 plasmid. +1 marks the transcriptional start site.
(B) Northern blot of HeLa cells infected with *Chlamydia* transformants that overexpressed either mCherry or IhtA after incubation with or without 50 ng/mL aTc starting at 16 hpi. IhtA levels are shown at 36 hpi. 5S rRNA served as a loading control.
(C) HeLa cells infected for 36 hours with mCherry or IhtA transformants that were either left uninduced or induced with aTc at 16 hpi were lysed and subjected to western blotting analysis with antibodies to HctA, HctB, and OmcB. MOMP and GAPDH served as loading controls for *Chlamydia* and host cells, respectively.
(D) HeLa cells infected with the IhtA transformant and induced as above were analyzed by RT-qPCR for the transcript levels of HctA, HctB, and OmcB at 36 hpi. 16S rRNA served as the reference gene. Transcript levels for each gene in the induced sample was compared to the average transcript levels of each respective gene in the uninduced control via the Pfaffl equation. Data is presented as mean ± SEM (n= 3).

We attempted an alternative approach to knockout IhtA using fluorescence-reported allelic exchange mutagenesis (FRAEM) (Mueller et al., 2017). This approach utilizes a suicide vector that contains the spectinomycin resistance and GFP reporter genes, flanked by the upstream and downstream regions of *ihtA* (Fig. 5A). We were successful in deleting IhtA from the genome (Fig. 5B) and observed a slight increase in HctA protein levels (Fig. 5C). However, we also observed polar effects of the cassette insertion into the *ihtA* gene locus as the expression of the downstream tRNA-thr was no longer detected by northern blot analysis (Fig. 5D). IhtA and tRNA-thr most likely share the same promoter as the σ^{66}-Chromatin immunoprecipitation (ChIP) experiment showed that σ^{66} has one binding site upstream of the *ihtA* gene (Fig. 5E). In addition, alongside knocking out *ihtA*, we attempted to knockout another sRNA, CtrR7, and were unsuccessful. These results further demonstrated the limitation of utilizing the knockout approach to study chlamydial sRNAs.

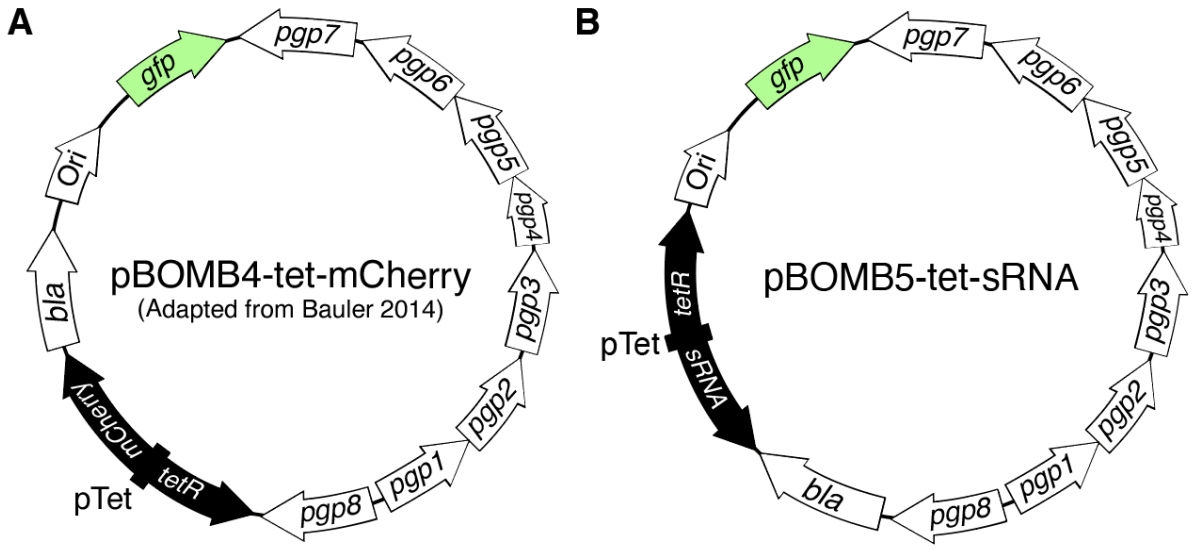

Figure 4. Plasmid map of pBOMB5-tet-sRNA.
The sRNA expression cassette was moved to prevent potential transcriptional read-through into the *bla* gene. The IncG terminator was placed downstream of the *bla* gene to prevent read-through into the sRNA expression cassette.

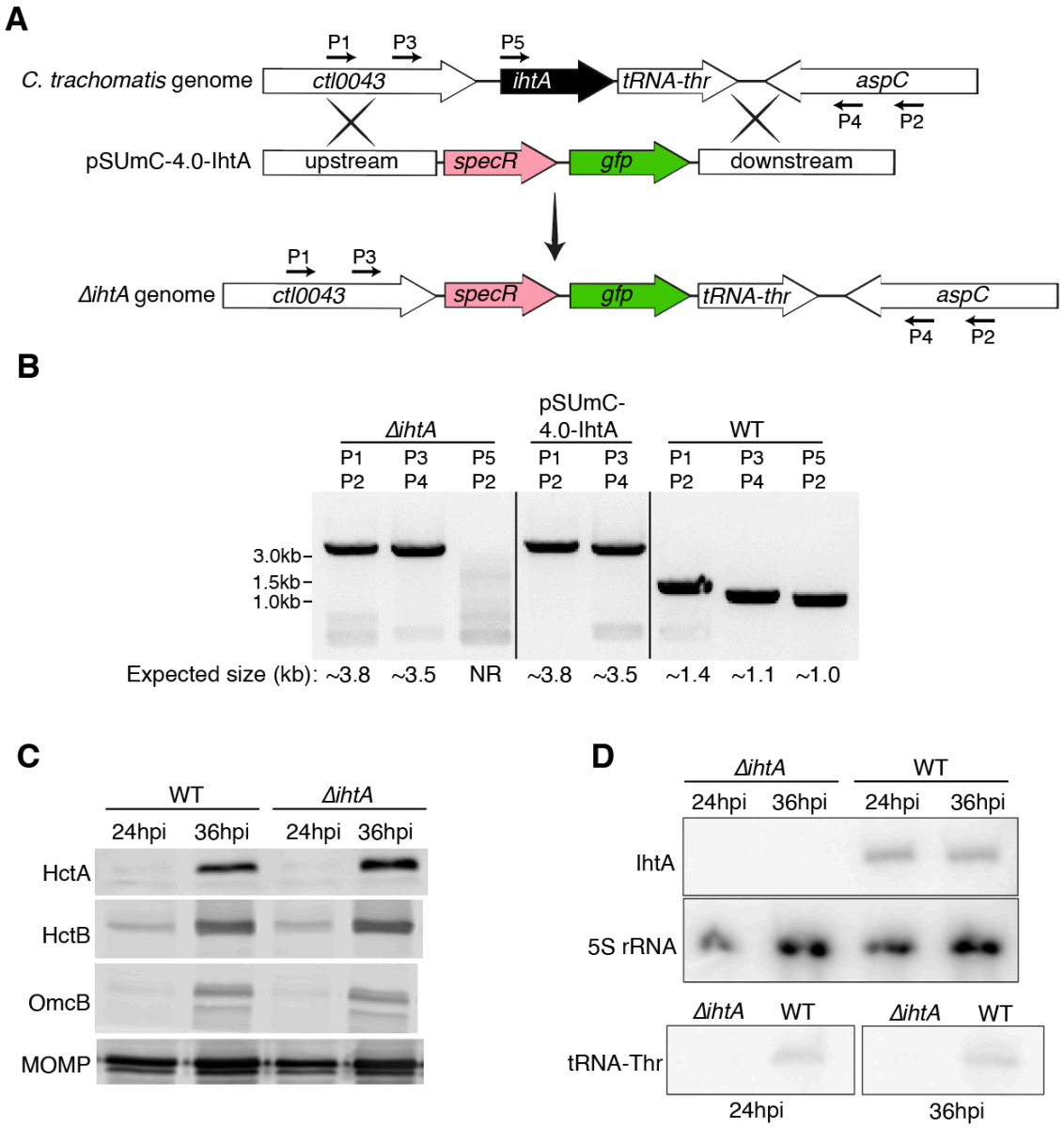
A
C. trachomatis genome
ctl0043
ihtA
tRNA-thr
aspC
P1
P3
P5
P4
P2
pSUmC-4.0-IhtA
upstream
specR
gfp
downstream
ΔihtA genome
B
ΔihtA
pSUmC-4.0-IhtA
WT
3.0kb
1.5kb
1.0kb
Expected size (kb): ~3.8 ~3.5 NR ~3.8 ~3.5 ~1.4 ~1.1 ~1.0
C
WT
ΔihtA
24hpi
36hpi
HctA
HctB
OmcB
MOMP
D
ΔihtA
WT
IhtA
5S rRNA
tRNA-Thr
24hpi
36hpi
E
53,000
53,500
54,000
(Gene)
Gene annotations (936)
IhtA
tRNA-Thr
25523
24_sig66_READ1
(Reads)
GCA_000068585.1
(Genome)
1,038,842bp

Figure 5. Knockout of IhtA results in polar effects on tRNA-Thr.
(A) Schematics of deleting *ihtA* through fluorescence-reported allelic exchange mutagenesis (FRAEM) (Mueller et al., 2016). *SpecR* encodes a spectinomycin resistance gene. Arrows mark the primers that were used to confirm *ihtA* gene deletion.
(B) Genomic DNA from *ihtA* mutant or wildtype *C. trachomatis* and the knockout vector (pSUmC-4.0-IhtA) were PCR amplified with the indicated primer sets.
(C) HeLa cells infected for 24 or 36 hours with *ihtA* mutant or WT *C. trachomatis* were lysed and subjected to western blotting analysis with antibodies to HctA, HctB, and OmcB. MOMP served as loading controls for *Chlamydia*.
(D) Northern blot of RNA extracted from HeLa cells infected with *ihtA* mutant or WT *C. trachomatis* at 24 and 36 hpi. IhtA and tRNA-thr levels are shown and 5S rRNA served as a loading control.
(E) HeLa cells infected with WT *C. trachomatis* were lysed and subjected to σ^{66}-ChIP analysis. Peak indicates the binding site of σ^{66} in the *Chlamydia* genome. σ^{66}-ChIP experiment was conducted by Dr. Syed Rizvi.

2.2 A reverse genetic screen identifies sRNAs that are involved in a productive chlamydial infection

We next used this sRNA overexpression system to screen putative *C. trachomatis* sRNAs for a potential role in the developmental cycle. We focused on 16 sRNAs that have been previously confirmed by northern blot analysis and whose transcription start sites have been mapped (Table 2) (AbdelRahman et al., 2011; Albrecht et al., 2010). Each sRNA was cloned into pBOMB5, and 14 of 16 were successfully transformed into *C. trachomatis*. Using this panel of transformants and the IhtA transformant, we induced the overexpression of individual sRNAs and measured effects on the production of infectious EBs with a progeny assay, which is performed with a secondary infection (Fig 6A).

Overexpression of six sRNAs caused measurable reductions in progeny production (Fig. 6B). The greatest defects were seen with overexpression of CtrR3, CtrR7, CtrR0332 (Fig. 7A-C), and CTIG648. CtrR3 overexpression decreased progeny by 68-fold at 32 hpi, compared to its uninduced control, and the severity of the defect was proportional to the aTc concentration used for induction (Fig. 8). Overexpression of CtrR7 and CTIG648 resulted in a 38-fold and 36-fold decrease in progeny at 32 hpi, respectively. The most drastic effect on progeny was seen with CtrR0332 overexpression, which resulted in a 132-fold decrease in progeny. In comparison, IhtA and CTIG270 transformants showed only a 2.8-fold and 7.7-fold reduction in progeny, respectively (Fig. 6B). Induction of the nine other sRNAs did not affect progeny, and of these, we verified overexpression for CtrR1 and CtrR4 by northern blot analysis (Figs.

7D). These results demonstrate that CtrR3, CtrR7, CtrR0332, CTIG648, CTIG270 and IhtA have important functions in the developmental cycle.

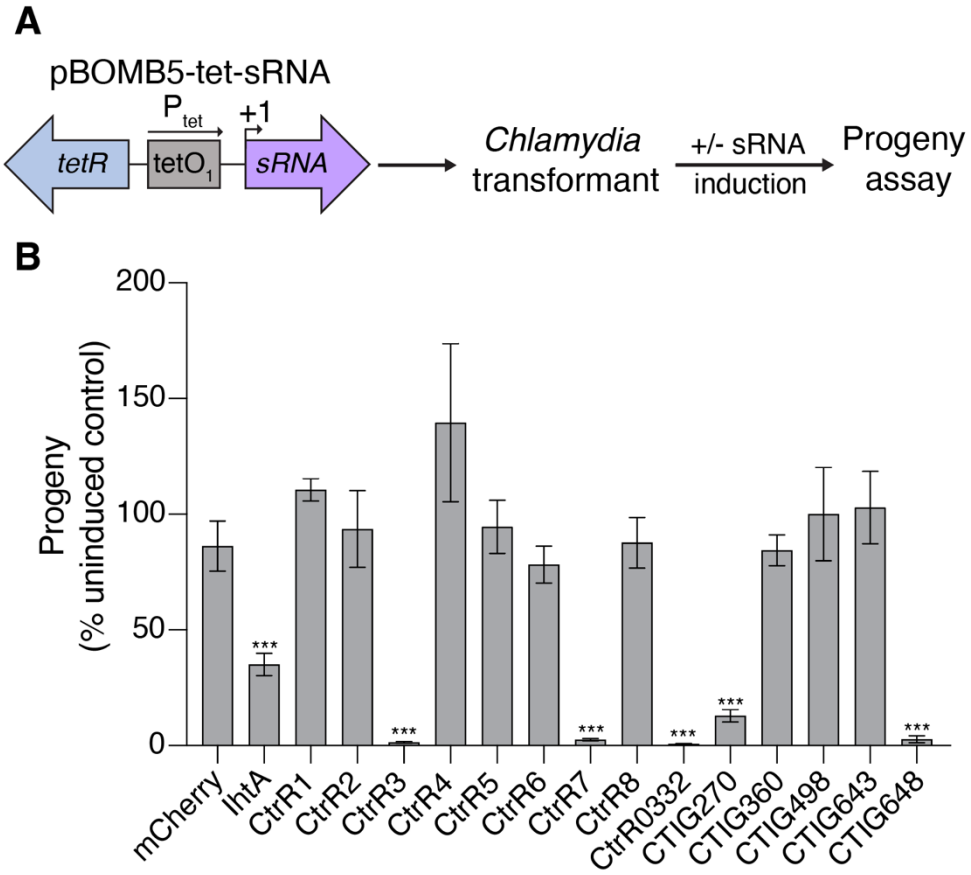

Figure 6. A screen to identify *C. trachomatis* sRNAs important for the *Chlamydia* developmental cycle.
(A) Schematic of the sRNA overexpression screen.
(B) For each transformant, the number of infectious EBs of induced samples is expressed as a percentage of the uninduced control samples. HeLa cells infected with transformants expressing mCherry or a sRNA were incubated in the absence or presence of 50 ng/mL aTc starting at 1 hpi. Lysates were collected at 32 hpi and analyzed for infectious progeny production in a secondary infection. Data are presented as mean ± SEM (n= 3), ****P*<0.001.

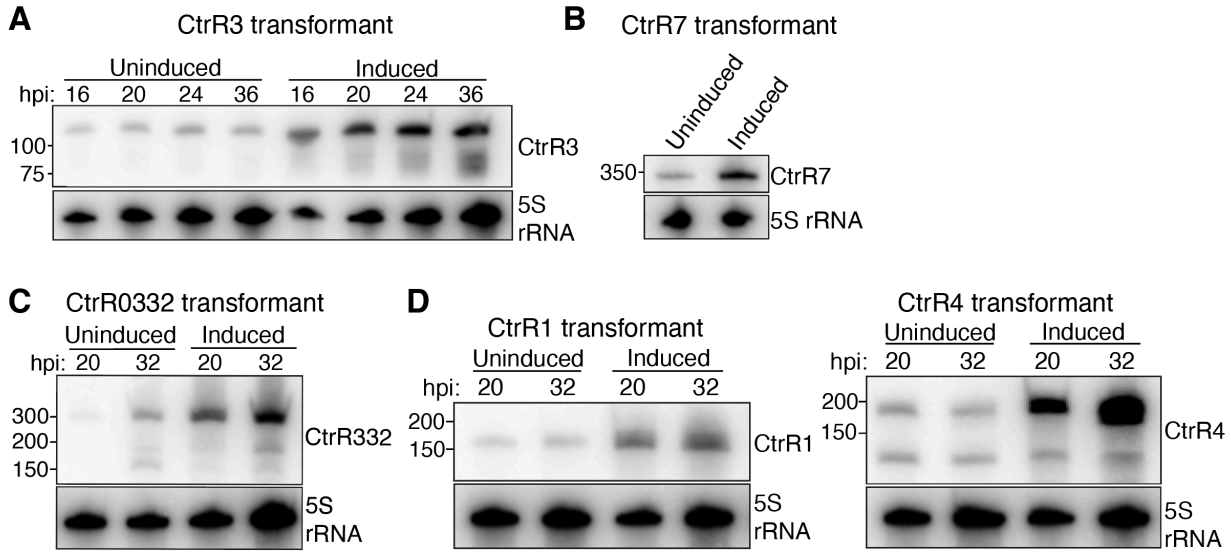

Figure 7. Overexpression of CtrR3, CtrR7, CtrR0332, CtrR1, and CtrR4. Northern blots of Hela cells infected with (A) CtrR3, (B) CtrR7, (C) CtrR0332, and (D) CtrR1 or CtrR4 transformants. CtrR3, CtrR0332, CtrR1, and CtrR4 transformants were induced at 1 hpi and analyzed at the indicated time points. CtrR7 transformant was induced at 16 hpi and analyzed at 32 hpi because CtrR7 overexpression from 1 hpi strongly impacted bacterial growth. CtrR3, CtrR7, CtrR0332, CtrR1 and CtrR4 levels are shown; and 5S rRNA served as a loading control.

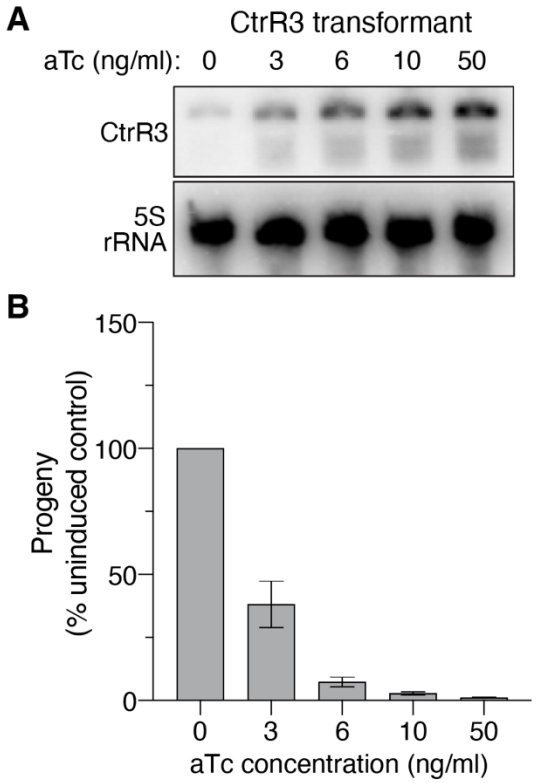

Figure 8. CtrR3 overexpression affects progeny in a dose-dependent manner.
(A) Northern blot analysis of total RNA extracted from HeLa cells that were infected with CtrR3 transformants and that were incubated with different amount of aTc from 1-32 hpi. Level of CtrR3 is shown; 5S rRNA served as loading control.
(B) Infectious EBs from samples in the same conditions as (A) were harvested at 32 hpi and quantified by progeny assay. The number of infectious EBs in the induced conditions is expressed as a percentage of the number of EBs in uninduced control samples. Data are presented as mean ± SEM (n= 3).

A

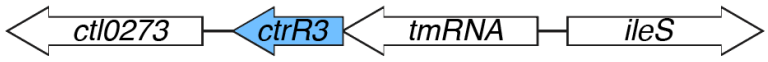
ctl0273
ctrR3
tmRNA
ileS

B

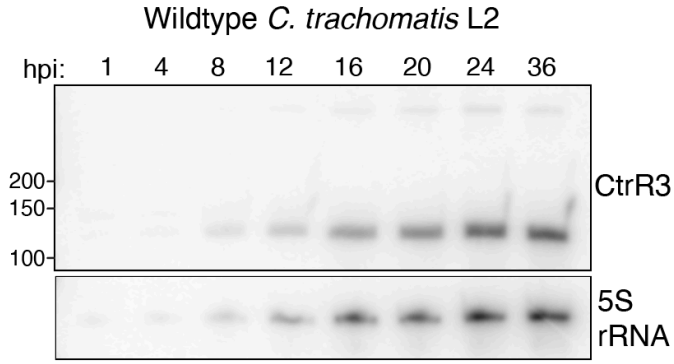
Wildtype C. trachomatis L2
hpi: 1 4 8 12 16 20 24 36
200
150
100
CtrR3
5S
rRNA

C

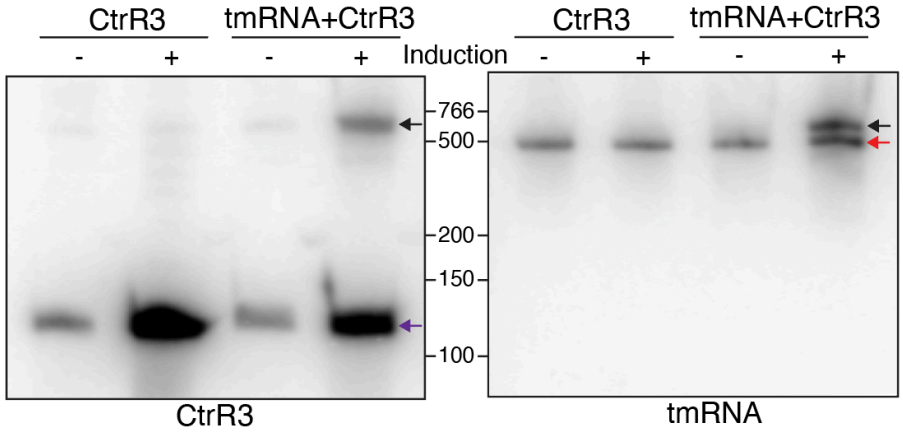
CtrR3
tmRNA+CtrR3
CtrR3
tmRNA+CtrR3
Induction
- + - + - + - +
766
500
200
150
100
CtrR3
tmRNA

D

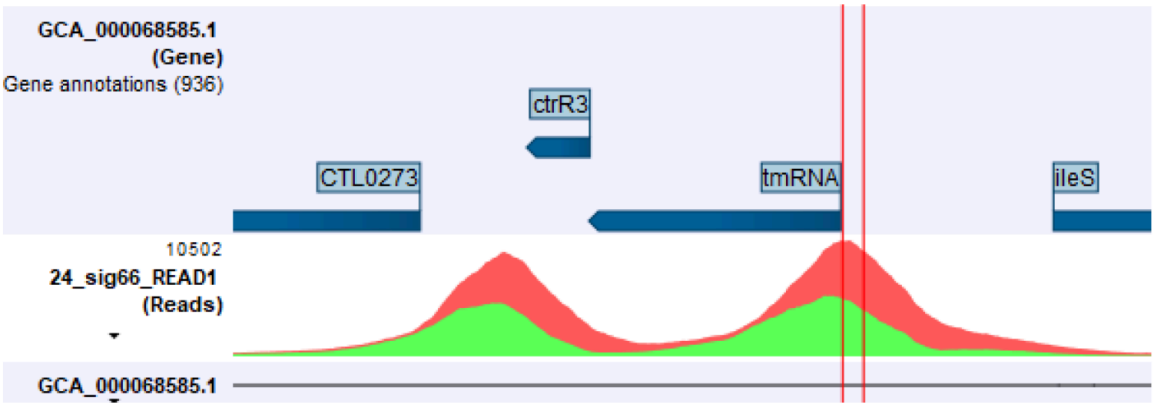
GCA_000068585.1
(Gene)
Gene annotations (936)
ctrR3
CTL0273
tmRNA
ileS
10502
24_sig66_READ1
(Reads)
GCA_000068585.1

Figure 9. CtrR3 is processed from pre-tmRNA.
(A) The position of the *ctrR3* gene in the *C. trachomatis* serovar L2 genome is shown.
(B) Total RNA isolated from HeLa cells that were infected with wildtype *C. trachomatis* serovar L2 was analyzed by northern blotting at the indicated times. Blots were probed for CtrR3 and 5S rRNA as loading control.
(C) HeLa cells were infected with the CtrR3 transformant or the tmRNA+CtrR3 transformant and were incubated with or without aTc at 1 hpi. Total RNA isolated from the infected cells was analyzed by northern blotting at 24 hpi. Blots were probed with CtrR3 and tmRNA oligonucleotides. Black arrows: tmRNA+CtrR3; red arrow: tmRNA; purple arrow: CtrR3.
(D) HeLa cells infected with WT *C. trachomatis* were lysed and subjected to σ^{66}-ChIP analysis. Peaks indicate the binding site of σ^{66} in the *Chlamydia* genome. σ^{66}-ChIP experiment was conducted by Dr. Syed Rizvi.

2.3 Characterization of CtrR3 overexpression effects on the developmental cycle

As CtrR3 overexpression caused a large defect in progeny production, we performed additional experiments to characterize this sRNA. CtrR3 is a *trans*-encoded sRNA located downstream of the tmRNA (Fig. 9A) and its endogenous expression was detected throughout the developmental cycle (Fig. 9B). Overexpression of the transcript containing both CtrR3 and tmRNA in *Chlamydia* showed increased levels of both RNAs under aTc induction via northern blot analysis (Fig. 9C). In addition, σ^{66}-ChIP showed a single binding site upstream of the *tmRNA* gene, suggesting that CtrR3 and tmRNA share the same promoter (Fig. 9D). These results indicate that CtrR3 and tmRNA are processed from the same transcript.

We next identified the stage in the developmental cycle that was disrupted by CtrR3 overexpression. CtrR3 overexpression only had a modest effect on RB replication, as shown by 1.9-fold and 1.6-fold decreases in genome copy number at 24 hpi and 36 hpi, respectively, compared to uninduced controls (Fig. 10A). In contrast, there was a 24-fold and 104-fold reduction in progeny at 24 and 36 hpi, respectively (Fig. 10B), and thus a disproportionate effect on EB production compared to RB replication (Fig. 10C). Progeny counts did not recover at later times, which indicates that this defect could not be attributed to a delay in EB production (48 and 60 hpi, Fig. 10D). This progeny defect was dependent on the timing of CtrR3 induction, as CtrR3 overexpression at 20 hpi or later did not affect progeny production (Fig. 10E)

We confirmed the defect in EB production with additional assays. Western blot analysis at 36 hpi showed that CtrR3 overexpression decreased expression of the EB-specific proteins HctB and OmcB, but not of MOMP, which is present in RBs and EBs

(Fig. 10F). Transmission electron microscopy at 36 hpi showed that CtrR3 overexpression produced inclusions full of RBs and dividing RBs, with very few EBs and intermediate bodies (IBs), which are RBs in the process of converting into EBs (Fig. 10G). This distribution of chlamydial developmental forms was strikingly different from uninduced control cells at this late time, which had predominantly EBs, with few RBs and IBs, similar to a wildtype infection (J. K. Lee et al., 2018). In addition, the RBs in the CtrR3 overexpressing condition appeared larger than the ones in control (Fig. 10H). These results show that the large progeny defect caused by CtrR3 overexpression was mainly due to a block in RB-to-EB conversion.

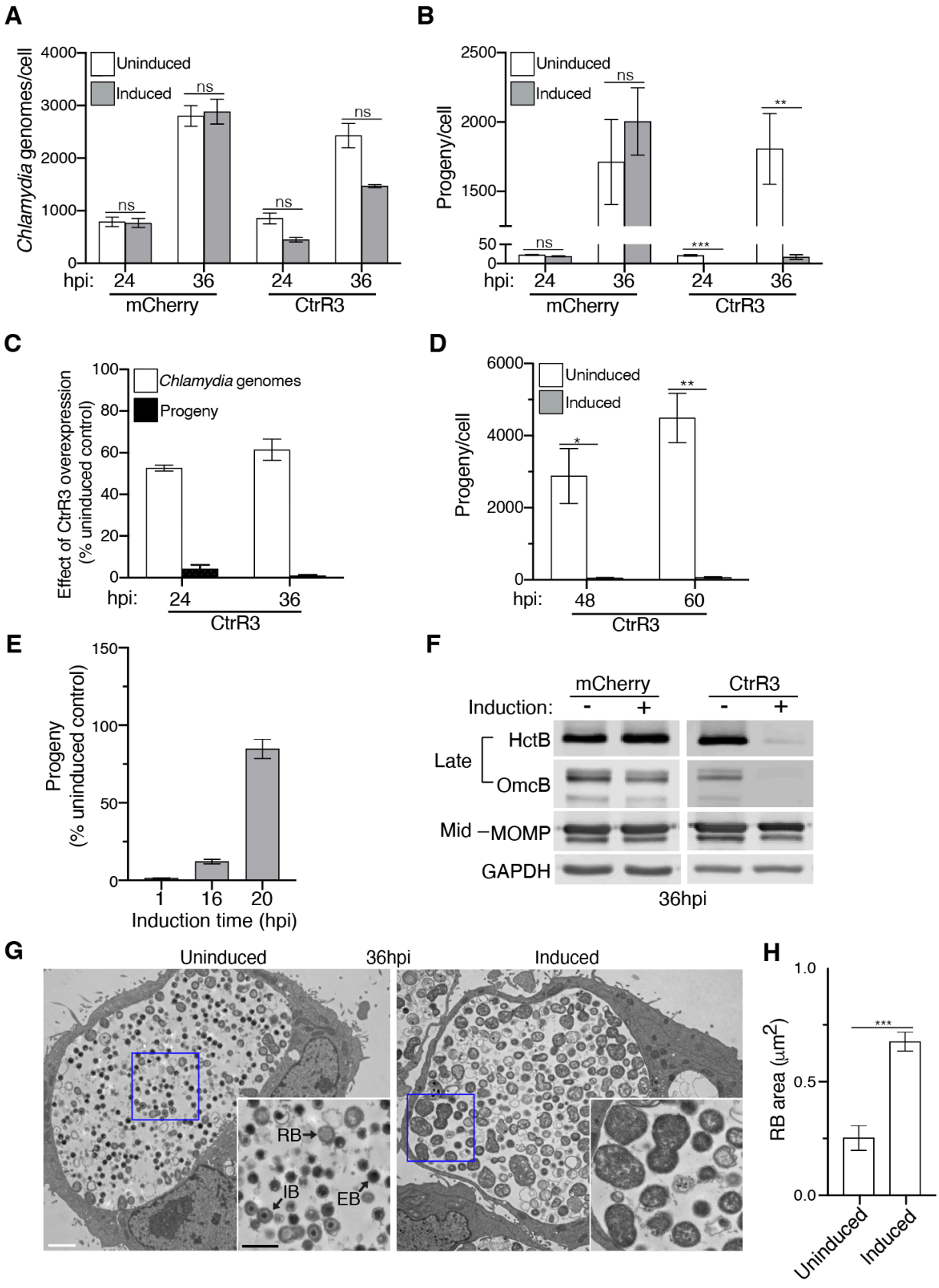
A
Chlamydia genomes/cell
Uninduced
Induced
ns
hpi: 24 36 24 36
mCherry
CtrR3
B
Progeny/cell
Uninduced
Induced
ns
**
***
hpi: 24 36 24 36
mCherry
CtrR3
C
Effect of CtrR3 overexpression (% uninduced control)
Chlamydia genomes
Progeny
hpi: 24 36
CtrR3
D
Progeny/cell
Uninduced
Induced
*
**
hpi: 48 60
CtrR3
E
Progeny (% uninduced control)
Induction time (hpi)
F
mCherry
CtrR3
Induction: - + - +
Late
HctB
OmcB
Mid
MOMP
GAPDH
36hpi
G
Uninduced
36hpi
Induced
RB
IB
EB
H
RB area (μm2)
***
Uninduced
Induced

Figure 10. CtrR3 overexpression resulted in an RB-to-EB conversion.
(A) The number of chlamydial genomes and (B) infectious EBs produced in HeLa cells infected either with the mCherry or the CtrR3 transformant were determined by qPCR and progeny assay, respectively, at the indicated time points and normalized to the number of host cells. mCherry or CtrR3 overexpression was induced as described in Fig 6B. Data are mean ± SEM (n= 3); ** $P \leq 0.01$ and *** $P < 0.001$.
(C) The numbers of chlamydial genomes and infectious EBs in CtrR3 overexpression samples are expressed as a percentage of their respective uninduced control to represent the relative effect of CtrR3 overexpression.
(D) The number of infectious EBs per cell was determined at the indicated time points in HeLa cells infected with the CtrR3 transformant that was incubated with aTc at 1 hpi. Data are mean ± SEM (n= 3); * $P \leq 0.5$, ** $P \leq 0.01$.
(E) HeLa cells were infected with the CtrR3 transformant and incubated with aTc at the 1, 16, 20 hpi. For each condition, the number of infectious EBs was determined at 32 hpi, normalized to the uninduced control and expressed as a percentage. Data are mean ± SEM (n= 3).
(F) Western blot analysis of lysates from Hela cells infected with the mCherry or CtrR3 transformants treated with aTc from 1-36 hpi. The levels of HctB and OmcB (late gene products) MOMP (mid gene product) are shown. GAPDH served as a loading control.
(G) Electron micrographs of CtrR3 transformant-infected HeLa cells at 36 hpi, in the absence or presence of aTc starting at 1 hpi. The chlamydial developmental forms are as indicated: RB, reticulate body; IB, intermediate body; and EB, elementary body. White scale bar: 2 μm, black scale bar: 1 μm.
(H) Area of 30 RBs was determined by ImageJ from EM images of inclusions of CtrR3 transformants that were either left uninduced or induced with aTc from 1-36 hpi. Data are mean ± SEM (n= 3 inclusions); *** $P < 0.001$.

2.4 Characterization of CtrR7 overexpression effects on the developmental cycle

CtrR7 is a *trans*-encoded sRNA that is located in the intergenic region between the *oppA4* and *ctl0742* genes (Fig. 11A). Its endogenous expression peaks between 20 and 24 hpi and decreases at 36 hpi (Fig. 11B). In contrast to CtrR3, overexpression of CtrR7 had a strong effect on RB replication as shown by a 9.3-fold and 21-fold decrease in genome copy at 24 and 36 hpi, respectively (Fig. 11C). CtrR7 overexpression caused a 14-fold and 47-fold decrease in progeny at 24 and 36 hpi (Fig. 11D), and thus, its deleterious effect on RB replication and EB production were proportional (Fig. 11E). This progeny defect caused by CtrR7 overexpression was not observed when the induction started at 20 hpi (Fig. 11F). Western blot analysis further demonstrated that CtrR7 overexpression affected the expression of both late (HctB and OmcB) and midcycle gene products (MOMP) (Fig. 11G). In addition, transmission electron microscopy at 36 hpi showed that CtrR7 overexpression resulted in an inclusion that was mostly empty except for a few RBs. In addition, some of these RBs appeared to be lysed within the inclusion (Fig. 11H). Lastly, CtrR7 overexpression did not cause the formation of multiple inclusions within a host cell (data not shown), which suggests that the inclusion membrane protein, IncA, involved in inclusion fusion is expressed (Weber et al., 2015). Because IncA is expressed and secreted exclusively by RBs, this provided additional evidence that the few chlamydiae we observed in EM are RBs. Taken together, these results suggest that the severe reduction in progeny caused by CtrR7 overexpression is mainly due to an RB replication defect.

Upon inspecting CtrR7 nucleotide sequences, we suspected that this sRNA may encode for a 53 amino acid small protein, which is conserved in *C. suis* and *C.*

muridarum (Fig 12A, B). To test this hypothesis, we inserted a 3xFlag tag at the C-terminus of the predicted ORF in the CtrR7 sequence and overexpressed this version of CtrR7, called CtrR7-Flag, in *C. trachomatis* (Fig 12A). Western blot analysis showed an overexpression of a 15kD protein, which is larger than the predicted size of 8.6 kD (Fig 12C). Immunofluorescence analysis demonstrated that the small protein may localized to the bacterial membrane, as it co-localized with a membrane protein (MOMP), in a ring-like structure (Fig 12D). Although the CtrR7 small protein is not bioinformatically predicted to have a transmembrane domain, it is predicted to have a Sec targeting signal peptide (Fig 12E).

To test if the small protein is necessary for the progeny defect caused by CtrR7 overexpression, we disrupted the ORF by introducing a nucleotide deletion that resulted in the formation of a premature stop codon and we called this sRNA CtrR7^{mut} (Fig. 13A). Predicted secondary structures of CtrR7^{mut} by RNAfold showed that the RNA secondary structure is similar to the predicted structure of the wildtype CtrR7 (Fig. 13A). Interestingly, overexpression of CtrR7^{mut} no longer caused a defect on progeny at 32 hpi (Fig. 13B), suggesting that the small protein is required for the deleterious effect of CtrR7 overexpression on the *C. trachomatis* developmental cycle.

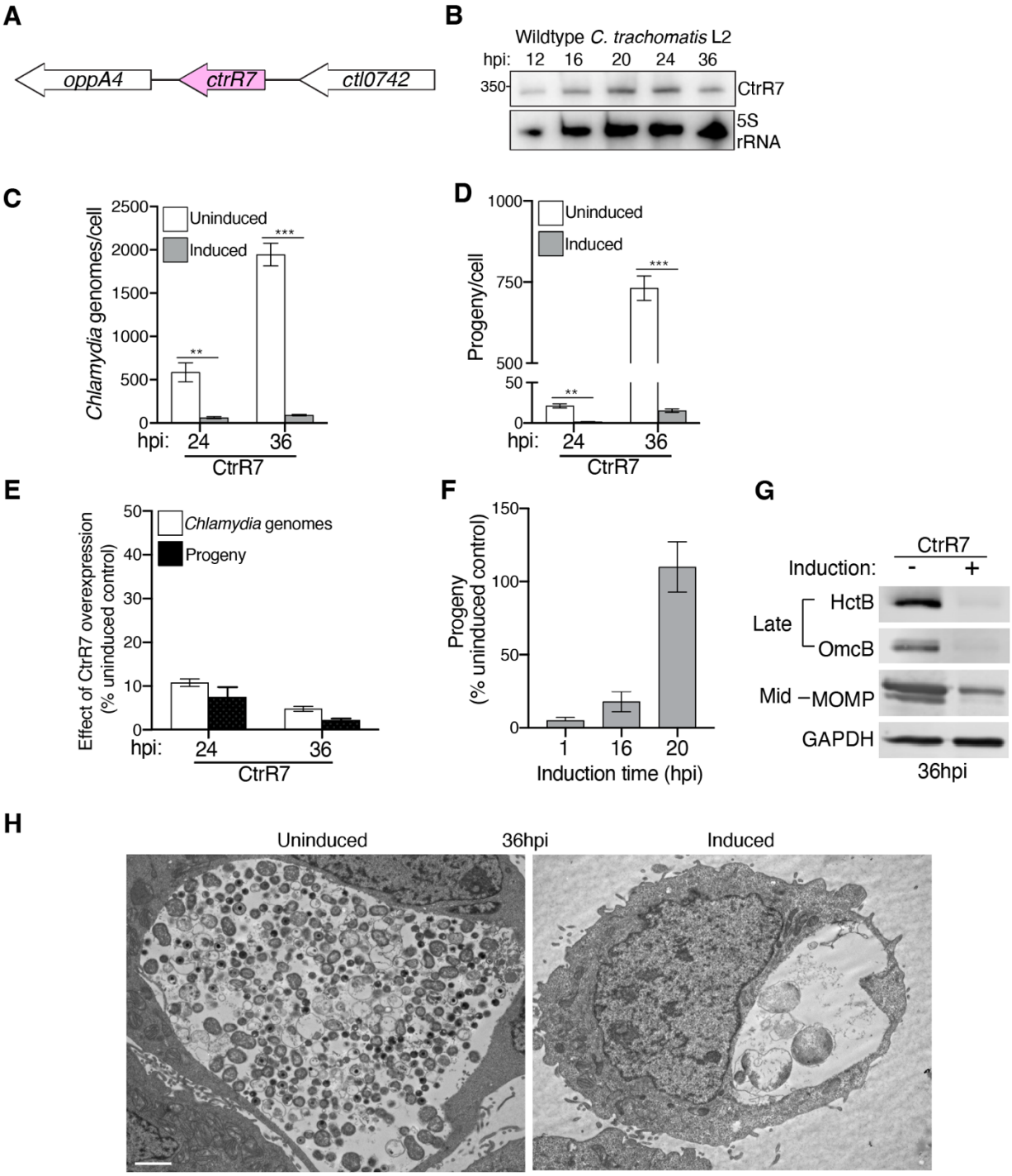

Figure 11. CtrR7 overexpression resulted in RB replication defect.
(A) The position of the *ctrR7* gene in the *C. trachomatis* serovar L2 genome is shown. (B) Total RNA extracted from HeLa cells that were infected with wildtype *C. trachomatis* serovar L2 was analyzed by northern blotting at the indicated times. Blots were probed for CtrR7 and 5S rRNA as loading control.

(C) The number of chlamydial genomes and (D) infectious EBs produced in HeLa cells infected with the CtrR7 transformant were determined by qPCR and progeny assay, respectively, at the indicated time points and normalized to the number of host cells. CtrR7 overexpression was induced as described in Fig 6B. Data are mean ± SEM (n= 3); $^{**}P \leq 0.01$ and $^{***}P < 0.001$.
(E) The numbers of chlamydial genomes and infectious EBs in CtrR7 overexpression samples are expressed as a percentage of their respective uninduced control to represent the relative effect of CtrR7 overexpression.
(F) HeLa cells were infected with the CtrR7 transformant and incubated with aTc at the 1, 16, 20 hpi. For each condition, the number of infectious EBs was determined at 32 hpi, normalized to the uninduced control and expressed as a percentage. Data are mean ± SEM (n= 3).
(G) Western blot analysis of lysates from HeLa cells infected with the CtrR7 transformants treated with aTc from 1-36 hpi. The levels of HctB and OmcB (late gene products) MOMP (mid gene product) are shown. GAPDH served as a loading control.
(H) Electron micrographs of CtrR7 transformant-infected HeLa cells at 36 hpi, in the absence or presence of aTc starting at 1 hpi. White scale bar: 2 μm.

A

CtrR7 nucleotide sequence

```
  1 gagcttacacagcttagatccgcttctattcttttctatagcatttttttcgaggagagaaag  63
 64 taagaagttcggattattcgtgaaatctacctattaaaaggagacgccaatgaaaaaattact 126
127 tttactcgcaatgttaacttctgctgccgctgctggttccgtttacgctgatgagactgaaga 189
190 agaaaaagaagtttcttctttagttgtttccctagcttgcgaaggggaagaaggtggagaaga 252
253 aactagagatcctattcgatagttttttctaaaagagagttgaattttcaactctctttttttt 317
```

Predicted RBS / Predicted ORF

3xFlag tag
(CtrR7-Flag)

B

```
C. trachomatis MKKLLLLAMLTSAAAAGSVYADETEEEKEVSSLVVSLACEGEEGGEETRDPIR*
      C. suis MKKLLLLALVLSSCA---LHAGDTEEEKNTDSFVTSLCCGGEEEGPKDGE*
C. muridarum MKKLLLLALLASSCS---VYAGDKEEEK-SDSLVAAFCCEGEETSQETKGE*
             ********   *       *   ****   * *    * ***
```

C

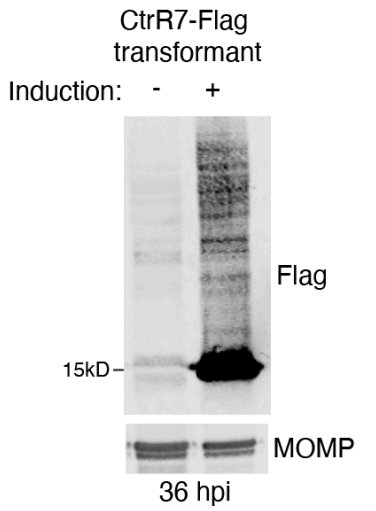

D

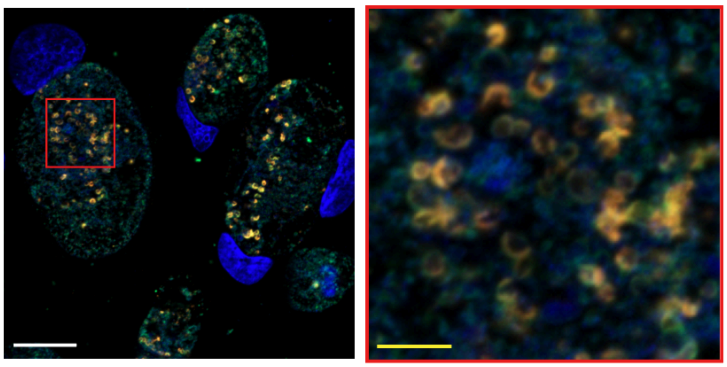

Induced / 36 hpi / Flag / MOMP / DNA

E

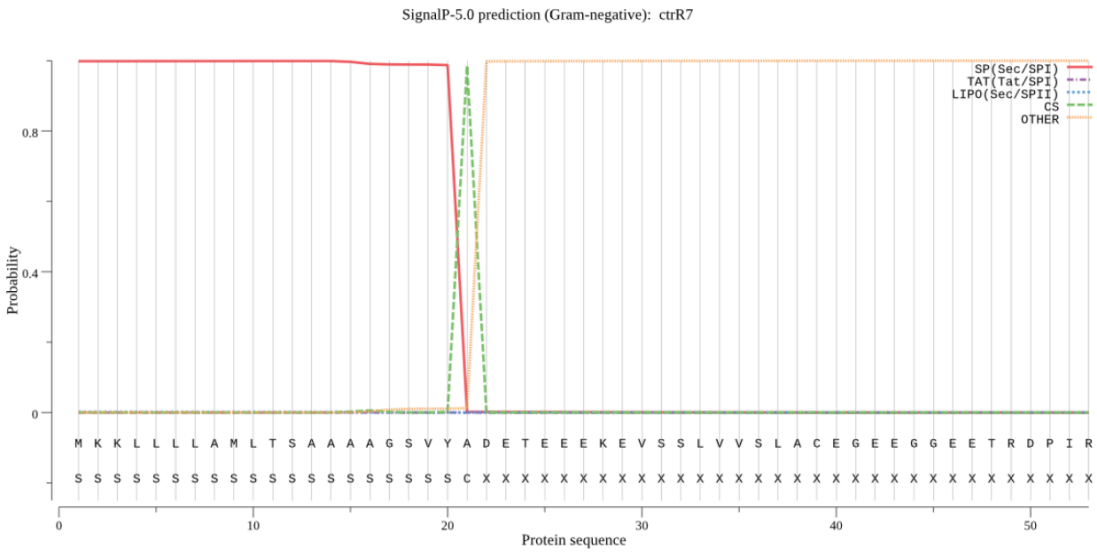

Figure 12. CtrR7 encodes a small membrane protein.
(A) Nucleotide sequence of CtrR7 in *Chlamydia trachomatis* serovar L2 is shown. The predicted ORF is highlighted in purple and the predicted RBS is marked in red. The arrow indicates the position where 3xFlag was inserted.
(B) Amino acid sequences of the predicted CtrR7 small protein in *Chlamydia trachomatis* serovar L2, *Chlamydia suis*, and *Chlamydia muridarum* are shown. Blue asterisks indicate the conserved amino acids.
(C) Western blot analysis of lysates from HeLa cells infected with the CtrR7-Flag transformants treated with or without aTc from 1-36 hpi. The blot was probed with Flag antibody and MOMP served as a loading control.
(D) Immunofluorescence image of HeLa cells infected with the CtrR7-Flag transformant and treated with aTc from 1-36 hpi is shown. CtrR7-Flag protein is visualized with Flag antibody (red), chlamydial membrane is visualized with MOMP antibody (green), and DNA is visualized by DAPI (blue). White scale bar: 20 μm. Yellow scale bar: 5 μm.
(E) Signal peptide prediction by SignalP-5.0. Green peak indicates the predicted cleavage site.

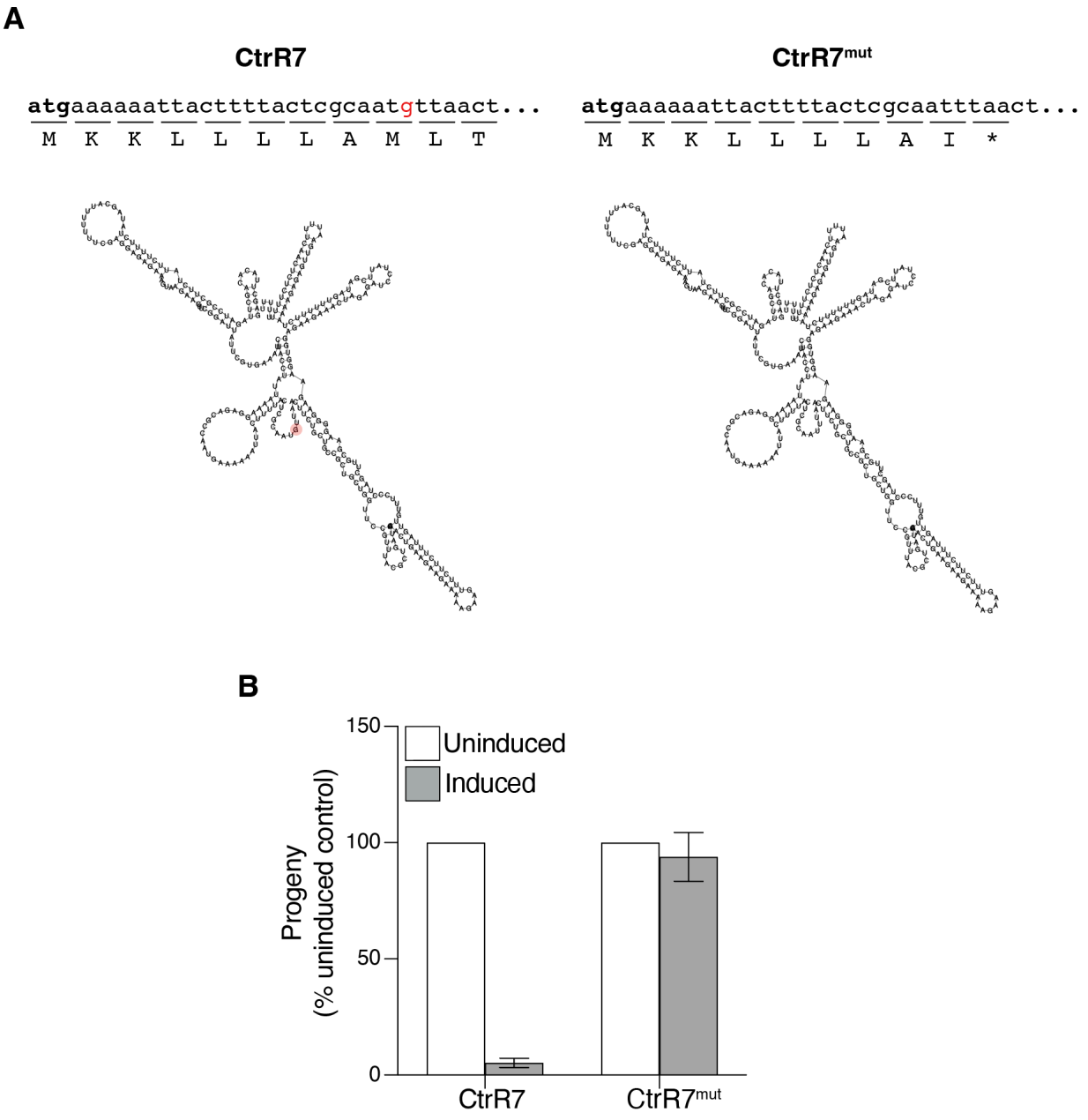

Figure 13. CtrR7 small protein is necessary for CtrR7 overexpression-induced progeny defect.
(A) Left: The wildtype CtrR7 protein codons and predicted secondary structure (RNAfold) are shown. The deleted nucleotide is indicated in red. Right: The mutated CtrR7 protein codons and predicted secondary structure are shown.
(B) Infectious EBs produced in HeLa cells infected with CtrR7 or CtrR7^{mut} transformants and were treated with aTc 1-32 hpi were determined using progeny assay. The numbers of infectious EBs in CtrR7 or CtrR7^{mut} overexpression samples are expressed as a percentage of their respective uninduced control to represent the relative effect of CtrR7 or CtrR7^{mut} overexpression. Data are mean ± SEM (n= 2).

2.5 Characterization of CtrR0332 overexpression effects on the developmental cycle

CtrR0332 is a *trans*-encoded sRNA that is located downstream of the late gene, *ltuB* (Fig. 14A). Northern blot analysis revealed that CtrR0332 is also expressed as a late gene (Fig. 14B). σ^{66}-ChIP study showed a single σ^{66}-dependent promoter upstream of *ltuB*, suggesting that the sRNA may be processed from the same transcript as *ltuB* (Fig 14C). Similar to CtrR3, overexpression of CtrR0332 had a modest effect on RB replication as shown by a 1.6-fold and 2.2-fold decrease in genome copy at 24 and 36 hpi compared to uninduced controls, respectively (Fig. 15A). CtrR0332 overexpression had 31.2-fold and 660-fold reduction in progeny at 24 and 36 hpi, respectively, and thus had a disproportionate effect on EB production compared to RB replication (Fig. 15B, C). Western blot analysis further demonstrated that CtrR0332 overexpression affected the expression of late (HctB and OmcB) and not the midcycle gene product (MOMP) (Fig. 15D). In addition, the effect on late gene expression and progeny was still observed when CtrR0332 overexpression was induced at 24 hpi (Fig. 15D, E). Lastly, transmission electron microscopy at 36 hpi showed that CtrR0332 overexpression resulted in an inclusion that contained only RBs that were larger than those observed in the uninduced control (Fig. 15F). The RBs also had small round fragments that were adjacent to the bacteria. These results suggest that CtrR0332 overexpression caused minimal RB defect and mostly an RB-to-EB conversion defect.

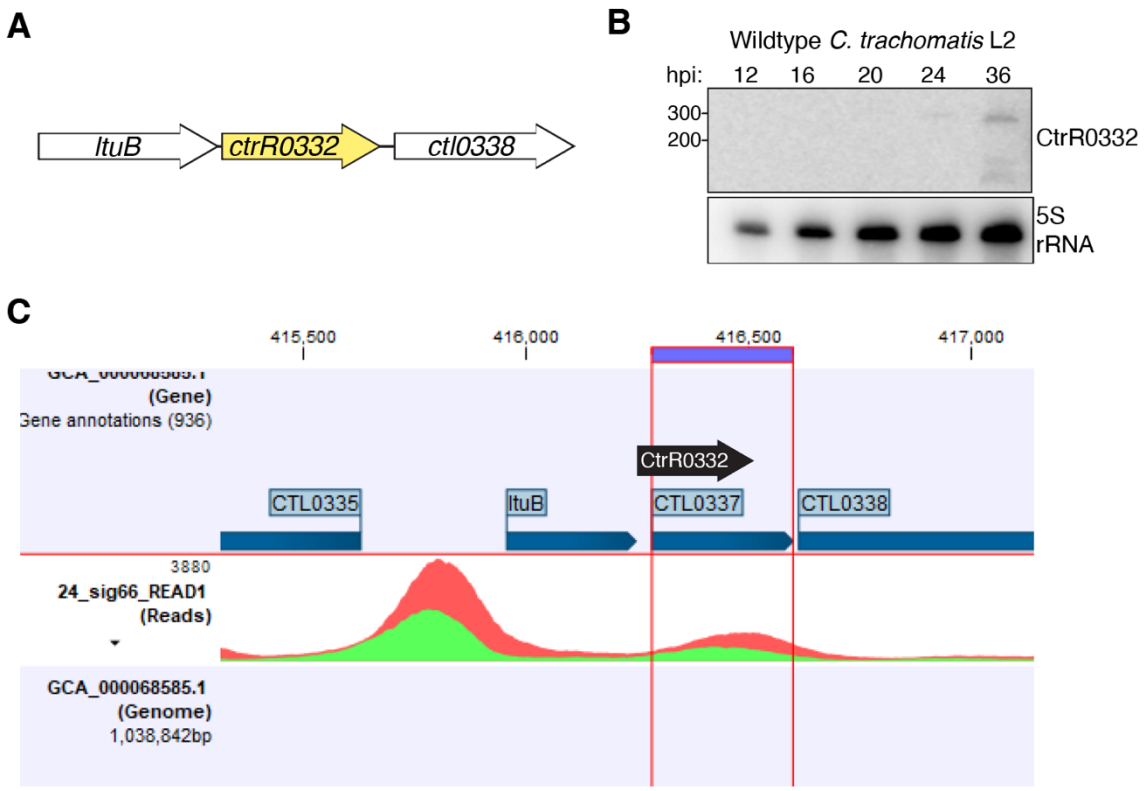

Figure 14. CtrR0332 is expressed as a late gene.
(A) The position of the *ctr0332* gene in the *C. trachomatis* serovar L2 genome is shown. (B) Total RNA extracted from HeLa cells that were infected with wildtype *C. trachomatis* serovar L2 was analyzed by northern blotting at the indicated times. Blots were probed for CtrR0332 and 5S rRNA as loading control.
(C) HeLa cells infected with WT *C. trachomatis* were lysed and subjected to σ^{66}-ChIP analysis at 24 hpi. Peaks indicate the binding site of σ^{66} in the *Chlamydia* genome. CTL0337 is a misannotated gene in the chlamydial genome. Position of CtrR0332 is shown in black arrow. σ^{66}-ChIP experiment was conducted by Dr. Syed Rizvi.

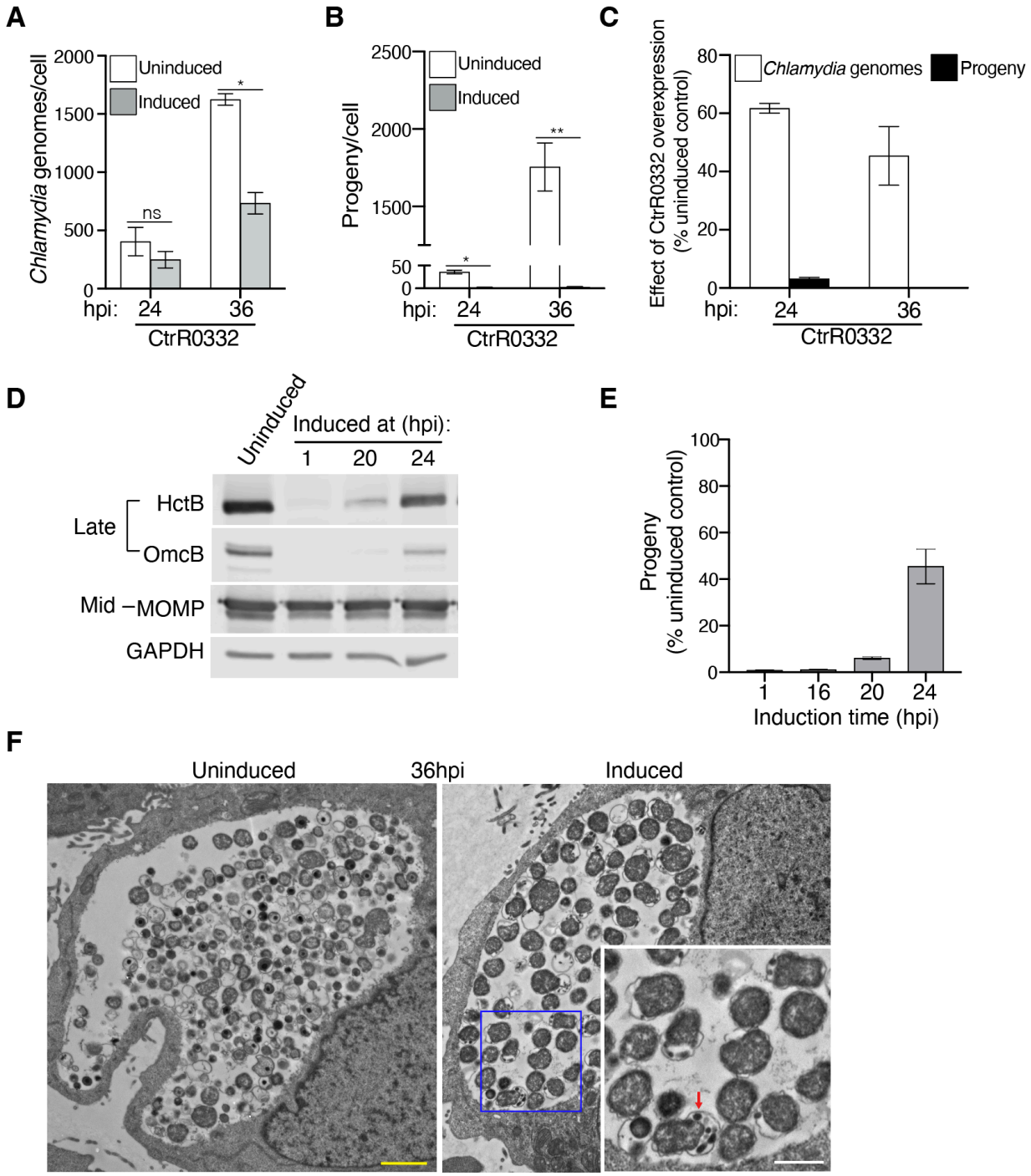

Figure 15. CtrR0332 overexpression resulted in an RB-to-EB conversion defect. (A) The number of chlamydial genomes and (B) infectious EBs produced in HeLa cells infected with the CtrR0332 transformant were determined by qPCR and progeny assay, respectively, at the indicated time points and normalized to the number of host cells. CtrR0332 overexpression was induced as described in Fig 6B. Data are mean ± SEM (n= 3); *$P \leq 0.05$ and **$P \leq 0.01$.

(C) The numbers of chlamydial genomes and infectious EBs in CtrR0332 overexpression samples are expressed as a percentage of their respective uninduced control to represent the relative effect of CtrR0332 overexpression.
(D) HeLa cells were infected with the CtrR0332 transformant and incubated with aTc at the 1, 16, 20, and 24 hpi. For each condition, lysates were collected at 36 hpi and were subjugated to Western blot analysis. The levels of HctB and OmcB (late gene products) MOMP (mid gene product) are shown. GAPDH served as a loading control.
(E) HeLa cells were infected with the CtrR0332 transformant and incubated with aTc at the 1, 16, 20, and 24 hpi. For each condition, the number of infectious EBs was determined at 32 hpi, normalized to the uninduced control and expressed as a percentage. Data are mean ± SEM (n= 3).
(F) Electron micrographs of HeLa cells infected with CtrR0332 transformants at 36 hpi, in the absence or presence of aTc starting at 1 hpi. Red arrow indicates small round fragments next to an RB. Yellow scale bar: 2 μm. White scale bar: 1 μm.

2.6 Identification of mRNA targets of CtrR3

For the remainder of this study, we used CtrR3 to develop a generalizable, multi-step approach to isolate and identify the mRNA targets of a sRNA in *Chlamydia*.

2.6a Identification of the target recognition sequence of CtrR3

To identify mRNA targets of CtrR3, we used a combined bioinformatic and mutational approach to identify the target recognition sequence, or seed region, of CtrR3. From the predicted secondary structure (RNAfold) (Lorenz et al., 2011) of CtrR3, we predicted its seed region to be in the large C-rich single-stranded hairpin loop, which has sequence complementarity to the ribosome binding site (RBS) sequence of bacterial mRNAs (Fig. 16A). In addition, the loop sequence is conserved from *C. suis* and *C. muridarum* (Fig. 16B).

To test if this sequence is important for CtrR3 function, we generated a transformant expressing CtrR3 with a C-to-U substitution at two positions in the potential anti-RBS sequence (CtrR3^{mut}) (Fig. 16A). We first tested if the two nucleotide substitutions affected the stability of CtrR3mut compared to CtrR3. To measure the stability of the sRNAs, we infected HeLa cells with either CtrR3^{mut} or CtrR3 transformants and first induced sRNA expression with aTc and then treated the cells with rifampicin, which halts prokaryotic transcription (Campbell et al., 2001; Ferreira et al., 2017). Northern blot analysis showed that CtrR3 and CtrR3^{mut} were both stable 60 minutes after rifampicin treatment (Fig 16C). In contrast, RT-qPCR analysis on the same samples showed that the EUO mRNA has a ½ life of ~17 minutes, demonstrating that the rifampicin treatment was effective (Fig 16D). These data suggest that the

mutations did not destabilize CtrR3^{mut}, as it still has comparable stability to CtrR3. We next demonstrated that overexpression of CtrR3^{mut} (Fig. 16E) no longer decreased progeny production (Fig. 16F), providing strong experimental evidence that this hairpin loop sequence is the seed region through which CtrR3 mediates its effects on EB production.

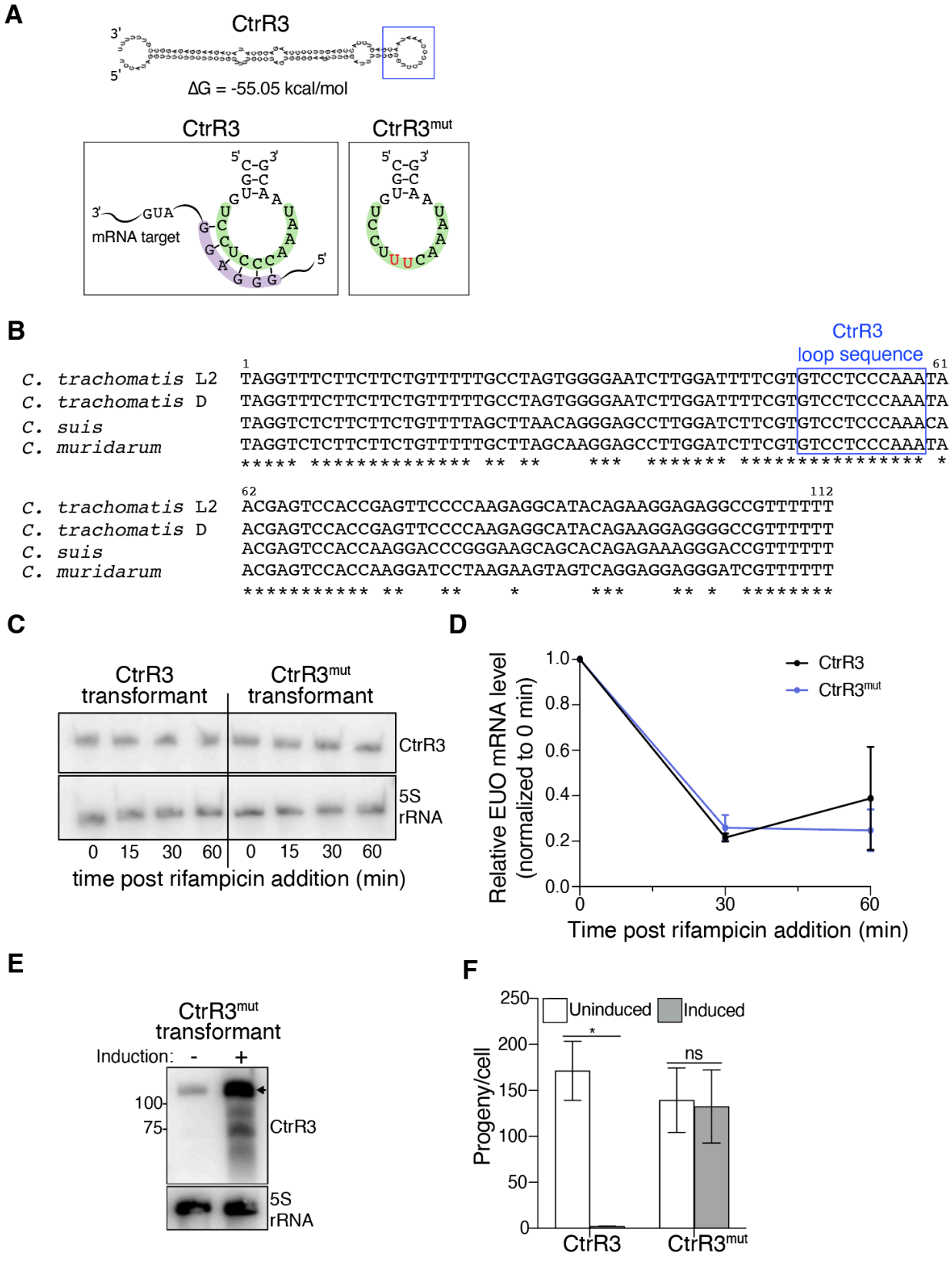
A
CtrR3
ΔG = -55.05 kcal/mol
CtrR3
CtrR3mut
mRNA target
B
CtrR3
loop sequence
C. trachomatis L2
C. trachomatis D
C. suis
C. muridarum
C
CtrR3
transformant
CtrR3mut
transformant
CtrR3
5S
rRNA
time post rifampicin addition (min)
D
Relative EUO mRNA level
(normalized to 0 min)
CtrR3
CtrR3mut
Time post rifampicin addition (min)
E
CtrR3mut
transformant
Induction:
CtrR3
5S
rRNA
F
Uninduced
Induced
Progeny/cell
ns
CtrR3
CtrR3mut

Figure 16. The C-rich hairpin sequence is necessary for CtrR3 function.
(A) The secondary structure of CtrR3 was predicted bioinformatically using the RNAfold software. The free energy of the thermodynamic ensemble is shown (∆G). The box on the left shows its C-rich hairpin sequence (highlighted in green) interacting with the RBS (highlighted in purple) of a putative mRNA target. The box on the right box shows the sequence for CtrR3^{mut} with two C-to-U substitutions.
(B) Sequences of CtrR3 in *Chlamydia trachomatis* serovar L2, serovar D, *Chlamydia suis*, and *Chlamydia muridarum* are shown. Asterisk indicates conserved sequences among the species. The blue box marks the sequences of the main loop in the CtrR3 predicted secondary structure.
(C) HeLa cells were infected with CtrR3 or CtrR3^{mut} transformants and were treated with 50 ng/mL of aTc first for 90 minutes followed by 10 µg/mL of rifampicin. Total RNA was extracted at 0, 15, 30, or 60 minutes post rifampicin treatment and subjugated to northern blot analysis. Blot was probed with an oligonucleotide that recognize by CtrR3 and CtrR3^{mut}. 5S rRNA served as loading control
(D) RT-qPCR of total RNA from (C) for the transcript level of EUO. 16S rRNA served as the reference gene and each sample was normalized to their respective 0 minute control. Data is presented as mean ± SEM (n= 2).
(E) Northern blot analysis of the CtrR3^{mut} transformant in the absence or presence of aTc from 1-32 hpi. CtrR3 and CtrR3^{mut} levels were detected by a probe that recognized both forms of the sRNA; 5S rRNA served as the loading control.
(F) The numbers of infectious EBs in Hela cells infected with either CtrR3 or CtrR3^{mut} transformants after treatment with aTc from 1 hpi were determined by progeny assay at 32 hpi and normalized to the number of host cells. Data are shown as mean ± SEM (n= 3); *$P \leq 0.05$.

2.6b MS2-affinity purification with RNA sequencing (MAPS)

To identify mRNAs that bind to CtrR3, we overexpressed CtrR3 tagged at the 5′ end with two MS2 hairpins (MS2-CtrR3). We used RNAfold (Lorenz et al., 2011) to check that these MS2 hairpins did not alter the predicted secondary structure of CtrR3 (Fig. 16A). We also constructed a control consisting of two MS2 hairpins followed by a rnpB T1 terminator (MS2-Control, Fig. 17A). MS2-CtrR3 and MS2-Control were individually cloned into pBOMB5 and successfully transformed into *C. trachomatis*. Using northern blot analysis, we confirmed that these tagged RNA constructs were detected and that the sRNA levels at 1 hour after aTc induction were comparable to sRNA levels at 2 or 6 hours after aTc induction (Fig. 17B).

We then performed MS2-affinity purification coupled with RNA sequencing (MAPS) on these transformants (Lalaouna et al., 2018; Lalaouna & Massé, 2015; Mercier et al., 2021). We infected HeLa cells with MS2-CtrR3 or MS2-Control transformants and induced MS2-sRNAs expression with aTc for one hour before lysing the cells at 30 hpi. We captured MS2-sRNAs and their interacting mRNAs using MS2-Maltose binding fusion proteins (MS2-MBP) that were bound to amylose resins. We verified that MS2-CtrR3 and MS2-Control were enriched in the eluted samples compared to the respective whole cell lysate (Fig. 17C), and analyzed the eluates by RNA-seq. We then performed a differential expression analysis to identify RNAs that were enriched in the MS2-CtrR3 library compared to the MS2-Control library. Using an enrichment cut-off of $\log_2$ fold change ≥ 2 (p-value ≤ 0.01), we identified 52 transcripts that were enriched in the MS2-CtrR3 library (Fig. 18).

2.6c Bioinformatic prioritization scheme

We performed a bioinformatics analysis to prioritize these CtrR3-interacting RNAs and to select likely mRNA targets of CtrR3. Using the program IntaRNA (Busch et al., 2008; Mann et al., 2017; Raden et al., 2018; Wright et al., 2014), which predicts sRNA-mRNA target base-pairing, we found that 34 of the 52 candidate mRNA targets showed sequence complementarity to the CtrR3 seed region (Table 3). We focused on four of these mRNAs, YtgB, CTL0389*,* CTL0015 and CTL0674, because they contained predicted CtrR3-interacting sequences located at their RBS, which is the site where sRNAs frequently bind to regulate protein expression (Fig. 18, Table 4).

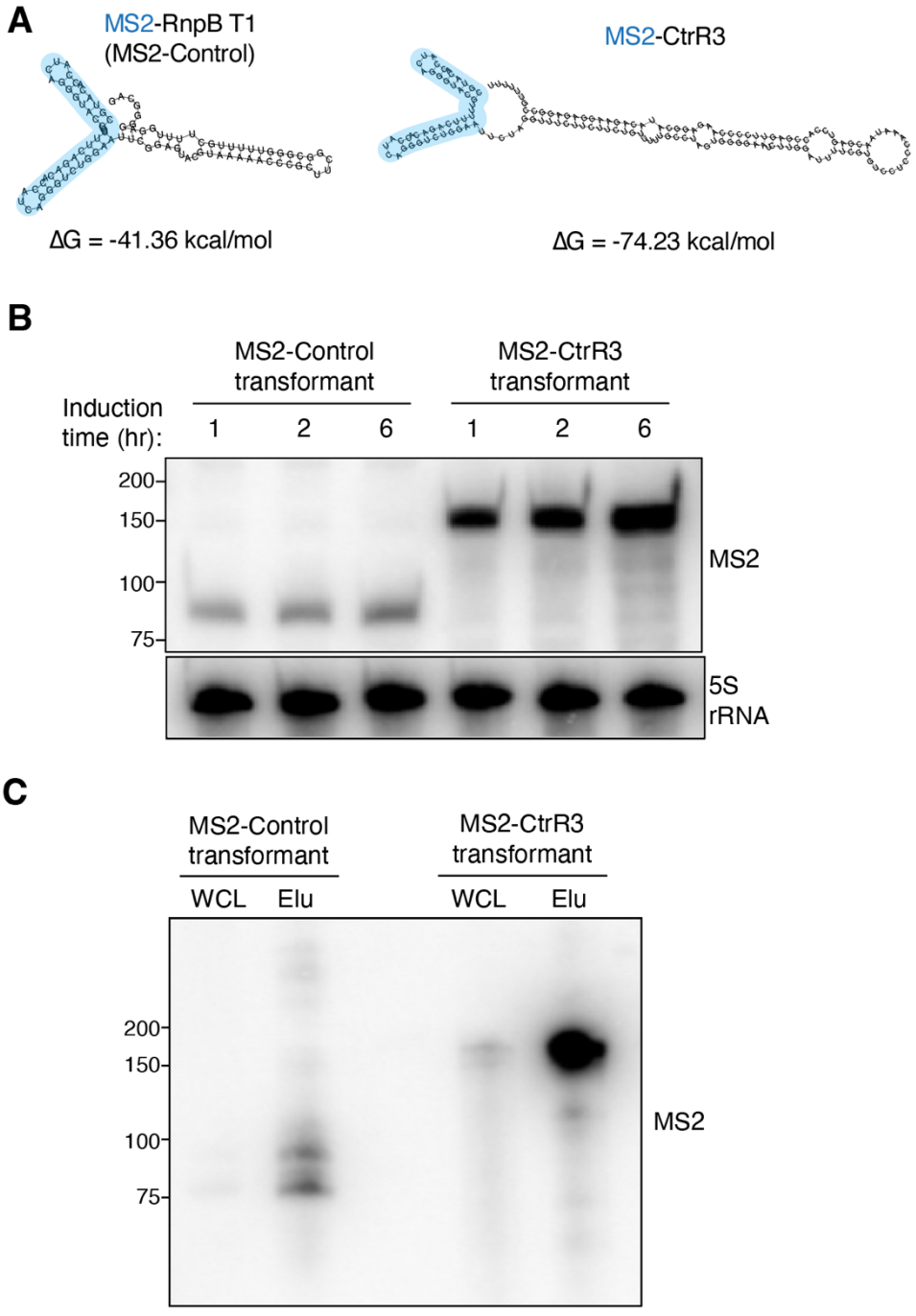

Figure 17. Aptamer affinity purification of MS2-CtrR3.
(A) The secondary structures of MS2-Control (MS2-RnpB T1) and MS2-CtrR3 were predicted bioinformatically using the RNAfold software. The free energy of the thermodynamic ensemble is shown (ΔG).

(B) Northern blot of lysates from MS2-Control and MS2-CtrR3 infected HeLas that were induced 1, 2, or 6 hours prior to collection at 30 hpi. Blot was probed with oligonucleotide against the MS2 sequence; 5S rRNA is shown as loading control.
(C) Northern blot analysis of the whole cell lysates (WCL) and eluted materials (Elu) of MS2-Control and MS2-CtrR3 infected HeLas that were induced at 29 hpi with aTc and collected at 30 hpi for MS2-affinity purification. Northern blot was probed with oligonucleotide against the MS2 sequence.

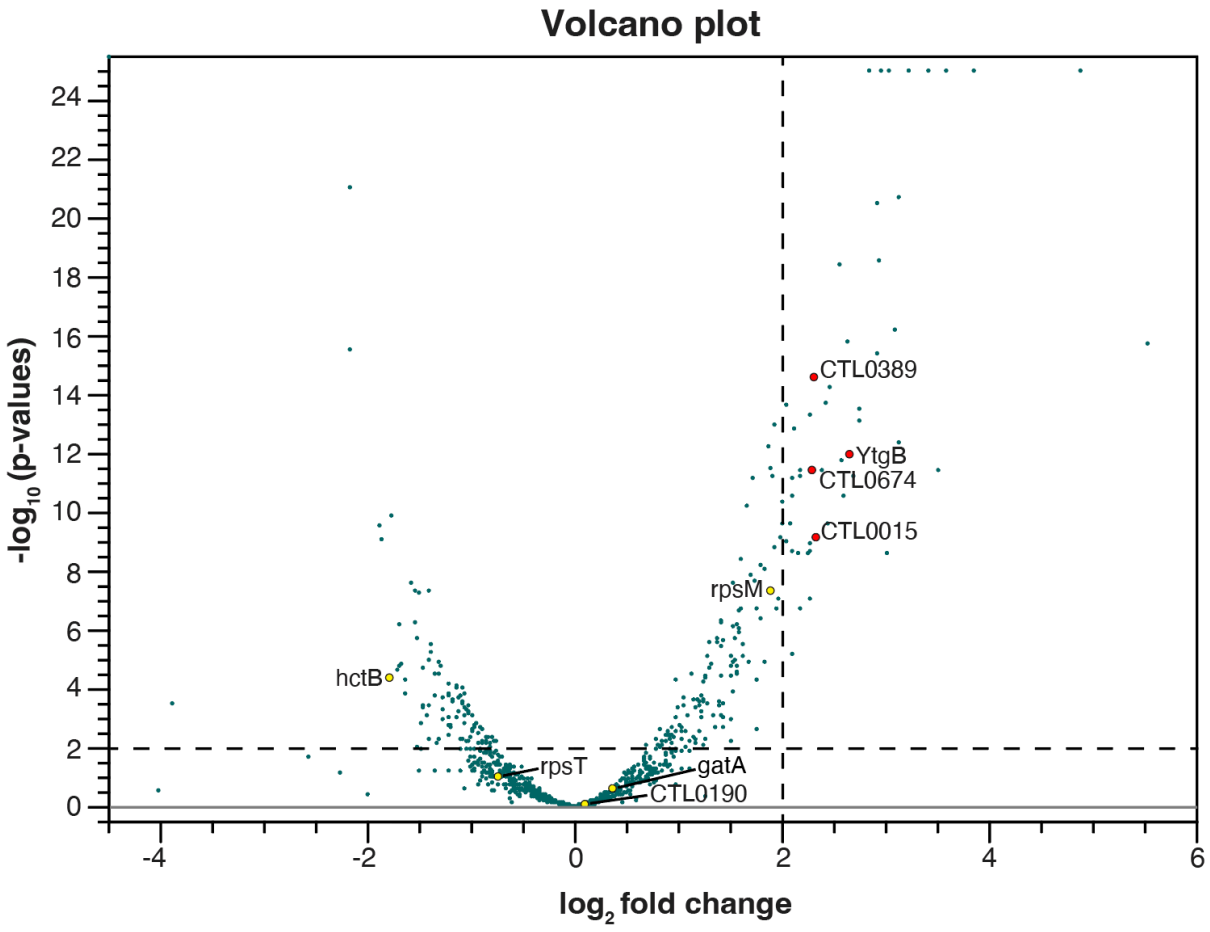

Figure 18. MAPS identifies putative mRNA targets of CtrR3.
Volcano plot demonstrating differential enrichment of the MS2-Control (left) vs MS2-CtrR3 (right) (n=2). Cut-off for enrichment was set at Log_2 fold ≥ 2 and p-value was set at ≤ 0.01 as indicated by the dashed lines. Enriched transcripts are marked with red dots. Also marked are unenriched transcripts that had been bioinformatically predicted to interact with CtrR3 target recognition sequence at the RBS (yellow dots).

2.6d Functional testing with translational fusion reporter assays

We tested these four candidates in translational fusion reporter assays, first in *E. coli* (Urban & Vogel, 2007), then in *Chlamydia*. For the *E. coli* analysis, we included five negative controls, which were *C. trachomatis* mRNAs predicted to have sequence complementarity to the CtrR3 seed region at or near the RBS, by the sRNA target prediction program TargetRNA2 (Kery et al., 2014), but not recovered in our MAPS analysis (Fig. 18, Table 4). For each of these nine mRNA candidates, we constructed a translational fusion reporter containing the region from -50 to +30 relative to the start codon, fused upstream of *gfp*. Co-expression of these translational fusion reporters with CtrR3 in *E. coli* decreased GFP levels for YtgB and CTL0389, but not for CTL0015, CTL0674 or the five control mRNAs (Fig. 19).

To confirm that YtgB and CTL0389 are bona fide CtrR3 targets, we developed an analogous translational fusion assay in *C. trachomatis* (Fig. 20A). This analysis required generation of a *C. trachomatis* transformant for each sRNA-target pair that we tested. As proof of principle, we first showed that overexpression of IhtA downregulated GFP reporter expression for its known target HctA, but not for the negative control HctB (Figs. 20B, C). We then tested CtrR3 overexpression and found that it significantly decreased GFP reporter expression for YtgB and CTL0389 (Figs. 21A, B). For both these targets, the level of downregulation was proportional to the aTc concentration used for induction (Fig. 21C). Importantly, GFP expression was not decreased when either YtgB and CTL0389 were co-expressed with CtrR3^{mut}, which contains a disrupted target recognition sequence (Fig. 21D). These data confirm our *E. coli* translational

fusion results and provide strong evidence that YtgB and CTL0389 are mRNA targets of CtrR3 in *C. trachomatis.*

We also performed reciprocal mutation experiments to test if CtrR3 directly interacts with CTL0389. In initial experiments, we made mutations in the RBS of the CTL0389 translational fusion reporter to complement the CtrR3^{mut} seed region (5'-GGGAGG-3' to 5'-GAAAGG-3'). However, CtrR3^{mut} did not downregulate this version of CTL0389 reporter (data not shown). We then generated a new reciprocal pair by making two CT→TC mutations in the seed region of CtrR3 (CtrR3m1) and introducing reciprocal mutations in the RBS of the CTL0389 GFP reporter (CTL0389m1::GFP) (Fig. 21E). Overexpression of CtrR3m1, but not wildtype CtrR3, decreased CTL0389m1 GFP reporter expression, providing genetic evidence of base-pairing between CtrR3 and CTL0389 mRNA.

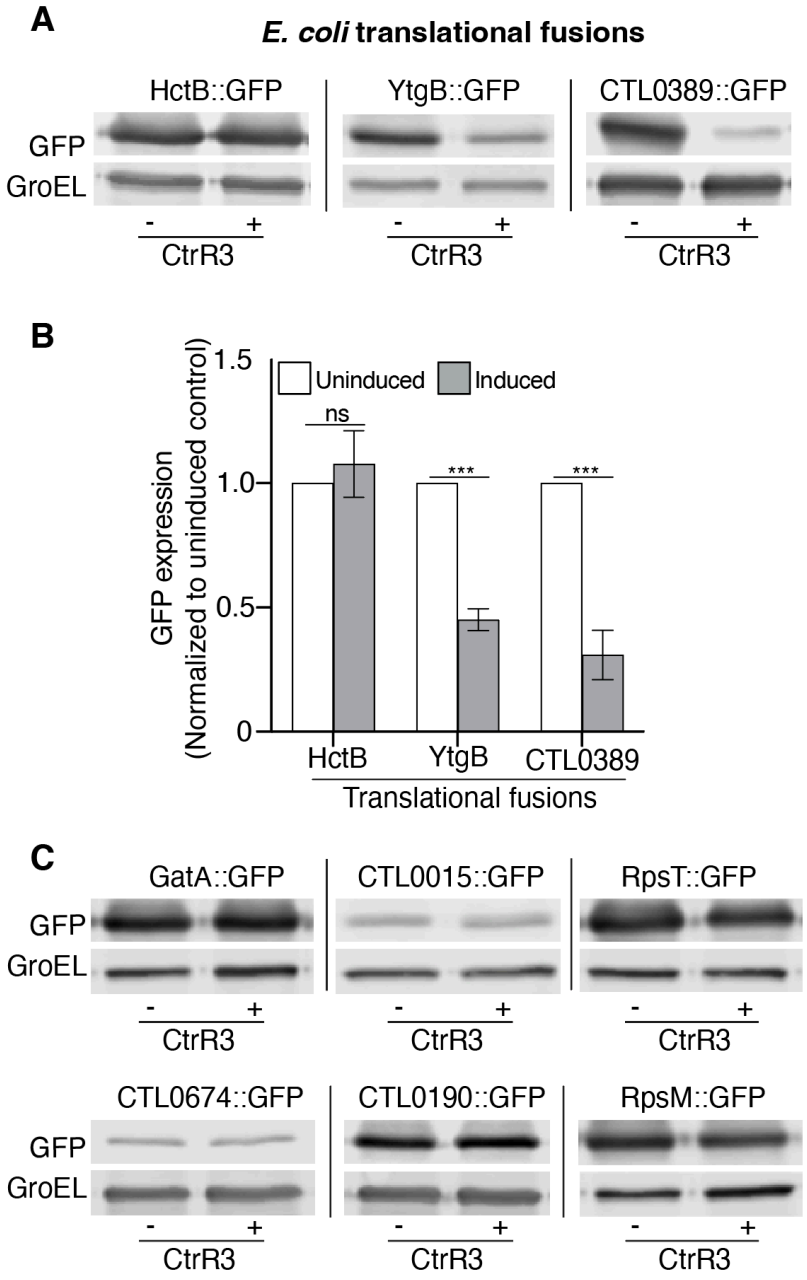

Figure 19. *E. coli* translational fusion assays identify YtgB and CTL0389 as potential targets of CtrR3.

(A) Western blots of lysates from *E. coli* co-expressing CtrR3 together with the reporter construct in which GFP was fused to of each candidate mRNA targets. CtrR3 was first expressed for 30 minutes with 200 ng/mL aTc. Subsequently, 0.02% arabinose was used to induce expression of GFP reporter constructs. The level of GFP is shown. *E. coli* GroEL served as a loading control.

(B) Quantification of the western blots in (A). GFP was normalized first to GroEL and then to the respective uninduced controls. Data are mean ± SEM (n= 3); ***$P \leq 0.001$.
(C) Western blot analysis of lysates from *E. coli* co-expressing CtrR3 together with 6 putative mRNA target sequences fused to GFP. Expression of CtrR3 or the translational fusion proteins was induced with aTc or arabinose, respectively. GFP levels are shown. GroEL served as a loading control.

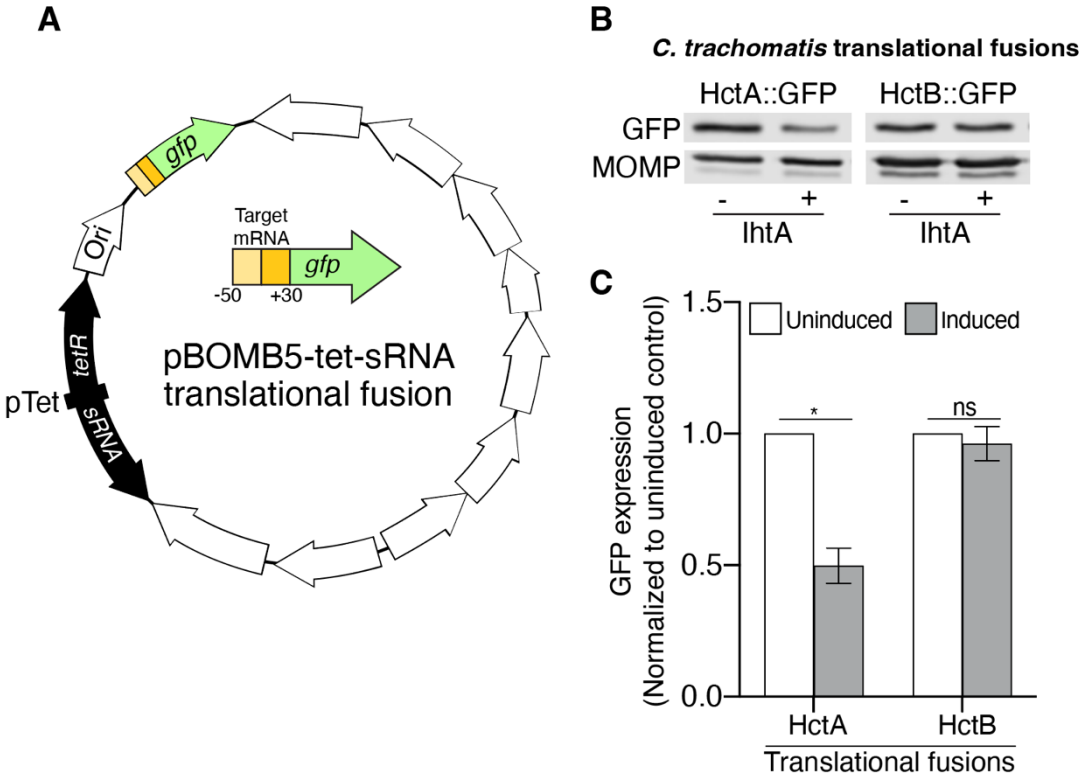

Figure 20. Development of a *Chlamydia* translational fusion assay.
(A) Plasmid map of pBOMB5-tet-sRNA translational fusion. The -50 to +30 region, relative to the translational start site, of the mRNA targets were fused upstream of the *gfp* in the pBOMB5 plasmid. Translational fusion is under the control of the *Neisseria meningitidis* constitutive promoter.
(B) Representative western blots of lysates from HeLa cells infected with *Chlamydia* transformants that co-expressed IhtA together with either HctA or HctB translational fusion proteins. Infected cells were induced with aTc at 20 hpi and lysates were collected at 24 hpi to avoid the deleterious effects of IhtA overexpression. The level of GFP is shown. MOMP served as a loading control for *Chlamydia*.
(C) Quantification of the western blot in (A). GFP was normalized first to MOMP, then to the respective uninduced controls. Data are mean ± SEM (n= 3); *$P \leq 0.05$.

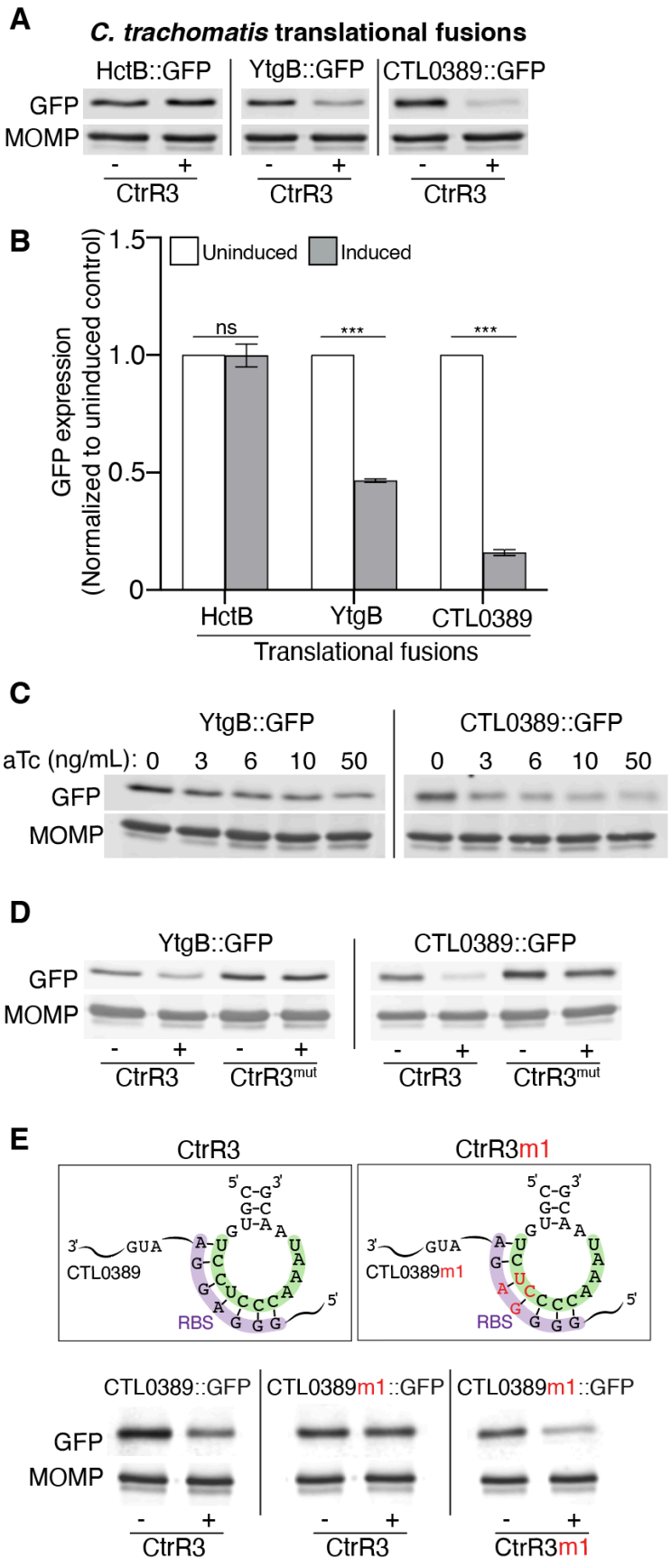
A
C. trachomatis translational fusions
HctB::GFP
YtgB::GFP
CTL0389::GFP
GFP
MOMP
- + - + - +
CtrR3 CtrR3 CtrR3
B
Uninduced
Induced
GFP expression (Normalized to uninduced control)
1.5
1.0
0.5
0
ns
***
***
HctB
YtgB
CTL0389
Translational fusions
C
YtgB::GFP
CTL0389::GFP
aTc (ng/mL): 0 3 6 10 50
0 3 6 10 50
GFP
MOMP
D
YtgB::GFP
CTL0389::GFP
GFP
MOMP
- + - + - + - +
CtrR3 CtrR3mut CtrR3 CtrR3mut
E
CtrR3
CtrR3m1
CTL0389
CTL0389m1
RBS
CTL0389::GFP
CTL0389m1::GFP
CTL0389m1::GFP
GFP
MOMP
- + - + - +
CtrR3 CtrR3 CtrR3m1

Figure 21. *C. trachomatis* translational fusion assays validate YtgB and CTL0389 as CtrR3 targets.
(A) Representative western blots of lysates from HeLa cells infected with transformants that co-expressed CtrR3 together with HctB, YtgB, or CTL0389 translational fusion proteins. To minimize deleterious effects of CtrR3 overexpression, samples were induced with aTc at 20 hpi and analyzed at 24 hpi. The level of GFP is shown. MOMP served as a loading control for *Chlamydia*.
(B) Quantification of the western blots in (A). GFP was normalized first to MOMP and then to the respective uninduced controls. Data are mean ± SEM (n= 3); ****P*≤0.001.
(C) Western blots of HeLa cells that were infected with transformants that co-expressed CtrR3 with either YtgB or CTL0389 translational fusion proteins. The infected cells were incubated with different amount of aTc at 20 hpi and samples were analyzed at 24 hpi. The level of GFP is shown. MOMP served as a loading control for *Chlamydia*.
(D) Western blots of lysates from HeLa cells infected with transformants that co-expressed the translational fusion proteins with either CtrR3 or $CtrR3^{mut}$. sRNA overexpression was induced as described in (A). The level of GFP is shown, and MOMP served as a loading control.
(E) Top: diagram of the compensatory mutations that were made to CtrR3 and the CTL0389 translational fusion. Each box shows the seed region (highlighted in green) of CtrR3 or CtrR3m1 interacting with the RBS (highlighted in purple) of either wildtype CTL0389 or CTL0389m1 translational fusion mRNAs. Bottom: representative western blots of lysates from HeLa cells infected with three different transformants that co-expressed CtrR3 together with either the CTL0389 or CTL0389m1 translational fusions, or CtrR3m1 together with the CTL0389m1 translational fusion. sRNA overexpression was induced as described in (A). The level of GFP is shown, and MOMP served as a loading control.

Discussion

Until now, functional studies of chlamydial sRNAs have been performed in *E. coli* but not in *Chlamydia* itself. The main impediment has been that *Chlamydia* genetics has not been possible until recently, and that new methodologic innovations, such as transformation of *Chlamydia,* have remained inefficient (Mueller et al., 2017; Rahnama & Fields, 2018). Studies in *E. coli* have demonstrated that two *C. trachomatis* sRNAs, IhtA and CTIG270, regulate their respective mRNA targets, HctA and FtsI (AbdelRahman et al., 2011; N. A. Grieshaber, Grieshaber, et al., 2006). While useful, this heterologous approach has two limitations: 1) target recognition between a chlamydial sRNA and its target transcripts may be different because *Chlamydia* lacks the RNA chaperone Hfq, which stabilizes sRNA-mRNA target interactions in *E. coli* (De Lay et al., 2013); and 2) potential roles of a chlamydial sRNA in the unique chlamydial developmental cycle cannot be investigated.

Our inducible sRNA overexpression system has a number of advantages. Most importantly, it allows a sRNA to be studied in the context of the chlamydial sRNA machinery and in the native environment of an infected host cell. Its inducible design allows the level and timing of sRNA expression to be controlled by adjusting the concentration and duration of aTc induction. Furthermore, it is versatile and can be applied in a reverse genetic screen to identify chlamydial sRNAs involved in a specific aspect of *Chlamydia* biology (e.g. the developmental cycle, host-pathogen interactions), which has been done in *E. coli* as well (Bak et al., 2015). Furthermore, the genetic system can be used to investigate sRNA target recognition and sRNA-mRNA interactions with functional studies.

An alternative strategy would be to delete the endogenous sRNA gene, but our results with knocking out IhtA demonstrated the limitations of this approach. Not only is gene deletion technically difficult in *Chlamydia*, this approach also requires the insertion of reporter genes into the targeted gene locus, which causes polar effects on downstream genes. We observed this phenomenon when we deleted IhtA and also saw the loss of tRNA-Thr expression. Polar effect can be eliminated by excising the reporter genes using the Cre-LoxP system (Keb et al., 2021), however, this requires a second round of transformation. Another limitation to the knockout approach is that *Chlamydia* has mostly essential genes as it has a reduced genome. This was demonstrated by our inability to knockout another sRNA, CtrR7, which is likely to be essential. Future investigation of sRNA functions could also utilize the inducible knockdown system (i.e. CRISPRi) that has just been optimized available last year (Ouellette, 2018; Ouellette et al., 2021). This approach blocks transcription by targeting the promoter, and thus may have limitations if the sRNA is processed from an mRNA or pre-tRNA transcript, as may be the case for IhtA (Fig. 5E).

We were surprised to find that we were able to delete IhtA from the *C. trachomatis* genome, suggesting that it is not essential. Grieshaber et al. previously proposed that IhtA represses HctA expression to prevent premature DNA condensation and RB-to-EB conversion in a normal developmental cycle. Based on our result, it is possible that IhtA is not essential for completion of the *Chlamydia* developmental cycle but could be important for other processes, such as persistence. During persistence, RBs remain viable but do not convert into EBs until the environmental stressor is gone. Coincidentally, persistent RBs also express high levels of IhtA and low levels of HctA

protein (AbdelRahman et al., 2011; N. A. Grieshaber, Grieshaber, et al., 2006). Thus, IhtA may be crucial for preventing persistent RBs from converting into EBs, allowing these RBs to remain dormant until the environment is optimal for the *Chlamydia* developmental cycle to continue. This model can be tested by comparing the progeny productions of wildtype strain and *⊿ihtA* strain that are in or coming out of persistence.

Our sRNA genetic system allowed us to identify chlamydial sRNAs whose overexpression had deleterious effects on the intracellular infection. We used a progeny defect as our read-out, but the same sRNA overexpression transformants can also be screened for other phenotypes, such as alteration of a known *Chlamydia*-host interaction. In our study, six sRNAs produced a progeny defect when overexpressed, which suggests that they each may have an important function in the developmental cycle. This conclusion is supported by published reports showing that two of these four sRNAs, IhtA and CTIG270, regulate proteins with roles in the *Chlamydia* infection. In studies with *E. coli*, IhtA decreased levels of HctA, which controls RB-to-EB conversion, and CTIG270 decreased expression of FtsI (Pbp3), which is involved in chlamydial division (AbdelRahman et al., 2011; N. A. Grieshaber, Grieshaber, et al., 2006; Ouellette et al., 2012). CtrR3, CtrR7, CtrR0332, and CTIG648, the four other sRNAs with an overexpression phenotype, are uncharacterized *trans*-encoded sRNAs that caused a much greater progeny defect than IhtA or CTIG270. We did not detect progeny defects with nine of the sRNAs that we tested, but we cannot exclude their potential involvement in *Chlamydia*-host interactions or pathogenesis *in vivo*. These negative findings also provide confidence that the progeny defects we observed in the screen are specific to the sRNAs that were identified.

Based on our screen and chlamydial sRNA conservation, we propose that CtrR3, CtrR7, CtrR0332, and CTIG648 are likely to have important roles in the *C. trachomatis* developmental cycle. This hypothesis is supported by the observation that individual overexpression of all four sRNAs caused a 30-fold or more reduction in progeny production, which is greater than the progeny defect observed with IhtA or CTIG270 overexpression. In addition, out of the four sRNAs identified, CtrR3, CtrR7, and CTIG648 have sequence motifs that are conserved in *C. suis* and *C. muridarum*, while CtrR0332 is conserved among *C. pneumoniae.* This observation provides further support that these sRNAs may have important functions in the *Chlamydia* developmental cycle.

Our results demonstrated that CtrR3 is processed from the pre-tmRNA transcript at the 3′ end. This is supported by the observation that overexpression of tmRNA+CtrR3 in *Chlamydia* increases levels of both RNAs. Additionally, we did not observe a higher level of CtrR3 in the uninduced tmRNA+CtrR3 transformant compared to the uninduced CtrR3 transformant, which should occur if CtrR3 has a promoter residing within the tmRNA sequence due to increased copy numbers from the plasmids. Consistent with this model is the observation that both CtrR3 and tmRNA may share the same promoter. The fact that CtrR3 is constitutively expressed also illustrates that the sRNA is processed from pre-tmRNA, which is a housekeeping RNA. Currently, we do not know which RNAse is responsible for cleaving CtrR3 from the pre-tmRNA. However, RNAse E and RNase Z have been shown to process the 3′ end of pre-tmRNA in *E. coli* and *B. subtilis* respectively (Gilet et al., 2015; Lin-Chao et al., 1999). We propose that CtrR3 is cleaved from pre-tmRNA via RNase Z (CTL0600) because RNAse Z

transcripts are detected at 8 hpi, a time when CtrR3 is detected, whereas RNase E (CafE) transcripts are detected starting at 16 hpi (Belland, Zhong, et al., 2003). Lastly, having CtrR3 processed from a larger transcript could be a strategy *Chlamydia* utilizes to express a sRNA despite having very few and small intergenic regions (Albrecht et al., 2010).

We hypothesize that CtrR3 overexpression does not directly interfere with RB-to-EB conversion, but instead, may act indirectly through effects on RBs. CtrR3 overexpression only decreased progeny if treatment was started before 20 hpi, which is a time in the developmental cycle when RBs are actively replicating but before RB-to-EB conversion can be detected (J. K. Lee et al., 2018). In addition, our EM studies revealed that CtrR3 overexpression increased RB size, compared to uninduced controls, although these RBs were not as big as the non-dividing aberrant bodies seen with classical chlamydial persistence (Beatty et al., 1993; Belland, Nelson, et al., 2003; Panzetta et al., 2018). The correlation between larger RBs and a block in RB-to-EB conversion is intriguing because RB size has been proposed as an intrinsic signal that controls conversion (J. K. Lee et al., 2018). According to this size control model, large RBs are unable to convert and have to get smaller through replication in order to differentiate into an EB. Thus, it is possible that CtrR3 overexpression may inhibit RB-to-EB conversion by altering RB size. This hypothesis can be tested by investigating if there is a correlation between RB size and progeny defect in CtrR3 transformants that are induced with different concentrations of aTc. Lastly, our analysis here demonstrates that we cannot draw definite conclusion on the function of a sRNA based on of the

sRNA overexpression phenotype, especially in cases when the overexpression phenotype can be achieved through direct or indirect mechanism.

Based on our results, we propose that CtrR7 is involved in the RB replication process. This is supported by our analysis of the CtrR7 overexpression phenotype, which showed a block in RB replication. However, our CtrR3 analysis demonstrated that it is difficult to conclude the function of a sRNA based on of its overexpression phenotype. This was largely due to our inability to rule out the possibility that CtrR3 overexpression indirectly blocked RB-to-EB conversion by affecting RBs. In contrast, we were able to show that CtrR7 overexpression directly affected RB replication by confirming that it does not affect EB-to-RB conversion. Our EM analysis suggests that bacteria overexpressing CtrR7 have successfully converted into an RB. Furthermore, we observed that induction of CtrR7 overexpression at 16 hpi, a time past the EB-to-RB conversion stage, still had an effect on progeny production. Additionally, in principle, the transcriptionally silent EB has to first differentiate into an RB to start transcription of the exogenous CtrR7. Thus, we propose that CtrR7 overexpression directly blocks RB replication and is likely to be involved in facilitating RB replication. In accordance with our model, the endogenous CtrR7 is expressed as a mid-cycle gene, which is expressed during RB replication.

We hypothesize that CtrR7 encodes a small periplasmic protein. Bacterial small proteins (~50 amino acid or less) are often membrane proteins that regulate nutrient transport (Kim et al., 2018; Storz et al., 2014; Yadavalli & Yuan, 2021). Similarly, the CtrR7 protein is likely a membrane protein as it co-localized with MOMP in the immunofluorescent analysis and is only present in larger bacteria, which are

presumably RBs. Interestingly, the small protein is not predicted to have a transmembrane domain, but it is predicted to have a signal peptide. This predicted signal peptide can be recognized by the SecYEG complex, which translocate unfolded protein through the inner membrane and into the periplasm (Natale et al., 2008; L. Wang et al., 2004). Thus, we propose that the small protein encoded in CtrR7 is a periplasmic protein.

We propose that the small protein is responsible for the block in RB replication observed in CtrR7 overexpression. This was strongly supported by the inability of CtrR7^{mut} overexpression to reduce progeny production. CtrR7^{mut} has a one nucleotide deletion that resulted in a premature stop codon in the ORF. More importantly, this deletion did not alter the predicted RNA secondary structure of CtrR7, which have preserved the hairpin structures important for sRNA function. Thus, if CtrR7 overexpression phenotype was due to a sRNA function, then CtrR7^{mut} should still cause a block in RB replication. From this analysis, we cannot conclude that CtrR7 only encodes a small protein and does not have a sRNA function. It is possible that CtrR7 can function as a sRNA, but the overexpression of the sRNA does not affect progeny production. Additionally, we cannot rule out the possibility that the deleted nucleotide is required for sRNA base-pairing with mRNA targets. The latter point can be resolved by demonstrating that the small protein alone is sufficient to cause the progeny defect.

We hypothesize that CtrR0332 has different function and targets from those of CtrR3, despite the fact that overexpression of both sRNAs resulted in an RB-to-EB conversion defect. Similar to CtrR3, overexpression of CtrR0332 resulted in the formation of larger RBs as observed in EM. However, unlike CtrR3, CtrR0332

overexpression caused the formation of “miniature” RBs adjacent to the larger RBs (Beatty et al., 1994). This phenomenon has been observed in aberrant RBs attempting to produce infectious EBs during persistence (Beatty et al., 1994). Another dissimilarity between the two sRNAs is that induction of CtrR3 overexpression at 20 hpi no longer had an effect on progeny production. In contrast, induction of CtrR0332 overexpression at 24 hpi, a time when RB-to-EB conversion is first detected, still had an effect on late gene expression and EB production (Belland, Nelson, et al., 2003; J. K. Lee et al., 2018). This suggests that CtrR0332 overexpression, compared to CtrR3 overexpression, is more likely to directly impair late gene expression and RB-to-EB conversion in *C. trachomatis*. In support of this hypothesis, endogenous CtrR3 is expressed constitutively, whereas endogenous CtrR0332 is expressed in late infection time.

Our analysis of CtrR3, CtrR7, and CtrR0332 shows how overexpression of these sRNAs caused different effects on the *C. trachomatis* infection. Based on assays of chlamydial genome number, progeny production, late gene expression and ultrastructural analysis, we propose that overexpression of CtrR3 and CtrR0332 disrupts RB-to-EB conversion, whereas overexpression CtrR7 mainly blocks RB replication. Upon further analysis, we also observed differences in the effects of CtrR3 and CtrR0332 overexpression as mentioned above. These differential effects demonstrate that 1) these sRNA most likely control different mRNA targets; 2) the overexpression phenotypes are specific for each sRNA and not due to general toxicity; and 3) it is possible to narrow down a progeny defect to a specific step in the developmental cycle. We do not yet know how CtrR3, CtrR0332, and CtrR7 overexpression inhibits RB-to-EB

conversion or RB replication, but they could do so through direct or indirect mechanisms. Further studies are ongoing to delineate the roles of these sRNAs in the *C. trachomatis* developmental cycle.

We utilized our sRNA genetic system in multiple complementary approaches to identify the mRNA targets of a chlamydial sRNA. For example, it allowed us to overexpress an MS2-tagged CtrR3 so that we could use MAPS as an unbiased method to identify interacting mRNA targets. This approach is attractive for chlamydial sRNA target identification because it does not rely on a sRNA chaperone protein, such as Hfq, as the bait to capture a sRNA and its bound targets. Our genetic approach also allowed us to identify the target recognition sequence of CtrR3, which we then used to prioritize candidate mRNA targets based on sequence complementary to the seed region. In this analysis, we focused on complementarity to the RBS (Storz et al., 2011; Waters & Storz, 2009), but there is also precedent for a sRNA to bind to the coding region of its mRNA targets (Carrier et al., 2018; Fröhlich et al., 2012; Lalaouna & Massé, 2015). Our MAPS analysis also recovered mRNAs lacking complementarity to the CtrR3 seed region, which are less likely to be bona fide targets. Since interactions identified through MAPS may be direct or indirect (Lalaouna et al., 2017; Lalaouna & Massé, 2015), it is important to confirm the regulation of the sRNA on a candidate mRNA target.

We paired our sRNA overexpression approach with a translational fusion reporter to test and validate candidate mRNA targets. This reporter approach is commonly used in other bacteria to demonstrate that a sRNA regulates specific mRNA targets (Sharma & Vogel, 2009b) and can distinguish between direct and indirect targets identified by MAPS (Lalaouna et al., 2017). However, translational fusion assays in *Chlamydia* are

labor-intensive because a transformant with a customized translational reporter has to be generated for each candidate target. For this reason, we first tested candidate targets with a translational fusion reporter in *E. coli* and then used the *C. trachomatis* translational fusion for confirmation. Using this approach, we identified YtgB, an ATPase for iron transport, and CTL0389, an uncharacterized inclusion membrane protein, as likely mRNA targets of CtrR3 (Thompson et al., 2012; Weber et al., 2015). We do not yet know if CtrR3 has other mRNA targets and which target(s) may mediate its observed progeny defect.

Our studies of CtrR3 target recognition shed light on how *C. trachomatis* sRNAs interact with their mRNA targets in the absence of Hfq. Small RNAs in *Mycobacterium,* and other gram-positive bacteria that lack Hfq and another RNA chaperone ProQ, are proposed to use C-rich motifs to interact with their mRNA targets (Jørgensen et al., 2020). For example, *Mycobacterium* sRNA 6C, which is named after the 6 C-nucleotides in its recognition motif, requires 5 of these 6 C-nucleotides to regulate its target (Mai et al., 2019). Our translational fusion studies with reciprocal compensatory mutations showed that an intact 5 C/G base-pairing was necessary for functional interactions between CtrR3 and the CTL0389 translational fusion reporter (Fig 7D). These findings are consistent with the *E. coli* studies conducted by Grieshaber et al. who showed that interactions between IhtA and HctA mRNA required 5 G/C interactions. This observation led these authors to propose that perfect complementarity with G/C-rich base-pairing is important for *Chlamydia* sRNA-mRNA binding to compensate for the absence of Hfq (N. A. Grieshaber et al., 2015).

Chapter concluding remarks

In summary, we have developed a *Chlamydia* sRNA overexpression system that provides a genetic means to study the function of a chlamydial sRNA during the intracellular infection. This approach is particularly suited for investigating the roles of sRNAs in the control of *Chlamydia*-specific functions, such as the developmental cycle, that cannot be studied with a heterologous system. Our overexpression system is versatile because 1) it can be readily used to screen sRNAs for effects on the infection; 2) it can be combined with mutational analyses to identify and validate the sRNA target recognition sequence; and 3) it can be used together with an unbiased approach, such as MAPS, followed by bioinformatic prediction and functional testing, to identify candidate mRNA targets. In the next chapter, we will investigate if a chlamydial sRNA could be modified to recognize a non-native mRNA target, as the basis for a novel conditional protein knockdown method in *Chlamydia*, as has been done in *E. coli* (Magistro et al., 2018; Nakashima et al., 2006). Thus, our sRNA overexpression system represents an advance for studying an important post-transcriptional mechanism of gene regulation and may help to elucidate the molecular mechanisms that control the intracellular *Chlamydia* infection.

Materials and Methods

DNA oligonucleotides and plasmids

DNA oligonucleotides and plasmids can be found in the Tables 5 and 6.

Antibodies used in this study

Primary antibodies used were polyclonal rabbit anti-HctA and polyclonal rabbit anti-HctB (gifts from Ted Hackstadt), monoclonal mouse anti-MOMP (gift from Ellena Peterson), polyclonal rabbit anti-OmcB (gift from Guangming Zhong), monoclonal mouse anti-Flag (M2Flag) (F3165, Sigma-Aldrich), monoclonal mouse anti-GFP (11814460001, Roche), polyclonal rabbit anti-GroEL (G6532, Sigma-Aldrich), and mouse anti-GAPDH (sc-47724, Santa Cruz). Secondary antibodies were goat anti-rabbit IgG LI-COR IRDYE 680 (926-680-71, Fisher Scientific) and goat anti-mouse IgG LI-COR IRDye 800 (926-32210; Fisher Scientific). Membranes were imaged on Odyssey CLx LI-COR machine.

Cell culture and *Chlamydia* infection

HeLa cells were obtained from ATCC and cultured at 37°C and 5.0% CO_2 in DMEM (11995-065, Gibco) supplemented with 10% FBS (S11550, Atlanta Biologicals). McCoy cells (ATCC) were also cultured in a similar condition.

Chlamydia infections were done by infecting near-confluent cell monolayers with *C. trachomatis* serovar L2 (ATCC) or *Chlamydia* transformants at an MOI of 3 in SPG (200 mM sucrose, 20 mM sodium phosphate and 5 mM glutamate; pH 7.2) followed by centrifugation at 700×*g* for 1 hour at room temperature. After centrifugation, the

inoculum was removed and replaced with DMEM containing 10% FBS. For induction of mCherry or sRNAs expression, infected cells were incubated with 50ng/mL of aTc (94664, Supelco) in complete DMEM media at the indicated times. For experiments with aTc inductions starting at 1 hpi, aTc was replenished at 16 hpi due to the short half-life of aTc at 37°C(Politi et al., 2014).

Chlamydia transformation

Transformation of *C. trachomatis* serovar L2 was performed as previously described(Y. Wang et al., 2011). In brief, *Chlamydia* EBs were incubated with 10 µg of plasmid and $CaCl_2$ buffer (10 mM TRIS pH 7.4 in 50mM $CaCl_2$), followed by spin infection of a cell monolayer. The inoculum was then removed and replaced with DMEM containing 10% FBS. At 10 hpi, the medium was replaced with complete DMEM containing 10 µg/mL of ampicillin (A9518, Sigma-Aldrich). At around 48 hpi, the infected host cell monolayer was disrupted via glass beads, with the collected EBs being used to infect a new cell monolayer. After this second spin infection, the infected cells were immediately incubated in complete DMEM containing 10 µg/mL of ampicillin or 100 µg/mL of spectinomycin and 1 µg/mL of cycloheximide (NC9651091, Chem Service Inc). This infection was labeled as passage 1 (P1). The previous two steps were repeated until P3, resulting in a selected population of *Chlamydia* transformants. To obtain a clonal population of transformants, EBs from P3 underwent two rounds of plaque purifications in McCoy cells as previously described (Skipp et al., 2005). IhtA knockout was conducted following protocol as previously described (Keb & Fields, 2020).

Progeny assay

Progeny assays were performed as previously described (K. J. Muñoz et al., 2021). In brief, at the indicated times, *Chlamydia*-infected cells were washed with 1×PBS and collected in SPG to harvest infectious EBs from the primary infection. Samples were subjected to one cycle of freeze-thaw to lyse the host cells, then serially diluted in SPG and used to re-infect a new monolayer of HeLa cells in the absence of aTc. At 27 hpi, cells were fixed with ice-cold methanol, followed by visualization of chlamydial inclusions with mouse anti-MOMP antibodies (gift from Ellena Peterson, UC Irvine) using immunofluorescence microscopy. The number of inclusions, determined in 10 fields of view using a 20× objective, was used to calculate the total number of infectious progeny (IFU/mL). Progeny per cell was determined by dividing IFU/mL by the number of host cells present at the time of the infection, which was determined through counting trypsinized cells on a hemocytometer.

Northern blot

Total RNA was prepared from *Chlamydia* infected cells using TRIzol (15-596-026, Invitrogen) and chloroform with Phase Lock Gel tubes (2302830, Quantabio). Northern blot was performed as previously described (Sheehan & Caswell, 2017). Briefly, 12 µg of RNA was resolved in 10% polyacrylamide gel with Tris-Borate-EDTA (TBE) and 7M urea. Low molecular-weight ladder (N3233, NEB) was radiolabeled with (γ-^{32}P)-ATP (Perkin Elmer) using polynucleotide kinase (M0201, NEB) to identify RNA sizes. RNA samples were then transferred to Hybond-N+ membrane (GERPN303N, Cytiva) and then UV cross-linked to the membrane. Membranes were prehybridized

with ULTRAhyb-Oligo buffer (AM8663, Invitrogen) for 30 minutes at 42°C. The oligonucleotide probes, which can be found in Table 5, were end labeled with γ-^{32}P-ATP and incubated with the membranes overnight. The following day, membranes were washed four times with 2x SSC, 1x SSC, 0.05x SSC, and 0.025x SSC (1x SSC is 0.15M NaCl and 0.015M sodium citrate) plus 0.1% SDS. Membranes were exposed to phosphor-imager screens and visualized by Typhoon TRIO+ Imager.

Western blot

Cell lysates were prepared by lysing *Chlamydia*-infected cells or *E. coli* cells directly in 2% SDS, followed by boiling the samples at 95°C for 5 min as previously described(K. J. Muñoz et al., 2021). Equal volumes of lysates were loaded and resolved by SDS-PAGE, followed by transferring onto nitrocellulose membranes.

RT-qPCR and qPCR

RT-qPCR was used to measure relative transcript levels in *Chlamydia*. Total RNA extracted from *Chlamydia*-infected cells was subjected to DNAse (FEREN0521, Thermo Scientific) treatment, followed by cDNA synthesis with qScript cDNA SuperMix (95048-025, QuantaBio). qPCR reactions were conducted on diluted cDNA with SsoAdvanced universal SYBR green supermix (1725271, Bio-Rad) and was run on a Bio-Rad thermocycler. qPCR of the *C. trachomatis 16s rRNA* gene was used as control for all samples. Primers used can be found in Table 5. PCR efficiencies were calculated using LinRegPCR software(Ruijter et al., 2009), and relative levels of mRNA abundance

compared to the uninduced control samples were calculated using the Pfaffl equation (Pfaffl, 2001).

The number of chlamydial genomes per host cell was measured by qPCR. Genome copy number was determined using a standard curve generated from a plasmid containing the *C. trachomatis euo* gene(K. J. Muñoz et al., 2021). The number of host cells was determined from PCR reactions of the host cell gene *gapdh*. *Chlamydia* genomes per host cell was calculated by normalizing genome copy number (*euo*) to *gapdh* values in each sample. Primer sequences to *euo* and *gapdh* can be found in Table 5. qPCR was performed using SsoAdvanced universal SYBR green supermix and analyzed on the Bio-Rad thermocycler.

Immunofluorescence microscopy

HeLa cells, grown on glass coverslips, were fixed with 100% cold methanol for 10 minutes and were subsequently incubated with blocking buffer (2% FBS, 0.1% Saponin) for 30 minutes at room temperature. After serial incubation of primary and secondary antibodies, coverslips were mounted with ProLong Glass Antifade containing NucBlue (Invitrogen, P36985). Immunofluorescence microscopy images were acquired on Zeiss Axiovert 200.

MS2-affinity purification coupled with RNA sequencing

MS2-affinity purification was conducted by modifying the protocol previously described (Mercier et al., 2021). Two 150 mm dishes of HeLa cells were infected with either the MS2-Control or the MS2-CtrR3 transformants at an MOI of 3. At 29 hpi,

50ng/mL of aTc was added to each plate to induce MS2-sRNA expression. At 30 hpi, infected HeLa cells were trypsinized, pelleted at 500 g for 5 minutes, and washed once in PBS. After PBS removal, the cell pellets were frozen with liquid nitrogen and stored at -80°C. Cell pellets were then thawed on ice and resuspended in Buffer A, which is composed of 20mM Tris-HCl pH 8, 150mM KCl, 1mM $MgCl_2$, 60U of SUPERase (Fischer Scientific AM2694), and 1mM DTT in DEPC-treated water. Resuspended cells were transferred to Matrix B tube (MP Biomedical 116911050-CF) and lysed with the Fast Prep-24 homogenizer (MP Biomedical) at 4.0 m/s for 15 seconds. Lysates were then transferred to a new Eppendorf tube after spinning down the matrix beads at 3000 g for 5 minutes. A small fraction of the lysate (whole cell lysate, WCL) was saved for northern blot analysis.

Prior to loading the lysates onto the columns, amylose resin (NEB E8021S) was added to the Poly-prep Chromatography columns (Bio-Rad #731150). The resin was washed with Buffer A (no SUPERase added) and then incubated with 6mL of MS2-MBP (~1,200 pmol) in Buffer A. The columns were washed once with Buffer A then the lysates were loaded onto the columns. After 3 washes with Buffer A, the MS2-sRNAs were eluted with Buffer E, which is composed of 150mM KCl, 1mM DTT, and 12mM maltose in DEPC-treated water. RNA from both the WCLs and eluates were extracted with 1:1 Acid-Phenol: Chloroform: IAA (Invitrogen AM9720) followed by one chloroform wash. The RNA was then precipitated in -20°C with GlycoBlue (Thermo Scientific AM9515) and 2.5 times in volume of 100% ethanol. The next day, precipitated RNAs were pelleted and washed once with 70% ethanol. RNA pellets were dried at room temperature and resuspended in nuclease-free water. Extracted RNAs were then

treated with Turbo DNase (Invitrogen AM2238) and re-extracted using the aforementioned method. From here the RNA integrity of the DNAse-treated RNAs was assessed by determining the 3':5' ratio of the cDNA(Die et al., 2011). After confirmation of the RNA qualities, the DNAse-treated RNAs subsequently underwent RNA sequencing (eluates only) or northern blot analysis(Die et al., 2011). MS2-affinity purification was done in duplicates.

MS2-enriched paired end libraries were sequenced on an Illumina NovaSeq 6000 sequencing platform in duplicate. Two MS2-CtrR3 enriched libraries were sequenced to 85 and 98 million reads each with 10 and 16 million reads, respectively, mapping to *Chlamydia trachomatis* L2 434/Bu genome (accession GCA_000068585.1) excluding reads mapped to rRNAs. Similarly, two MS2-Control libraries were sequenced to a total of 102 and 78 million reads of which 10 and 6 million reads were mapped to the *Chlamydia* genome, excluding reads mapped to rRNA. All mappings and data analysis were performed on Qiagen CLC Genomics Workbench (version 21.0.5) software with high stringency settings (mismatch cost 2, and insertion and deletion cost 3, length and similarity fraction 0.8 each, maximum number of hits for a read to 10, and minimum read count fusion table to 5). The differential expression statistical analysis was done with MS2-CtrR3 Vs. MS2-Control libraries using “Differential Expression in Two Groups” function filtering for average expression for False Discovery Rate (FDR) correction. The p-value reported are FDR p-value. Default RNA-seq analysis method in CLC Genomics Workbench software counts fragments (FPKM) instead of individual reads. This method is more accurate as only unbroken fragment pairs are assigned a read, removing low quality read fragments from the analysis.

E. coli culture conditions and co-expression study

E. coli strain DHFα (NEB5-alpha) were grown in LB (Miller) under aerobic conditions at 37°C. Where appropriate, antibiotics were used at the following concentrations: 100 μg/mL ampicillin (A9518, Sigma-Aldrich) and 25 μg/ml chloramphenicol (C0378, Sigma-Aldrich). Co-expression studies were conducted by co-transforming *E. coli* with the high-copy pRSETC plasmid containing the sRNA under the Tet-inducible promoter and the low-copy pBAD33.1 plasmid containing the translational fusion protein under the control of an arabinose-inducible promoter. Overnight culture of the co-transformed *E. coli* was diluted to an OD_{600} of 0.1 and grown to an OD_{600} of 0.5. sRNA expression was induced with 200 ng/mL aTc for 30 minutes, followed by induction of the translational fusion protein expression with 0.02% arabinose. Bacteria were collected 90 minutes post arabinose induction. Lysates, prepared through incubation 2% SDS, were subjected to SDS-PAGE and western blot analysis.

EM

For transmission electron microscopy analysis, *Chlamydia*-infected cells were fixed in 2% paraformaldehyde (100503-917, VWR) and 2.5% glutaraldehyde (NC9861069, Polysciences) in 0.1M cacodylate buffer for 2 hours at room temperature. Samples were processed and imaged by Dr. Wandy Beatty at Washington University, School of Medicine.

Statistical analyses

For each experiment, 3 independent biological replicates were performed, and the results are presented as mean ± SEM. Data were analyzed by unpaired, two-tailed t-tests with Welch's correction on Graph Pad PRISM software version 8.

Plasmid construction

All plasmids were constructed with Gibson assembly via the NEBuilder HiFi DNA assembly mastermix (E2621, NEB) and subsequently transformed into *E. coli* strain DHFα (NEB5-alpha). The plasmid constructs were then confirmed via Sanger sequencing using Retrogen Inc.

To construct pBOMB5-tet-IhtA, the Tet-inducible mCherry expression cassette was first removed from pBOMB4-tet-mCherry using primer pairs P1+P2 and P3+P4. Subsequently, IncG terminator and the IhtA overexpression cassette was placed downstream of the *bla* gene using primer pairs P1+P5, P6+P7, P8+P9, P10+P11, and P12+P4. To overexpress mCherry and other sRNAs in the pBOMB5 plasmid, primer pairs P1+P13 and P10+P4 were used to amplify the vector backbone of pBOMB5-tet-IhtA. IhtA was then replaced by using primer pairs from P28 to P57. pBOMB5-tet-tmRNA+CtrR3 was constructed in a similar fashion with the primer pairs P32+P58.

IhtA knockout plasmid was constructed by using primer pairs P1+P16, P4+P17, and P18+19 with pSUmC 4.0 (Keb & Fields, 2020) as template. The 5F and 3F homology regions were amplified with primer pairs P24+P25 and P22+P23.

pBOMB5-tet-CtrR7-Flag was made with primer pairs P1+P60 and P4+P59 using pBOMB5-tet-CtrR7 as template. The two fragments were linked by P61. pBOMB5-tet-

CtrR7^{mut} was made using primer pairs P1+P63 and P4+P62 with pBOMB5-tet-CtrR7 as template.

pBOMB5-tet-MS2-CtrR3 was generated with primer pairs P1+P64 and P10+P4 using pBOMB5-tet-CtrR3 as template. The two fragments were joined by P65. pBOMB5-tet-MS2-RnpB T1 was made using primer sets P1+P66 and P67+P4 using pBOMB5-tet-MS2-CtrR3 as template. These two fragments were joined by P68. pBOMB5-tet-CtrR3^{mut} was generated with primer pairs P69+P4 and P1+P70 using pBOMB5-tet-CtrR3 as template.

pRSETC-tet-CtrR3 was constructed with primer pairs P71+P72 for the pRSETC vector backbone and P73+P74 for the CtrR3 overexpression cassette amplified from the pBOMB5-tet-CtrR3 plasmid. To generate the plasmid for arabinose-inducible translational fusion expression, pBAD33.1 vector backbone was amplified with P75+P76. GFP was amplified from the pBOMB5-tet-sRNA plasmid using primer pairs P77+P78. The -50 to +30 region of each putative mRNA targets were amplified with primer pairs P79 to P96.

The pBOMB5-tet-sRNA translational fusion plasmid was generated by amplifying the vector backbone using P1+P97 and P77+P4 using either pBOMB5-tet-IhtA or pBOMB5-tet-CtrR3 as templates. The -50 to +30 region of *hctA*, *hctB*, *ytgB*, *ctl0389* were amplified using primer pairs P98+P99, P100+P80, P101+P82, P102+P84 respectively. Plasmid with CtrR3^{mut} co-expressing with YtgB or CTL0389 translational fusion proteins were generated with primer pairs P69+P4 and P1+P70 using pBOMB5-tet-CtrR3-YtgB::GFP and pBOMB5-tet-CtrR3-CTL0389::GFP as templates, respectively. Plasmid with CtrR3 co-expressing with CTL0389m1 translational fusion protein were

generated with primers pair P1+P104 and P103+P4 using pBOMB5-tet-CtrR3-CTL0389::GFP as template. The two fragments were then assembled using P105 link oligonucleotide. Plasmid with CtrR3m1 co-expressing CTL0389m1::GFP was generated with primer pairs P1+P70 and P106+P4 using pBOMB5-tet-CtrR3-CTL0389m1::GFP as template. The two fragments were assembled using P107 link oligonucleotide.

Bioinformatic predictions of CtrR3 targets

IntaRNA (Busch et al., 2008; Mann et al., 2017; Wright et al., 2014) was used to analyze the 52 transcripts that were enriched $\geq$ 2 Log_2-fold in MAPS analysis to identify likely mRNA targets of CtrR3. This bioinformatic tool predicts base-pairing between a query sRNA and specific candidate mRNAs entered into the program. The entire CtrR3 sequence was entered as query ncRNA in the IntaRNA prediction site. For each mRNA transcript, 50 nucleotides upstream of the start codon, the coding sequence, and 50 nucleotides downstream of the stop codon were entered into the prediction site. The mRNA sequences were obtained from *Chlamydia trachomatis* 434/Bu genome (GCA_000068585.1). The parameters were set to default except for the “Min. number of base-pairs in seed” was set to 6. The list of putative mRNA targets was first narrowed down by identifying those with sequence complementarity to the CtrR3 seed region (49-61 nt). We then prioritized mRNAs which had sequence complementarity at their RBS (i.e. A/G-rich sequences upstream of the start codon).

TargetRNA2 (Lorenz et al., 2011) was utilized to identify mRNA targets that were also predicted to base-pair with the CtrR3 seed region at or near the RBS but were not identified in the MAPS analysis. This bioinformatic tool predicts sites of complementarity

base-pairing with the sRNA sequence in the genome, which is beneficial for when candidate mRNAs are not known. The hairpin loop sequence 5'-TGTCCTCCCAAATAAC-3' of CtrR3 was entered into the TargetRNA2 prediction site against the *Chlamydia trachomatis* 434/Bu genome (GCA_000068585.1). The constraints were set to search 50 nucleotides upstream and 30 nucleotides downstream of the translational start site. The hybridization seed was set to 6 nucleotides and P-value threshold was set to 0.5. Similar to the IntaRNA analysis, the list of predicted mRNA targets was further narrowed down by selecting for candidates that were predicted to base-pair with the seed region at the RBS, upstream of the RBS, or 5′ coding region of the mRNA.

Acknowledgments

We would like to thank Dr. Clay Caswell at Virginia Tech for his expertise on bacterial sRNA and assistance on experimental designs. We also thank Dr. Kenneth Fields at University of Kentucy for providing us with the pSUmC 4.0 plasmid. We would like to thank Dr. Marie-Claude Carrier at University of Sherbrooke, Liang Liu and Dr. Yongsheng Shi at University of California, Irvine, for their assistance and expertise on MS2 affinity purification. We would also like to thank Dr. Caswell, Dr. James Budnick, and members of the Tan and Sütterlin Labs for helpful comments on this manuscript. We thank Dr. Wandy Beatty at Washington University, School of Medicine, for producing the EM images. We also thank the UCI Microbiome Initiative for providing us with the homogenizer, and the UCI Genomic High Throughput Facility for conducting RNA sequencing for MAPS. This research was supported by grants from the National Institutes of Health (R01 AI044198 to M.T. and R01 AI151212 to C.S and M.T.). K.W. was supported by a National Institutes of Health T32 training grant (AI141346). Portion of this chapter is a pre-print of the material as it appears in “A reverse genetic approach for studying sRNAs in *Chlamydia trachomatis*” (revision submitted to *mBio*). The co-authors listed in this manuscript (Lauren Sheehan, Cuper Ramirez, Asha Densi, Syed Rizvi, Christine Sütterlin, and Ming Tan) directed and supervised research which forms the basis for the thesis.

Tables

Table 2. List of chlamydial sRNAs investigated in this study

sRNA	Identified in which study?	*trans* or *cis* ?	Transformed into *Ctr*
CtrR1	Albrecht 2010	*cis* to *aspC*	X
CtrR2	Albrecht 2010	*trans*	X
CtrR3	Albrecht 2010	*trans*	X
CtrR4	Albrecht 2010 AbdelRahman 2011 (CTIG153)	*cis* to *ycfV*	X
CtrR5	Albrecht 2010 AbdelRahman 2011 (CTIG241)	*trans*	X
CtrR6	Albrecht 2010 AbdelRahman 2011 (CTIG356)	*trans*	X
CtrR7	Albrecht 2010	*trans*	X
CtrR8	Albrecht 2010	*cis* to *ctl0812* (L2); *ct550* (D)	X
CtrR0332	Albrecht 2010	*trans*	X
CTIG270	AbdelRahman 2011	*cis* to *ftsI*	X
CTIG327	AbdelRahman 2011	*trans*	
CTIG360	AbdelRahman 2011	*trans* / riboswitch to *bioY*	X
CTIG498	AbdelRahman 2011	*trans*	X
CTIG504	AbdelRahman 2011	*trans*	
CTIG643	Albrecht 2010 AbdelRahman 2011	*trans*	X
CTIG684	AbdelRahman 2011	*trans*	X

Table 3. List of transcripts enriched in MAPS

Name	Max group mean	Log_2 fold change	Fold change	P-value	FDR p-value
ndk	67450.19	5.537525	46.44736	1.28919E-18	7.20338E-17
CTL0290	896.9667	4.884712	29.54234	3.03986E-52	2.71763E-49
ribC	1115.746	3.860462	14.52496	2.0206E-51	9.03208E-49
CTL0362	314.1781	3.591056	12.05079	8.19839E-36	1.83234E-33
folP	3625.127	3.51727	11.44995	5.74344E-14	1.65633E-12
atpI	447.9776	3.420895	10.71006	1.35375E-35	2.4205E-33
CTL0720	820.7484	3.234615	9.41274	1.26892E-39	3.78139E-37
radA	205.1244	3.229565	9.379851	8.36826E-31	1.06875E-28
CTL0323	1026.317	3.141088	8.821893	3.55252E-23	2.64663E-21
CTL0060	3507.647	3.125692	8.728249	1.85195E-14	5.70913E-13
ompH	456.4041	3.087755	8.501723	1.21489E-18	7.20338E-17
CTL0019	124.8349	3.039162	8.220135	2.74039E-30	3.06239E-28
pmpD	943.1394	3.026614	8.14895	1.28271E-10	1.97715E-09
CTL0138	978.2469	2.951098	7.733376	3.2931E-31	4.90671E-29
folA	1142.363	2.947101	7.711978	7.91786E-21	5.44505E-19
CTL0748	212.9091	2.928257	7.611904	1.14644E-17	5.39432E-16
CTL0895	216.4341	2.91415	7.537834	1.02358E-23	9.15082E-22
tdk	362.331	2.849241	7.206211	3.30736E-29	3.28531E-27
CTL0552	189.1133	2.751797	6.735558	1.12008E-15	4.00539E-14
CTL0447	168.8854	2.750022	6.727275	3.14125E-15	1.08011E-13
gspG	230.6808	2.694593	6.473709	2.97482E-13	6.8192E-12
YtgB	651.0923	2.664135	6.338474	6.06452E-14	1.69428E-12
CTL0661	589.8281	2.630953	6.19435	4.87185E-18	2.56202E-16
rpsU	529.644	2.599784	6.061961	1.5103E-12	3.06866E-11
CTL0390	480.5612	2.574468	5.956512	8.74279E-14	2.3685E-12
kdsB	230.1479	2.564464	5.915353	1.1799E-20	7.53451E-19
CTL0594	881.3212	2.471571	5.546475	1.81645E-16	7.73289E-15
CTL0830	111.288	2.444774	5.444402	1.21273E-11	2.25871E-10
rnc	77.65273	2.4165	5.338744	3.70436E-16	1.50532E-14
CTL0473	2099.082	2.382701	5.215122	2.08067E-13	5.02734E-12
CTL0015	261.8779	2.334142	5.042509	3.48274E-11	5.98764E-10
CTL0389	320.0356	2.316142	4.979987	8.03282E-17	3.59067E-15
CTL0674	119.0459	2.295047	4.9077	1.72746E-13	4.41242E-12
folX	112.8934	2.280205	4.857469	6.94561E-09	8.27916E-08

CTL0477	80.72546	2.27855	4.8519	1.21304E-10	1.92131E-09
infC	541.8581	2.277326	4.847785	1.0197E-15	3.79838E-14
rpmI	128.5642	2.26419	4.803846	7.65153E-11	1.24372E-09
CTL0309	344.4438	2.258718	4.78566	1.5072E-10	2.24573E-09
dnaX_1	71.92109	2.187961	4.556611	3.23537E-13	7.23106E-12
dppD	408.8421	2.179023	4.528468	2.00255E-08	2.31365E-07
dnaA	131.1617	2.177833	4.524734	1.95342E-13	4.85099E-12
CTL0831	330.902	2.164895	4.484337	1.59767E-10	2.3415E-09
lpxB	106.3507	2.124893	4.361708	5.90704E-15	1.88603E-13
CTL0061	434.3979	2.104318	4.299943	5.8557E-13	1.24643E-11
CTL0384	140.5384	2.104027	4.299076	8.17675E-07	7.16668E-06
CTL0675	140.3912	2.096128	4.275603	1.05241E-12	2.18803E-11
CTL0511	679.1575	2.094615	4.271123	1.99114E-10	2.8711E-09
CTL0361	26.05648	2.078937	4.224957	1.56715E-11	2.85356E-10
fabF	1745.602	2.041514	4.116774	1.3929E-10	2.1106E-09
CTL0016	103.1742	2.041231	4.115966	6.62444E-16	2.57489E-14
sucC	536.2973	2.003194	4.008866	2.79549E-12	5.55371E-11
CTL0880	124.2135	2.001551	4.004304	2.02695E-11	3.55312E-10

Complementary to CtrR3 seed region in the coding region
Complementary to CtrR3 seed region in the RBS

Table 4. List of candidate mRNA targets of CtrR3 tested in this study

Gene name	Predicted mRNA binding sites (5′ to 3′)
ctl0389	(−16)C**GGGAGGA**G**A**G(−6)
ytgB	(−17)**AUUGGGAGG**GA(−7)
ctl0015	(−12)A**GGGAGG**GG**A**U(−2)
ctl0674	(−9)U**UUUGGGAG**A(+1)
gatA	(−51)G**UUGGGAGGA**UU(−40)
rpsT	(−13)A**UUGGGAG**A**GA**UU(−1)
rpsM	(−15)A**GGGAGG**C(−8)
ctl0190	(−10)G**GGGAGGA**GG**A**(+1)
hctB	(+9)G**UUGGGAG**U**ACA**A(+21)

Enriched in MAPS
Not enriched in MAPS

Table 5. List of DNA oligonucleotides used in this study

Name	Description	Sequence (5' to 3')
P1	pBOMB4 vector forward	GGATAGACATTAGCTACAGAATC
P2	Δcassette reverse	GACCGGTACCTGCAGGACGTCGGATCCGTGAT
P3	Δcassette forward	CTGCAGGTACCGGTCGACCATTCAAATATG
P4	pBOMB4 vector reverse	GATTCTGTAGCTAATGTCTATCC
P5	*bla* reverse	AATCACATGTCATCCTTACCAATGCTTAATCAGTGAGG
P6	lncG terminator forward	GGATGACATGTGATTCGCG
P7	lncG terminator reverse	GTACCACCGGTGGATCCGTCGACGCG
P8	lhtA forward	ATCCACCGGTGGTACAAAAAGCCA
P9	lhtA reverse	TTGATAGAGTTATTTTACCAAAGTTGGTATTCTAACGCCATGGAATAGC
P10	pTet forward	TGGTAAAATAACTCTATCAACGATAGAGTGTC
P11	pTetR reverse	AACTTGGTCTGACAGTTAAGACCCACTTTCACATTTAAGTTG
P12	pBOMB5 vector forward	CTGTCAGACCAAGTTTACTCATATATAC
P13	pBOMB5 vector reverse	GTACCACCGGTGGATCCGTCGACGCG
P14	mCherry forward	ATCCACCGGTGGTACTTATTTGTACAGCTCATCC
P15	mCherry reverse	AGAGTTATTTTACCACGAGGAGCTTAAACATGGTCTCTAAGG
P16	pSumC4.0 vector reverse	CGGTACCTGCAGTGACGG
P17	pSumC4.0 vector forward	GCGTCAGACCCCGTAGAAAG
P18	pSumC4-Aadgfp forward	GTCGACCATTCCTACTTCG
P19	pSumC4-Aadgfp reverse	CCTGCAGGTCATAACTTCG
P20	lhtA-5F forward	TCACTGCAGGTACCGGTCGACCTAGAGATCCACGAACAGTC
P21	lhtA-5F reverse	GAAGTAGGAATGGTCGACGCAACTCTTATAACATTATTCC
P22	lhtA-3F forward	GAAGTTATGACCTGCAGGATGGAGTTAGCCTAAATAGCTC
P23	lhtA-3F reverse	TACGGGGTCTGACGCCCTGCAGGCGCAGAAAGCATCTGACG
P24	P1 lhtA KO check forward	GACTACAAGTTCCGGATGG
P25	P2 lhtA KO check reverse	GTAAATCAGGCAGGCACG
P26	P3 lhtA KO check forward	GTATCCGGAGTGCCGTTAC
P27	P4 lhtA KO check reverse	CCTACGTTGTGGAACAGCG
P28	CtrR1 forward	ATCCACCGGTGGTACAAAACCCCAGGCAGAGCG
P29	CtrR1 reverse	AGAGTTATTTTACCATTCCTAGGCAGAGTAATTCG
P30	CtrR2 forward	ATCCACCGGTGGTACGCTTCATGCTAACATGATTTTTTG
P31	CtrR2 reverse	AGAGTTATTTTACCAACAAATCTTATTAACTAAATAGTTTATAAAG
P32	CtrR3 forward	ATCCACCGGTGGTACGAATCGGGGAAAAATTTCAATAAAAAAC
P33	CtrR3 reverse	AGAGTTATTTTACCATAGGTTTCTTCTTCTGTTTTTGC
P34	CtrR4 forward	ATCCACCGGTGGTACAAAAGTGCCACCGAGAAGAG
P35	CtrR4 reverse	AGAGTTATTTTACCAGTAGATGTTTGGGTAAGGGG
P36	CtrR5 forward	ATCCACCGGTGGTACAAAAAAAGCCCGAAAAGCAACCC
P37	CtrR5 reverse	AGAGTTATTTTACCAGGTTTATCTAGTTTTTGCTAGTGAC
P38	CtrR6 forward	ATCCACCGGTGGTACAAAAACCTTAAGAATTTTGGGTTGTTC
P39	CtrR6 reverse	AGAGTTATTTTACCAGACGGCTGGGTCCCTC
P40	CtrR8 forward	ATCCACCGGTGGTACGGAGAAACGGCAGTGAGTTTAG
P41	CtrR8 reverse	AGAGTTATTTTACCAATTAACAGCACTGTCAGCAAGTTC
P42	CtrR0332 forward	ATCCACCGGTGGTACAAAAAAAAACGCAAGGCTCTGGGCCTTGCG
P43	CtrR0332 reverse	AGAGTTATTTTACCATCAAATAAAAAACTAATAAGTGGGATTAAC
P44	CTIG643 forward	ATCCACCGGTGGTACAAAAAGAGTTCTCAATACTTCAAGAC
P45	CTIG643 reverse	AGAGTTATTTTACCACCCGGGAAAACTCATCGTC
P46	CTIG327 forward	ATCCACCGGTGGTACAAAAAGGTCTGAGCTTCGGTAAG
P47	CTIG327 reverse	AGAGTTATTTTACCAATTTAAGCCAATTCACAGAAAAAAGTAAG
P48	CTIG270 forward	ATCCACCGGTGGTACTCCTGTATTTTCGAGAATAGCTTC
P49	CTIG270 reverse	AGAGTTATTTTACCAAAATGTTTTGTTTGTGAGATATAATTATG
P50	CTIG360 forward	ATCCACCGGTGGTACCTAAACAAGCTAAGAACAAGGAC
P51	CTIG360 reverse	AGAGTTATTTTACCAAGTTTTTCTGGGTAAATCTCCATG
P52	CTIG498 forward	ATCCACCGGTGGTACTAGGTTTTTTTCTCAAAGTGTATCG
P53	CTIG498 reverse	AGAGTTATTTTACCATCTATACAATTAGTTTTTGAAAAAGACTTC
P54	CTIG504 forward	ATCCACCGGTGGTACAAAAACGACGAGGACCCTAAAG
P55	CTIG504 reverse	AGAGTTATTTTACCATAGCTTTTCCAGTCGTGCGTG
P56	CTIG684 forward	ATCCACCGGTGGTACAAAAAAAAGAAAGACAGCCTAGGG
P57	CTIG684 reverse	AGAGTTATTTTACCACCAACAAGTTTTTTTCTTAAGGGC
P58	tmRNA+CtrR3 reverse	AGAGTTATTTTACCAGGGGGTGTAAAGGTTTCGAC
P59	CtrR7-Flag vector forward	GTCTTTGTAGTCTCCGCTACTACCTCGAATAGGATCTCTAGTTTCTTC
P60	CtrR7-Flag vector reverse	GATTACAAGGATGACGATGACAAGTAGTTTTTTCTAAAAGAGAGTTGAATTTTC
P61	CtrR7-Flag link	GTCATCCTTGTAATCGATGTCATGATCTTTATAATCACCGTCATGGTCTTTGTAGTCTCC
P62	CtrR7mut vector forward	TTGCGAGTAAAAGTAATTTTTTCATTGGCG
P63	CtrR7mut vector reverse	TACTTTTACTCGCAATTTAACTTCTGCTGCCGCTGCTGG
P64	pBOMB5 MS2-CtrR3 reverse	CAGACACCATCAGGGTCTGGAATTCTAGGTTTCTTCTTCTGTTTTTGC
P65	pBOMB5 MS2-CtrR3 link	CCCTGATGGTGTCTGAAAAACGTACCCTGATGGTGTACGTGGTAAAATAACTCT

P66	pBOMB5 MS2-RnpB T1 reverse	CTTTTGGAGGGGCAGGTACCACCGGTGGATCCGTCGACGCG
P67	pBOMB5 MS2-RnpB T1 forward	GTTTTTACGTACTCCGAATTCCAGACCCTGATGGTG
P68	pBOMB5 MS2-RnpB T1 link	CTGCCCCTCCAAAAGCAAAAACCCGCCGAAGCGGGTTTTTACGTACTCC
P69	CtrR3mut vector forward	TGGACTCGTTATTTGAAAGGACACGAAAATCCAAGATTCC
P70	CtrR3mut vector reverse	CAAATAACGAGTCCACCGAG
P71	pRSETC vector forward	CAGCCTGAATGGCG
P72	pRSETC vector reverse	ATTTCGCGGGATCGAGATC
P73	pRSETC CtrR3 forward	TCGATCCCGCGAAATGAATCGGGGAAAAATTTCAATAAAAAAC
P74	pRSETC tetR reverse	CGCCATTCAGGCTGCTTAAGACCCACTTTCACATTTAAGTTG
P75	pBAD33.1 vector forward	CTGTTGTTTGTCGGTGAACG
P76	pBAD33.1 vector reverse	GAGCTCGAATTCGCTAGCC
P77	pBAD33.1 gfp forward	AGTAAAGGAGAAGCACTTTTCAC
P78	pBAD33.1 gfp reverse	ACCGACAAACAACAGTTACTTGTATAGTTCATCCATGC
P79	pBAD33.1 hctB::gfp forward	AGCGAATTCGAGCTCCTCCTTGTCGATAGATCAAATAAG
P80	hctB::gfp reverse	TGCTTCTCCTTTACTGCGTTTCTTTTGTACTCCCAAC
P81	pBAD33.1 ytgB::gfp forward	AGCGAATTCGAGCTCGTTCCAGCACAATGTTCGCAC
P82	ytgB::gfp reverse	TGCTTCTCCTTTACTGGACCAAGCAATTGCATTATCTC
P83	pBAD33.1 ctl0389::gfp forward	AGCGAATTCGAGCTCCGAAGCTTCGATAGAAAGTAAGG
P84	ctl0389::gfp reverse	TGCTTCTCCTTTACTGTAACCGTATACACATGCGC
P85	pBAD33.1 ctl0015::gfp forward	AGCGAATTCGAGCTCCTGGCAGATCGCCAATTTG
P86	pBAD33.1 ctl0015::gfp reverse	TGCTTCTCCTTTACTTAACAGCACCCATACTCCTAAG
P87	pBAD33.1 rpsT::gfp forward	AGCGAATTCGAGCTCGTTCTTTGCGTTAAAGATAACAG
P88	pBAD33.1 rpsT::gfp reverse	TGCTTCTCCTTTACTGACTTTCTTGCTCGGTTTTC
P89	pBAD33.1 ctl0674::gfp forward	AGCGAATTCGAGCTCGCAGACACCACTACAATTTCAG
P90	pBAD33.1 ctl0674::gfp reverse	TGCTTCTCCTTTACTCAAAGAACAGAGAATAGAGATCATG
P91	pBAD33.1 ctl0190::gfp forward	AGCGAATTCGAGCTCGCGTAATGAGAAAGATTCCCCTA
P92	pBAD33.1 ctl0190::gfp reverse	TGCTTCTCCTTTACTTCCTCCTACACACTTATTCCGC
P93	pBAD33.1 rpsM::gfp forward	AGCGAATTCGAGCTCAACAATTTTTGACCTAAGATGC
P94	pBAD33.1 rpsM::gfp reverse	TGCTTCTCCTTTACTAGGAATATCTATTCCAATGATG
P95	pBAD33.1 gatA::gfp forward	AGCGAATTCGAGCTCTCCCGTGTCGTTGGGAG
P96	pBAD33.1 gatA::gfp reverse	TGCTTCTCCTTTACTTCTTAATTCTAAAGCACTCTTACG
P97	pBOMB5 nMen vector reverse	GTAAATTTGATAAAAACCTAAAAACATCG
P98	pBOMB5 hctA::gfp forward	TTTTATCAAATTTACATTAAAACTGAAAAAAATAGTTTAAAACAAC
P99	pBOMB5 hctA::gfp reverse	TGCTTCTCCTTTACTCATTTTTTTTGCCGTATCTTTTAGC
P100	pBOMB5 hctB::gfp forward	TTTTATCAAATTTACCTCCTTGTCGATAGATCAAATAAG
P101	pBOMB5 ytgB::gfp forward	TTTTATCAAATTTACGTTCCAGCACAATGTTCGCAC
P102	pBOMB5 ctl0389::gfp forward	TTTTATCAAATTTACCGAAGCTTCGATAGAAAGTAAGG
P103	pBOMB5 ctl0389m1::gfp forward	AGAGCAGTTATGGCTTGTTGCG
P104	pBOMB5 ctl0389m1::gfp reverse	CCGCAGGATTTCCTTACTTTC
P105	pBOMB5 ctl0389m1::gfp link	AAGGAAATCCTGCGGCGGGGAGAGAGCAGTTATGGCT
P106	pBOMB5 ctrR3m1 forward	GACACGAAAATCCAAGATTCC
P107	pBOMB5 ctrR3m1 link	TGGACTCGTTATTTGGGGAGACACGAAAATCCAA
P108	hctA RT forward	CGTAAAGAGTCCATTAAAGCAG
P109	hctA RT reverse	CTACTGTTTTTGTAGCGCGAAC
P110	hctB RT forward	TAGCTGTTGCTTTCTTAGCTA
P111	hctB RT reverse	CTGTAGCAGCTCGTAAGCCTGTA
P112	omcB RT forward	TTAGAGACCTCTATGGCAGAGT
P113	omcB RT reverse	AACCGGAGCAACCTTTTTACG
P114	16s rRNA RT forward	GGAAACGGCCGCTAATACCG
P115	16s rRNA RT reverse	GTAGGCCTTTACCCCACCAAC
P116	lhtA northern probe	GAGTCAGAAGCTATTCCATGGCGT
P117	tRNA-thr northern probe	CGCGTTACGAATGCGTTGCTCTACC
P118	CtrR1 northern probe	CTAAGCGACTACCCTAATCGAATTAC
P119	CtrR3 northern probe	ACTCGTTATTTGGGAGGACACGAA
P120	CtrR4 northern probe	AGACACGGTCACCCCTAACTACCA
P121	CtrR7 northern probe	GAAGCGGATCTAAGCTGTGTAAGC
P122	CtrR0332 northern probe	GCAATAAAGTGCATCTCTGTAGC
P123	tmRNA northern probe	CCGTATTTAGGTAACAACTTTGC
P124	CtrR3mut northern probe	CCCCACTAGGCAAAAACAGAAGAAG
P125	MS2 northern probe	CAGACCCTGATGGTGTCTGAAAAAC
P126	5s rRNA northern probe	TTCGGAATGGTGTCAGGTGTTTCCCTCTC
P127	euo qPCR and RT forward	TTATTCCGTGGGACAAGTGG
P128	euo qPCR and RT reverse	TGCAAGACTTTTCCCTTTGC
P129	gapdh qPCR forward	AGGCGCTCACTGTTCTCTCCC
P130	gapdh qPCR reverse	CGCAAGGCTCGTAGACGCGC

Table 6. List of plasmids and strains generated in this study

Plasmids used to transform in *C. trachomatis* serovar L2

Name	Description	Marker	Source
pBOMB4-tet-mCherry	Tet-inducible protein expression plasmid	AmpR	Bauler 2014
pBOMB4-Δcassette	pBOMB4-tet-mCherry without the expression cassette	AmpR	This study
pBOMB5-tet-lhtA	Tet-inducible lhtA expression plasmid. Only one tet operator and expression cassette is placed downstream of *bla* gene	AmpR	This study
pBOMB5-tet-mCherry	Tet-inducible mCherry expression plasmid	AmpR	This study
pSUmC 4.0-lhtA knockout	Used for lhtA knockout by allelic exchange. GFP and SpecR cassette flanked by ~3kb homology to the 5' and 3' of *ihtA*	SpecR	This study
pBOMB5-tet-CtrR1	Tet-inducible CtrR1 expression plasmid	AmpR	This study
pBOMB5-tet-CtrR2	Tet-inducible CtrR2 expression plasmid	AmpR	This study
pBOMB5-tet-CtrR3	Tet-inducible CtrR3 expression plasmid	AmpR	This study
pBOMB5-tet-CtrR4	Tet-inducible CtrR4 expression plasmid	AmpR	This study
pBOMB5-tet-CtrR5	Tet-inducible CtrR5 expression plasmid	AmpR	This study
pBOMB5-tet-CtrR6	Tet-inducible CtrR6 expression plasmid	AmpR	This study
pBOMB5-tet-CtrR8	Tet-inducible CtrR8 expression plasmid	AmpR	This study
pBOMB5-tet-CtrR0332	Tet-inducible CtrR0332 expression plasmid	AmpR	This study
pBOMB5-tet-CTIG643	Tet-inducible CTIG643 expression plasmid	AmpR	This study
pBOMB5-tet-CTIG327	Tet-inducible CTIG327 expression plasmid	AmpR	This study
pBOMB5-tet-CTIG270	Tet-inducible CTIG270 expression plasmid	AmpR	This study
pBOMB5-tet-CTIG360	Tet-inducible CTIG360 expression plasmid	AmpR	This study
pBOMB5-tet-CTIG498	Tet-inducible CTIG498 expression plasmid	AmpR	This study
pBOMB5-tet-CTIG504	Tet-inducible CTIG504 expression plasmid	AmpR	This study
pBOMB5-tet-CTIG684	Tet-inducible CTIG684 expression plasmid	AmpR	This study
pBOMB5-tet-MS2-CtrR3	Tet-inducible MS2-CtrR3 expression plasmid	AmpR	This study
pBOMB5-tet-MS2-RnpB T1	Tet-inducible MS2-RnpB T1 expression plasmid	AmpR	This study
pBOMB5-tet-CtrR3mut	Tet-inducible CtrR3mut expression plasmid	AmpR	This study
pBOMB5-lhtA-hctA::gfp	Tet-inducible lhtA expression + hctA translational fusion	AmpR	This study
pBOMB5-lhtA-hctB::gfp	Tet-inducible lhtA expression + hctB translational fusion	AmpR	This study
pBOMB5-CtrR3-hctB::gfp	Tet-inducible CtrR3 expression + hctB translational fusion	AmpR	This study
pBOMB5-CtrR3-ytgB::gfp	Tet-inducible CtrR3 expression + ytgB translational fusion	AmpR	This study
pBOMB5-CtrR3-ctl0389::gfp	Tet-inducible CtrR3 expression + ctl0389 translational fusion	AmpR	This study
pBOMB5-CtrR3mut-ytgB::gfp	Tet-inducible CtrR3mut expression + ytgB translational fusion	AmpR	This study
pBOMB5-CtrR3mut-ctl0389::gfp	Tet-inducible CtrR3mut expression + ctl0389 translational fusion	AmpR	This study
pBOMB5-CtrR3-ctl0389m1::gfp	Tet-inducible CtrR3 expression + ctl0389m1 translational fusion	AmpR	This study
pBOMB5-CtrR3m1-ctl0389m1::gfp	Tet-inducible CtrR3m1 expression + ctl0389m1 translational fusion	AmpR	This study

Plasmids used to transform in *E. coli* (NEB5-alpha)

Name	Description	Marker	Source
pRSETC	IPTG-inducible protein expression plasmid	AmpR	Thermo
pRSETC-tet-CtrR3	Tet-inducible CtrR3 expression plasmid	AmpR	This study
pRSETC-tet-CtrR3mut	Tet-inducible CtrR3mut expression plasmid	AmpR	This study
pBAD33.1	Arabinose-inducible protein expression plasmid	CmR	Chung 2010
pBAD33.1-hctB::gfp	Arabinose-inducible hctB::gfp expression plasmid	CmR	This study
pBAD33.1-ytgB::gfp	Arabinose-inducible ytgB::gfp expression plasmid	CmR	This study
pBAD33.1-ctl0389::gfp	Arabinose-inducible ctl0389::gfp expression plasmid	CmR	This study
pBAD33.1-ctl0015::gfp	Arabinose-inducible ctl0015::gfp expression plasmid	CmR	This study
pBAD33.1-rpsT::gfp	Arabinose-inducible rpsT::gfp expression plasmid	CmR	This study
pBAD33.1-ctl0674::gfp	Arabinose-inducible ctl0674::gfp expression plasmid	CmR	This study
pBAD33.1-ctl0190::gfp	Arabinose-inducible ctl0190::gfp expression plasmid	CmR	This study
pBAD33.1-rpsM::gfp	Arabinose-inducible rpsM::gfp expression plasmid	CmR	This study
pBAD33.1-gatA::gfp	Arabinose-inducible gatA::gfp expression plasmid	CmR	This study

Chapter 3: Development of a sRNA-mediated conditional knockdown system in *Chlamydia trachomatis*

Abstract

The molecular mechanism of *Chlamydia trachomatis* pathogenesis remains largely unexplored due to the scarcity of genetic tools in this important obligate intracellular pathogen. In addition, *Chlamydia* has a reduced genome with mostly essential genes, which cannot be investigated using gene deletion approaches. Recently, the CRISPR interference (CRISPRi) system for conditional gene knockdown has been described in *C. trachomatis*. Although powerful, CRISPRi cannot be utilized to investigate the function of genes in an operon as it causes polar effects on downstream or upstream genes. In the present work, we describe a novel sRNA-mediated conditional knockdown system in *C. trachomatis*. We demonstrate that our system can silence a non-essential protein, IncA, in an inducible and reversible manner. We further test the sRNA-mediated knockdown system by targeting a gene in an operon, IncG, and show that knockdown of IncG does not inhibit the protein expression of an upstream gene, IncE. We also demonstrate the power of our genetic system by silencing an essential gene, MOMP, in *C. trachomatis*. Overall, this sRNA-mediated gene knockdown system is an important addition to *Chlamydia* genetics and a great complement to the CRISPRi approach.

Introduction

A conditional knockdown system is needed for investigating gene functions in *C. trachomatis*. *Chlamydia* has a reduced genome that encompasses mostly essential genes. Pan-genomic analysis showed that approximately 700 ORFs, 75% of the chlamydial genome, are part of the 'core' genome, which likely contains genes that are crucial for chlamydial infection (Sigalova et al., 2019). The functions of these genes cannot be investigated via current knockout approaches, such as type II introns or allelic exchange (C. M. Johnson & Fisher, 2013; Keb et al., 2021; J. H. Shaw et al., 2018; Weber & Faris, 2019). Thus, conditional knockdown systems in *C. trachomatis* are required to elucidate the functions of the majority of genes in the chlamydial genome.

A knockdown system in *C. trachomatis* that has been recently described is CRISPR interference (CRISPRi) (Ouellette, 2018; Ouellette et al., 2021). The CRISPRi system involves a complex formed by the single guide RNA (sgRNA) and the catalytically inactive form of Cas9 (dCas9). The sgRNA base pairs with a target sequence in the genome that is upstream of a protospacer adjacent motif (PAM) sequence, which is recognized by the dCas9. The presence of dCas9 will physically block RNA polymerase from transcribing the gene of interest (Bikard et al., 2013; Qi et al., 2013). In the chlamydial CRISPRi system, the sgRNA is constitutively expressed whereas dCas9 is inducibly expressed, making this a conditional knockdown system. Ouellete et al. has demonstrated the power of this system by repressing IncA expression in an inducible and reversible manner (Ouellette et al., 2021). More importantly, the group also showed that they can knockdown the essential chlamydial gene *clpP2* (Wood et al., 2020).

However, the chlamydial CRISPRi system has some limitations. One issue with CRISPRi is that it can cause polar effects. This system represses the transcription of a target gene and as a consequence, will also prevent the expression of downstream or upstream genes. Thus, CRISPRi is not suitable for investigating the function of genes in an operon. This will greatly limit the number of genes that can be studied in *C. trachomatis* with CRISPRi as more than 40% of the chlamydial genes are predicted to be in an operon via MicrobesOnline (Alm et al., 2005). The ability to knockdown a specific gene may also be restricted by the available PAM sites in the chlamydial genome. Ouellette et. al. addressed this limitation by extending the system to include dCas12, which recognizes a different PAM site from dCas9 (Ouellette et al., 2021; Terns, 2018). However, further expansion of the number of available PAM sites would require optimization of additional CRISPR/Cas systems in *Chlamydia*. Additionally, different sgRNA sequences must be individually tested in *C. trachomatis* to evaluate their efficacy, which requires generating separate chlamydial transformants. Thus, *Chlamydia* genetics would benefit from having an additional conditional knockdown system.

Small RNA (sRNA)-mediated gene silencing is an alternative system for conditional knockdown in prokaryotes. Briefly, sRNAs are engineered to target the RBS of a specific mRNA. The sRNA will prevent the expression of the mRNA by blocking translation initiation and/or destabilizing the mRNA (Man et al., 2011; Na et al., 2013; Nakashima et al., 2006; Noh et al., 2017, p. 201). Importantly, sRNA-mediated knockdown has also been used to specifically target a gene in an operon without causing polar effects on downstream or upstream genes in *E. coli* (Goh et al., 2015).

Additionally, this knockdown system is titratable as sRNA-mediated regulation depends on the stoichiometry between the levels of the sRNA and the mRNA target (Noh et al., 2017, p. 201). However, this also indicates that engineered sRNAs must be expressed at a sufficient level for efficient gene silencing. Groups have circumvented this issue by increasing the stability of the sRNA via placing the target sequence adjacent to a Hfq-binding site or in a hairpin secondary structure (Na et al., 2013; Nakashima et al., 2006; Noh et al., 2017).

In this chapter, we describe a novel sRNA-mediated conditional knockdown system in *C. trachomatis*. We demonstrate that the knockdown system can repress the expression of IncA in an inducible and reversible manner. In addition, we can restore IncA expression using our complementation system. We then used the sRNA-mediated knockdown system to target a specific gene in an operon. We also show that we can silence an essential chlamydial protein with our genetic system. Overall, our sRNA-mediated knockdown system is an important addition to *C. trachomatis* genetics and help elucidate the molecular function of chlamydial genes.

Results

3.1 Development of a conditional knockdown system in *Chlamydia*

3.1a Knockdown of IncA as proof of principle

To develop an inducible knockdown system in *C. trachomatis*, we utilized the pBOMB5 plasmid to overexpress an engineered sRNA that contains an anti-sense sequence to a specific mRNA target. Our strategy for designing the sRNA is to use CtrR3 as a scaffold and replace the main loop of CtrR3 with an anti-sense RNA (asRNA) sequence (Fig. 22A). We took this approach because our previous work indicated that the loop sequence is the target recognition site of CtrR3 (Fig. 16A). Additionally, CtrR3 is a stable sRNA (Fig. 16C) that would allow for high expression of the anti-sense RNA.

As a proof of principle study, we attempted to knockdown a non-essential protein, IncA. IncA is an inclusion membrane protein that is required for homotypic fusion between chlamydial inclusions (Hackstadt et al., 1999; Weber et al., 2016) and thus, lack of IncA in *C. trachomatis* results in multiple inclusions in a single host cell (C. M. Johnson & Fisher, 2013; Ouellette, 2018; Ouellette et al., 2021; Weber et al., 2016). To knockdown IncA, we designed different lengths of asRNAs against the RBS of the IncA mRNA and cloned them into the CtrR3 sRNA (Fig 22A). We used *E. coli* translational fusion to test the knockdown efficiency of the sRNA with 10, 30, or 60 bp targeting sequence. Western blot analysis demonstrated that the co-expression of the 30 bp anti-sense sequence caused the greatest reduction in IncA translational fusion levels (Fig. 22B). This engineered sRNA, which we called C3-IncA, was cloned into pBOMB5 and subsequently transformed into *C. trachomatis*. Immunofluorescence analysis at 24 hpi

showed that induction of C3-IncA expression in *Chlamydia* resulted in a loss of IncA staining at the inclusion membrane, as well as the formation of multiple inclusions within a host cell (Fig. 22C). This effect was not seen in *Chlamydia* overexpressing CtrR3^{mut}, suggesting that the IncA knockdown was specific to the anti-sense sequence. These results demonstrated that we can utilize our system to knockdown a targeted protein.

To measure off-target effects in our system, we conducted progeny assays on the C3-IncA transformant. Previous work demonstrated that knockout or knockdown of IncA has no effect on infectious EB production (Ouellette et al., 2021; Weber et al., 2016). Overexpression of C3-IncA with 50 ng/ml aTc knocked down IncA (Fig. 23A) but caused an 8.4-fold decrease in progeny at 32 hpi compared to the uninduced control (Fig. 23B). This suggests that the level of C3-IncA produced with 50 ng/ml of aTc is affecting expression of off-target mRNAs. To circumvent this issue, we induced C3-IncA expression with 3 or 10 ng/ml of aTc. Overexpression of C3-IncA with 3 ng/ml of aTc was able to decrease IncA protein (Fig. 23A) but no longer caused a defect in progeny (Fig. 23B). RT-qPCR also showed that induction of C3-IncA expression with 3 ng/ml caused a 3-fold reduction in the mRNA levels of IncA but not EUO (Fig. 23C). These results suggest that we can titrate the expression of the sRNA to minimize off-target effects.

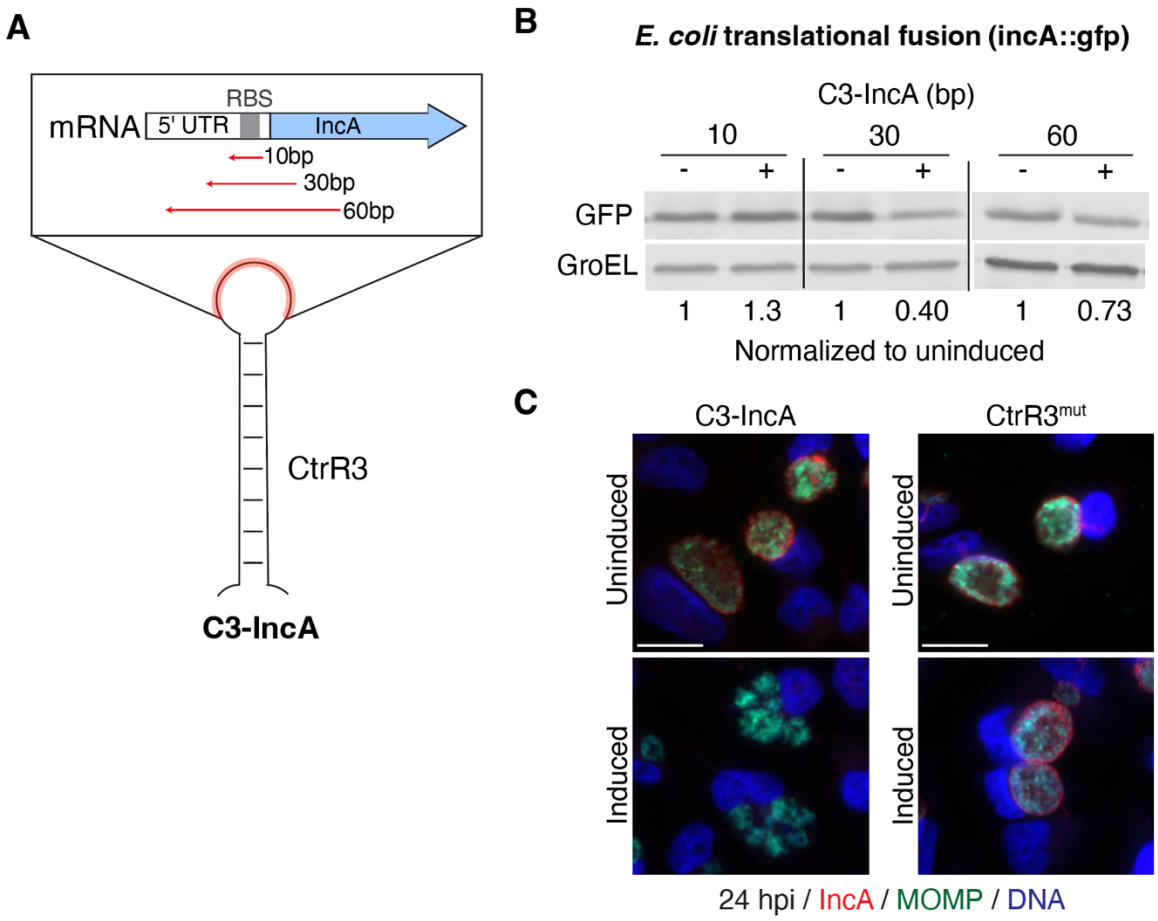

Figure 22. Development of a sRNA-mediated knockdown system in *C. trachomatis*.
(A) Schematic of the engineered sRNA designed to knockdown IncA.
(B) Western blot analysis of lysates from *E. coli* co-expressing IncA translational fusion GFP with C3-IncA that has a 10 bp, a 30 bp, or a 60 bp asRNA sequence. GFP levels are shown and GroEL served as loading control. Normalized values are shown below where GFP was normalized first to GroEL and then to the respective uninduced controls.
(C) Immunofluorescence images of HeLa cells infected with either C3-IncA or CtrR3^{mut} transformants and treated with 50 ng/mL aTc from 1-24 hpi are shown. IncA staining is shown in red. *C. trachomatis* was detected with the MOMP antibody (green), and DNA was detected by DAPI (blue). White scale bar: 20 μm.

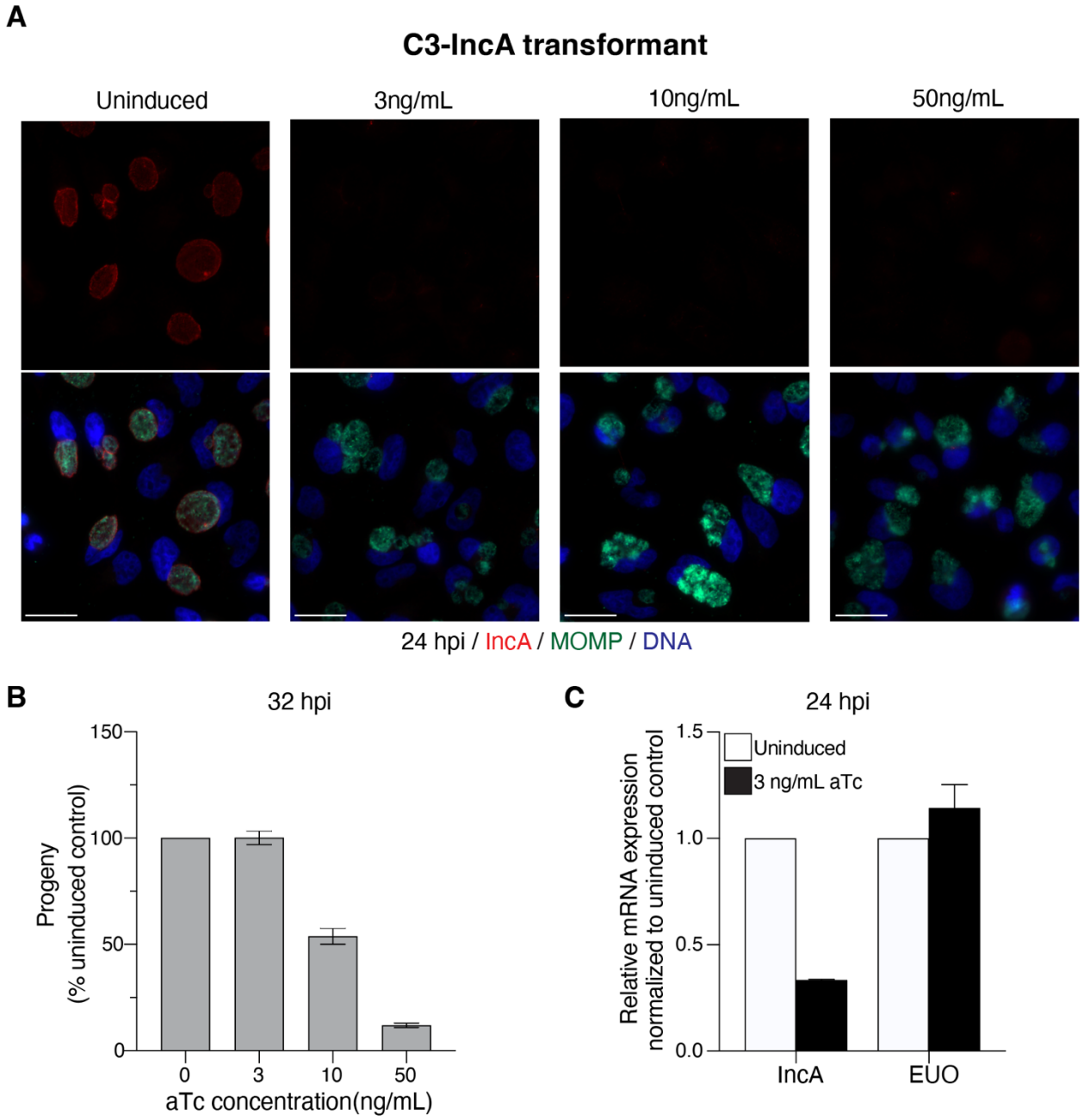

Figure 23. Low aTc concentration can minimize off-target effects.
(A) Immunofluorescence images of HeLa cells infected with C3-IncA transformants and were treated with 3 ng/mL, 10 ng/mL, or 50 ng/mL of aTc from 1-24 hpi are shown. IncA staining is shown in red. *C. trachomatis* was detected with the MOMP antibody (green) and DNA was detected by DAPI (blue). White scale bar: 50 μm.
(B) Infectious EBs produced from HeLa cells infected with C3-IncA transformants and incubated with different amount of aTc from 1-32 hpi were quantified by progeny assay.

The number of infectious EBs in the induced conditions is expressed as a percentage of the number of EBs in uninduced control samples. Data are mean ± SEM (n= 2).
(C) RT-qPCR of total RNA extracted from HeLa cells infected with C3-IncA transformants and treated with 3 ng/mL of aTc from 1-24 hpi for the transcript levels of IncA and EUO. 16S rRNA and GAPDH served as the reference genes and each sample was normalized to their respective uninduced control. Data is presented as mean ± SEM (n= 2).

3.1b Knockdown of IncA in C. trachomatis is reversible

We next tested if our inducible knockdown system is reversible. We induced C3-IncA expression with 3 ng/ml of aTc from 1 hpi. At 20 hpi, we washed out the inducer and collected samples 4 or 6 hours after (24 and 26 hpi). We also conducted the same experiment without removing aTc as negative control. Immunofluorescence analysis detected IncA protein staining 4 and 6 hours after aTc removal (Fig. 24). In contrast, IncA remained undetectable in the control. This data demonstrated that the knockdown of a target is reversible.

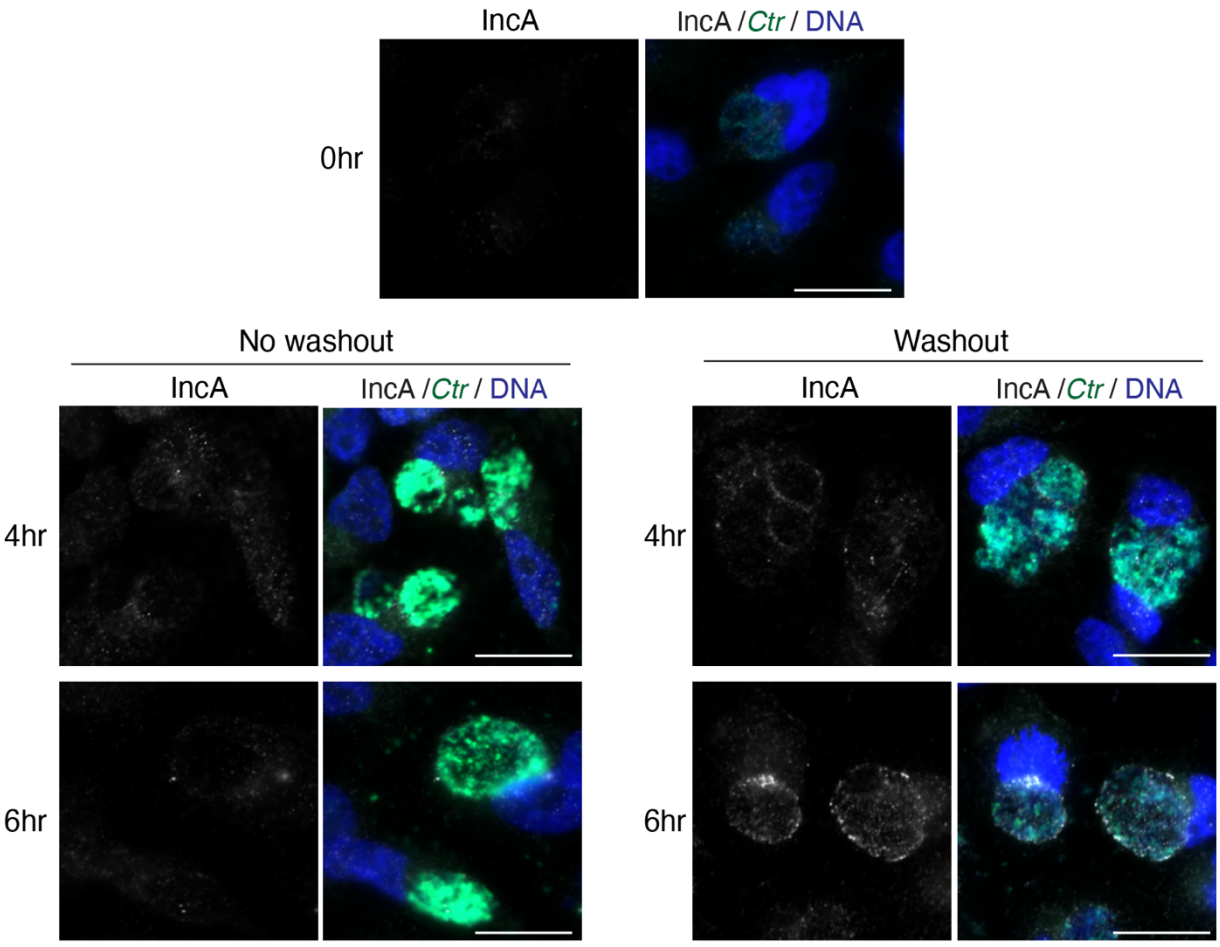

Figure 24. IncA knockdown is reversible.
Immunofluorescence images of HeLa cells that were infected with C3-IncA transformants and treated with 3 ng/mL of aTc from 1-20 hpi. At 20 hpi (0hr), aTc was either left in the media or washed out, and samples were analyzed 4 and 6 hr after. IncA staining is shown in gray. *C. trachomatis* was detected with MOMP antibody (green) and DNA was detected with DAPI (blue). White scale bar: 20 μm.

3.1c Targeting RBS is required for sRNA-mediated knockdown of IncA

To define the base-pair requirement for C3-IncA to regulate the IncA mRNA, we conducted a mutational analysis. We generated six versions of C3-IncA (5nt1-5nt6) with each version containing 5 nucleotide substitutions that resulted in a loss of base-pairing to a specific region of the IncA mRNA (Fig. 25A). We then utilized *E. coli* to test the ability of the mutated C3-IncAs to regulate the expression of the IncA translational fusion. Western blot analysis demonstrated that mutations in the anti-RBS of C3-IncA (5nt4) abrogated the ability of the sRNA to downregulate the GFP levels of the IncA translational fusion (Fig. 25B). To a lesser extent, mutations in C3-IncA sequence that base-pairs with the 5' coding region of the mRNA (5nt1 and 5nt2) also decreased protein levels of IncA translational fusion. To further test if the RBS is the more important target site, we designed a new anti-sense sequence that targets the RBS but not the 5' coding region (C3-IncA2) (Fig. 25C). Using *E. coli* translational fusion, we observed that co-expression of C3-IncA2 was able to decrease the GFP level of the IncA translational fusion. More importantly, overexpression of C3-IncA2 in *C. trachomatis* also resulted in the lack of IncA staining by immunofluorescence analysis and the multiple inclusions phenotype (Fig. 26B). Overall, these analyses suggest that targeting the RBS is required for the sRNA-mediated knockdown system.

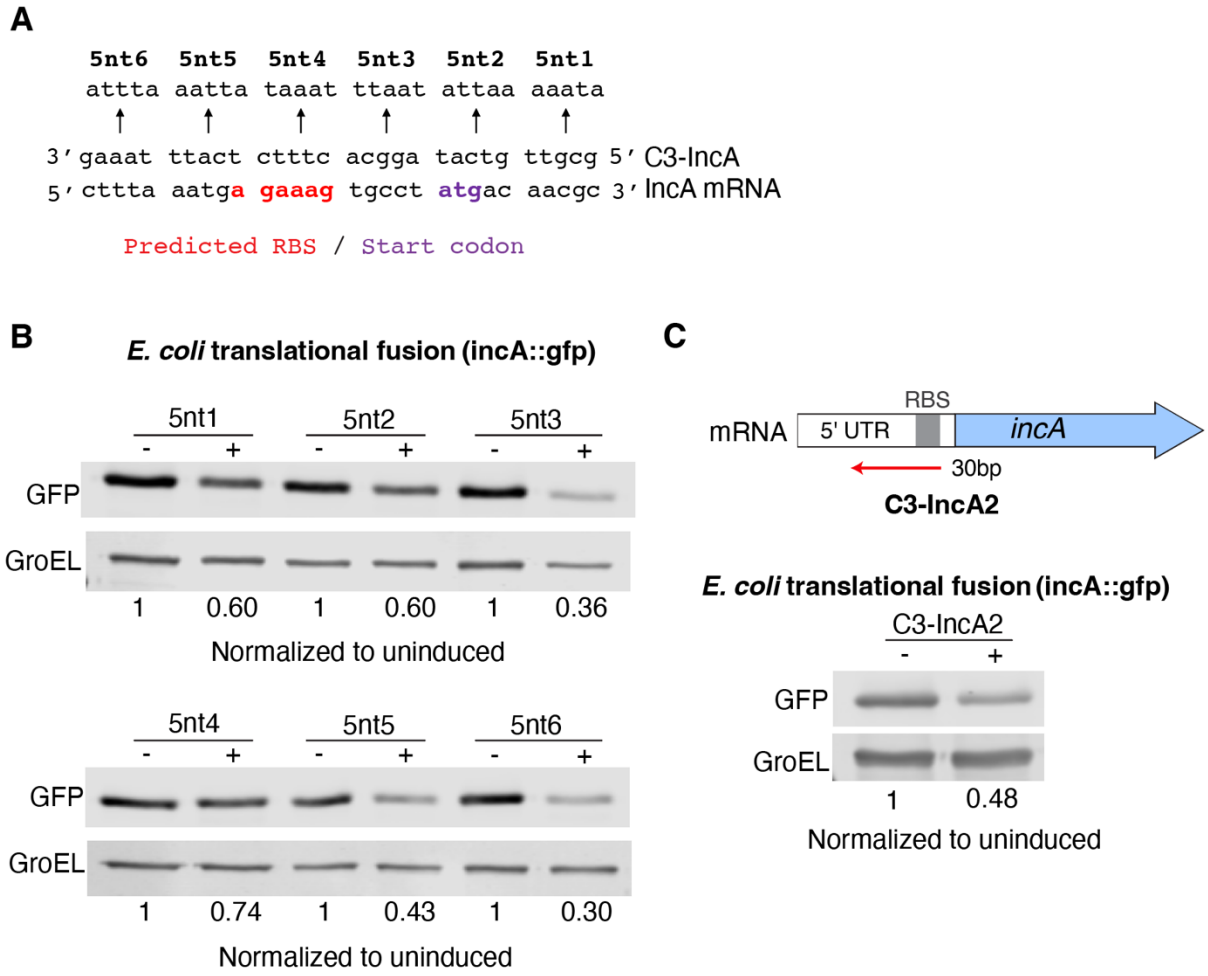

Figure 25. Targeting the RBS is required from IncA knockdown.
(A) Schematic of the C3-IncA anti-sense sequence and the IncA mRNA sequence. Mutations made for 6 different versions of the C3-IncA (5nt1-5nt6) are indicated by the arrows.
(B) Western blots of lysates from *E. coli* co-expressing IncA translational fusion GFP with each of the 6 mutated versions of C3-IncA. GFP levels are shown and GroEL serves as a loading control. Normalized values are shown below where GFP was normalized first to GroEL and then to the respective uninduced controls.
(C) Top: Schematic of C3-IncA2. Bottom: Western blots of lysates from *E. coli* co-expressing IncA translational fusion GFP with C3-IncA2. GFP levels are shown and GroEL serves as a loading control. Normalized values are shown below where GFP was normalized first to GroEL and then to the respective uninduced controls.

3.1d Complementation of IncA in the knockdown system

To complement IncA in our knockdown system, we aimed to co-express CtrR3-IncA2 with an exogenous IncA protein. The complement IncA protein was designed to have a C-terminal Flag tag and be driven under a Tet promoter (Fig 26A). This Tet promoter sequence originated from the chlamydial shuttle plasmid pASK and differs from the one driving the sRNA expression. This is because we wanted to prevent having identical sequences on the plasmid, which may cause recombination in *C. trachomatis*. In addition, we removed the second Tet operator in this promoter sequence to ensure that the complementation plasmid has a total of two Tet operators. Importantly, the 5' UTR sequence of *incA-flag* also originated from the pASK plasmid and contains an RBS that does not form complementarity base-pairing with CtrR3-IncA2. As a negative control, we designed a plasmid that co-expresses CtrR3-IncA2 with mCherry (Fig. 26A)

Next, we generated transformants that either harbored the control or the complementation plasmid. Control transformant induced with 3 ng/mL aTc resulted in mCherry expression (data not shown) and IncA knockdown at 24 hpi (Fig. 26B). This demonstrated that co-expression of CtrR3-IncA2 with mCherry does not affect the ability of the sRNA to knockdown its target. In contrast, immunofluorescence analysis showed that aTc induction on the complementation transformant had similar IncA staining compared to the uninduced control at 24 hpi (Fig. 26C). In addition, immunofluorescence analysis using the Flag antibody showed co-localization with IncA at the inclusion membrane (Fig. 26D), demonstrating that the complementing IncA is exogenously expressed. The uninduced sample had some signal at the inclusion

membrane, suggesting that the Tet promoter driving the complementation protein is leaky. Overall, these data provide evidence that we can perform complementation in our knockdown system.

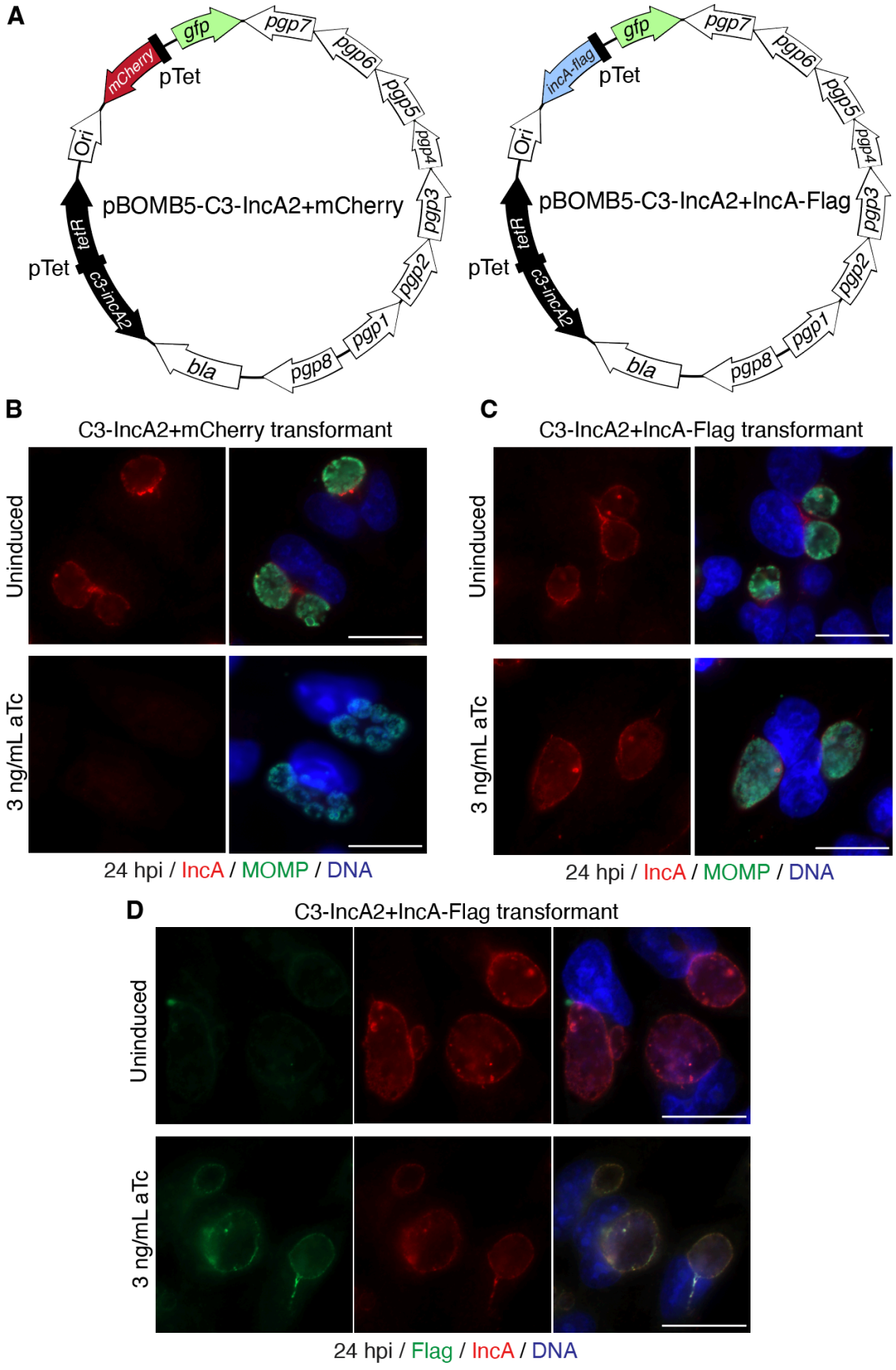
A
gfp
pgp7
pgp6
pgp5
pgp4
pgp3
pgp2
pgp1
pgp8
bla
c3-incA2
tetR
pTet
Ori
mCherry
pBOMB5-C3-IncA2+mCherry
incA-flag
pBOMB5-C3-IncA2+IncA-Flag
B
C3-IncA2+mCherry transformant
C
C3-IncA2+IncA-Flag transformant
Uninduced
3 ng/mL aTc
24 hpi / IncA / MOMP / DNA
D
C3-IncA2+IncA-Flag transformant
24 hpi / Flag / IncA / DNA

Figure 26. Complementation of IncA knockdown.
(A) Plasmid maps of the control (mCherry) and the complementation (IncA-Flag) plasmids.
(B, C) Immunofluorescence images of HeLa cells infected with (B) C3-IncA2+mCherry or (C) C3-IncA2+IncA-Flag transformants and were treated with 3 ng/mL of aTc from 1-24 hpi are shown. IncA staining is shown in red. *C. trachomatis* was detected with the MOMP antibody (green) and DNA was detected with DAPI (blue). White scale bar: 20 μm.
(D) Immunofluorescence images of infected HeLa cells with the same condition as (C). IncA staining is shown in red. IncA-Flag was detected with the Flag antibody (green) and DNA was detected with DAPI (blue). White scale bar: 20 μm.

3.2 Knockdown of a gene in an operon

We tested if the knockdown system is able to downregulate the expression of a specific gene in an operon. The operon we chose to test is the incDEFG operon because we have available antibodies to the inclusion membrane proteins, IncE and IncG. We designed a 30 bp asRNA sequence against the IncG mRNA, which targeted a portion of the RBS (Fig. 27A). We chose this anti-sense sequence because it gave us the least number of bioinformatically predicted off-targets via TargetRNA2 (data not shown) (Kery et al., 2014). The anti-sense sequence was cloned into CtrR3 (C3-IncG) and confirmed by *E. coli* translational fusion to downregulate IncG translational fusion GFP level (data not shown).

We then cloned C3-IncG into pBOMB5 and successfully transformed the plasmid into *C. trachomatis*. Immunofluorescence analysis at 24 hpi demonstrated that induction of C3-IncG expression with 3 ng/mL and 10 ng/mL of aTc resulted in the loss of IncG (Fig. 27B). Knockdown of IncG also resulted in the loss of 14-3-3β recruitment to the inclusion membrane, which is a host protein that is proposed to interact with IncG (Fig. 27C) (Scidmore & Hackstadt, 2001). In contrast, overexpression of C3-IncG did not affect IncE protein expression by immunofluorescence analysis at 24 hpi (Figs. 28A, B), suggesting that C3-IncG is able to knockdown IncG without depleting another protein encoded in the operon. Immunofluorescence analysis with IncE antibodies also showed multiple inclusions under the C3-IncG overexpressing condition, suggesting that IncG may be required for inclusions fusion (Fig. 28A). Additionally, antibodies against the bacterial membrane protein, MOMP, showed larger chlamydiae in the induced cells compared to the uninduced control, which may indicate that C3-IncG overexpression

had deleterious effects on the chlamydial infection (Fig. 28A). Overall, these data suggest that C3-IncG overexpression is able to specifically knockdown IncG without largely affecting the protein levels of IncE.

Next, we investigated if the transcript levels of IncE and IncG are affected by C3-IncG overexpression. RT-qPCR analysis at 24 hpi showed that overexpression of C3-IncG starting at 1hpi resulted in a 1.7-fold and 1.8-fold decrease in IncE and IncG transcript levels, respectively (Fig. 29A). In contrast, the levels of EUO and IncA mRNA remained unaffected compared to the uninduced control (Fig. 29A). To minimize the confounding factor that C3-IncG overexpression at 1 hpi had a deleterious effect on *C. trachomatis*, we also induced C3-IncG expression at 16 hpi and analyzed at 24 hpi. In this condition, 16S rRNA levels were no longer affected by C3-IncG overexpression (Fig. 29B), whereas IncE and IncG mRNA levels were still decreased (Fig. 29A). This result suggests that C3-IncG overexpression may destabilize the entire incDEFG operon mRNA.

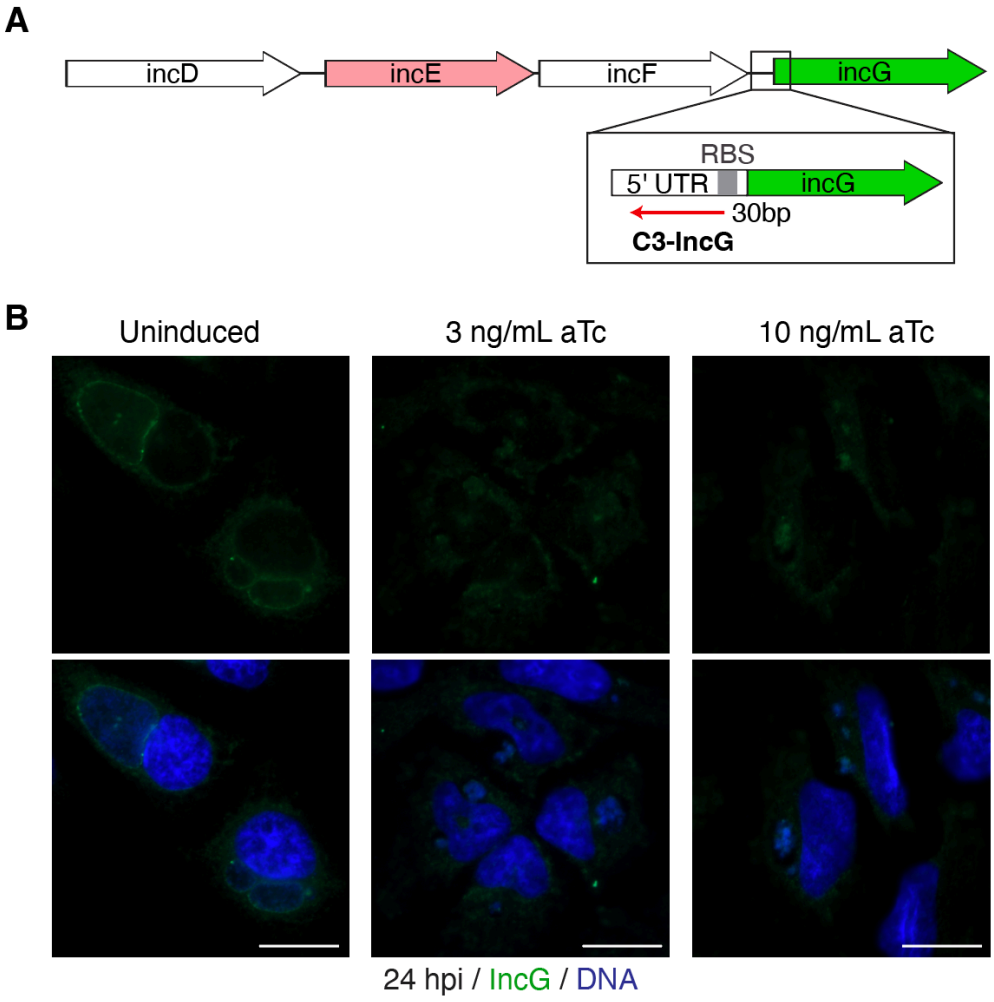
A
incD
incE
incF
incG
RBS
5' UTR
incG
30bp
C3-IncG
B
Uninduced
3 ng/mL aTc
10 ng/mL aTc
24 hpi / IncG / DNA
C
Uninduced
3 ng/mL aTc
24 hpi / IncG / 14-3-3β / DNA

Figure 27. Knockdown of a gene in an operon, IncG.
(A) Schematic of the IncDEFG operon and the target site of C3-IncG.
(B) Immunofluorescence images of HeLa cells infected C3-IncG+mCherry and treated with 3 ng/mL or 10 ng/mL of aTc from 1-24 hpi are shown. IncG staining is shown in green and DNA was detected with DAPI (blue). White scale bar: 20 μm.
(C) Immunofluorescence images of infected HeLa cells with the same condition as (B). IncG staining is shown in green and 14-3-3β staining is shown in red. DNA was detected with DAPI (blue). White scale bar: 20 μm. These images were produced by Dr. Janina Ehses.

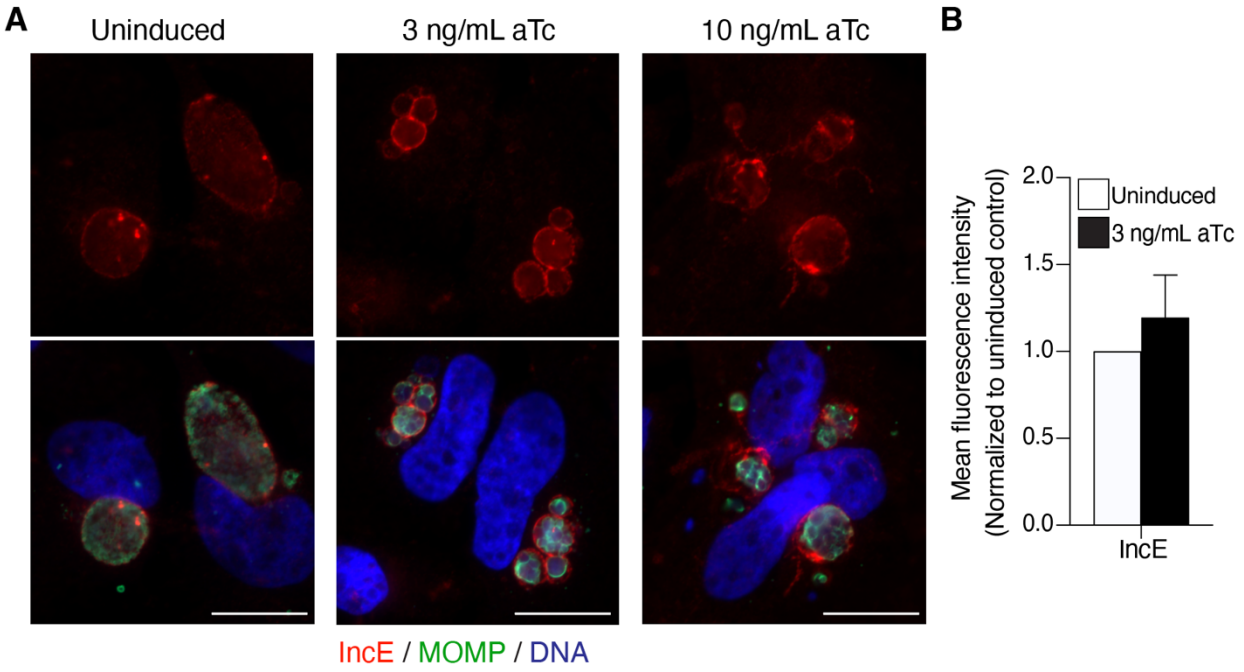

Figure 28. Knockdown of IncG does not affect IncE protein expression.
(A) Immunofluorescence images of infected HeLa cells with the same condition as (Fig. 27B). IncE staining is shown in red. *C. trachomatis* was detected with MOMP antibody (green) and DNA was detected with DAPI (blue). White scale bar: 20 μm.
(B) Mean fluorescence intensity was calculated from immunofluorescence images of HeLa cells infected with C3-IncG+mCherry and treated with 3 ng/mL of aTc from 1-24 hpi using ImageJ. Mean fluorescence intensity was calculated by dividing average intensity density of an inclusion by the area of the inclusion. The mean fluorescence intensity of 3 ng/mL aTc sample was then normalized to the uninduced control. For each experiment, at least 100 inclusions were analyzed. Data is presented as mean ± SEM (n= 2). This quantification was conducted by Dr. Janina Ehses.

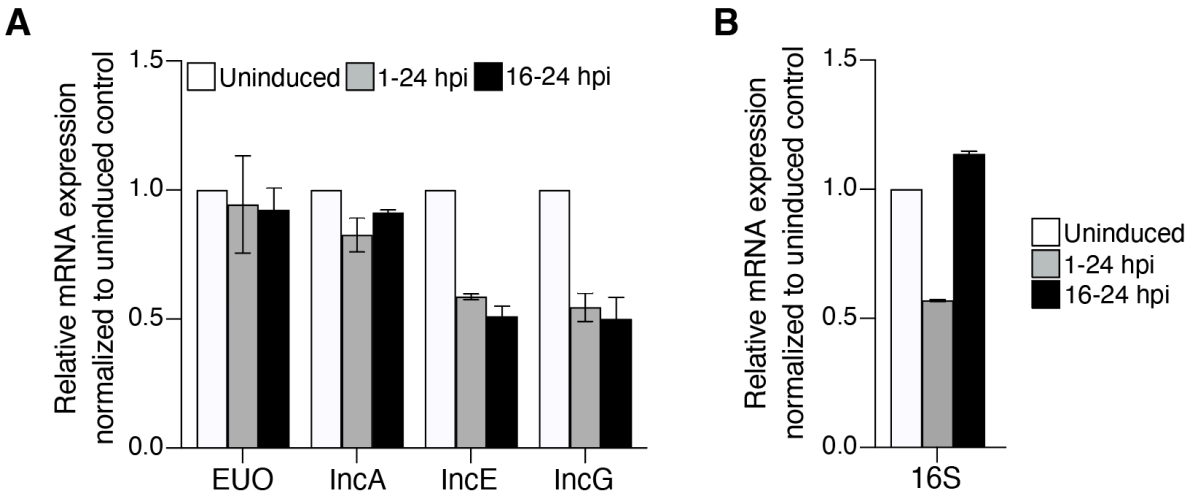

Figure 29. C3-IncG overexpression destabilizes the IncDEFG operon.
HeLa cells infected with C3-IncG+mCherry transformants and treated with 3 ng/mL of aTc from 1-24 hpi or 16-24 hpi were analyzed by RT-qPCR for (A) EUO, IncA, IncE, and IncG. 16S rRNA and GAPDH served as reference genes. (B) shows RT-qPCR for 16S rRNA levels with GAPDH served as a reference gene. Each experimental condition was normalized to the respective uninduced control. Data is presented as mean ± SEM (n= 2). This data was completed with the help of Dr. Janina Ehses.

3.3 Knockdown of an essential chlamydial gene

To investigate if we can silence an essential gene using our system, we knock downed the chlamydial major outer membrane protein (MOMP or OmpA). MOMP is proposed to provide cell wall rigidity to EBs (Hatch, 1996, p. 199), to function as a general porin in the outer membrane (G. Sun et al., 2007), and to act as an adhesion protein for host attachment (Su et al., 1990; Swanson & Kuo, 1994). Following our general knockdown approach, we designed a 30 bp asRNA that includes an anti-RBS to the MOMP mRNA and cloned it into CtrR3 (C3-MOMP) (Fig. 30A). We first confirmed that C3-MOMP can downregulate its target in *E. coli* translational fusion (data not shown) and subsequently cloned it into pBOMB5, which was used to transform *C. trachomatis*. Western blot analysis at 24 hpi showed that C3-MOMP overexpression decreased MOMP protein levels in an aTc dose-dependent manner (Fig. 30B, C). This regulation is specific to MOMP because overexpression of C3-MOMP at 3 ng/mL did not affect the levels of the chlamydial housekeeping protein Hsp60 (Figs. 30D, E). Immunofluorescence analysis at 24 hpi of the transformant overexpressing C3-MOMP showed sparse MOMP intensity at the bacterial membrane, whereas the expression of an inclusion membrane protein, IncE, remained unaffected (Fig. 30F). In addition, C3-MOMP transformant induced with aTc resulted in the formation of few large aberrant RBs in the inclusion under phase-contrast microscopy, which resembles ampicillin induced-persistence (Fig. 30G) (Beatty et al., 1994; Hogan et al., 2004; Panzetta et al., 2018; Skilton et al., 2009). Lastly, overexpression of C3-MOMP caused a 16.3-fold decrease in progeny compared to the uninduced control at 32 hpi (Fig. 30H). Overall,

these results demonstrated that our system can knockdown an essential protein in *C. trachomatis*.

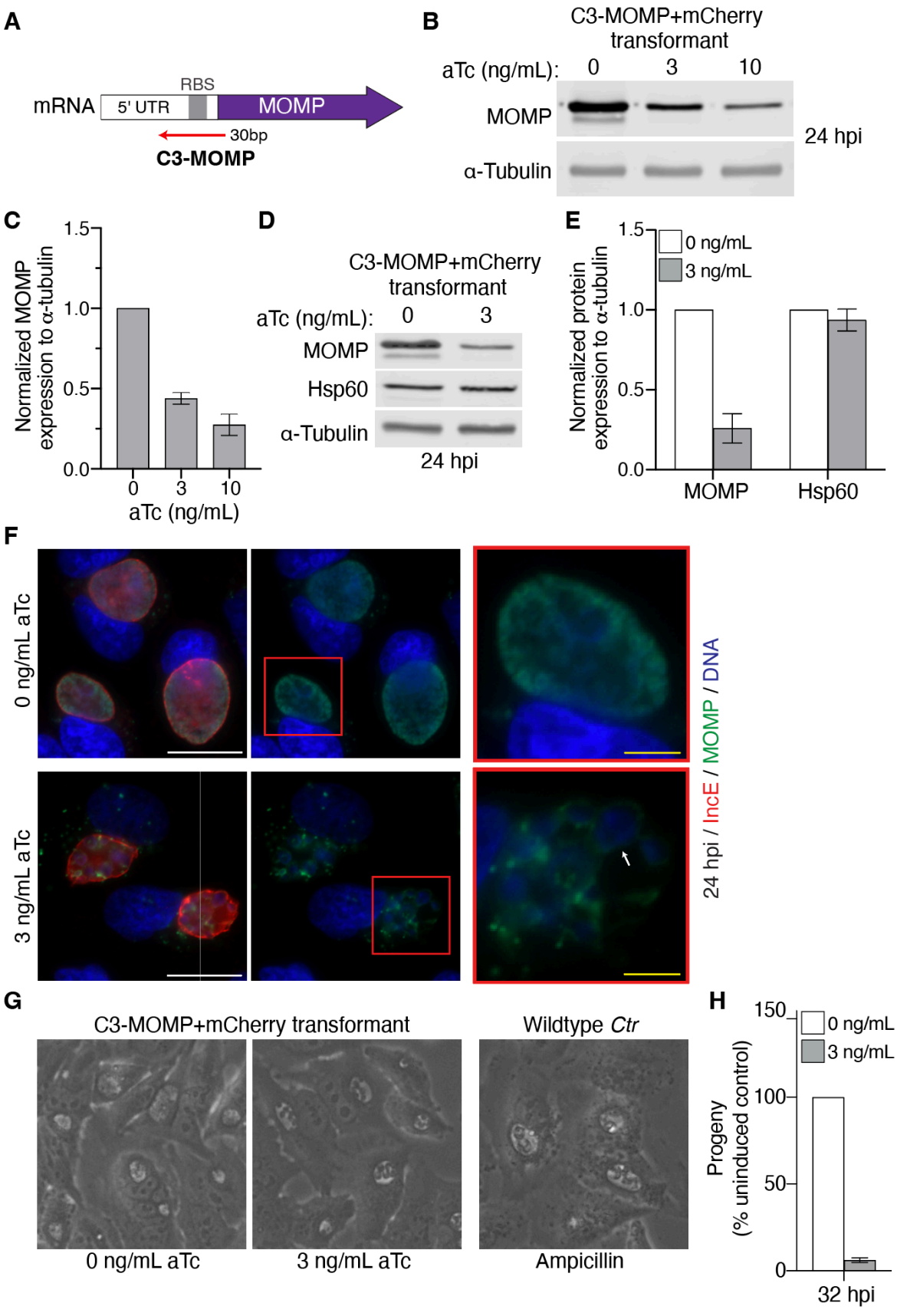
A
mRNA
RBS
5' UTR
MOMP
30bp
C3-MOMP
B
C3-MOMP+mCherry transformant
aTc (ng/mL): 0 3 10
MOMP
α-Tubulin
24 hpi
C
Normalized MOMP expression to α-tubulin
1.5
1.0
0.5
0.0
0 3 10
aTc (ng/mL)
D
C3-MOMP+mCherry transformant
aTc (ng/mL): 0 3
MOMP
Hsp60
α-Tubulin
24 hpi
E
Normalized protein expression to α-tubulin
0 ng/mL
3 ng/mL
MOMP
Hsp60
F
0 ng/mL aTc
3 ng/mL aTc
24 hpi / IncE / MOMP / DNA
G
C3-MOMP+mCherry transformant
Wildtype Ctr
0 ng/mL aTc
3 ng/mL aTc
Ampicillin
H
Progeny (% uninduced control)
150
100
50
0
0 ng/mL
3 ng/mL
32 hpi

Figure 30. Knockdown of an essential protein, MOMP.
(A) Schematic of the MOMP mRNA and the target site of C3-MOMP.
(B) Western blot analysis of lysates from HeLa cells infected with C3-MOMP+mCherry transformants and treated with 3 or 10 ng/mL of aTc from 1-24 hpi. MOMP levels are shown and α-tubulin served as loading control.
(C) Quantification of the western blots in (B). MOMP was normalized first to α-tubulin and then to the uninduced control. Data are mean ± SEM (n= 2).
(D) Western blot analysis of lysates from (B). MOMP and Hsp60 levels are shown. α-tubulin served as loading control.
(E) Quantification of the western blots in (D). MOMP and Hsp60 were first normalized to α-tubulin and then to their respective uninduced controls. Data are mean ± SEM (n= 2).
(F) Immunofluorescence images of HeLa cells infected with C3-MOMP+mCherry transformants and treated with 3 ng/mL of aTc from 1-24 hpi are shown. IncE staining is shown in red and MOMP staining is shown in green. DNA was detected with DAPI (blue). White arrow indicates a single aberrant RB. White scale bar: 20 μm; yellow scale bar: 5 μm.
(G) Phase contrast images of HeLa cells infected with C3-MOMP+mCherry transformants or wildtype *C. trachomatis* serovar L2 and treated with 3 ng/mL of aTc or 10 μg/mL of ampicillin from 1-24 hpi are shown.
(H) Infectious EBs produced by HeLa cells infected with C3-IncA transformants and incubated with or without 3 ng/mL of aTc from 1-32 hpi were quantified by progeny assay. The number of infectious EBs in the induced conditions is expressed as a percentage of the number of EBs in uninduced control samples. Data are mean ± SEM (n= 2).

Discussion

Although the CRISPRi system has been described in *C. trachomatis*, we provide justification for developing a second knockdown system. For example, CRISPRi blocks expression on a transcriptional level and causes polar effects, resulting in the silencing of upstream and downstream genes in an operon (Table 7 and 8). In contrast, the sRNA-mediated knockdown system blocks the translation of specific mRNA target and has been shown to not cause polar effects in *E. coli* (Goh et al., 2015). Additionally, testing the knockdown efficiency of sgRNAs is labor-intensive as it requires the generation of individual chlamydial transformants. For our approach, we can test the efficacy of each engineered sRNA in an *E. coli* translational fusion, which has a faster turn-around time (Table 8). Lastly, both approaches have the potential to have off-target effects as well as limited target sites, thus it is imperative to have two systems to provide options and versatility when knocking down a specific gene. CRISPRi and our system can also be utilized to separately knockdown the same gene to demonstrate the specificity of the knockdown to a certain phenotype.

In this study, we developed a novel sRNA-mediated conditional knockdown system in *C. trachomatis* by overexpressing a version of CtrR3 that has its loop sequence modified to target a specific mRNA. The strength of our approach is that the engineered sRNA expression is inducible, titratable, and reversible. The control of the timing of the sRNA expression will be beneficial to investigate the role of the targeted protein during a specific time in the developmental cycle. In addition, controlling the level of sRNA expression can also minimize off-target effects.

The present study indicates that a 30 bp long asRNA sequence is optimal for efficient protein knockdown. We were surprised to observe that the 10 bp anti-sense sequence did not affect IncA translational fusion, since it was designed to mimic the wildtype CtrR3 by having a similar loop sequence length and an anti-RBS sequence. We propose that this lack of regulation is due to a weak interaction between the asRNA and the IncA mRNA, which only has 4 G/C base-pairing, whereas CtrR3 has 5 G/C interactions with its mRNA targets. Similarly, the 60 bp anti-sense RNA sequence had minimal regulation on IncA translational fusion expression. This could be a result of a large loop sequence that either destabilizes the sRNA structure or forms additional secondary structures in the loop, thus hindering binding to the IncA mRNA. Overall, we believe that the 30 bp sequence worked best because it had a long enough complementarity with the mRNA to establish a strong interaction, but not too long to disrupt the sRNA structure.

Our work on defining the mRNA target site requirement for efficient knockdown is useful when designing an asRNA sequence. From the *E. coli* translational fusion study, we know that the asRNA sequence has to include the RBS of the mRNA. In the later part of this chapter, we will demonstrate that including a portion of the RBS in the target sequence is also sufficient for an efficient knockdown. Knowing this rule allows us to have options when designing an asRNA sequence. Different asRNA sequences can be entered into a bioinformatic software (i.e. TargetRNA2 or IntaRNA) to predict potential off-targets. The asRNA sequence with the least number of predicted off-targets can then be prioritized and tested in the *E. coli* translational fusion assay.

We took the approach of expressing the complementing protein under a Tet inducible promoter. The complement protein has to be under an inducible promoter to prevent exogenous protein expression, which may be toxic to *Chlamydia* during the transformation process. This approach worked well in complementing IncA knockdown, however, it does not allow for separate control of the expression of the sRNA and the complement protein. This could pose an issue when we are trying to complement a high expressing protein and are using low aTc concentration to prevent off-target effects. Our lab is currently devising ways to increase the expression of the complement protein via altering the Tet promoter sequence and/or adding a transcriptional terminator. Alternatively, translation of the complement protein can be controlled by a synthetic riboswitch E, which can be induced with theophylline (N. A. Grieshaber et al., 2022).

We were surprised to observe that C3-IncG overexpression blocked the protein expression of only IncG but not IncE, and yet, mRNA levels of both genes were decreased. This observation is consistent with the model that the mechanism of sRNA repression is mostly on the level of blocking translational initiation, rather than mRNA target destabilization (Rice & Vanderpool, 2011; Waters & Storz, 2009). In addition, the mRNAs that are not yet destabilized are still capable of translating IncE proteins. Lastly, translation of IncE may occur before the IncG target site is transcribed, as translation and transcription are coupled in prokaryotes (Irastortza-Olaziregi & Amster-Choder, 2021; Miller et al., 1970). We also cannot rule out the possibility that an overall decreased in IncE mRNA levels will eventually lead to a decreased in IncE protein at later time points (i.e. 36 hpi). We are currently working to determine if the phenotypes we observed, such as multiple inclusions and larger bacteria, are a result of an IncG

knockdown, which can be addressed by IncG complementation. Overall, our knockdown system has the potential to downregulate a specific gene in an operon without largely affecting the protein expression of an upstream gene in the same operon and therefore, may be an important addition to the *C. trachomatis* genetic toolbox.

Based on our results, we hypothesize that C3-IncG expression leads to destabilization of the incDEFG operon. We propose this occurs when C3-IncG binds to the IncG mRNA and induces RNase cleavage at or near the binding site. Cleavage of IncG mRNA will result in the loss of the downstream transcriptional terminator and subsequently, in the destabilization of the incDEFG mRNA (He et al., 2020). Nonetheless, the fact that the engineered sRNA destabilizes the target transcript may be beneficial. This feature would allow us to measure the transcript level to verify the knockdown of a target gene instead of relying on available antibodies. However, our data also indicates that quantifying changes in transcript level may not be an accurate way to measure changes in protein levels of a non-targeted gene (i.e. IncE).

For both IncA and IncG knockdown, we observed that the engineered sRNA destabilizes the mRNA target. This is in contrast with IhtA, in which IhtA overexpression affected the protein but not the mRNA level of HctA (Fig. 3). The differential effects between the chlamydial sRNA and the engineered sRNA could be due to the differences in length between the target sequences. We hypothesize that the 30 bp of perfect complementarity between the engineered sRNA and the mRNA target allows for RNA cleavage by RNase III, resulting in mRNA destabilization. RNase III is an endoribonuclease that processes double-stranded RNA and it has been shown to cleave, either one or both strands, at the interaction site between the anti-sense sRNA

and the mRNA target (Court et al., 2013; Georg & Hess, 2011). For a dsRNA to be bound and cleaved by RNase III, however, the helix has to be approximately 22 bp long (Court et al., 2013). This requirement for RNase III cleavage suggests that the 7 bp interaction between an endogenous chlamydial sRNA and its mRNA target is not sufficient for RNase III processing. Thus, we propose that engineered sRNA-mRNA interaction is cleaved by RNase III, whereas chlamydial sRNA-mRNA interaction is not.

We also utilized the knockdown system to target MOMP, an essential chlamydial protein. We have reasons to suspect that our knockdown is specific to MOMP as we did not observe a defect in the expression of two other chlamydial proteins under C3-MOMP overexpressing conditions. In addition, we expressed C3-MOMP at 3 ng/mL, a concentration that did not produce off-target effects when we knocked down IncA. We are currently confirming the specificity of the knockdown via MOMP complementation.

Our result suggests that MOMP might be involved in RB division. This is due to the presence of aberrant RBs in C3-MOMP overexpressing transformants, which resembled the ones found in ampicillin-treated *C. trachomatis*. The formation of aberrant RBs is largely due to a block in chlamydial cell division (Panzetta et al., 2018; Skilton et al., 2009). Interestingly, MOMP has recently been shown to be highly enriched in the daughter cell membrane during polarized division in *C. trachomatis* (Cox et al., 2020), suggesting that it may have a role in RB division. In addition, MOMP or OmpA in other gram-negative bacteria can anchor the bacterial outer membrane to the peptidoglycan layer (Park et al., 2012). This interaction can play a role in outer membrane constriction during bacterial cell division (Egan, 2018). Thus, it is plausible that the loss of MOMP in *Chlamydia* may result in a block of chlamydial cell division due

to the inability of outer membrane constriction. This hypothesis can be tested by conducting EM analysis which may show the separation between outer and inner membrane. Alternatively, we can use immunofluorescence analysis to determine the relative position of MOMP to the peptidoglycan layer, which can be visualized by EDA-DA, an analog of D-alanine dipeptide (Liechti et al., 2014).

Overall, we propose the following steps to knockdown a specific target. 1) Design a 30 bp long asRNA sequence that has an anti-RBS sequence. 2) Replace the loop sequence of CtrR3 with the asRNA sequence (C3-sRNA). 3) Use *E. coli* translational fusion to test the ability of the C3-sRNA to downregulate the expression of its target. 4) Clone C3-sRNA into the pBOMB5 plasmid and transform it into *C. trachomatis*. 5) Test the ability of C3-sRNA to knockdown its target in *Chlamydia* using antibody or RT-qPCR. 6) Complement the knockdown to show specificity.

Chapter concluding remarks

In this chapter, we described a novel sRNA-mediated conditional knockdown system in *Chlamydia*. This system is inducible, titratable, and reversible, allowing for fine-tuned control of the knockdown. Specificity of the knockdown can be potentially validated through our complementation system. In addition, our sRNA-mediated knockdown system has the potential to silence a specific gene in an operon. More importantly, it can be utilized to knockdown essential genes to study their molecular function. We propose that our knockdown system complements the CRISPRi approach and together, both will play an important role in investigating the molecular mechanism of *C. trachomatis* pathogenesis.

Materials and Methods

The following Material and Methods are described in Chapter 2 Materials and Methods: **Cell culture and *Chlamydia* infection, *Chlamydia* transformation, Western blot, Immunofluorescence microscopy, RT-qPCR, *E. coli* culture conditions and co-expression study**

DNA oligonucleotides and plasmids

DNA oligonucleotides and plasmids can be found in the Tables 9 and 10.

Antibodies used in this study

Primary antibodies used were monoclonal mouse anti-GFP (11814460001, Roche), polyclonal rabbit anti-GroEL (G6532, Sigma-Aldrich), monoclonal mouse anti-MOMP (gift from Ellena Peterson), polyclonal rabbit anti-IncA (gift from Guangming Zhong), monoclonal mouse anti-Flag (M2Flag) (F3165, Sigma-Aldrich), polyclonal rabbit anti-IncG (gift from Guangming Zhong), polyclonal rabbit anti-14-3-3β (K-19) (sc-629, Santa Cruz), polyclonal rabbit anti-IncE (gift from Joanne Engel), monoclonal mouse anti-Hsp60 (GroEL) (gift from Rick Morrison), and polyclonal rabbit anti-α-tubulin (ab18251, Abcam). Secondary antibodies for immunofluorescence microscopy: Donkey anti-Rabbit IgG Alexa Fluor 488 (Invitrogen, A21206), Donkey anti-Rabbit IgG Alexa Fluor 555 (Invitrogen, A31572), Donkey anti-Mouse IgG Alexa Fluor 488 (Invitrogen, A21202), and Donkey anti-Mouse IgG Alexa Fluor 555 (Invitrogen, A31570), Secondary antibodies for western blot: goat anti-rabbit IgG LI-COR IRDYE 680 (926-680-71, Fisher Scientific) and goat anti-mouse IgG LI-COR IRDye 800 (926-32210; Fisher Scientific).

Plasmid construction

All plasmids were generated with Gibson assembly via the NEBuilder HiFi DNA assembly mastermix (E2621, NEB) and subsequently transformed into *E. coli* strain DHFα (NEB5-alpha). The plasmid sequences were then confirmed via Sanger sequencing using Retrogen Inc.

The pRSETC-C3-IncA (10bp), (30bp), and (60bp) were constructed with primer sets P1+P2, P3+P4, P5+P6, respectively, using pRSETC-CtrR3 as template. pRSETC-C3-IncA (60bp) also required P7 oligonucleotide as link.

pBAD33.1 incA::gfp, incG::gfp, and momp::gfp plasmids were generated by amplifying the pBAD33.1 ctl0389::gfp vector backbone primer set P8+P9. The amplicons made with primer sets P10+P11 (incA), P35+P36 (incG), and P38+P39 (momp) using *C. trachomatis* serovar L2 genomic DNA as template were then assembled into the the vector backbone.

pBOMB5-tet-C3-IncA was constructed by using primers P14+P15 and P16+P17 to amplify the vector backbone from pBOMB5-tet-CtrR3. Then, primer set P12+P13 was used to amplify C3-IncA (10bp) from pBAD33.1 C3-IncA (10bp) plasmid.

The pRSETC-5nt plasmids were constructed by amplifying the vector backbone (pRSETC-CtrR3) with P18+P2 and utilizing P19-P25 to link the vector backbone. pRSETC-C3-IncA2, C3-IncG, and C3-MOMP plasmids were constructed in a similar fashion but with P25, P34, and P37 as oligonucleotides, respectively, to link the vector backbone.

pBOMB5-tet-C3-IncA+mCherry and C3-IncA+IncA-Flag plasmids were constructed by utilizing primer sets P14+P27 and P17+P26 to amplify the vector backbone, pBOMB5-tet-C3-IncA. Tet promoter driving mCherry or IncA-Flag expression was amplified from pASK (gift from Scott Hefty). mCherry was amplified from pBOMB5-tet-mCherry using P30+P31 and IncA-Flag was amplified using P32+P33.

Acknowledgments

We would like to thank Dr. Scott Hefty from University of Kentucky for providing us with the pASK -GFP-L2 plasmid. We also thank Dr. Guangming Zhong at University of Texas Health Science Center and Dr. Joanne Engel at University of California, San Francisco for providing us with IncG and IncE antibodies, respectively. This research was supported by grants from the National Institutes of Health (R01 AI044198 to M.T. and R01 AI151212 to C.S and M.T.). K.W. was supported by a National Institutes of Health T32 training grant (AI141346). The text of this chapter is a pre-print of the material as it appears in “Development of a sRNA-mediated conditional knockdown system in *Chlamydia trachomatis*”. The co-authors listed in this publication (Cuper Ramirez, Janina Ehses, Christine Sütterlin, and Ming Tan) directed and supervised research which forms the basis for the chapter.

Tables

Table 7. Mechanism of action: CRISPRi vs sRNA-mediated knockdown.

	CRISPRi	**sRNA-mediated knockdown**
Component(s)	sgRNA and dCas9	sRNA
Target site	Promoter or ORF of a gene	5'UTR of mRNA (RBS)
Mechanism of repression	Block transcription	Block translation

Table 8. Characteristics of CRISPRi vs sRNA-mediated knockdown.

CRISPRi	sRNA-mediated knockdown
Study essential genes	
Inducible	
Reversible	
Off-target	
Limited target sites	
Strong repression	Potential incomplete repression
Polar effect	Potential to not have polar effect
dCas9 toxicity	No dCas9 toxicity
Titrating repression may be difficult	Titratable repression
Requires minimal sgRNA and dCas9 expression	Requires strong sRNA expression
Testing individual sgRNA requires separate transformants	Testing engineered sRNA is quick

Table 9. List of DNA oligonucleotides used in this study.

Name	Description	Sequence (5' to 3')
P1	pRSETC-C3-IncA (10bp) forward	TCGGTGGACTCGTTATGAGAAAGTGACACGAAAATCCAAGATTCC
P2	pRSETC-C3-IncA (10bp) reverse	TAACGAGTCCACCGAGTTCC
P3	pRSETC-C3-IncA (30bp) forward	AATGAGAAAGTGCCTATGACAACGCACACGAAAATCCAAGATTCC
P4	pRSETC-C3-IncA (30bp) reverse	AGGCACTTTCTCATTTAAAGTAACGAGTCCACCGAGTTCC
P5	pRSETC-C3-IncA (60bp) forward	TGCCTATGACAACGCCTACTCTAATACACGAAAATCCAAGATTCC
P6	pRSETC-C3-IncA (60bp) reverse	TAAAGTTCTCTGAAACCAGATCCTATAACGAGTCCACCGAGTTCC
P7	pRSETC-C3-IncA (60bp) link	GGTTTCAGAGAACTTTAAATGAGAAAGTGCCTATGACAACGCCT
P8	pBAD33.1 vector reverse	GAGCTCGAATTCGCTAGCC
P9	pBAD33.1 gfp forward	AGTAAAGGAGAAGCACTTTTCAC
P10	pBAD33.1 incA::gfp forward	AGCGAATTCGAGCTCTATAAAGCCCTAGGATCTGG
P11	pBAD33.1 incA::gfp reverse	TGCTTCTCCTTTACTAGGAGTCACGATTAGAGTAGG
P12	CtrR3 forward	ATCCACCGGTGGTACGAATCGGGGAAAAATTTCAATAAAAAAC
P13	CtrR3 reverse	AGAGTTATTTTACCATAGGTTTCTTCTTCTGTTTTTGC
P14	pBOMB4 vector forward	GGATAGACATTAGCTACAGAATC
P15	pBOMB5 vector reverse	GTACCACCGGTGGATCCGTCGACGCG
P16	pTet forward	TGGTAAAATAACTCTATCAACGATAGAGTGTC
P17	pBOMB4 vector reverse	GATTCTGTAGCTAATGTCTATCC
P18	pRSETC-5nt forward	ACACGAAAATCCAAGATTCCC
P19	pRSETC-5nt1 link	TCGGTGGACTCGTTACTTTAAATGAGAAAGTGCCTATGACTTTATACACGAAAATCCAAG
P20	pRSETC-5nt2 link	TCGGTGGACTCGTTACTTTAAATGAGAAAGTGCCTTAATTAACGCACACGAAAATCCAAG
P21	pRSETC-5nt3 link	TCGGTGGACTCGTTACTTTAAATGAGAAAGAATTAATGACAACGCACACGAAAATCCAAG
P22	pRSETC-5nt4 link	TCGGTGGACTCGTTACTTTAAATGAATTTATGCCTATGACAACGCACACGAAAATCCAAG
P23	pRSETC-5nt5 link	TCGGTGGACTCGTTACTTTATTAATGAAAGTGCCTATGACAACGCACACGAAAATCCAAG
P24	pRSETC-5nt6 link	TCGGTGGACTCGTTATAAATAATGAGAAAGTGCCTATGACAACGCACACGAAAATCCAAG
P25	pRSETC-IncA2 link	TCGGTGGACTCGTTATCTGGTTTCAGAGAACTTTAAATGAGAAAGACACGAAAATCCAAG
P26	pBOMB5 comp vector forward	TTGCTCACATGGAATTCGATGC
P27	pBOMB5 comp vector reverse	GCCAGCAAAAGGCCAGGAAC
P28	pBOMB5 comp ptet forward	CATACCGGTATCTCCTTCTTAAAG
P29	pBOMB5 comp ptet reverse	ATTCCATGTGAGCAAAATTCCTAAGATCTGTTGACTC
P30	pBOMB5 comp mCherry forward	TGGCCTTTTGCTGGCTTATTTGTACAGCTCATCCATGCC
P31	pBOMB5 comp mCherry reverse	GGAGATACCGGTATGGTCTCTAAGGGCGAGGAAG
P32	pBOMB5 comp IncA-Flag forward	TGGCCTTTTGCTGGCTTACTTATCGTCGTCATCCTTG
P33	pBOMB5 comp IncA-Flag reverse	GAAGGAGATACCGGTATGACGACTCCTACTCTAATCGTGACTCCTC
P34	pRSETC-C3-IncG link	TCGGTGGACTCGTTAACAAGAAACGAAATTTGATAAAGGGATAGGACACGAAAATCCAAG
P35	pBAD33.1 incG::gfp forward	AGCGAATTCGAGCTCAGCTTTTTTAATGACAAGAAACGAAATTTG
P36	pBAD33.1 incG::gfp reverse	TGCTTCTCCTTTACTGCTCGACAAGACTTTGTCAC
P37	pRSETC-C3-MOMP link	TCGGTGGACTCGTTAGCTAATTATACAATTTAGAGGTAAGAATGAACACGAAAATCCAAG
P38	pBAD33.1 momp::gfp forward	AGCGAATTCGAGCTCAAAAAGATAGCGAGCACAAAGAG
P39	pBAD33.1 momp::gfp reverse	TGCTTCTCCTTTACTCACTAATACCGATTTCAAGAG
P40	RT IncA forward	GCAGGGAATGCTCTTTATCTAC
P41	RT IncA reverse	CTTGAGATACAGCAGAGAGG
P42	RT Euo forward	TTATTCCGTGGGACAAGTGG
P43	RT Euo reverse	TGCAAGACTTTTCCCTTTGC
P44	RT IncG forward	CGTACAATCAATGCCTGTTATAG
P45	RT IncG reverse	GCAGATATGGAAGAACAGCAG
P46	RT IncE forward	CTTGTCGAGCGTACAATCAATG
P47	RT IncE reverse	GGAAGAACAGCAGCAGTGC
P48	RT 16S rRNA forward	GGAAACGGCCGCTAATACCG
P49	RT 16S rRNA reverse	GTAGGCCTTTACCCCACCAAC
P50	RT gapdh forward	TGCACCACCAACTGCTTAGC
P51	RT gapdh reverse	GGCATGGACTGTGGTCATGAG

Table 10. List of Plasmids and strains generated in this study.

Plasmids used to transform in *C. trachomatis* serovar L2

Name	Description	Marker	Source
pBOMB5-tet-C3-IncA (30bp)	Tet-inducible C3-IncA (30bp) expression plasmid	AmpR	This study
pBOMB5-tet-C3-IncA2+mCherry	Tet-inducible C3-IncA2 and mCherry expression plasmid	AmpR	This study
pBOMB5-tet-C3-IncA2+IncA-Flag	Tet-inducible C3-IncA2 and IncA-Flag expression plasmid	SpecR	This study
pBOMB5-tet-C3-IncG+mCherry	Tet-inducible C3-IncG and mCherry expression plasmid	AmpR	This study
pBOMB5-tet-C3-MOMP+mCherry	Tet-inducible C3-MOMP and mCherry expression plasmid	AmpR	This study

Plasmids used to transform in *E. coli* (NEB5-alpha)

Name	Description	Marker	Source
pRSETC-tet-C3-IncA (10bp)	Tet-inducible C3-IncA (10bp) expression plasmid	AmpR	This study
pRSETC-tet-C3-IncA (30bp)	Tet-inducible C3-IncA (30bp) expression plasmid	AmpR	This study
pRSETC-tet-C3-IncA (60bp)	Tet-inducible C3-IncA (60bp) expression plasmid	AmpR	This study
pRSETC-tet-5nt1	Tet-inducible 5nt1 expression plasmid	AmpR	This study
pRSETC-tet-5nt2	Tet-inducible 5nt2 expression plasmid	AmpR	This study
pRSETC-tet-5nt3	Tet-inducible 5nt3 expression plasmid	AmpR	This study
pRSETC-tet-5nt4	Tet-inducible 5nt4 expression plasmid	AmpR	This study
pRSETC-tet-5nt5	Tet-inducible 5nt5 expression plasmid	AmpR	This study
pRSETC-tet-5nt6	Tet-inducible 5nt6 expression plasmid	AmpR	This study
pRSETC-tet-C3-IncA2	Tet-inducible C3-IncA2 expression plasmid	AmpR	This study
pRSETC-tet-C3-IncG	Tet-inducible C3-IncG expression plasmid	AmpR	This study
pRSETC-tet-C3-MOMP	Tet-inducible C3-MOMP expression plasmid	AmpR	This study
pBAD33.1-incA::gfp	Arabinose-inducible incA::gfp expression plasmid	CmR	This study
pBAD33.1-incG::gfp	Arabinose-inducible incG::gfp expression plasmid	CmR	This study
pBAD33.1-momp::gfp	Arabinose-inducible momp::gfp expression plasmid	CmR	This study

Chapter 4: General Discussion

Impact and Summary

The goal of this work was to advance our understanding of post-transcriptional gene regulation in *Chlamydia trachomatis* by studying chlamydial sRNAs. Prior to this study, relatively little was known about sRNAs in *Chlamydia*. Although chlamydial sRNAs have been identified, their function and mRNA targets remained unknown. One *trans*-encoded sRNA, IhtA, has been proposed to regulate HctA expression. However, this hypothesis was formulated based on work done in *E. coli* and has never been tested in *C. trachomatis*, which is crucial as *Chlamydia* lacks the sRNA chaperone protein, Hfq. Importantly, it was not known if sRNAs can regulate gene expression in *C. trachomatis* or if they have an important function in chlamydial infection. The knowledge gap in the function of chlamydial sRNAs was largely attributed to the previous lack of genetic tools in this obligate intracellular pathogen.

To investigate the function of chlamydial sRNAs, we developed a novel inducible sRNA overexpression system in *C. trachomatis*. The power of this system is that it allowed us to investigate chlamydial sRNAs in their native environment. As we have shown, the sRNA overexpression system is versatile and can be used to study many different aspects of a chlamydial sRNA. We first utilized the system to confirm that IhtA negatively regulates HctA expression in *C. trachomatis* (Ch 2.1). Our work also provided experimental evidence that chlamydial sRNAs may have important functions in the *C. trachomatis* developmental cycle. This hypothesis is based on our genetic screen, which identified 4 uncharacterized sRNAs (i.e. CtrR3, CtrR7, CtrR0332, CTIG648) whose overexpression caused a severe reduction in infectious EB production (Ch 2.2). We further showed that overexpression of 3 of these sRNAs affected different steps in

the developmental cycle, as overexpression of CtrR3 and CtrR0332 resulted mostly in an RB-to-EB conversion defect, whereas CtrR7 overexpression caused an RB replication defect (Ch 2.3-2.5). Additionally, we applied the genetic system through a multi-step approach to identify YtgB and CTL0389 as mRNA targets of CtrR3 (Ch 2.6). Lastly, we expanded the *Chlamydia* genetic toolbox by successfully utilizing the overexpression approach to develop a novel sRNA-mediated conditional knockdown system in *C. trachomatis* (Ch 3). Overall, this study represents a major advance in the field of chlamydial sRNAs, and the genetic systems we have developed will help unravel the function and mechanism of post-transcriptional regulation in *C. trachomatis*.

In the following sections, I will discuss and speculate on some remaining unanswered questions regarding the overall functions of chlamydial sRNAs, the mechanism of chlamydial sRNA regulation, and the current approach we can take to define the function of a specific chlamydial sRNA.

What are the functions of chlamydial sRNAs?

We propose that the overall function of chlamydial sRNAs in *C. trachomatis* is to provide an additional level of gene regulation by regulating individual mRNA targets. *C. trachomatis* has limited means to differentiate gene expression transcriptionally, as it only possesses three sigma factors and 12-15 transcription factors (Domman & Horn, 2015). For example, around 650 midcycle genes are transcriptionally upregulated simultaneously, chlamydial sRNAs could act as a means to further differentiate their expression (e.g. temporally) via regulating a subset of target genes. In addition, unlike transcription factors which often turn target genes “on” or “off”, chlamydial sRNAs may

have the ability to modulate the expression level of their mRNA targets because the mechanism of sRNA regulation is typically based on stoichiometry. Thus, we hypothesize that by having chlamydial sRNAs (i.e. post-transcriptional regulation) in addition to transcriptional regulation, *Chlamydia* can generate complex and customized gene expression patterns to orchestrate the intricate developmental cycle of *C. trachomatis*.

Based on published reports on bacterial sRNAs and our work, we propose that there are three classes of chlamydial sRNAs that differ in their expression profiles. Class I sRNAs are constitutively expressed throughout the developmental cycle. Class II sRNAs are only expressed during a certain time frame in the developmental cycle. Class III sRNAs are similar to the traditional bacterial sRNAs, in that their expressions are induced under certain stress conditions.

Class I: constitutive chlamydial sRNAs

We hypothesize that this class of chlamydial sRNAs has a constitutively active promoter and/or is processed from a housekeeping RNA. This hypothesis is based on two *E. coli* sRNAs that are expressed constitutively: ChiX, which has a constitutively active promoter, and 3'ETS^{LeuZ}, which is processed from a pre-tRNA (Figueroa-Bossi et al., 2009; Lalaouna et al., 2015). Based on these criteria, we propose that CtrR3 is a prototype of Class I chlamydial sRNAs as we showed that it is expressed throughout the developmental cycle and that it is likely cleaved from a pre-tmRNA (Ch 2.3). In addition, we demonstrated that CtrR3 has a long half-life and is stable, which is a feature that may also contribute to its constitutive expression (Ch 2.6). Currently, it is unclear if there

are additional Class I sRNAs in *C. trachomatis* besides CtrR3. In principle, these sRNAs could be processed from housekeeping RNA such as tRNAs or SRP (4.5S RNA). For example, CtrR1 and CTIG504 could be processed from tRNA-thr and tRNA-leu, respectively, based on their genomic locations.

Because the expression of Class I sRNAs is constitutive, we anticipate that these sRNAs modulate the expression of their mRNA targets. One of the ways to achieve this is for the sRNA to set a concentration threshold for which the mRNA target has to overcome to express the target protein. This model is supported by studies conducted on the function of 3'ETS^{LeuZ} (Lalaouna et al., 2015). Lalaouna et al. showed that 3'ETS^{LeuZ} negatively regulates the expression of RyhB, a sRNA involved in the iron-starvation response (Lalaouna et al., 2015; Massé & Gottesman, 2002). During iron-rich conditions, the repressor Fur is bound to Fe^{2+} and represses transcription of RyhB (Massé & Gottesman, 2002). The authors proposed that the repression is incomplete and that there is some expression of RyhB whose activity is then blocked by 3'ETS^{LeuZ}. During iron-depleted conditions, RyhB expression is induced and is functional as its level overcomes the concentration threshold set by 3'ETS^{LeuZ}. This mechanism is in place to regulate intracellular iron levels because iron overload can result in the formation of reactive oxidative species, which is toxic to bacteria (Braun, 1997; Frawley & Fang, 2014).

We speculate that CtrR3 may be functioning similarly to 3'ETS^{LeuZ}. When the intracellular iron level is high, the chlamydial repressor YtgR binds to Fe^{2+} and represses the transcription of the YtgABCD operon, which encodes an iron import complex (Pokorzynski et al., 2019). In this condition, CtrR3 could further prevent iron

import and iron overload in *C. trachomatis* by blocking the translation of existing YtgB mRNAs. In contrast, when the intracellular iron level is low, transcription of YtgB is de-repressed and YtgB mRNA level can overcome the CtrR3 concentration threshold, allowing YtgB protein to be made. Our model is supported by the fact that *Chlamydia trachomatis* does not have a bacterioferritin homolog, an iron-storage protein found in most bacteria, suggesting that it requires stringent regulation on iron import (Andrews, 1998). One way to test our model is to decrease endogenous CtrR3 level or activity, and subsequently measure oxidative stress in *C. trachomatis* as an indirect measurement of iron toxicity. CtrR3 level or activity can be decreased via either CRISPRi or overexpressing an RNA with multiple CtrR3 binding sites, and oxidative stress in *Chlamydia* could be potentially measured with CellROX™. If the model holds true, diminishing CtrR3 level or activity should increase oxidative stress in the bacteria.

Class II: developmental-regulated chlamydial sRNAs

We propose that this class of chlamydial sRNAs is developmentally expressed, similar to the temporal expression of chlamydial genes (i.e. early, midcycle, and late genes). This suggests that the promoters of these sRNAs are transcriptionally regulated through the same mechanisms as the promoters of other genes in the same temporal group (Table 1). Chlamydial sRNAs may also achieve a specific temporal expression profile by being processed from an mRNA transcript. For example, we proposed that CtrR0332, which is expressed during late infection time, is processed from the mRNA transcript of a late gene, *ltuB* (Ch 2.5). Based on the time-course analyses of sRNA expression conducted by AbdelRahman et al. and our group, we anticipate that most of

the identified chlamydial sRNAs fall under this class, including IhtA, CtrR7, and CtrR0332 (AbdelRahman et al., 2011).

Due to their expression pattern, Class II sRNAs may fine-tune the temporal expression of target genes on a post-transcriptional level. Transcriptional regulation in *Chlamydia* occurs in broad strokes, in which multiple genes from the same temporal class are transcribed simultaneously. In addition, after early and midcycle genes are expressed, the mRNA levels for these genes often remain constant throughout the developmental cycle (Belland, Zhong, et al., 2003). As such, a midcycle gene that is transcribed starting at 8 hpi may still be translated during late infection time. In this case, a sRNA that is expressed late (i.e. CtrR0332) could shut off the translation of a midcycle mRNA target to ensure that the encoded protein is only made during a specific time frame in the developmental cycle.

Because Class II chlamydial sRNAs may have the ability to temporally control the expression of their target genes, we propose that these sRNAs can function as regulators of a specific step in the developmental cycle. This is exemplified by CtrR0332, which we speculate to be a late-expressed sRNA that hinders bacterial division during RB-to-EB conversion. We hypothesize that CtrR0332 negatively regulates RB division because overexpression of CtrR0332 resulted in a modest decrease in genome copy, no late gene expression, and the presence of “miniature” RBs attached to larger RBs by electron microscopy (Ch 2.5). These three phenotypes are also associated with chlamydial persistence (Beatty et al., 1993, p. 1, 1994; Belland, Nelson, et al., 2003). During persistence, RBs do not undergo cell division, resulting in the formation of aberrant RBs, which are thought to maintain DNA replication and do not

express late genes (Belland, Nelson, et al., 2003; Hogan et al., 2004; Skilton et al., 2009). In addition, RBs in the process of exiting persistence have been shown to produce “miniature” RBs next to aberrant RBs by electron microscopy (Beatty et al., 1994; Wyrick, 2010). Based on these similarities, we propose that CtrR0332 overexpression produces some degree of persistence by hindering RB division. Taking into consideration that CtrR0332 is expressed as a late gene, we hypothesize that this sRNA is expressed during RB-to-EB conversion to prevent RBs from further dividing. As such, we anticipate CtrR0332 negatively regulates midcycle mRNA targets that encode bacterial division proteins, such as MreB, a chlamydial protein proposed to direct RB division (Ranjit et al., 2020). Additionally, we propose that CtrR0332 is binding and inhibiting the activity of a protein involved in RB division. This model will be discussed in a later section.

Class III: stress-induced chlamydial sRNAs

Based on sRNA function in other bacteria, we speculate that there are chlamydial sRNAs that are only expressed under certain stress conditions. Several stress conditions have been studied in *C. trachomatis*, including nutrient starvation, iron depletion, IFN-γ treatment, and beta-lactam antibiotics treatment, all of which lead to persistence (Brockett & Liechti, 2021; Hogan et al., 2004; Panzetta et al., 2018). Currently, we have not explored any stress conditions that may induce the expression of the sRNAs investigated in this study. AbdelRahman and colleagues, however, have observed increased expression of specific sRNAs after 24 and 48 hours post carbenicillin treatment, which induces chlamydial persistence (AbdelRahman et al.,

2011). These results are hard to interpret because stress-induced persistence in *C. trachomatis* causes significant changes in the chlamydial transcriptome (Belland, Nelson, et al., 2003; Ouellette et al., 2006). Thus, it is difficult to conclude if a sRNA is induced directly or indirectly by a stressor. To circumvent this issue, it would be more appropriate to induce stress for a short duration and subsequently test if the levels of sRNAs are altered.

We also speculate that the RNA-seq and microarray studies that were conducted to discover chlamydial sRNAs may not have identified any Class III sRNAs (AbdelRahman et al., 2011; Albrecht et al., 2010). This is because bacterial sRNAs that are induced under a specific stress condition are usually not expressed or are lowly expressed during normal bacteria growth (Hör et al., 2020). Both the deep sequencing and the microarray studies were performed in *C. trachomatis* undergoing the normal developmental cycle. In the future, it would be worthwhile to place *Chlamydia*-infected cells under different stress conditions and conduct small RNA-seq. Similar approaches have been utilized to uncover sRNAs involved in iron starvation conditions in *Mycobacterium tuberculosis* (Gerrick et al., 2018). If successful, it would be powerful because the chlamydial sRNAs that are identified under certain stress conditions are likely to have a physiological role or function in the stress response.

We anticipate that, compared to other gram-negative bacteria, *C. trachomatis* may have relatively few Class III sRNAs. The induction of sRNA expression in *E. coli* is mediated by the two-component signal transduction system (TCS) and/or regulated by specific transcription factors, both of which can sense the presence or absence of a stressor in the bacterial environment (Brosse et al., 2016; Mei et al., 2015; Storz et al.,

2011). The *Chlamydia* genome, however, is predicted to have only one intact TCS (Koo & Stephens, 2003) and 15 transcription factors (Domman & Horn, 2015; Rosario CJ, 2020); whereas *E. coli* has 30 TCS and 300 transcription factors (Yamamoto et al., 2005). This observation supports the concept that *Chlamydia* grows in a stable environment (i.e. the inclusion) and is likely to encounter few stressors (Rosario CJ, 2020). Interestingly, the one intact chlamydial TCS, the CtcB-CtcC system, activates an alternative sigma factor, σ^{54} (Soules et al., 2020). Although it is not known what the CtcB-CtcC system is sensing, identifying sRNAs that are part of the σ^{54} regulon would be another approach to discovering Class III chlamydial sRNAs.

Additional chlamydial sRNA functions

In addition to the three classes of chlamydial sRNAs proposed above, we postulate that *C. trachomatis* could potentially have dual function sRNAs. This class of sRNAs has two functions: 1) regulates mRNA targets through base-pairing and 2) encodes a small protein (Storz et al., 2014). The two functions are often related and regulate the same biological processes. For example, the *E. coli* dual-function sRNA, SgrS, encodes a small protein called SgrT. SgrT blocks the activity of PtsG, a glucose transporter, whereas SgrS base-pairs with and negatively regulates the expression of mRNA targets, including PtsG, that are involved in sugar uptake (Raina et al., 2018; Vanderpool & Gottesman, 2004; Wadler & Vanderpool, 2007; Wassarman et al., 2001). In our work, we discovered that CtrR7, an uncharacterized sRNA, encodes a small protein (Ch 2.4).

We speculate that the CtrR7 small protein regulates the activity of oligopeptide transport in *C. trachomatis*. There is precedent for a bacterial small protein to regulate membrane transport complexes (Garai & Blanc-Potard, 2020). In some cases, the gene encoding the small protein is located near the genes of its protein targets (Storz et al., 2014). For example, the *S. Typhimurium* small protein KdpF stabilizes the KdpABC potassium transport complex, which is encoded by an operon located downstream of the *kdpF* gene (Gannoun-Zaki et al., 2014; Garai & Blanc-Potard, 2020; Gaßel et al., 1999; Storz et al., 2014). Interestingly, the *ctrR7* gene is located downstream of the *oppA4*, *oppB2*, and *oppC2* operon, which encodes a hypothetical oligopeptide transporter complex. In addition, OppA4 is a substrate-binding protein located in the periplasm, which is where we propose the CtrR7 small peptide is localized. Thus, we speculate that the CtrR7 small protein binds and represses the activity of OppA4 in the periplasm, thereby reducing oligopeptide transport in *C. trachomatis*. This model also explains why we observed a block in RB replication when CtrR7 is overexpressed (Ch 2.4). Our lab is currently determining if CtrR7 also has a sRNA function. If it does, we would predict the sRNA to regulate mRNA targets that are also involved in oligopeptide transport.

In addition to dual-function sRNAs, we anticipate that certain chlamydial sRNA can bind and inhibit protein function. There is precedent for a sRNA to function through this mechanism, including *E. coli* 6S RNA, which regulates transcription by acting as a decoy promoter site for σ^{70} RNAP (Wassarman, 2007). We proposed earlier that CtrR0332 could hamper *Chlamydia* cell division by interacting and blocking the activity of a protein involved in RB division. This model is mainly supported by dissertation work

from the Rudel lab, which demonstrated that CtrR0332 binds to a putative SNF2-related helicase called CTL0077 (Klepsch, 2019). SWI/SNF and related proteins are found in eukaryotes and they mobilize the nucleosome to alter gene expression (Pazin & Kadonaga, 1997). Interestingly, CTL0077 is in the same operon as MreB, a protein that directs RB division, and both are expressed as midcycle genes (Belland, Zhong, et al., 2003). This suggests that the putative helicase could be involved in altering gene expression to promote chlamydial cell division. Taken together, we speculate that CtrR0332 is expressed as a late gene to bind and inhibit CTL0077 activity, resulting in downregulation of RB division during RB-to-EB conversion. In support of this model, long non-coding RNAs in eukaryotes can also bind to SWI/SNF complex subunits to act as a decoy and repress their activity (Tang et al., 2017). In addition, both CtrR0332 and CTL0077 are conserved in *Chlamydia spp*., suggesting that an interaction between the sRNA and the putative helicase is likely to be conserved. We can test the model by affinity purifying MS2-CtrR0332 in *C. trachomatis* and examine if we can co-purify the CTL0077 protein, and vice versa. Additionally, we can knockdown CTL0077 in *C. trachomatis* and test if the knockdown generates a phenotype similar to the one we observed with CtrR0332 overexpression (i.e. RB-to-EB impairment, persistent-like phenotype).

How do chlamydial sRNAs regulate their mRNA targets?

Is there a sRNA chaperone protein in *C. trachomatis*?

In many gram-negative bacteria, the RNA chaperone Hfq protects sRNAs from degradation and helps facilitate the sRNA-mRNA interaction. On the genomic sequence

level, there does not appear to be an Hfq homolog in *Chlamydia*. The lack of Hfq in *Chlamydia* is further supported by the fact that the chlamydial RNase E homolog is missing the C-terminal domain, which is utilized to interact with Hfq in *E. coli* (Ikeda et al., 2011). The *C. trachomatis* genome does, however, encode an YbeY protein, which is a conserved endoribonuclease that is required for bacterial rRNA processing (e.g. 16S rRNA) (Davies et al., 2010; Grinwald & Ron, 2013; Jacob et al., 2013). More recently, YbeY has been proposed to be involved in sRNA regulation (Pandey et al., 2011, 2014; Vercruysse et al., 2014). This is because YbeY is an RNA-binding protein that shares structural similarities to the MID domain of the eukaryotic protein, Argonaute (AGO), which binds to small RNAs in eukaryotes (Mallory & Vaucheret, 2009; Nowotny & Yang, 2009; Pandey et al., 2011, 2014). In addition, deletion of *ybeY* in *Sinorhizobium meliloti* caused a similar phenotype as a *hfq* mutant, including altered levels of sRNAs and their mRNA targets (Pandey et al., 2014). Thus, it is possible that the *C. trachomatis* YbeY is also involved in chlamydial sRNA-mediated regulation. This hypothesis can be tested by knocking down YbeY and assessing the changes in sRNA and mRNA levels. Alternatively, a temperature-sensitive mutant for YbeY (CTL0681) has been isolated in *C. trachomatis* that can be investigated in a similar fashion (Brothwell et al., 2016). We can also utilize the MS2-affinity purification to examine if YbeY could be pulled down by a sRNA or conduct MS2-sRNA purification coupled with mass spectrometry to identify sRNA-interacting proteins.

<u>How do chlamydial sRNAs bind to their targets?</u>

To compensate for the apparent lack of an sRNA chaperone in *Chlamydia*, we propose that a chlamydial sRNA requires perfect complementarity with its mRNA for at least 7 base pairs, of which 5 are G/C interactions. In reciprocal mutation experiments, we showed that a 5 G/C interaction must be maintained for CtrR3 to regulate CTL0389 translational fusion expression (Ch 2.6). The minimal base-pairing length is supported by our observation that CtrR3 is predicted to form an 8 and a 7 base-pair interaction with YtgB and CTL0389, respectively (Ch 2.6). This requirement may explain why putative mRNA targets that have 5 G/C interactions but only a 6 base-pair interaction with CtrR3 (e.g. RpsM, CTL0015) were not regulated by this sRNA in the translational fusion assay. Nonetheless, this rule needs to be confirmed with our *C. trachomatis* translation fusion system and may not be generalizable to other chlamydial sRNAs. Interestingly, the interaction between IhtA and HctA mRNA also satisfies these two requirements (N. A. Grieshaber et al., 2015). Our model is further supported by the observations that sRNAs in Hfq-deficient bacteria (i.e. *Mycobacterium tuberculosis*) also utilize G/C-rich sequences to bind and regulate their mRNA targets (Gerrick et al., 2018; Jørgensen et al., 2020; Mai et al., 2019).

How do chlamydial sRNAs repress the expression of their mRNA targets?

We anticipate that when a chlamydial sRNA binds to the RBS of an mRNA target, it blocks translation initiation but does not destabilize the target transcript. This model is supported by the observation that IhtA overexpression decreased the protein level, but not the mRNA level, of HctA (Ch 2.1). These findings differed from what has been typically observed with bacterial sRNAs which, upon binding to their mRNA

targets, destabilize the transcript. Transcript destabilization is often achieved through the recruitment of the degradosome to the sRNA-mRNA interaction site by Hfq (Ikeda et al., 2011; Massé et al., 2003; Morita et al., 2005; Prévost et al., 2011). The degradosome is a complex that facilitates mRNA decay of untranslated transcripts in bacteria (Kaberdin et al., 1998; Kido et al., 1996; Sheehan et al., 2020; Tejada-Arranz et al., 2020; Vargas-Blanco & Shell, 2020). The bacterial degradosome is composed of RNase E (RNase Y in *B. subtlis*), PNPase, an RNA helicase (RhlB), and enolase. The N-terminal domain of RNase E is the catalytic domain, whereas the C-terminal domain acts as a scaffold and binds to other proteins in the degradosome (Carpousis, 2007; Vargas-Blanco & Shell, 2020).

Interestingly, *C. trachomatis* does not have an identifiable RhlB homolog and the RNase E homolog does not have the C-terminal tail, suggesting that *Chlamydia* may not have a degradosome or may have an alternative mRNA degradation complex. In addition, as an obligate intracellular bacterium, *C. trachomatis* possesses mRNA with longer half-lives than those in extracellular (e.g. *E. coli*) or facultative intracellular bacteria (e.g. *M. tuberculosis*) (Ferreira et al., 2017). Overall, we postulate that chlamydial sRNAs do not destabilize their mRNA target due to the lack of Hfq and the lack of an efficient mRNA degradation machinery. This form of sRNA regulation could be energetically favorable for *Chlamydia* as the bacterium would not have to re-synthesize the mRNA targets once the sRNA level has been depleted. Our model can be tested by co-expressing the *E. coli* sRNA RyhB with its mRNA target SodB in *Chlamydia*. RyhB blocks the translation of the SodB mRNA and destabilizes the transcript (Prévost et al., 2011). However, transcript destabilization, but not translation

block, requires Hfq and the degradosome. Thus, if our model holds true, RyhB would block SodB translation but not cause transcript destabilization in *C. trachomatis*.

How do we define the function of a specific chlamydial sRNA?

To define the function of a specific chlamydial sRNA, we need to combine clues from 1) the endogenous expression pattern of the sRNA, 2) the phenotypes resulting from altered levels of sRNA in *C. trachomatis*, 3) the mRNA targets and the effect of the sRNA on the target, and 4) the function of the mRNA targets. In the above sections, we have discussed and demonstrated how the expression pattern of a sRNA can provide crucial insight into sRNA function. In the following section, we will discuss how the other clues provide insights about sRNA function that can be further investigated.

Phenotypes resulting from altered levels of sRNA

By altering the levels of sRNA in *Chlamydia*, we are changing the expression of specific mRNA targets, which may result in phenotypes. In principle, characterization of the phenotype can thereby, provide insight into the function of the mRNA targets as well as the sRNA. Our work illustrates, however, that the overexpression phenotype alone may not allow us to draw firm conclusions about endogenous sRNA function. For example, CtrR3 overexpression inhibited RB-to-EB conversion, but we could not definitively conclude that CtrR3 is a regulator of conversion (Ch 2.3). This is because CtrR3 overexpression may be blocking RB-to-EB conversion indirectly by affecting an upstream mechanism. We observed that CtrR3 overexpression caused an increase in RB size. A link between RB size and RB-to-EB conversion has been proposed by our

lab, in which RBs must reduce to a certain size threshold to initiate conversion. Thus, CtrR3 overexpression may cause an RB-to-EB conversion defect by affecting RB size. In addition, like any genetic system, there is always the possibility that the phenotype is a result of off-target effects, such as expressing the exogenous sRNA when it is not normally present or at too high of a level.

Nonetheless, we can utilize the known properties of a chlamydial sRNA and additional approaches to help interpret the overexpression phenotype. In the case of CtrR3, we know that endogenous CtrR3 is constitutively expressed, making it less likely to regulate a specific step in the developmental cycle, such as RB-to-EB conversion. We can also use complementary approaches, such as decreasing the sRNA level or activity, in conjunction with the overexpression phenotype to elucidate the function of the endogenous sRNA. For example, based on our proposed model for CtrR3, if downregulation of endogenous CtrR3 results in smaller RBs and earlier conversion, this would provide direct evidence that CtrR3 regulates RB size. Our lab is currently working on this complementary approach by knocking down endogenous CtrR3 with CRISPRi and overexpressing an RNA with multiple CtrR3 binding sites to decrease CtrR3 activity.

mRNA targets of a chlamydial sRNA

Perhaps the most important clue to elucidating the function of a chlamydial sRNA is the identification of its mRNA targets. Due to chlamydial sRNA biology, however, there are limitations to the approaches we can utilize to identify the targets. The first limitation is the apparent lack of sRNA chaperone proteins (i.e. Hfq or ProQ), which

prevents us from using approaches that rely on utilizing sRNA chaperone proteins as bait to capture sRNA-mRNA target complexes. These techniques include cross-linking immunoprecipitation-sequencing (CLIP-seq), RNA immunoprecipitation-sequencing (RIP-seq), UV crosslinking, ligation and sequencing of hybrids (CLASH), and RNA interaction by ligation and sequencing (RIL-seq) (Saliba et al., 2017). Additionally, we have to be cautious when using mRNA target prediction software (e.g. TargetRNA2, IntaRNA), because these platforms were built to predict sRNA-mRNA interactions in gram-negative bacteria, which often occur in the context of Hfq (Busch et al., 2008; Gerrick et al., 2018; Kery et al., 2014). A second limitation is that chlamydial sRNAs do not appear to destabilize their mRNA targets. This prevents us from overexpressing a specific sRNA for a short duration and subsequently using RNA-seq to identify mRNA targets.

To circumvent these limitations, we combined sRNA overexpression with MAPS to identify mRNAs that interact with CtrR3 in an Hfq-independent manner (Ch 2.6). In the future with more advanced chlamydial genetic tools, our MAPS system can be improved by tagging the endogenous sRNA with MS2 aptamers on the chromosome. Another approach to identifying mRNA targets of a chlamydial sRNA is via high-throughput global sRNA target identification by ligation and sequencing (Hi-GRIL-Seq), which has been shown to capture Hfq-independent sRNA-mRNA target interactions (Zhang et al., 2017). Hi-GRIL-Seq requires expression of T4 RNA ligase in bacteria to ligate the sRNA to its mRNA targets, creating sRNA-mRNA chimeras that can subsequently be detected through sequencing (K. Han et al., 2016; Zhang et al., 2017). Overexpression of the sRNA also improves the detection of the chimera (K. Han et al.,

2016). Thus, our complementation plasmid described in Chapter 3 can be utilized to co-express a sRNA and T4 RNA ligase to conduct Hi-GRIL-Seq in *C. trachomatis*. mRNA targets can also be identified by overexpressing a sRNA and conducting Ribo-Seq, which measures the translation efficiency of each mRNA (J. Wang et al., 2015). One drawback of this approach is that separating host from chlamydial ribosomes may be difficult. Targets identified from these approaches can be confirmed either through checking the target protein level with an antibody or utilizing the chlamydial translational fusion system we have developed in this study.

After identifying the mRNA targets of a chlamydial sRNA, it would valuable if we can connect the mRNA targets back to the sRNA overexpression phenotype to help understand the sRNA function. One question that remains from our work is if the downregulation of YtgB and/or CTL0389 caused the block in RB-to-EB conversion that we observed from CtrR3 overexpression. Answering this question, however, may not be straightforward. This is because the CtrR3 overexpression phenotype could be a combined result of CtrR3 downregulating multiple targets, including the ones that have yet to be identified. A way to address this question is to test if exogenous expression of YtgB or CTL0389 can rescue the CtrR3 overexpression phenotype, which can be accomplished using our complementation vector. Alternatively, we can knockdown YtgB or CTL0389 separately and investigate if they phenocopy CtrR3 overexpression at some level (e.g. increases RB size or decrease EB production). The identification of additional CtrR3 targets would also help address this question, which can be achieved by testing more targets identified in the CtrR3 MAPS or utilizing the aforementioned approaches.

The function of the mRNA targets

The function of an mRNA target is crucial in defining the function of the sRNA. For example, YtgB is predicted to be the cytosolic ATPase for iron transport based on previous work and protein homology (Luo et al., 2019; Pokorzynski et al., 2017; Thompson et al., 2012). This information led us to hypothesize that CtrR3 functions as a sRNA that modulates intracellular iron levels in *C. trachomatis*. Unfortunately, many proteins remained uncharacterized in the chlamydial genome due to the lack of genetic tools. Such is the case for CTL0389, which is an inclusion membrane protein (Inc) with no known function (Bauler & Hackstadt, 2014). There are some indications that CTL0389 may be essential for chlamydial infection. Bonner et al. subjected *Chlamydia trachomatis* serovar K to serial passage *in vitro* and observed that the *ctl0389* gene remained stable, whereas the downstream gene in the operon, *ctl0390*, accumulated frameshift mutations rapidly (Bonner et al., 2015). This suggests that CTL0389 expression may be necessary for the completion of the developmental cycle. In support of this model, there are currently no *ctl0389* mutants available in either transposon or chemical mutagenesis studies (Andersen et al., 2021; Brothwell et al., 2016). To better understand CtrR3 function, future work includes defining CTL0389 function by ectopically expressing CTL0389 in a host cell to identify interacting host or chlamydial proteins. Additionally, CTL0389 expression can be silenced in *C. trachomatis* with our knockdown system to gain a better understanding of CTL0389 function.

Chapter concluding remarks

In conclusion, the present work has furthered our understanding of chlamydial sRNAs. It has led us to propose five different classes of sRNAs and their functions in *C. trachomatis*. Our data has allowed us to predict the function of several sRNAs, including putative roles for CtrR3 in modulating chlamydial iron levels, CtrR0332 in regulating RB-to-EB conversion, and a CtrR7-encoded small protein in controlling RB replication. Further characterizations of these novel regulators are required to test and confirm these hypotheses, including the use of MAPS to identify mRNA targets of CtrR7 and CtrR0332. Moreover, our work has improved our knowledge of the mechanism of chlamydial sRNA regulation, such as the base-pairing requirements for a sRNA to target an mRNA in *Chlamydia*. Overall, the study described in this dissertation is an important step toward uncovering the mechanism and the role of post-transcriptional regulation in the pathogenesis and the developmental cycle of *C. trachomatis*.

Chapter 5: *Chlamydia* and HPV induce centrosome amplification in the host cell through additive mechanisms

Graphical Abstract

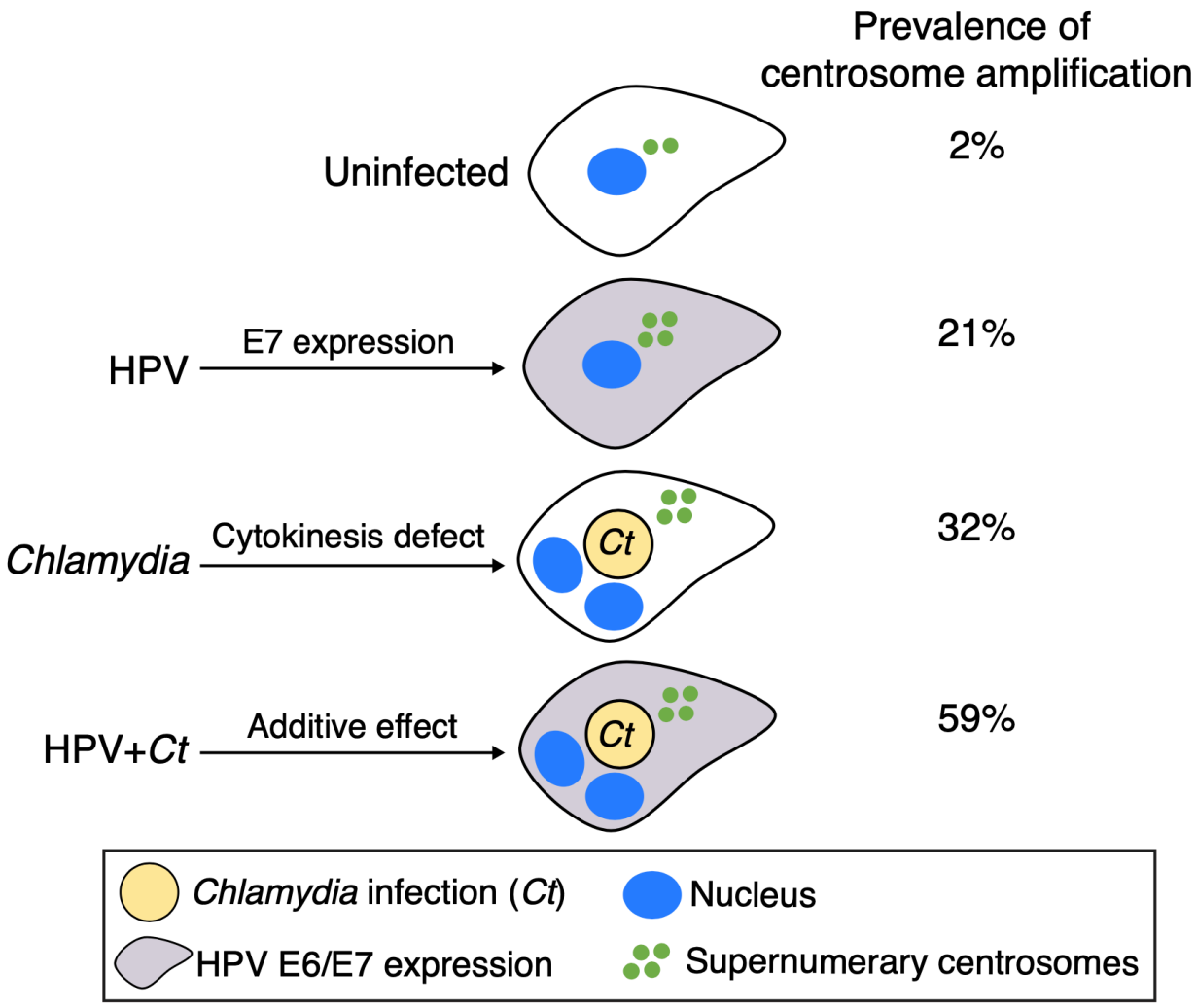

HPV and *Chlamydia* have additive effects on the prevalence of centrosome amplification when present in the same host cell. While HPV primarily causes centriole overduplication through expression of the oncoprotein E7, *Chlamydia* causes cytokinesis defects, which then lead to centrosome amplification and multinucleation in the host cell.

Abstract

Based on epidemiology studies, *Chlamydia trachomatis* has been proposed as a co-factor for human papillomavirus (HPV) in the development of cervical cancer. These two intracellular pathogens have been independently reported to induce the production of extra centrosomes, or centrosome amplification, which is a hallmark of cancer cells. We developed a cell culture model to systematically measure the individual and combined effects of *Chlamydia* and HPV on the centrosome in the same host cell. We found that *C. trachomatis* caused centrosome amplification in a greater proportion of cells than HPV and that the effects of the two pathogens on the centrosome were additive. Furthermore, centrosome amplification induced by *Chlamydia*, but not by HPV, strongly correlated with multinucleation and required progression through mitosis. Our results suggest that *C. trachomatis* and HPV induce centrosome amplification through different mechanisms with the chlamydial effect being largely due to a failure in cytokinesis that also results in multinucleation. Our findings provide support for *C. trachomatis* as a co-factor for HPV in carcinogenesis and offer mechanistic insights into how two infectious agents may cooperate to promote cancer.

Introduction

Each year, cervical cancer causes 300,000 deaths in the world, making it the fourth most common cancer in women (Arbyn et al., 2018). Human papillomavirus (HPV) is its main etiologic agent, with 90% of cervical carcinomas linked to “high-risk” HPV types, such as HPV16 and 18 (N. Muñoz et al., 2003). However, not all women infected with HPV develop cervical cancer, which suggests that additional factors are involved in carcinogenesis. A number of co-factors, including smoking, long-term use of oral contraceptives, and *Chlamydia trachomatis* infection, have been proposed (Appleby et al., 2007; Fonseca-Moutinho, 2011; Silva et al., 2014). The evidence for *C. trachomatis* as co-factor is based on sero-epidemiology studies showing that women with cervical cancer were more likely to have had a prior *Chlamydia* infection (Smith et al., 2002; Zhu et al., 2016).

HPV contributes to oncogenesis through multiple mechanisms. It causes aberrant proliferation of host cells, which supports viral DNA replication (Münger et al., 2004). It also promotes genomic instability in an infected host cell by inactivating cell cycle checkpoints, dysregulating host DNA repair pathways, and inducing centrosome abnormalities (Thomas & Laimins, 1998; Banerjee et al., 2011; Spardy et al., 2009; S. Duensing et al., 2000). As a consequence, HPV-infected cells accumulate cellular mutations while undergoing enhanced proliferation, which together lead to malignant transformation.

The centrosome, an organelle with a key role in microtubule organization, is dysregulated in many cancer cells (Salisbury et al., 1999; Chan, 2011). Normal diploid cells have a single centrosome, which duplicates in parallel to DNA in S-phase of the

cell cycle. Cancer cells often contain extra, or supernumerary, centrosomes, which is a phenomenon called centrosome amplification (Lingle et al., 1998; Pihan et al., 1998). Such supernumerary centrosomes contribute to carcinogenesis by leading to chromosome missegregation, genomic instability, and enhanced cell invasiveness (Ganem et al., 2009; Godinho et al., 2014). Centrosome amplification is caused by at least three distinct mechanisms, which include cell-cell fusion, cytokinesis defects, and dysregulation of the centrosome duplication machinery (Godinho & Pellman, 2014).

High risk HPV induces centrosome amplification through its oncoproteins E6 and E7. Co-expression of E6 and E7 is sufficient to increase centrosome number in normal human keratinocytes, which leads to multipolar spindles and ultimately to genomic instability (S. Duensing et al., 2000). Additionally, mice expressing E6 and E7 have cervical and skin lesions containing cells with multiple centrosomes (Schaeffer et al., 2004). E7 expression has been proposed to promote centrosome amplification by altering the centrosome duplication machinery, whereas the mechanism for E6-induced centrosome amplification is less understood (A. Duensing et al., 2006; S. Duensing & Münger, 2002).

C. trachomatis also induces centrosome amplification (Grieshaber et al. 2006; Johnson et al. 2009). Tissue culture cells infected with this obligate intracellular bacterium formed extra centrosomes in interphase and multipolar spindles in mitosis (S. S. Grieshaber et al., 2006). Intriguingly, these phenotypes persisted after the cells were cured of the infection. *C. trachomatis* has been proposed to induce centrosome abnormalities by dysregulating the centrosome duplication machinery and by causing cytokinesis defects in host cells (K. A. Johnson et al., 2009; Alzhanov et al., 2009). An

important caveat is that prior mechanistic investigations were mostly done in *C. trachomatis*-infected HeLa cells, which contain HPV-18 DNA (Schwarz et al., 1985). Thus, these studies measured the combined effects of *Chlamydia* and HPV on the centrosome, but not the individual contribution of *C. trachomatis*.

In the present study, we investigated the respective roles of HPV and *Chlamydia* in causing centrosome abnormalities. To accomplish this goal, we developed a cell culture system that allowed us to determine the individual and combined effects of these two sexually transmitted pathogens on the centrosome in the same host cell. Our results provide biologic plausibility for a role of *Chlamydia* as a co-factor for HPV in the development of cervical cancer.

Results

An experimental system for studying the effects of *Chlamydia* and HPV on the centrosome

We developed a cell culture model that allowed us to separate the effects of HPV and *Chlamydia trachomatis* (referred to as *Chlamydia* hereafter) on the centrosome in the same human cell (Fig. 31A). We used retinal pigment epithelial cells (RPE-1) as the host cell because these diploid epithelial cells are neither cancerous nor transformed by HPV, unlike HeLa or A2EN cells that are commonly utilized for *Chlamydia* infection (Buckner et al., 2016). To mimic the effects of HPV on the centrosome, we generated an RPE-1 cell line that stably expresses the viral oncoproteins HPV16 E6 and E7 (referred to as "HPV cells") (Fig. 32). Prior studies showed that ectopic co-expression of the HPV oncoproteins E6 and E7 was sufficient to induce centrosome amplification (S. Duensing et al., 2000; S. Duensing & Münger, 2002). Ectopic E6/E7 expression is proposed to mimic the effect of HPV on the centrosome, with the advantage that this approach does not require a stratified epithelium typically used in an HPV infection model (Bienkowska-Haba et al., 2018). However, because we are not performing actual HPV infections, we cannot exclude the possibility that other HPV factors may contribute to the phenotypes measured in this study. RPE-1 cells transduced with an empty vector lacking these viral oncogenes served as a negative control ("control cells").

We infected either control cells with *C. trachomatis* to produce "*Chlamydia* cells", or HPV cells to generate "HPV+*Chlamydia* cells". For these infections, we used *C. trachomatis* serovar L2 because this strain has been used as an experimental model to study *C. trachomatis*-induced centrosome amplification (S. S. Grieshaber et al., 2006;

K. A. Johnson et al., 2009). This strain is representative of other *C. trachomatis* strains, such as the genital serovars D and G, that produce comparable levels of centrosome amplification (S. S. Grieshaber et al., 2006).

We then compared the percentage of control, HPV, *Chlamydia* and HPV+*Chlamydia* cells with amplified centrosomes. We detected centrosomes by immunofluorescence microscopy with antibodies to the centrosomal marker proteins γ-tubulin and centrin2, which stain the pericentriolar material (PCM) and centrioles, respectively. Centrosome amplification was defined as cells harboring more than 2 centrosomes (n>2 γ-tubulin dots) (Fig. 31B).

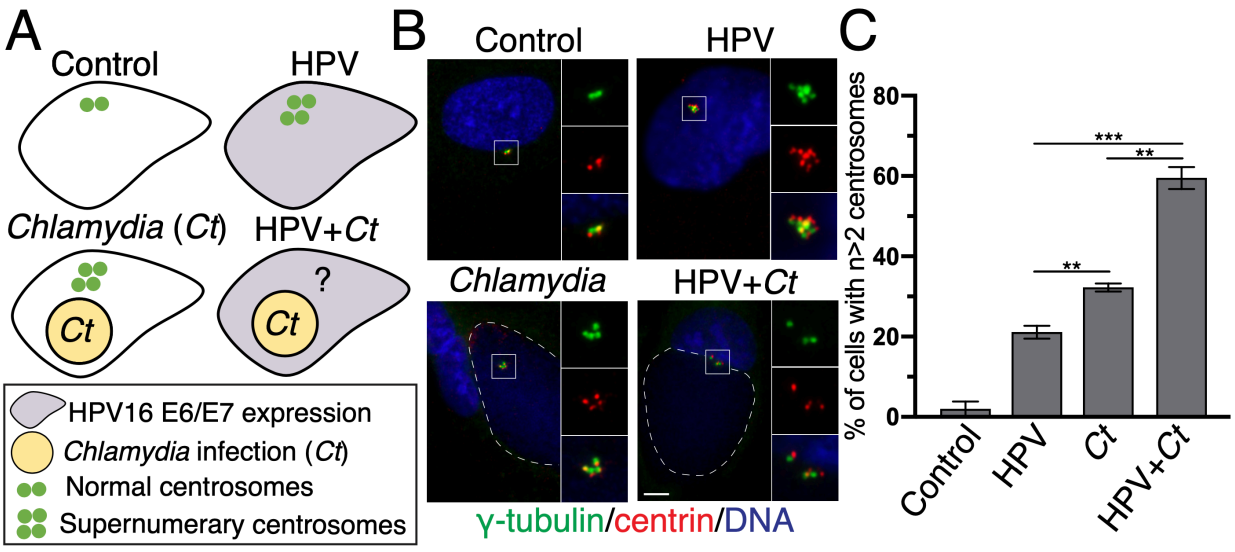

Figure 31. *Chlamydia* and HPV have additive effects on the host cell centrosome
(A) Schematic representation of the experimental design to study the separate and combined effect of *Chlamydia* and HPV on the centrosome. Control cells are RPE-1 cells transfected with an empty plasmid. "HPV cells" are RPE-1 cells that stably express HPV16 oncoproteins E6 and E7 (gray cell). "*Chlamydia* cells" are RPE-1 cells infected with *Chlamydia trachomatis* (yellow circle), while "HPV+*Chlamydia"* cells are RPE-1 cells that stably express HPV16 oncoproteins and that are infected with *C. trachomatis*. Individual centrosomes are presented as green dots.
(B) Control RPE-1 cells or HPV cells, grown on coverslips, were either mock-infected or infected with *C. trachomatis* L2 at an MOI of 3. Samples were fixed at 36 hours post infection (hpi). Centrosomes were visualized with antibodies to γ-tubulin (green) and centrin (red), host and chlamydial DNA was detected with DAPI (blue). Chlamydial inclusions are outlined with white dashed lines. Scale bar: 5 μm.
(C) The percentage of host cells with supernumerary centrosomes (n>2 centrosomes) from the four different conditions is shown. 100 cells were analyzed for each condition. For the samples with a *Chlamydia* infection, only infected cells were examined and quantified. Data are represented as mean ± SD (n=3); ***P*≤0.01 and ****P*<0.001.

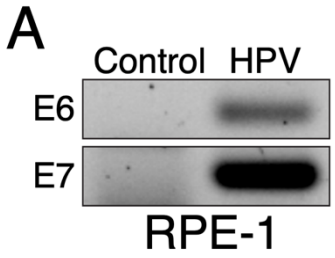

Figure 32. Confirmation of E6 and E7 expression in HPV cells
Reverse transcription PCR (RT-PCR) analysis of HPV cells to confirm that they express the viral oncogenes E6 and E7. RPE-1 cells transfected with the empty plasmid served as the control.

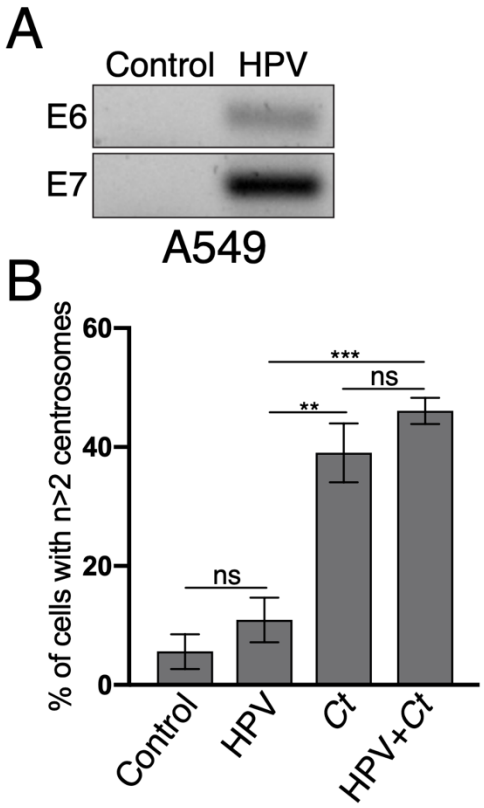

Figure 33. *Chlamydia* and HPV have additive effects on centrosome amplification in A549 cells
(A) RT-PCR of A549 cells that stably express HPV16 E6 and E7 to confirm viral oncogene expression. Control cells are A549 cells transfected with an empty plasmid. These cell lines were a generous gift from Dr. Ashok Aiyar, LSU
(B) The percentage of cells with supernumerary centrosomes for each of the four experimental conditions is shown. 100 cells were analyzed for each condition at 36hpi. Data are represented as mean ± SD (n=3); $^{**}P \leq 0.01$, $^{***}P < 0.001$, ns: not statistically significant.

Chlamydia and HPV dysregulated centrosome number in an additive manner

This systematic approach revealed different effects of these two pathogens on the centrosome. Control cells had only few supernumerary centrosomes (Prevalence of 1.9%). *Chlamydia* cells showed a higher prevalence of amplified centrosomes than HPV cells (Prevalence of 32.2% vs 21.1%) (Fig. 31C), but the highest percentage of extra centrosomes (59.5%) was seen in HPV+*Chlamydia* cells. These data demonstrated that *Chlamydia* had a greater effect on the centrosome than HPV, and that together, they caused more centrosome amplification than either infectious agent alone (Fig. 31C). Thus, HPV and *Chlamydia* cause centrosome amplification in a host cell through additive mechanisms.

We also examined effects of HPV and *Chlamydia* on the centrosome of A549 cells, which are HPV-negative lung carcinoma cells. Similar to our results with RPE-1 cells, there was a greater prevalence of centrosome amplification in *Chlamydia* cells when compared to HPV cells. However, because E6/E7 expression did not cause a statistically significant increase in the percentage of A549 cells with amplified centrosomes, we were unable to test if the effects of HPV and *Chlamydia* on centrosome amplification are additive (Fig. 33). We conclude from these experiments that unlike for HPV, the prominent effects of *Chlamydia* in dysregulating centrosome number is independent of the cell type used as the host cell.

Chlamydia- and HPV-induced centrosome amplification did not disrupt the function of the centrosome in organizing microtubules

We next tested if *Chlamydia* and HPV altered the function of the centrosome, which organizes microtubules by controlling their nucleation and anchoring. HPV, *Chlamydia* and HPV+*Chlamydia* cells all formed a radial array of interphase microtubules that was indistinguishable from that of control cells (Fig. 34A). There was also no difference in the growth kinetics of microtubules as measured in regrowth assays (Fig. 34B).

We further analyzed spindle formation to assess centrosome function in mitosis (Fig. 34C). HPV and HPV+*Chlamydia* cells showed a higher prevalence of abnormal spindles, including multipolar and pseudo-bipolar spindles, than control or *Chlamydia* cells (Figs. 34C and 34D). This finding suggests that the abnormal interphase centrosomes in HPV and HPV+*Chlamydia* cells may promote the formation of abnormal mitotic spindles. In contrast, while a high percentage of *Chlamydia* cells had supernumerary centrosomes in interphase (Fig. 31C), only few of these cells actually progressed into mitosis and formed abnormal spindles. We conclude that all cells with abnormal centrosomes were able to form mitotic spindles and that cell cycle progression to reach mitosis may be disrupted in *Chlamydia* cells with supernumerary centrosomes.

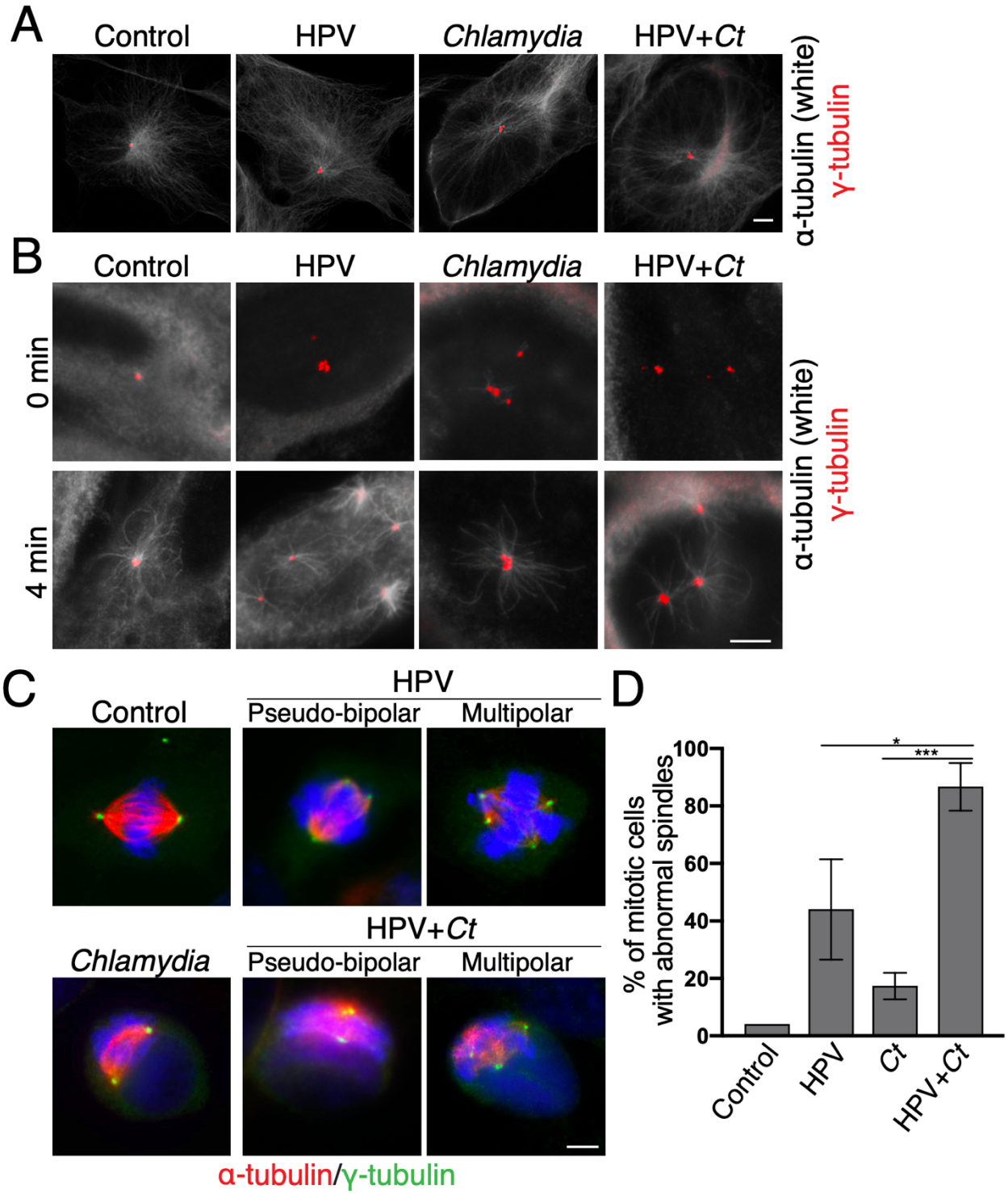
A
Control
HPV
Chlamydia
HPV+Ct
α-tubulin (white)
γ-tubulin
B
Control
HPV
Chlamydia
HPV+Ct
0 min
4 min
α-tubulin (white)
γ-tubulin
C
Control
HPV
Pseudo-bipolar
Multipolar
Chlamydia
HPV+Ct
Pseudo-bipolar
Multipolar
α-tubulin/γ-tubulin
D
% of mitotic cells with abnormal spindles
100
80
60
40
20
0
*
***
Control
HPV
Ct
HPV+Ct

Figure 34. Centrosome amplification does not disrupt centrosome function
(A) Immunofluorescence images of mock or *Chlamydia*-infected RPE-1 or HPV cells fixed at 36hpi in interphase. Microtubules were visualized with α-tubulin antibodies (white) and centrosomes were detected with γ-tubulin antibodies (red). Scale bar: 5μm.
(B) Microtubule regrowth assays are shown for cells of each of the four experimental conditions. Cells were incubated on ice to depolymerize microtubules (0 min) and then shifted to 37ºC for 4 minutes to allow microtubule nucleation and polymerization (4 min). Cells were fixed at the indicated time points and analyzed by immunofluorescence microscopy, detecting microtubules and centrosomes as described in (A). Scale bar: 5μm.
(C) Immunofluorescence images of mitotic cells in the samples in (A). Mitotic spindles were identified with antibodies to α-tubulin antibodies (red) and centrosomes were visualized with γ-tubulin antibodies (green). DNA was visualized with DAPI (blue). Scale bar: 5μm.
(D) The percentage of mitotic cells with abnormal spindles in each of the four conditions is shown. Both pseudo-bipolar (centrosome clustering) and multipolar spindles were considered abnormal. 50 mitotic cells were analyzed for each condition. For the samples with a *Chlamydia* infection, only infected cells were examined and quantified. Data are represented as mean ± SD (n=3); $*P \leq 0.05$ and $***P < 0.001$.

Chlamydia cells with amplified centrosomes are multinucleated and defective in cell cycle progression

We observed that *Chlamydia* was more likely to cause host cell multinucleation than HPV. 32.9% of *Chlamydia* cells and 32.1% of HPV+*Chlamydia* cells were multinucleated, compared to only 3.9% of HPV cells and 1.0% of control cells (Fig. 35A). In *Chlamydia* cells, multinucleation and centrosome amplification were often present in the same cell. Consistent with this observation, we determined a ϕ coefficient of 0.94 between the two phenotypes, which indicates a strong correlation (Fig. 35B). In contrast, HPV cells had a low ϕ coefficient of 0.23. HPV+*Chlamydia* cells displayed an intermediate correlation (ϕ coefficient = 0.49), consistent with a mixed effect (Fig. 35B).

As multinucleation can cause cells to arrest in the G1 phase of the cell cycle (Ganem et al., 2009; Hart et al., 2021), we compared cell cycle progression in mono- and multinucleated *Chlamydia* and HPV+*Chlamydia* cells. Mononucleated *Chlamydia* and HPV+*Chlamydia* cells, as well as multi-nucleated HPV+*Chlamydi*a, incorporated EdU, a marker for S-phase entry, to similar extents (Fig. 36). In contrast, the percentage of EdU-positive multinucleated *Chlamydia* cells was reduced (Fig. 36), suggesting that these cells become arrested in a pre-S-phase stage of the cell cycle, likely in G1.

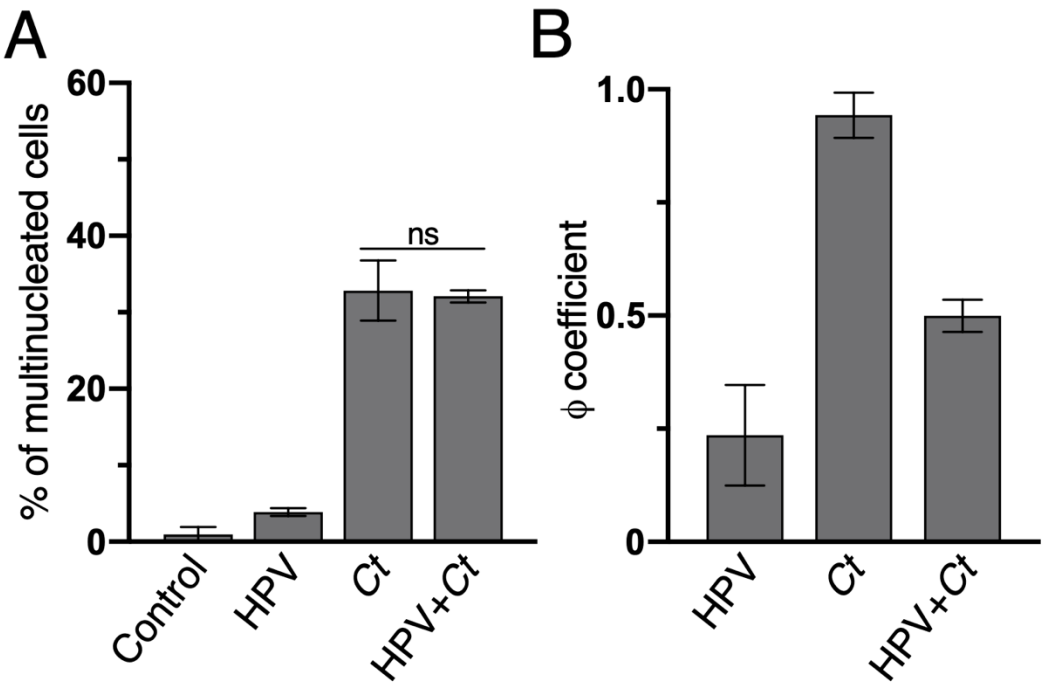

Figure 35. Multinucleation is strongly correlated with centrosome amplification in *Chlamydia* cells but not in HPV cells

(A) The percentage of multinucleated host cells described in Figure 1C is shown. 100 cells were examined for each condition. For *Chlamydia* cells, only infected cells were counted. Data are shown as mean ± SD (n=3); ns: not statistically significant.

(B) ϕ coefficients between multinucleation and centrosome amplification were calculated for the HPV, *Chlamydia*, and HPV+*Chlamydia* cells of Figure 1C. ϕ coefficients range from -1 to 1, with -1 or +1 indicating perfect negative or positive relationships, respectively, while 0 shows no relationship between the two phenotypes. The control sample was not included due to low level of centrosome amplification in these cells. Data are shown as mean ± SD (n=3).

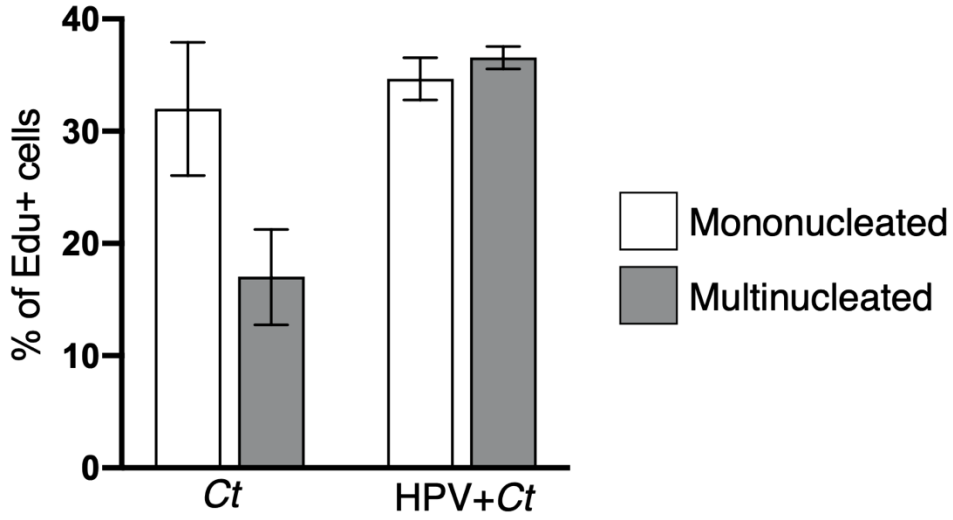

Figure 36. Multinucleation prevents cell cycle progression in *Chlamydia* cells but not in HPV+*Chlamydia* cells

Control or HPV cells, grown on coverslips, were infected with *C. trachomatis* at an MOI of 3. Samples were incubated with EdU for 30 minutes prior to fixation at 36 hpi. The percentage of either mono-nucleated or multinucleated EdU positive cells is shown. 60 cells were analyzed for each condition. Data are represented as mean ± SD (n=2).

Chlamydia-induced centrosome amplification and multinucleation result from a cytokinesis defect

The strong correlation between centrosome amplification and multinucleation in *Chlamydia* cells is indicative of a cytokinesis defect in the host cell, a reported consequence of *Chlamydia* infection (Alzhanov et al., 2009; H. S. Sun et al., 2016). To test this hypothesis, we counted the number of Cep164-positive foci in HPV, *Chlamydia*, and HPV+*Chlamydia* cells, focusing on cells with supernumerary centrosomes (Fig. 37). In a normal mitotic cell, the two mature Cep164-positive centrioles are passed on to the two daughter cell after cytokinesis (Schmidt et al., 2012). The presence of two mature centrioles in the same cell is therefore a strong indicator of a cytokinesis defect. Greater than 60% of *Chlamydia* cells had two Cep164-positive foci, whereas HPV cells contained predominantly a single Cep164 focus. HPV+*Chlamydia* cells showed an intermediate phenotype (Fig. 37).

As a complementary approach, we prevented *Chlamydia*, HPV and HPV+*Chlamydia* cells from reaching cytokinesis by blocking cell cycle progression either in S-phase or G2 and then measuring the prevalence of amplified centrosomes and multinucleation in each cell population. We induced a cell cycle arrest in S-phase by treating cells with thymidine. We also arrested cells in G2 by first synchronizing cells in S-phase, with thymidine treatment and washout, and then incubating them with the G2 inhibitor RO-3306 (Ma & Poon, 2017). Each of these cell cycle manipulations decreased the prevalence of multinucleation as well as centrosome amplification in *Chlamydia* cells, but not in HPV cells (Figs. 38A and 38B). Once again, HPV+*Chlamydia* cells showed an intermediate phenotype. Thus, multinucleation and

centrosome amplification are closely linked in *Chlamydia* cells, with both phenotypes depending on progression through the cell cycle. Together, these results indicate that centrosome amplification in *Chlamydia*, but not in HPV cells, may be the consequence of a cytokinesis defect. They also provide further support that these pathogens contribute to centrosome abnormalities through different mechanisms in the same host cell.

Our experimental set-up allowed us to examine an alternative model in which centrosome amplification in *Chlamydia* cells was proposed to cause multinucleation (Brown et al., 2014). To test this order of events, we prevented centrosome duplication through the use of the Plk4 inhibitor centrinone, which has been shown to block new centriole assembly in RPE-1 cells (Wong et al., 2015). Centrinone treatment significantly reduced centrosome amplification in HPV, *Chlamydia* and HPV+*Chlamydia* cells (Fig. 39A), which is consistent with published results on Plk4 inhibition (K. A. Johnson et al., 2009; Korzeniewski et al., 2011). However, centrinone treatment did not prevent multinucleation in *Chlamydia* cells (Fig. 39B), suggesting that centrosome amplification is not necessary for *Chlamydia*-induced multinucleation.

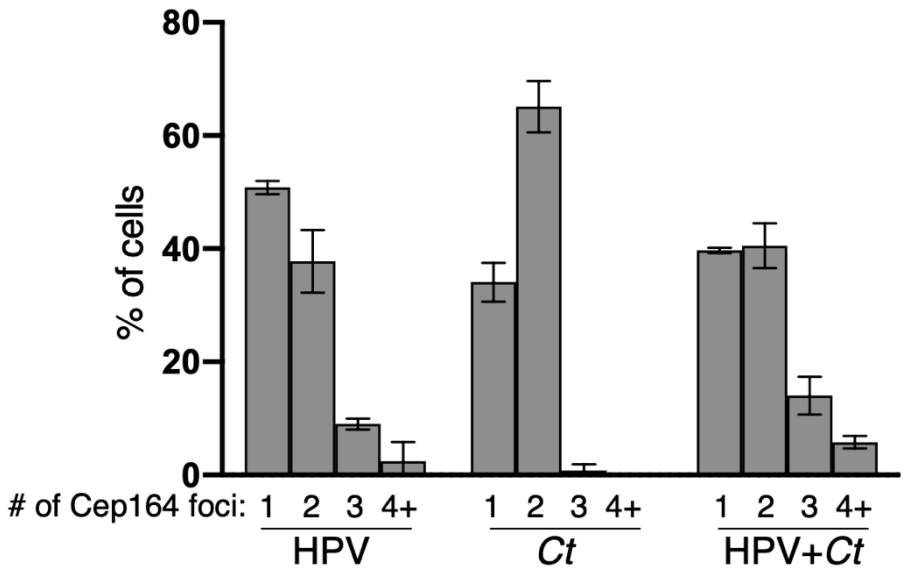

Figure 37. The amplified centrosomes in *Chlamydia* cells contain mostly two Cep164-positive mature centrioles

HPV, *Chlamydia* and HPV+*Chlamydia* cells at 36 hpi were stained with antibodies to γ-tubulin to detect centrosome amplification and Cep164 to mark mature mother centrioles. The percentage of Cep164-positive centrioles is shown for those cells that has amplified centrosomes (n>2 γ-tubulin foci). 60 cells were analyzed for each condition. Data are represented as mean ± SD (n=2).

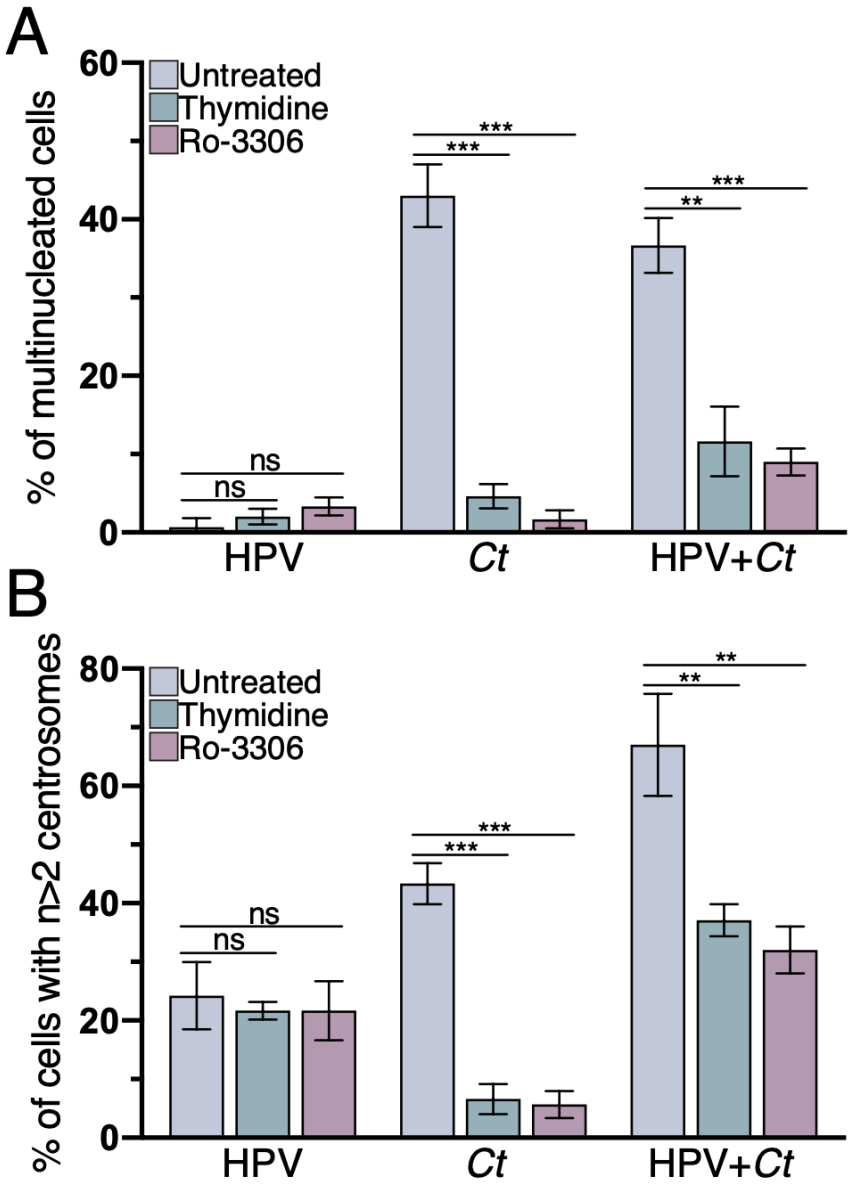

Figure 38. Multinucleation and centrosome amplification in *Chlamydia*-infected cells require mitotic progression

The cells of our four experimental conditions were arrested in S-phase with thymidine, or in G2 by the addition of RO-3306. Untreated samples were incubated in equivalent volume of DMSO. The percentage of cells with (A) multiple nuclei and (B) supernumerary centrosomes is shown. 100 cells were analyzed for each condition at 36hpi. Data are represented as mean ± SD (n=3); $^{**}P \leq 0.01$, $^{***}P < 0.001$, ns: not statistically significant.

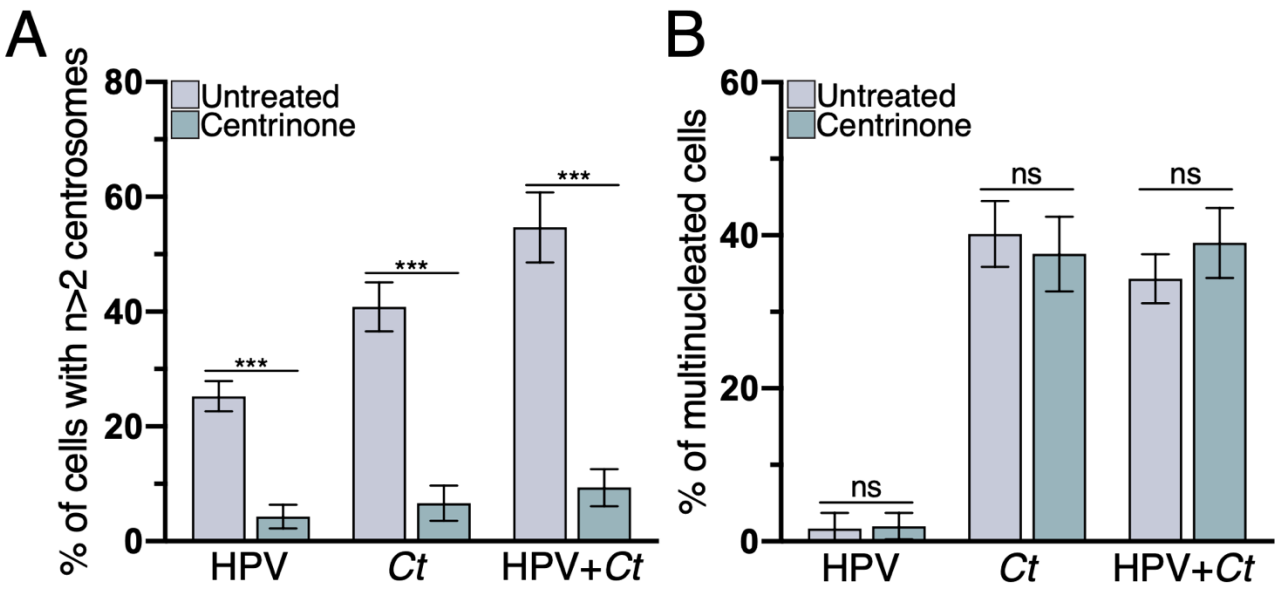

Figure 39. Multinucleation in *Chlamydia*-infected cells does not depend on centrosome amplification

The percentage of HPV, *Chlamydia*, and HPV+*Chlamydia* cells with (A) supernumerary centrosomes or (B) multiple nuclei after treatment with the Plk4 inhibitor centrinone is shown. Untreated samples were incubated in equivalent volume of DMSO. 100 cells were analyzed for each condition at 36hpi. Data are represented as mean ± SD (n=3); ***P<0.001.

Discussion

To investigate how *C. trachomatis* could contribute to HPV-mediated carcinogenesis, we measured the respective effects of these intracellular pathogens on the centrosome in the same host cell. We found that *Chlamydia* induced more cells to have amplified centrosomes than HPV and that these pathogens together caused an even higher percentage of cells with supernumerary centrosomes. These additive effects, together with our mechanistic analyses, suggest that *Chlamydia* and HPV induce centrosome amplification through different mechanisms. This study thus provides evidence that *C. trachomatis,* as a co-factor for HPV, may contribute to the development of cervical cancer by enhancing centrosome defects.

Chlamydia has been reported to cause centrosome amplification (S. S. Grieshaber et al., 2006; K. A. Johnson et al., 2009). These prior cell culture studies have predominantly used transformed cell lines that have an HPV background, such as HeLa cells (S. S. Grieshaber et al., 2006; K. A. Johnson et al., 2009; Knowlton et al., 2013). Although *Chlamydia* was found to also induce centrosome amplification in HPV-negative cell lines, such as NIH3T3 or HFF, these studies did not separate or compare the effects on the centrosome caused by either *Chlamydia*, HPV, or both pathogens together (S. S. Grieshaber et al., 2006; K. A. Johnson et al., 2009; Knowlton et al., 2013). Furthermore, comparing centrosome amplification between different *Chlamydia*-infected HPV-negative and positive cell lines can be difficult. We avoided these issues by developing a cell culture model that uses the same cellular background to measure the respective effects of *Chlamydia* and HPV on the centrosome.

HPV has been shown to induce centrosome amplification through its oncoproteins E6 and E7. E7 is proposed to be the primary driver of centrosome amplification in an HPV infection. This conclusion is based on data showing that E7 dysregulates the centrosome duplication machinery in a Cdk2-dependent manner (A. Duensing et al., 2006) and that transient E7 expression is sufficient to cause centrosome amplification (S. Duensing et al., 2001; S. Duensing & Münger, 2002). In contrast, E6 has been proposed to play a lesser role in centrosome amplification by disabling the p53-dependent checkpoint (S. Duensing et al., 2001; S. Duensing & Münger, 2002). The loss of this checkpoint could lead to a cytokinesis defect (Bunz et al., 1998; S. Duensing et al., 2001), in which the nucleus and the two centrosomes duplicate normally, but the cell fails to divide, resulting in a multinucleated cell with extra centrosomes (Cosenza & Krämer, 2016).

This present study compared the mechanisms through which *Chlamydia* and HPV produce supernumerary centrosomes. We propose that *Chlamydia*-induced centrosome amplification is the result of a cytokinesis defect. This idea is supported by the observation that centrosome amplification in *Chlamydia* cells strongly correlated with host cell multinucleation and required progression through mitosis. Additionally, most *Chlamydia* cells with supernumerary centrosomes had two Cep164-positive foci. In contrast, centrosome amplification in HPV cells did not correlate with multinucleation and was independent of cell cycle progression. Furthermore, most HPV cells with amplified centrosomes only contained one mature Cep164-positive mother centriole.

Together, these data suggest that HPV and *Chlamydia* induce centrosome defects through different mechanisms in the same host cell. While HPV primarily

dysregulate the centrosome duplication machinery through E7 (S. Duensing et al., 2001; S. Duensing & Münger, 2002), *Chlamydia* appears to cause centrosome dysregulation by disrupting cytokinesis. Consistent with this model, blocking cell cycle progression in HPV+*Chlamydia* cells partially reduced the prevalence of amplified centrosomes because it eliminated the contribution of *Chlamydia*, but not HPV, to this phenotype. Overall, our results suggest that these two pathogens activate two distinct pathways to induce centrosome dysregulation, although the respective contribution of each pathway to centrosome amplification appears to be cell type specific (Fig. 33).

Chlamydia is proposed to block cytokinesis through multiple mechanisms, including the physical presence of the inclusion and expression of the chlamydial proteins, CT223 (IPAM) or the protease CPAF (Greene 2001, Alzanov, 2009, Sun 2011, Brown 2014). The latter two studies both described evidence for a link between multinucleation and centrosome amplification, but Brown and colleagues suggested that multinucleation is the consequence of CPAF-induced centrosome amplification in *Chlamydia*-infected cells (Brown et al., 2014). Our data, however, suggests that the cytokinesis defect is upstream of the other two phenotypes because centrinone treatment blocked centrosome amplification in *Chlamydia* cells, but did not prevent multinucleation. Currently, it is not clear if centrosome amplification and multinucleation are functionally linked or if they are two independent consequences of the cytokinesis defect.

The presence of *Chlamydia* and HPV in the same cells produced a high prevalence of abnormal spindles but did not to affect the function of the centrosome in organizing microtubules in interphase or mitosis. As supernumerary centrosomes can

lead to spindle defects, we propose that *Chlamydia* and HPV together produce abnormal spindles by altering centrosome number rather than function. These abnormal spindles may lead to chromosome mis-segregation and aneuploidy (Zhou et al., 1998), thereby providing a mechanism by which *Chlamydia* may contribute to HPV-induced carcinogenesis.

Our study provides evidence for *Chlamydia*-induced cell cycle dysregulation in the host cell. We observed that fewer multinucleated *Chlamydia* cells progressed through the cell cycle than either mononucleated *Chlamydia* or multinucleated HPV+*Chlamydia* cells (Fig. 36). Thus, in addition to the known effect on cytokinesis, which leads to centrosome amplification and multinucleation, *Chlamydia* appears to disrupt progression through interphase. This *Chlamydia*-induced cell cycle arrest is likely in G1 and may be the consequence of either centrosome amplification or multinucleation. Centrosome amplification and multinucleation have been reported to lead to a G1 arrest through p53-dependent or p53-independent mechanisms, respectively (Hart et al., 2021; Mikule et al., 2007). However, as *Chlamydia* infection is known to induce p53 degradation, the presence of multiple nuclei in an infected cells is more likely to induce this G1 arrest in a p53-independent manner (González et al., 2014; Hart et al., 2021; Siegl et al., 2014). In HPV+*Chlamydia* cells, the presence of E6 and E7 may release the G1 arrest, possibly by degrading retinoblastoma protein (pRB) (Boyer et al., 1996; Giacinti & Giordano, 2006), resulting in cell cycle progression and the formation of aberrant mitotic spindles .

We hypothesize that these combined effects on the centrosome occur through co-infection, with HPV infection preceding the *Chlamydia* infection. Both sexually

transmitted agents are highly prevalent, making co-infection likely. These pathogens each infect the stratified epithelia of the cervix, but they do so at different locations, with HPV infecting basal cells (Spurgeon & Lambert, 2017), while *Chlamydia* infects the superficial cell layer (Murall et al., 2019). It is known, however, that HPV-infected basal cells divide, differentiate and migrate to the epithelial surface (Pinidis et al., 2016), thus providing a population of HPV-infected cells that can be infected acutely by *Chlamydia*. Our HPV/*Chlamydia* cell culture model mimics this sequence of events by taking cells expressing HPV E6 and E7 and then infecting them with *C. trachomatis*.

Our data is consistent with a 'hit-and-run' model, in which *C. trachomatis* infects a cervical cell that has an on-going HPV infection and contributes to HPV-induced carcinogenesis by augmenting centrosomal defects in these cells. *Chlamydia* typically causes a lytic infection, but we propose that some co-infected cells survive the *Chlamydia* infection and have enhanced centrosomal defects that promote their progression into cancer cells. This model is supported by data showing that cervical cancer cells do not have evidence of active *Chlamydia* infection (Wallin et al., 2002). In addition, cervical cancer has been associated with serological evidence of past, rather than current, *Chlamydia* infection (Wallin et al., 2002). There is also evidence that cells can be cleared of a *C. trachomatis* infection with antibiotics, while retaining amplified centrosome number (S. S. Grieshaber et al., 2006) or can survive through a non-lytic process called extrusion (Hybiske & Stephens, 2007).

Our findings provide biologic plausibility for *C. trachomatis* as a co-factor for HPV in carcinogenesis and have implications for the management of HPV and *C. trachomatis* infections. Based on this study, HPV-infected women who have had a prior *C.*

trachomatis infection may be at a higher risk for the development of cervical cancer. Our findings suggest that current screening for cervical cancer, which is based on Pap smear identification of premalignant cells and HPV test may not be adequate (Fontham et al., 2020). Enhanced screening for past *C. trachomatis* infection could be performed with an antibody blood test, but not with the standard *C. trachomatis* test, which is a nucleic acid amplification test (NAAT) that only detects an active or resolving infection (Meyer, 2016). If *Chlamydia* does contribute to cervical cancer, there will also be a greater need to identify and treat active infections and to develop a vaccine.

Materials and Methods

Antibodies used in this study

Primary antibodies: anti-Centrin (Millipore, 04-1624), anti-γ-tubulin (Abcam, ab11321), anti-α-tubulin (Sigma, T5168), anti-Cep164 (Santa Cruz, sc-240226). Secondary antibodies for immunofluorescence microscopy: Donkey anti-Rabbit IgG Alexa Fluor 488 (Invitrogen, A21206), Donkey anti-Mouse IgG Alexa Fluor 555 (Invitrogen, A31570), Goat anti-Rat IgG Alexa Fluor 564 (Invitrogen, A11081), Donkey anti-Goat IgG Alexa Fluor 488 (Invitrogen, A21202).

Cell culture and *Chlamydia* infection

The parental hTERT-RPE-1 cell line was obtained from ATCC and cultured at 37°C and 5.0% CO_2 in DMEM (Gibco, 11995-065) supplemented with 10% FBS (Atlanta Biologicals, S11550). A549 cells stably expressing HPV16 E6/E7 were a generous gift from Dr. Ashok Aiyar (LSU New Orleans) and were grown in DMEM supplemented with 10% FBS.

Chlamydia infection was done by infecting near-confluent cell monolayers with *C. trachomatis* serovar L2 (ATCC) at an MOI of 3 in SPG (200 mM sucrose, 20 mM sodium phosphate and 5 mM glutamate; pH 7.2) followed by centrifugation at 700×*g* for 1 hour at room temperature. As control, cells were mock infected with SPG alone. After centrifugation, the inoculum was removed and replaced with DMEM containing 10% FBS. The same infection conditions were used for RPE-1 and A549 cells.

Generation of RPE-1 cell lines expressing HPV16 E6/E7 oncoproteins

The pLXSN-HPV16 E6/E7 retroviral vector was obtained from Addgene (Plasmid #52394). From this vector, the pLXSN-Empty control vector was generated using Gibson assembly with forward primer 5′-TCCTCTAGAGTCCTGTAATCCTACCATGGCTGATCCTGCAG-3′ and reverse primer 5′-GATTACAGGACTCTAGAGGATC-3′. The pLXSN retroviral vectors and helper plasmid were co-transfected in 293T cells with calcium phosphate (293T cells and helper plasmid were generous gifts from Dr. Aimee Edinger, UC Irvine). Viral particles were collected 48 hours post transfection and used to infect RPE-1 cell monolayers with 10ug/mL polybrene (Sigma). Colonies were pooled after 10 days of selection with 600ug/mL G418 (Fisher, BP-918). HPV16 E6/E7 expressions were confirmed via RT-PCR. Forward primer 5′-GCAAGCAACAGTTACTGCG-3′ and reverse primer 5′-GGTTTCTCTACGTGTTCTTG-3′ were used to detect HPV16 E6 expression and primer pair 5′-CAGCTCAGAGGAGGAGGATG-3′ and 5′-GCCCATTAACAGGTCTTCCA-3′ were used to detect HPV16 E7 expression.

Immunofluorescence microscopy

Cells, grown and infected on glass coverslips, were fixed in 100% ice-cold methanol for 10 minutes. Cells were permeabilized and incubated in blocking buffer (2% FBS, 0.1% Triton) for 30 minutes at room temperature. *C. trachomatis* and host cell DNA was stained with NucBlue (Invitrogen, P36985). Centrosomes were detected with antibodies to Centrin to observe centrioles, Cep164 to mark mother centrioles and γ-tubulin to observe pericentriolar material. Mitotic spindles and microtubule regrowth

were visualized with anti-α-tubulin antibody. Coverslips were mounted with ProLong Glass Antifade containing NucBlue (Invitrogen, P36985). Immunofluorescence microscopy images were acquired on a Zeiss Axiovert 200M microscope.

Microtubule regrowth assay

Cells grown on coverslips in growth medium supplemented with 25mM HEPES, were first incubated on ice for 40 minutes to depolymerize microtubules and then shifted to room temperature for 4 minutes to allow microtubule regrowth. Cells were rinsed for 40 seconds with microtubule buffer (60mM PIPES, 25mM HEPES, 10mM EGTA, 2mM $MgCl_2$, 0.25nM Nocodazole, 0.25nM Paclitaxel, pH 6.9) and fixed with ice-cold methanol for 7 minutes prior to immunofluorescence microscopy analysis with antibodies to α-tubulin and γ-tubulin.

Pharmacological inhibition of cell cycle progression and centrosome duplication

Mock or *Chlamydia*-infected RPE-1 cells were arrested in S-phase by incubating them with 2mM thymidine (ACROS Organics, 226740050) in standard growth medium for 24 hours, starting at 12 hpi. Cells were arrested in G2 by first incubating them with 2mM thymidine for 18 hours, followed by release from the thymidine block for 6 hours and incubation with 10μM RO-3306 (TOCRIS, cat # 4181) in standard medium for 12 hours. Both the S-phase and the G2 arrest experiments were analyzed at 36 hpi using immunofluorescence microscopy.

To inhibit centrosome duplication, *Chlamydia*, HPV and HPV+*Chlamydia* cells were incubated with 125nM of the Plk4 inhibitor centrinone (MedChemExpress HY-

18682) in standard growth medium starting at 1 hpi. The experiment was evaluated by immunofluorescence microscopy at 36 hpi.

EdU labeling

Cells undergoing S-phase were identified using the Click-iT EdU Cell Proliferation kit (Invitrogen, C10337). Control or HPV cells were grown on coverslips and infected with *Chlamydia* at an MOI of 3. At 36 hpi, cells were incubated with 10μM EdU for 30 minutes and fixed with 4% PFA. EdU labeled cells were detected following the manufacturer's protocol.

Statistical analyses

For each experiment, 3 independent biological replicates were performed, and the results are presented as mean ± SD. Data were analyzed by unpaired, two-tailed t-tests with Welch's correction on Graph Pad PRISM software version 8.

Acknowledgments

We would like to thank Dr. Karl Munger for his input and guidance on generating our HPV16 E6 and E7-expressing RPE-1 cell line, and Dr. Aimee Edinger and Brendan Finicle for their assistance with lentiviral transductions. We also thank Dr. Ashok Aiyar for generously providing us with the A549 cell lines. This research was supported by the California Cancer Research Consortium (CCRC grant # 582146 to C.S.) and the National Institutes of Health (R21 AI128723 and R01 AI153410 to M.T. and C.S.). K.W. was supported by a National Institutes of Health T32 training grant (AI141346). K.J.M was supported by a National Science Foundation graduate research fellowship (ID 2018262334). The text of this chapter is a reprint of the material as it appears in "*Chlamydia* and HPV induce centrosome amplification in the host cell through additive mechanisms". The co-authors listed in this publication (Karissa Muñoz, Ming Tan, and Christine Sütterlin) directed and supervised research which forms the basis for the thesis/dissertation.

General References

AbdelRahman, Y. M., Rose, L. A., & Belland, R. J. (2011). Developmental expression of non-coding RNAs in Chlamydia trachomatis during normal and persistent growth. *Nucleic Acids Research*, *39*(5), 1843–1854. https://doi.org/10.1093/nar/gkq1065

Agaisse, H., & Derré, I. (2014). Expression of the effector protein IncD in Chlamydia trachomatis mediates recruitment of the lipid transfer protein CERT and the endoplasmic reticulum-resident protein VAPB to the inclusion membrane. *Infection and Immunity*, *82*(5), 2037–2047. https://doi.org/10.1128/IAI.01530-14

Albrecht, M., Sharma, C. M., Reinhardt, R., Vogel, J., & Rudel, T. (2010). Deep sequencing-based discovery of the Chlamydia trachomatis transcriptome. *Nucleic Acids Research*, *38*(3), 868–877. https://doi.org/10.1093/nar/gkp1032

Alm, E. J., Huang, K. H., Price, M. N., Koche, R. P., Keller, K., Dubchak, I. L., & Arkin, A. P. (2005). The MicrobesOnline Web site for comparative genomics. *Genome Research*, *15*(7), 1015–1022. https://doi.org/10.1101/gr.3844805

Almeida, F., Luís, M. P., Pereira, I. S., Pais, S. V., & Mota, L. J. (2018). The Human Centrosomal Protein CCDC146 Binds Chlamydia trachomatis Inclusion Membrane Protein CT288 and Is Recruited to the Periphery of the Chlamydia-Containing Vacuole. *Frontiers in Cellular and Infection Microbiology*, *8*. https://www.frontiersin.org/article/10.3389/fcimb.2018.00254

Alzhanov, D. T., Weeks, S. K., Burnett, J. R., & Rockey, D. D. (2009). Cytokinesis is blocked in mammalian cells transfected with Chlamydia trachomatis gene CT223. *BMC Microbiology*, *9*, 2. https://doi.org/10.1186/1471-2180-9-2

Andersen, S. E., Bulman, L. M., Steiert, B., Faris, R., & Weber, M. M. (2021). Got mutants? How advances in chlamydial genetics have furthered the study of effector proteins. *Pathogens and Disease*, *79*(2), ftaa078. https://doi.org/10.1093/femspd/ftaa078

Andrews, S. C. (1998). Iron storage in bacteria. *Advances in Microbial Physiology*, *40*, 281–351. https://doi.org/10.1016/s0065-2911(08)60134-4

Appleby, P., Beral, V., Berrington de González, A., Colin, D., Franceschi, S., Goodhill, A., Green, J., Peto, J., Plummer, M., & Sweetland, S. (2007). Cervical cancer and hormonal contraceptives: Collaborative reanalysis of individual data for 16,573 women with cervical cancer and 35,509 women without cervical cancer from 24 epidemiological studies. *Lancet (London, England)*, *370*(9599), 1609–1621. https://doi.org/10.1016/S0140-6736(07)61684-5

Arbyn, M., Smith, S. B., Temin, S., Sultana, F., Castle, P., & Collaboration on Self-Sampling and HPV Testing. (2018). Detecting cervical precancer and reaching

underscreened women by using HPV testing on self samples: Updated meta-analyses. *BMJ (Clinical Research Ed.)*, *363*, k4823. https://doi.org/10.1136/bmj.k4823

Auer, D., Hügelschäffer, S. D., Fischer, A. B., & Rudel, T. (2020). The chlamydial deubiquitinase Cdu1 supports recruitment of Golgi vesicles to the inclusion. *Cellular Microbiology*, *22*(5), e13136. https://doi.org/10.1111/cmi.13136

Bachmann, N. L., Polkinghorne, A., & Timms, P. (2014). Chlamydia genomics: Providing novel insights into chlamydial biology. *Trends in Microbiology*, *22*(8), 464–472. https://doi.org/10.1016/j.tim.2014.04.013

Bak, G., Lee, J., Suk, S., Kim, D., Young Lee, J., Kim, K., Choi, B.-S., & Lee, Y. (2015). Identification of novel sRNAs involved in biofilm formation, motility, and fimbriae formation in Escherichia coli. *Scientific Reports*, *5*, 15287. https://doi.org/10.1038/srep15287

Banerjee, N. S., Wang, H.-K., Broker, T. R., & Chow, L. T. (2011). Human papillomavirus (HPV) E7 induces prolonged G2 following S phase reentry in differentiated human keratinocytes. *The Journal of Biological Chemistry*, *286*(17), 15473–15482. https://doi.org/10.1074/jbc.M110.197574

Barry, C. E., Brickman, T. J., & Hackstadt, T. (1993). Hc1-mediated effects on DNA structure: A potential regulator of chlamydial development. *Molecular Microbiology*, *9*(2), 273–283. https://doi.org/10.1111/j.1365-2958.1993.tb01689.x

Barry, C. E., Hayes, S. F., & Hackstadt, T. (1992). Nucleoid condensation in Escherichia coli that express a chlamydial histone homolog. *Science (New York, N.Y.)*, *256*(5055), 377–379. https://doi.org/10.1126/science.256.5055.377

Bastidas, R. J., & Valdivia, R. H. (2016). Emancipating Chlamydia: Advances in the Genetic Manipulation of a Recalcitrant Intracellular Pathogen. *Microbiology and Molecular Biology Reviews*, *80*(2), 411–427. https://doi.org/10.1128/MMBR.00071-15

Batteiger BE, Tan M. (2019). Chlamydia trachomatis (trachoma and urogenital infections). In *In Bennett JE, Dolin R, Blaser MJ (ed), Mandell, Douglas, and Bennett's principles and practice of infectious diseases, 9th ed Elsevier Inc., Philadelphia, PA.* (pp. 2301–2319).

Bauler, L. D., & Hackstadt, T. (2014). Expression and targeting of secreted proteins from Chlamydia trachomatis. *Journal of Bacteriology*, *196*(7), 1325–1334. https://doi.org/10.1128/JB.01290-13

Beatty, W. L., Byrne, G. I., & Morrison, R. P. (1993). Morphologic and antigenic characterization of interferon gamma-mediated persistent Chlamydia trachomatis

infection in vitro. *Proceedings of the National Academy of Sciences of the United States of America*, *90*(9), 3998–4002.

Beatty, W. L., Morrison, R. P., & Byrne, G. I. (1994). Persistent chlamydiae: From cell culture to a paradigm for chlamydial pathogenesis. *Microbiological Reviews*, *58*(4), 686–699.

Beatty, W. L., Morrison, R. P., & Byrne, G. I. (1995). Reactivation of persistent Chlamydia trachomatis infection in cell culture. *Infection and Immunity*, *63*(1), 199–205. https://doi.org/10.1128/iai.63.1.199-205.1995

Belland, R. J., Nelson, D. E., Virok, D., Crane, D. D., Hogan, D., Sturdevant, D., Beatty, W. L., & Caldwell, H. D. (2003). Transcriptome analysis of chlamydial growth during IFN-γ-mediated persistence and reactivation. *Proceedings of the National Academy of Sciences*, *100*(26), 15971–15976. https://doi.org/10.1073/pnas.2535394100

Belland, R. J., Zhong, G., Crane, D. D., Hogan, D., Sturdevant, D., Sharma, J., Beatty, W. L., & Caldwell, H. D. (2003). Genomic transcriptional profiling of the developmental cycle of Chlamydia trachomatis. *Proceedings of the National Academy of Sciences of the United States of America*, *100*(14), 8478–8483. https://doi.org/10.1073/pnas.1331135100

Bennett, J. E., Dolin, R., & Blaser, M. J. B. (2014). *Mandell, Douglas, and Bennett's Principles and Practice of Infectious Diseases: 2-Volume Set*. Elsevier Health Sciences.

Betts-Hampikian, H. J., & Fields, K. A. (2010). The Chlamydial Type III Secretion Mechanism: Revealing Cracks in a Tough Nut. *Frontiers in Microbiology*, *1*, 114. https://doi.org/10.3389/fmicb.2010.00114

Bienkowska-Haba, M., Luszczek, W., Myers, J. E., Keiffer, T. R., DiGiuseppe, S., Polk, P., Bodily, J. M., Scott, R. S., & Sapp, M. (2018). A new cell culture model to genetically dissect the complete human papillomavirus life cycle. *PLoS Pathogens*, *14*(3), e1006846. https://doi.org/10.1371/journal.ppat.1006846

Bikard, D., Jiang, W., Samai, P., Hochschild, A., Zhang, F., & Marraffini, L. A. (2013). Programmable repression and activation of bacterial gene expression using an engineered CRISPR-Cas system. *Nucleic Acids Research*, *41*(15), 7429–7437. https://doi.org/10.1093/nar/gkt520

Bonner, C., Caldwell, H. D., Carlson, J. H., Graham, M. R., Kari, L., Sturdevant, G. L., Tyler, S., Zetner, A., & McClarty, G. (2015). Chlamydia trachomatis virulence factor CT135 is stable in vivo but highly polymorphic in vitro. *Pathogens and Disease*, *73*(6), ftv043. https://doi.org/10.1093/femspd/ftv043

Bouvier, M., Sharma, C. M., Mika, F., Nierhaus, K. H., & Vogel, J. (2008). Small RNA binding to 5' mRNA coding region inhibits translational initiation. *Molecular Cell*, *32*(6), 827–837. https://doi.org/10.1016/j.molcel.2008.10.027

Boyer, S. N., Wazer, D. E., & Band, V. (1996). E7 protein of human papilloma virus-16 induces degradation of retinoblastoma protein through the ubiquitin-proteasome pathway. *Cancer Research*, *56*(20), 4620–4624.

Braun, V. (1997). Avoidance of iron toxicity through regulation of bacterial iron transport. *Biological Chemistry*, *378*(8), 779–786.

Brickman, T. J., Barry, C. E., & Hackstadt, T. (1993a). Molecular cloning and expression of hctB encoding a strain-variant chlamydial histone-like protein with DNA-binding activity. *Journal of Bacteriology*, *175*(14), 4274–4281.

Brickman, T. J., Barry, C. E., & Hackstadt, T. (1993b). Molecular cloning and expression of hctB encoding a strain-variant chlamydial histone-like protein with DNA-binding activity. *Journal of Bacteriology*, *175*(14), 4274–4281. https://doi.org/10.1128/jb.175.14.4274-4281.1993

Brockett, M. R., & Liechti, G. W. (2021). Persistence Alters the Interaction between Chlamydia trachomatis and Its Host Cell. *Infection and Immunity*, *89*(8), e00685-20. https://doi.org/10.1128/IAI.00685-20

Brosse, A., Korobeinikova, A., Gottesman, S., & Guillier, M. (2016). Unexpected properties of sRNA promoters allow feedback control via regulation of a two-component system. *Nucleic Acids Research*, *44*(20), 9650–9666. https://doi.org/10.1093/nar/gkw642

Brothwell, J. A., Muramatsu, M. K., Toh, E., Rockey, D. D., Putman, T. E., Barta, M. L., Hefty, P. S., Suchland, R. J., & Nelson, D. E. (2016). Interrogating Genes That Mediate Chlamydia trachomatis Survival in Cell Culture Using Conditional Mutants and Recombination. *Journal of Bacteriology*, *198*(15), 2131–2139. https://doi.org/10.1128/JB.00161-16

Brown, H. M., Knowlton, A. E., Snavely, E., Nguyen, B. D., Richards, T. S., & Grieshaber, S. S. (2014). Multinucleation during C. trachomatis infections is caused by the contribution of two effector pathways. *PloS One*, *9*(6), e100763. https://doi.org/10.1371/journal.pone.0100763

Buckner, L. R., Amedee, A. M., Albritton, H. L., Kozlowski, P. A., Lacour, N., McGowin, C. L., Schust, D. J., & Quayle, A. J. (2016). Chlamydia trachomatis Infection of Endocervical Epithelial Cells Enhances Early HIV Transmission Events. *PloS One*, *11*(1), e0146663. https://doi.org/10.1371/journal.pone.0146663

Bunz, F., Dutriaux, A., Lengauer, C., Waldman, T., Zhou, S., Brown, J. P., Sedivy, J. M., Kinzler, K. W., & Vogelstein, B. (1998). Requirement for p53 and p21 to sustain G2 arrest after DNA damage. *Science (New York, N.Y.)*, *282*(5393), 1497–1501. https://doi.org/10.1126/science.282.5393.1497

Busch, A., Richter, A. S., & Backofen, R. (2008). IntaRNA: Efficient prediction of bacterial sRNA targets incorporating target site accessibility and seed regions. *Bioinformatics (Oxford, England)*, *24*(24), 2849–2856. https://doi.org/10.1093/bioinformatics/btn544

Campbell, E. A., Korzheva, N., Mustaev, A., Murakami, K., Nair, S., Goldfarb, A., & Darst, S. A. (2001). Structural Mechanism for Rifampicin Inhibition of Bacterial RNA Polymerase. *Cell*, *104*(6), 901–912. https://doi.org/10.1016/S0092-8674(01)00286-0

Carpousis, A. J. (2007). The RNA degradosome of Escherichia coli: An mRNA-degrading machine assembled on RNase E. *Annual Review of Microbiology*, *61*, 71–87. https://doi.org/10.1146/annurev.micro.61.080706.093440

Carrier, M.-C., Lalaouna, D., & Massé, E. (2018). Broadening the Definition of Bacterial Small RNAs: Characteristics and Mechanisms of Action. *Annual Review of Microbiology*, *72*(1), 141–161. https://doi.org/10.1146/annurev-micro-090817-062607

CDC. (2021, January 25). *STI Prevalence, Incidence, and Cost Estimates Infographic*. Centers for Disease Control and Prevention. https://www.cdc.gov/std/statistics/prevalence-2020-at-a-glance.htm

Chan, J. Y. (2011). A clinical overview of centrosome amplification in human cancers. *International Journal of Biological Sciences*, *7*(8), 1122–1144. https://doi.org/10.7150/ijbs.7.1122

Cheng, E., & Tan, M. (2012). Differential effects of DNA supercoiling on Chlamydia early promoters correlate with expression patterns in midcycle. *Journal of Bacteriology*, *194*(12), 3109–3115. https://doi.org/10.1128/JB.00242-12

Chiarelli, T. J., Grieshaber, N. A., Omsland, A., Remien, C. H., & Grieshaber, S. S. (2020). Single-Inclusion Kinetics of Chlamydia trachomatis Development. *MSystems*, *5*(5), e00689-20. https://doi.org/10.1128/mSystems.00689-20

Clausen, J. D., Christiansen, G., Holst, H. U., & Birkelund, S. (1997). Chlamydia trachomatis utilizes the host cell microtubule network during early events of infection. *Molecular Microbiology*, *25*(3), 441–449. https://doi.org/10.1046/j.1365-2958.1997.4591832.x

Collingro, A., Tischler, P., Weinmaier, T., Penz, T., Heinz, E., Brunham, R. C., Read, T. D., Bavoil, P. M., Sachse, K., Kahane, S., Friedman, M. G., Rattei, T., Myers, G. S. A., & Horn, M. (2011). Unity in variety—The pan-genome of the Chlamydiae. *Molecular Biology and Evolution*, *28*(12), 3253–3270. https://doi.org/10.1093/molbev/msr161

Cortina, M. E., Ende, R. J., Bishop, R. C., Bayne, C., & Derré, I. (2019). Chlamydia trachomatis and Chlamydia muridarum spectinomycin resistant vectors and a transcriptional fluorescent reporter to monitor conversion from replicative to infectious bacteria. *PloS One*, *14*(6), e0217753. https://doi.org/10.1371/journal.pone.0217753

Cosenza, M. R., & Krämer, A. (2016). Centrosome amplification, chromosomal instability and cancer: Mechanistic, clinical and therapeutic issues. *Chromosome Research: An International Journal on the Molecular, Supramolecular and Evolutionary Aspects of Chromosome Biology*, *24*(1), 105–126. https://doi.org/10.1007/s10577-015-9505-5

Court, D. L., Gan, J., Liang, Y.-H., Shaw, G. X., Tropea, J. E., Costantino, N., Waugh, D. S., & Ji, X. (2013). RNase III: Genetics and Function; Structure and Mechanism. *Annual Review of Genetics*, *47*, 405–431. https://doi.org/10.1146/annurev-genet-110711-155618

Cox, J. V., Abdelrahman, Y. M., & Ouellette, S. P. (2020). Penicillin-binding proteins regulate multiple steps in the polarized cell division process of Chlamydia. *Scientific Reports*, *10*(1), 12588. https://doi.org/10.1038/s41598-020-69397-x

da Cunha, M., Milho, C., Almeida, F., Pais, S. V., Borges, V., Maurício, R., Borrego, M. J., Gomes, J. P., & Mota, L. J. (2014). Identification of type III secretion substrates of Chlamydia trachomatis using Yersinia enterocolitica as a heterologous system. *BMC Microbiology*, *14*(1), 40. https://doi.org/10.1186/1471-2180-14-40

Davies, B. W., Köhrer, C., Jacob, A. I., Simmons, L. A., Zhu, J., Aleman, L. M., Rajbhandary, U. L., & Walker, G. C. (2010). Role of Escherichia coli YbeY, a highly conserved protein, in rRNA processing. *Molecular Microbiology*, *78*(2), 506–518. https://doi.org/10.1111/j.1365-2958.2010.07351.x

De Lay, N., Schu, D. J., & Gottesman, S. (2013). Bacterial Small RNA-based Negative Regulation: Hfq and Its Accomplices. *The Journal of Biological Chemistry*, *288*(12), 7996–8003. https://doi.org/10.1074/jbc.R112.441386

DeMars, R., Weinfurter, J., Guex, E., Lin, J., & Potucek, Y. (2007). Lateral Gene Transfer In Vitro in the Intracellular Pathogen Chlamydia trachomatis. *Journal of Bacteriology*, *189*(3), 991–1003. https://doi.org/10.1128/JB.00845-06

Dersch, P., Khan, M. A., Mühlen, S., & Görke, B. (2017). Roles of Regulatory RNAs for Antibiotic Resistance in Bacteria and Their Potential Value as Novel Drug Targets. *Frontiers in Microbiology*, *8*, 803. https://doi.org/10.3389/fmicb.2017.00803

Desnoyers, G., & Massé, E. (2012). Noncanonical repression of translation initiation through small RNA recruitment of the RNA chaperone Hfq. *Genes & Development*, *26*(7), 726–739. https://doi.org/10.1101/gad.182493.111

Dickinson, M. S., Anderson, L. N., Webb-Robertson, B.-J. M., Hansen, J. R., Smith, R. D., Wright, A. T., & Hybiske, K. (2019). Proximity-dependent proteomics of the Chlamydia trachomatis inclusion membrane reveals functional interactions with endoplasmic reticulum exit sites. *PLOS Pathogens*, *15*(4), e1007698. https://doi.org/10.1371/journal.ppat.1007698

Die, J. V., Obrero, Á., González-Verdejo, C. I., & Román, B. (2011). Characterization of the 3':5' ratio for reliable determination of RNA quality. *Analytical Biochemistry*, *419*(2), 336–338. https://doi.org/10.1016/j.ab.2011.08.012

Domman, D., & Horn, M. (2015). Following the Footsteps of Chlamydial Gene Regulation. *Molecular Biology and Evolution*, *32*(12), 3035–3046. https://doi.org/10.1093/molbev/msv193

Douglas, A. L., & Hatch, T. P. (2000). Expression of the transcripts of the sigma factors and putative sigma factor regulators of Chlamydia trachomatis L2. *Gene*, *247*(1–2), 209–214. https://doi.org/10.1016/s0378-1119(00)00094-9

Duensing, A., Liu, Y., Tseng, M., Malumbres, M., Barbacid, M., & Duensing, S. (2006). Cyclin-dependent kinase 2 is dispensable for normal centrosome duplication but required for oncogene-induced centrosome overduplication. *Oncogene*, *25*(20), 2943–2949. https://doi.org/10.1038/sj.onc.1209310

Duensing, S., Duensing, A., Crum, C. P., & Münger, K. (2001). Human papillomavirus type 16 E7 oncoprotein-induced abnormal centrosome synthesis is an early event in the evolving malignant phenotype. *Cancer Research*, *61*(6), 2356–2360.

Duensing, S., Lee, L. Y., Duensing, A., Basile, J., Piboonniyom, S., Gonzalez, S., Crum, C. P., & Munger, K. (2000). The human papillomavirus type 16 E6 and E7 oncoproteins cooperate to induce mitotic defects and genomic instability by uncoupling centrosome duplication from the cell division cycle. *Proceedings of the National Academy of Sciences of the United States of America*, *97*(18), 10002–10007. https://doi.org/10.1073/pnas.170093297

Duensing, S., & Münger, K. (2002). Human papillomaviruses and centrosome duplication errors: Modeling the origins of genomic instability. *Oncogene*, *21*(40), 6241–6248. https://doi.org/10.1038/sj.onc.1205709

Dumoux, M., Menny, A., Delacour, D., & Hayward, R. D. (2015). A Chlamydia effector recruits CEP170 to reprogram host microtubule organization. *Journal of Cell Science*, *128*(18), 3420–3434. https://doi.org/10.1242/jcs.169318

Dutta, T., & Srivastava, S. (2018). Small RNA-mediated regulation in bacteria: A growing palette of diverse mechanisms. *Gene*, *656*, 60–72. https://doi.org/10.1016/j.gene.2018.02.068

Egan, A. J. F. (2018). Bacterial outer membrane constriction. *Molecular Microbiology*, *107*(6), 676–687. https://doi.org/10.1111/mmi.13908

Elwell, C., Mirrashidi, K., & Engel, J. (2016). Chlamydia cell biology and pathogenesis. *Nature Reviews. Microbiology*, *14*(6), 385–400. https://doi.org/10.1038/nrmicro.2016.30

Falkow, S. (1988). Molecular Koch's postulates applied to microbial pathogenicity. *Reviews of Infectious Diseases*, *10 Suppl 2*, S274-276. https://doi.org/10.1093/cid/10.supplement_2.s274

Ferreira, R., Borges, V., Borrego, M. J., & Gomes, J. P. (2017). Global survey of mRNA levels and decay rates of Chlamydia trachomatis trachoma and lymphogranuloma venereum biovars. *Heliyon*, *3*(7), e00364. https://doi.org/10.1016/j.heliyon.2017.e00364

Figueroa-Bossi, N., Valentini, M., Malleret, L., & Bossi, L. (2009). Caught at its own game: Regulatory small RNA inactivated by an inducible transcript mimicking its target. *Genes & Development*, *23*(17), 2004–2015. https://doi.org/10.1101/gad.541609

Fonseca-Moutinho, J. A. (2011). Smoking and cervical cancer. *ISRN Obstetrics and Gynecology*, *2011*, 847684. https://doi.org/10.5402/2011/847684

Fontham, E. T. H., Wolf, A. M. D., Church, T. R., Etzioni, R., Flowers, C. R., Herzig, A., Guerra, C. E., Oeffinger, K. C., Shih, Y.-C. T., Walter, L. C., Kim, J. J., Andrews, K. S., DeSantis, C. E., Fedewa, S. A., Manassaram-Baptiste, D., Saslow, D., Wender, R. C., & Smith, R. A. (2020). Cervical cancer screening for individuals at average risk: 2020 guideline update from the American Cancer Society. *CA: A Cancer Journal for Clinicians*, *70*(5), 321–346. https://doi.org/10.3322/caac.21628

Frawley, E. R., & Fang, F. C. (2014). The Ins and Outs of Bacterial Iron Metabolism. *Molecular Microbiology*, *93*(4), 609–616. https://doi.org/10.1111/mmi.12709

Fröhlich, K. S., Papenfort, K., Berger, A. A., & Vogel, J. (2012). A conserved RpoS-dependent small RNA controls the synthesis of major porin OmpD. *Nucleic Acids Research*, *40*(8), 3623–3640. https://doi.org/10.1093/nar/gkr1156

Fröhlich, K. S., Papenfort, K., Fekete, A., & Vogel, J. (2013). A small RNA activates CFA synthase by isoform-specific mRNA stabilization. *The EMBO Journal*, *32*(22), 2963–2979. https://doi.org/10.1038/emboj.2013.222

Ganem, N. J., Godinho, S. A., & Pellman, D. (2009). A mechanism linking extra centrosomes to chromosomal instability. *Nature*, *460*(7252), 278–282. https://doi.org/10.1038/nature08136

Gannoun-Zaki, L., Belon, C., Dupont, C., Hilbert, F., Kremer, L., & Blanc-Potard, A.-B. (2014). Overexpression of the Salmonella KdpF membrane peptide modulates expression of kdp genes and intramacrophage growth. *FEMS Microbiology Letters*, *359*(1), 34–41. https://doi.org/10.1111/1574-6968.12559

Garai, P., & Blanc-Potard, A. (2020). Uncovering small membrane proteins in pathogenic bacteria: Regulatory functions and therapeutic potential. *Molecular Microbiology*, *114*(5), 710–720. https://doi.org/10.1111/mmi.14564

Gaßel, M., Möllenkamp, T., Puppe, W., & Altendorf, K. (1999). The KdpF Subunit Is Part of the K+-translocating Kdp Complex of Escherichia coli and Is Responsible for Stabilization of the Complex in Vitro *. *Journal of Biological Chemistry*, *274*(53), 37901–37907. https://doi.org/10.1074/jbc.274.53.37901

Georg, J., & Hess, W. R. (2011). Cis-antisense RNA, another level of gene regulation in bacteria. *Microbiology and Molecular Biology Reviews: MMBR*, *75*(2), 286–300. https://doi.org/10.1128/MMBR.00032-10

Gerrick, E. R., Barbier, T., Chase, M. R., Xu, R., François, J., Lin, V. H., Szucs, M. J., Rock, J. M., Ahmad, R., Tjaden, B., Livny, J., & Fortune, S. M. (2018). Small RNA profiling in Mycobacterium tuberculosis identifies MrsI as necessary for an anticipatory iron sparing response. *Proceedings of the National Academy of Sciences*, *115*(25), 6464–6469. https://doi.org/10.1073/pnas.1718003115

Ghosh, S., Ruelke, E. A., Ferrell, J. C., Bodero, M. D., Fields, K. A., & Jewett, T. J. (2020). Fluorescence-Reported Allelic Exchange Mutagenesis-Mediated Gene Deletion Indicates a Requirement for Chlamydia trachomatis Tarp during In Vivo Infectivity and Reveals a Specific Role for the C Terminus during Cellular Invasion. *Infection and Immunity*, *88*(5), e00841-19. https://doi.org/10.1128/IAI.00841-19

Giacinti, C., & Giordano, A. (2006). RB and cell cycle progression. *Oncogene*, *25*(38), 5220–5227. https://doi.org/10.1038/sj.onc.1209615

Gilet, L., DiChiara, J. M., Figaro, S., Bechhofer, D. H., & Condon, C. (2015). Small stable RNA maturation and turnover in Bacillus subtilis. *Molecular Microbiology*, *95*(2), 270–282. https://doi.org/10.1111/mmi.12863

Gitsels, A., Sanders, N., & Vanrompay, D. (2019). Chlamydial Infection From Outside to Inside. *Frontiers in Microbiology*, *10*, 2329. https://doi.org/10.3389/fmicb.2019.02329

Godinho, S. A., & Pellman, D. (2014). Causes and consequences of centrosome abnormalities in cancer. *Philosophical Transactions of the Royal Society of London. Series B, Biological Sciences*, *369*(1650). https://doi.org/10.1098/rstb.2013.0467

Godinho, S. A., Picone, R., Burute, M., Dagher, R., Su, Y., Leung, C. T., Polyak, K., Brugge, J. S., Théry, M., & Pellman, D. (2014). Oncogene-like induction of cellular invasion from centrosome amplification. *Nature*, *510*(7503), 167–171. https://doi.org/10.1038/nature13277

Goh, S., Hohmeier, A., Stone, T. C., Offord, V., Sarabia, F., Garcia-Ruiz, C., & Good, L. (2015). Silencing of Essential Genes within a Highly Coordinated Operon in Escherichia coli. *Applied and Environmental Microbiology*, *81*(16), 5650–5659. https://doi.org/10.1128/AEM.01444-15

González, E., Rother, M., Kerr, M. C., Al-Zeer, M. A., Abu-Lubad, M., Kessler, M., Brinkmann, V., Loewer, A., & Meyer, T. F. (2014). Chlamydia infection depends on a functional MDM2-p53 axis. *Nature Communications*, *5*(1), 5201. https://doi.org/10.1038/ncomms6201

Gottesman, S., & Storz, G. (2011). Bacterial small RNA regulators: Versatile roles and rapidly evolving variations. *Cold Spring Harbor Perspectives in Biology*, *3*(12), a003798. https://doi.org/10.1101/cshperspect.a003798

Grieshaber, N. A., Chiarelli, T. J., Appa, C. R., Neiswanger, G., Peretti, K., & Grieshaber, S. S. (2022). Translational gene expression control in Chlamydia trachomatis. *PLOS ONE*, *17*(1), e0257259. https://doi.org/10.1371/journal.pone.0257259

Grieshaber, N. A., Grieshaber, S. S., Fischer, E. R., & Hackstadt, T. (2006). A small RNA inhibits translation of the histone-like protein Hc1 in Chlamydia trachomatis. *Molecular Microbiology*, *59*(2), 541–550. https://doi.org/10.1111/j.1365-2958.2005.04949.x

Grieshaber, N. A., Runac, J., Turner, S., Dean, M., Appa, C., Omsland, A., & Grieshaber, S. S. (2021). The sRNA Regulated Protein DdbA Is Involved in Development and Maintenance of the Chlamydia trachomatis EB Cell Form.

Frontiers in Cellular and Infection Microbiology, *11*. https://www.frontiersin.org/article/10.3389/fcimb.2021.692224

Grieshaber, N. A., Sager, J. B., Dooley, C. A., Hayes, S. F., & Hackstadt, T. (2006). Regulation of the Chlamydia trachomatis Histone H1-Like Protein Hc2 Is IspE Dependent and IhtA Independent. *Journal of Bacteriology*, *188*(14), 5289–5292. https://doi.org/10.1128/JB.00526-06

Grieshaber, N. A., Tattersall, J. S., Liguori, J., Lipat, J. N., Runac, J., & Grieshaber, S. S. (2015). Identification of the base-pairing requirements for repression of hctA translation by the small RNA IhtA leads to the discovery of a new mRNA target in Chlamydia trachomatis. *PloS One*, *10*(3), e0116593. https://doi.org/10.1371/journal.pone.0116593

Grieshaber, S. S., Grieshaber, N. A., Miller, N., & Hackstadt, T. (2006). Chlamydia trachomatis causes centrosomal defects resulting in chromosomal segregation abnormalities. *Traffic (Copenhagen, Denmark)*, *7*(8), 940–949. https://doi.org/10.1111/j.1600-0854.2006.00439.x

Grinwald, M., & Ron, E. Z. (2013). The Escherichia coli translation-associated heat shock protein YbeY is involved in rRNA transcription antitermination. *PloS One*, *8*(4), e62297. https://doi.org/10.1371/journal.pone.0062297

Guillier, M., & Gottesman, S. (2008). The 5’ end of two redundant sRNAs is involved in the regulation of multiple targets, including their own regulator. *Nucleic Acids Research*, *36*(21), 6781–6794. https://doi.org/10.1093/nar/gkn742

Hackstadt, T., Baehr, W., & Ying, Y. (1991). Chlamydia trachomatis developmentally regulated protein is homologous to eukaryotic histone H1. *Proceedings of the National Academy of Sciences of the United States of America*, *88*(9), 3937–3941. https://doi.org/10.1073/pnas.88.9.3937

Hackstadt, T., Scidmore-Carlson, M. A., Shaw, E. I., & Fischer, E. R. (1999). The Chlamydia trachomatis IncA protein is required for homotypic vesicle fusion. *Cellular Microbiology*, *1*(2), 119–130. https://doi.org/10.1046/j.1462-5822.1999.00012.x

Haggerty, C. L., Gottlieb, S. L., Taylor, B. D., Low, N., Xu, F., & Ness, R. B. (2010). Risk of sequelae after Chlamydia trachomatis genital infection in women. *The Journal of Infectious Diseases*, *201 Suppl 2*, S134-155. https://doi.org/10.1086/652395

Han, K., Tjaden, B., & Lory, S. (2016). GRIL-Seq, a method for identifying direct targets of bacterial small regulatory RNA by in vivo proximity ligation. *Nature Microbiology*, *2*, 16239. https://doi.org/10.1038/nmicrobiol.2016.239

Han, Y., & Derré, I. (2017). A Co-infection Model System and the Use of Chimeric Proteins to Study Chlamydia Inclusion Proteins Interaction. *Frontiers in Cellular and Infection Microbiology*, *7*, 79. https://doi.org/10.3389/fcimb.2017.00079

Harris, S. R., Clarke, I. N., Seth-Smith, H. M. B., Solomon, A. W., Cutcliffe, L. T., Marsh, P., Skilton, R. J., Holland, M. J., Mabey, D., Peeling, R. W., Lewis, D. A., Spratt, B. G., Unemo, M., Persson, K., Bjartling, C., Brunham, R., de Vries, H. J. C., Morré, S. A., Speksnijder, A., … Thomson, N. R. (2012). Whole-genome analysis of diverse Chlamydia trachomatis strains identifies phylogenetic relationships masked by current clinical typing. *Nature Genetics*, *44*(4), 413–419, S1. https://doi.org/10.1038/ng.2214

Hart, M., Adams, S. D., & Draviam, V. M. (2021). Multinucleation associated DNA damage blocks proliferation in p53-compromised cells. *Communications Biology*, *4*(1), 1–11. https://doi.org/10.1038/s42003-021-01979-5

Hassan, H., & Troxell, B. (2013). Transcriptional regulation by Ferric Uptake Regulator (Fur) in pathogenic bacteria. *Frontiers in Cellular and Infection Microbiology*, *3*. https://www.frontiersin.org/article/10.3389/fcimb.2013.00059

Hatch, T. P. (1996). Disulfide cross-linked envelope proteins: The functional equivalent of peptidoglycan in chlamydiae? *Journal of Bacteriology*, *178*(1), 1–5.

He, Z., Duan, Y., Zhai, W., Zhang, X., Shi, J., Zhang, X., & Xu, Z. (2020). Evaluating Terminator Strength Based on Differentiating Effects on Transcription and Translation. *ChemBioChem*, *21*(14), 2067–2072. https://doi.org/10.1002/cbic.202000068

Hegemann, J. H., & Moelleken, K. (2012). Chlamydial adhesion and adhesins. In *Intracellular Pathogens 1: Chlamydiales Vol. 1* (1st ed., pp. 97–125). American Society for Microbiology Press.

Herring, A., & Richens, J. (2006). Lymphogranuloma venereum. *Sexually Transmitted Infections*, *82*(Suppl 4), iv23–iv25. https://doi.org/10.1136/sti.2006.023143

Hogan, R. J., Mathews, S. A., Mukhopadhyay, S., Summersgill, J. T., & Timms, P. (2004). Chlamydial Persistence: Beyond the Biphasic Paradigm. *Infection and Immunity*, *72*(4), 1843–1855. https://doi.org/10.1128/IAI.72.4.1843-1855.2004

Hör, J., Matera, G., Vogel, J., Gottesman, S., & Storz, G. (2020). Trans-Acting Small RNAs and Their Effects on Gene Expression in Escherichia coli and Salmonella enterica. *EcoSal Plus*, *9*(1). https://doi.org/10.1128/ecosalplus.ESP-0030-2019

Hui, M. P., Foley, P. L., & Belasco, J. G. (2014). Messenger RNA degradation in bacterial cells. *Annual Review of Genetics*, *48*, 537–559. https://doi.org/10.1146/annurev-genet-120213-092340

Hybiske, K., & Stephens, R. S. (2007). Mechanisms of host cell exit by the intracellular bacterium Chlamydia. *Proceedings of the National Academy of Sciences*, *104*(27), 11430–11435. https://doi.org/10.1073/pnas.0703218104

Ikeda, Y., Yagi, M., Morita, T., & Aiba, H. (2011). Hfq binding at RhlB-recognition region of RNase E is crucial for the rapid degradation of target mRNAs mediated by sRNAs in Escherichia coli. *Molecular Microbiology*, *79*(2), 419–432. https://doi.org/10.1111/j.1365-2958.2010.07454.x

Iosub, I. A., van Nues, R. W., McKellar, S. W., Nieken, K. J., Marchioretto, M., Sy, B., Tree, J. J., Viero, G., & Granneman, S. (2020). Hfq CLASH uncovers sRNA-target interaction networks linked to nutrient availability adaptation. *ELife*, *9*, e54655. https://doi.org/10.7554/eLife.54655

Irastortza-Olaziregi, M., & Amster-Choder, O. (2021). Coupled Transcription-Translation in Prokaryotes: An Old Couple With New Surprises. *Frontiers in Microbiology*, *11*. https://www.frontiersin.org/article/10.3389/fmicb.2020.624830

Jacob, A. I., Köhrer, C., Davies, B. W., RajBhandary, U. L., & Walker, G. C. (2013). Conserved bacterial RNase YbeY plays key roles in 70S ribosome quality control and 16S rRNA maturation. *Molecular Cell*, *49*(3), 427–438. https://doi.org/10.1016/j.molcel.2012.11.025

Jiwani, S., Alvarado, S., Ohr, R. J., Romero, A., Nguyen, B., & Jewett, T. J. (2013). Chlamydia trachomatis Tarp harbors distinct G and F actin binding domains that bundle actin filaments. *Journal of Bacteriology*, *195*(4), 708–716. https://doi.org/10.1128/JB.01768-12

Johnson, C. M., & Fisher, D. J. (2013). Site-Specific, Insertional Inactivation of incA in Chlamydia trachomatis Using a Group II Intron. *PLOS ONE*, *8*(12), e83989. https://doi.org/10.1371/journal.pone.0083989

Johnson, K. A., Tan, M., & Sütterlin, C. (2009). Centrosome abnormalities during a Chlamydia trachomatis infection are caused by dysregulation of the normal duplication pathway. *Cellular Microbiology*, *11*(7), 1064–1073. https://doi.org/10.1111/j.1462-5822.2009.01307.x

Jordan, S., Nelson, D., & Geisler, W. (2020). Chapter 1: Chlamydia trachomatis Infections. In *In Chlamydia Biology: From genome to disease* (pp. 1–30). Caister Academic Press, Norfolk, UK.

Jørgensen, M. G., Pettersen, J. S., & Kallipolitis, B. H. (2020). sRNA-mediated control in bacteria: An increasing diversity of regulatory mechanisms. *Biochimica et Biophysica Acta (BBA) - Gene Regulatory Mechanisms*, *1863*(5), 194504. https://doi.org/10.1016/j.bbagrm.2020.194504

Kaberdin, V. R., Miczak, A., Jakobsen, J. S., Lin-Chao, S., McDowall, K. J., & von Gabain, A. (1998). The endoribonucleolytic N-terminal half of Escherichia coli RNase E is evolutionarily conserved in Synechocystis sp. And other bacteria but not the C-terminal half, which is sufficient for degradosome assembly. *Proceedings of the National Academy of Sciences*, *95*(20), 11637–11642. https://doi.org/10.1073/pnas.95.20.11637

Kannan, R. M., Gérard, H. C., Mishra, M. K., Mao, G., Wang, S., Hali, M., Whittum-Hudson, J. A., & Hudson, A. P. (2013). Dendrimer-enabled transformation of Chlamydia trachomatis. *Microbial Pathogenesis*, *65*, 29–35. https://doi.org/10.1016/j.micpath.2013.08.003

Keb, G., Ferrell, J., Scanlon, K. R., Jewett, T. J., & Fields, K. A. (2021). Chlamydia trachomatis TmeA Directly Activates N-WASP To Promote Actin Polymerization and Functions Synergistically with TarP during Invasion. *MBio*, *12*(1), e02861-20. https://doi.org/10.1128/mBio.02861-20

Keb, G., & Fields, K. A. (2020). Markerless Gene Deletion by Floxed Cassette Allelic Exchange Mutagenesis in Chlamydia trachomatis. *JoVE (Journal of Visualized Experiments)*, *155*, e60848. https://doi.org/10.3791/60848

Kery, M. B., Feldman, M., Livny, J., & Tjaden, B. (2014). TargetRNA2: Identifying targets of small regulatory RNAs in bacteria. *Nucleic Acids Research*, *42*(W1), W124–W129. https://doi.org/10.1093/nar/gku317

Kido, M., Yamanaka, K., Mitani, T., Niki, H., Ogura, T., & Hiraga, S. (1996). RNase E polypeptides lacking a carboxyl-terminal half suppress a mukB mutation in Escherichia coli. *Journal of Bacteriology*, *178*(13), 3917–3925. https://doi.org/10.1128/jb.178.13.3917-3925.1996

Kim, S., Song, I., Eom, G., & Kim, S. (2018). A Small Periplasmic Protein with a Hydrophobic C-Terminal Residue Enhances DegP Proteolysis as a Suicide Activator. *Journal of Bacteriology*, *200*(3), e00519-17. https://doi.org/10.1128/JB.00519-17

Kintner, J., Lajoie, D., Hall, J., Whittimore, J., & Schoborg, R. V. (2014). Commonly prescribed β-lactam antibiotics induce C. trachomatis persistence/stress in culture at physiologically relevant concentrations. *Frontiers in Cellular and Infection Microbiology*, *4*, 44. https://doi.org/10.3389/fcimb.2014.00044

Klepsch, M. A. (2019). *Small RNA-binding complexes in Chlamydia trachomatis identified by Next-Generation Sequencing techniques*. Doctoral dissertation, Julius-Maximilians-Universität Würzburg.

Knowlton, A. E., Fowler, L. J., Patel, R. K., Wallet, S. M., & Grieshaber, S. S. (2013). Chlamydia induces anchorage independence in 3T3 cells and detrimental

cytological defects in an infection model. *PloS One*, *8*(1), e54022. https://doi.org/10.1371/journal.pone.0054022

Koo, I. C., & Stephens, R. S. (2003). A Developmentally Regulated Two-component Signal Transduction System in Chlamydia*. *Journal of Biological Chemistry*, *278*(19), 17314–17319. https://doi.org/10.1074/jbc.M212170200

Korzeniewski, N., Treat, B., & Duensing, S. (2011). The HPV-16 E7 oncoprotein induces centriole multiplication through deregulation of Polo-like kinase 4 expression. *Molecular Cancer*, *10*(1), 61. https://doi.org/10.1186/1476-4598-10-61

LaBrie, S. D., Dimond, Z. E., Harrison, K. S., Baid, S., Wickstrum, J., Suchland, R. J., & Hefty, P. S. (2019). Transposon Mutagenesis in Chlamydia trachomatis Identifies CT339 as a ComEC Homolog Important for DNA Uptake and Lateral Gene Transfer. *MBio*, *10*(4), e01343-19. https://doi.org/10.1128/mBio.01343-19

Lalaouna, D., Carrier, M.-C., Semsey, S., Brouard, J.-S., Wang, J., Wade, J. T., & Massé, E. (2015). A 3′ External Transcribed Spacer in a tRNA Transcript Acts as a Sponge for Small RNAs to Prevent Transcriptional Noise. *Molecular Cell*, *58*(3), 393–405. https://doi.org/10.1016/j.molcel.2015.03.013

Lalaouna, D., Desgranges, E., Caldelari, I., & Marzi, S. (2018). MS2-Affinity Purification Coupled With RNA Sequencing Approach in the Human Pathogen Staphylococcus aureus. *Methods in Enzymology*, *612*, 393–411. https://doi.org/10.1016/bs.mie.2018.08.022

Lalaouna, D., & Massé, E. (2015). Identification of sRNA interacting with a transcript of interest using MS2-affinity purification coupled with RNA sequencing (MAPS) technology. *Genomics Data*, *5*, 136–138. https://doi.org/10.1016/j.gdata.2015.05.033

Lalaouna, D., Prévost, K., Eyraud, A., & Massé, E. (2017). Identification of unknown RNA partners using MAPS. *Methods*, *117*, 28–34. https://doi.org/10.1016/j.ymeth.2016.11.011

Lambowitz, A. M., & Zimmerly, S. (2004). Mobile group II introns. *Annual Review of Genetics*, *38*, 1–35. https://doi.org/10.1146/annurev.genet.38.072902.091600

Lampe, D. J., Akerley, B. J., Rubin, E. J., Mekalanos, J. J., & Robertson, H. M. (1999). Hyperactive transposase mutants of the Himar1 mariner transposon. *Proceedings of the National Academy of Sciences of the United States of America*, *96*(20), 11428–11433. https://doi.org/10.1073/pnas.96.20.11428

Lan, J., van den Brule, A. J., Hemrika, D. J., Risse, E. K., Walboomers, J. M., Schipper, M. E., & Meijer, C. J. (1995). Chlamydia trachomatis and ectopic pregnancy:

Retrospective analysis of salpingectomy specimens, endometrial biopsies, and cervical smears. *Journal of Clinical Pathology*, *48*(9), 815–819. https://doi.org/10.1136/jcp.48.9.815

Lee, J., Cox, J. V., & Ouellette, S. P. (2020). Critical Role for the Extended N Terminus of Chlamydial MreB in Directing Its Membrane Association and Potential Interaction with Divisome Proteins. *Journal of Bacteriology*, *202*(9), e00034-20. https://doi.org/10.1128/JB.00034-20

Lee, J. K., Enciso, G. A., Boassa, D., Chander, C. N., Lou, T. H., Pairawan, S. S., Guo, M. C., Wan, F. Y. M., Ellisman, M. H., Sütterlin, C., & Tan, M. (2018). Replication-dependent size reduction precedes differentiation in Chlamydia trachomatis. *Nature Communications*, *9*(1), 45. https://doi.org/10.1038/s41467-017-02432-0

Liechti, G. W., Kuru, E., Hall, E., Kalinda, A., Brun, Y. V., VanNieuwenhze, M., & Maurelli, A. T. (2014). A new metabolic cell-wall labelling method reveals peptidoglycan in Chlamydia trachomatis. *Nature*, *506*(7489), 507–510. https://doi.org/10.1038/nature12892

Lin-Chao, S., Wei, C.-L., & Lin, Y.-T. (1999). RNase E is required for the maturation of ssrA RNA and normal ssrA RNA peptide-tagging activity. *Proceedings of the National Academy of Sciences*, *96*(22), 12406–12411. https://doi.org/10.1073/pnas.96.22.12406

Lingle, W. L., Lutz, W. H., Ingle, J. N., Maihle, N. J., & Salisbury, J. L. (1998). Centrosome hypertrophy in human breast tumors: Implications for genomic stability and cell polarity. *Proceedings of the National Academy of Sciences of the United States of America*, *95*(6), 2950–2955. https://doi.org/10.1073/pnas.95.6.2950

Lorenz, R., Bernhart, S. H., Höner Zu Siederdissen, C., Tafer, H., Flamm, C., Stadler, P. F., & Hofacker, I. L. (2011). ViennaRNA Package 2.0. *Algorithms for Molecular Biology: AMB*, *6*, 26. https://doi.org/10.1186/1748-7188-6-26

Luo, Z., Neville, S. L., Campbell, R., Morey, J. R., Menon, S., Thomas, M., Eijkelkamp, B. A., Ween, M. P., Huston, W. M., Kobe, B., & McDevitt, C. A. (2019). Structure and Metal Binding Properties of Chlamydia trachomatis YtgA. *Journal of Bacteriology*, *202*(1), e00580-19. https://doi.org/10.1128/JB.00580-19

Ma, H. T., & Poon, R. Y. C. (2017). Synchronization of HeLa Cells. *Methods in Molecular Biology (Clifton, N.J.)*, *1524*, 189–201. https://doi.org/10.1007/978-1-4939-6603-5_12

Magistro, G., Magistro, C., Stief, C. G., & Schubert, S. (2018). A simple and highly efficient method for gene silencing in Escherichia coli. *Journal of Microbiological Methods*, *154*, 25–32. https://doi.org/10.1016/j.mimet.2018.10.003

Mai, J., Rao, C., Watt, J., Sun, X., Lin, C., Zhang, L., & Liu, W. (2019). Mycobacterium tuberculosis 6C sRNA binds multiple mRNA targets via C-rich loops independent of RNA chaperones. *Nucleic Acids Research*, *47*. https://doi.org/10.1093/nar/gkz149

Mallory, A. C., & Vaucheret, H. (2009). ARGONAUTE 1 homeostasis invokes the coordinate action of the microRNA and siRNA pathways. *EMBO Reports*, *10*(5), 521–526. https://doi.org/10.1038/embor.2009.32

Man, S., Cheng, R., Miao, C., Gong, Q., Gu, Y., Lu, X., Han, F., & Yu, W. (2011). Artificial trans-encoded small non-coding RNAs specifically silence the selected gene expression in bacteria. *Nucleic Acids Research*, *39*(8), e50. https://doi.org/10.1093/nar/gkr034

Mann, M., Wright, P. R., & Backofen, R. (2017). IntaRNA 2.0: Enhanced and customizable prediction of RNA–RNA interactions. *Nucleic Acids Research*, *45*(W1), W435–W439. https://doi.org/10.1093/nar/gkx279

Massé, E., Escorcia, F. E., & Gottesman, S. (2003). Coupled degradation of a small regulatory RNA and its mRNA targets in Escherichia coli. *Genes & Development*, *17*(19), 2374–2383. https://doi.org/10.1101/gad.1127103

Massé, E., & Gottesman, S. (2002). A small RNA regulates the expression of genes involved in iron metabolism in Escherichia coli. *Proceedings of the National Academy of Sciences*, *99*(7), 4620–4625. https://doi.org/10.1073/pnas.032066599

Mehlitz, A., & Rudel, T. (2013). Modulation of host signaling and cellular responses by Chlamydia. *Cell Communication and Signaling: CCS*, *11*, 90. https://doi.org/10.1186/1478-811X-11-90

Mei, H., Tang, Q., Li, X., Wang, Y., Wang, J., & He, J. (2015). Insights into sRNA Genes Regulated by Two-Component Systems in the Bacillus cereus Group. *Current Bioinformatics*, *10*. https://doi.org/10.2174/1574893610041509221510 28

Melamed, S., Adams, P. P., Zhang, A., Zhang, H., & Storz, G. (2020). RNA-RNA Interactomes of ProQ and Hfq Reveal Overlapping and Competing Roles. *Molecular Cell*, *77*(2), 411-425.e7. https://doi.org/10.1016/j.molcel.2019.10.022

Mercier, N., Prévost, K., Massé, E., Romby, P., Caldelari, I., & Lalaouna, D. (2021). MS2-Affinity Purification Coupled with RNA Sequencing in Gram-Positive

Bacteria. *JoVE (Journal of Visualized Experiments)*, *168*, e61731. https://doi.org/10.3791/61731

Meyer, T. (2016). Diagnostic Procedures to Detect Chlamydia trachomatis Infections. *Microorganisms*, *4*(3). https://doi.org/10.3390/microorganisms4030025

Mikule, K., Delaval, B., Kaldis, P., Jurcyzk, A., Hergert, P., & Doxsey, S. (2007). Loss of centrosome integrity induces p38—P53—P21-dependent G1—S arrest. *Nature Cell Biology*, *9*(2), 160–170. https://doi.org/10.1038/ncb1529

Miller, O. L., Hamkalo, B. A., & Thomas, C. A. (1970). Visualization of bacterial genes in action. *Science (New York, N.Y.)*, *169*(3943), 392–395. https://doi.org/10.1126/science.169.3943.392

Mital, J., Lutter, E. I., Barger, A. C., Dooley, C. A., & Hackstadt, T. (2015). Chlamydia trachomatis inclusion membrane protein CT850 interacts with the dynein light chain DYNLT1 (Tctex1). *Biochemical and Biophysical Research Communications*, *462*(2), 165–170. https://doi.org/10.1016/j.bbrc.2015.04.116

Mojica, F. J. M., Díez-Villaseñor, C., García-Martínez, J., & Almendros, C. (2009). Short motif sequences determine the targets of the prokaryotic CRISPR defence system. *Microbiology (Reading, England)*, *155*(Pt 3), 733–740. https://doi.org/10.1099/mic.0.023960-0

Møller, T., Franch, T., Udesen, C., Gerdes, K., & Valentin-Hansen, P. (2002). Spot 42 RNA mediates discoordinate expression of the E. coli galactose operon. *Genes & Development*, *16*(13), 1696–1706. https://doi.org/10.1101/gad.231702

Morita, T., Maki, K., & Aiba, H. (2005). RNase E-based ribonucleoprotein complexes: Mechanical basis of mRNA destabilization mediated by bacterial noncoding RNAs. *Genes & Development*, *19*(18), 2176–2186. https://doi.org/10.1101/gad.1330405

Moulder, J. W. (1991). Interaction of chlamydiae and host cells in vitro. *Microbiology and Molecular Biology Reviews*, *55*(1), 143–190.

Mueller, K. E., Wolf, K., & Fields, K. A. (2016). Gene Deletion by Fluorescence-Reported Allelic Exchange Mutagenesis in Chlamydia trachomatis. *MBio*, *7*(1), e01817-01815. https://doi.org/10.1128/mBio.01817-15

Mueller, K. E., Wolf, K., & Fields, K. A. (2017). Chlamydia trachomatis transformation and allelic exchange mutagenesis. *Current Protocols in Microbiology*, *45*, 11A.3.1-11A.3.15. https://doi.org/10.1002/cpmc.31

Münger, K., Baldwin, A., Edwards, K. M., Hayakawa, H., Nguyen, C. L., Owens, M., Grace, M., & Huh, K. (2004). Mechanisms of human papillomavirus-induced

oncogenesis. *Journal of Virology*, *78*(21), 11451–11460. https://doi.org/10.1128/JVI.78.21.11451-11460.2004

Muñoz, K. J., Wang, K., Sheehan, L. M., Tan, M., & Sütterlin, C. (2021). The Small Molecule H89 Inhibits Chlamydia Inclusion Growth and Production of Infectious Progeny. *Infection and Immunity*, *89*(7), e00729-20. https://doi.org/10.1128/IAI.00729-20

Muñoz, N., Bosch, F. X., de Sanjosé, S., Herrero, R., Castellsagué, X., Shah, K. V., Snijders, P. J. F., Meijer, C. J. L. M., & International Agency for Research on Cancer Multicenter Cervical Cancer Study Group. (2003). Epidemiologic classification of human papillomavirus types associated with cervical cancer. *The New England Journal of Medicine*, *348*(6), 518–527. https://doi.org/10.1056/NEJMoa021641

Murall, C. L., Jackson, R., Zehbe, I., Boulle, N., Segondy, M., & Alizon, S. (2019). Epithelial stratification shapes infection dynamics. *PLOS Computational Biology*, *15*(1), e1006646. https://doi.org/10.1371/journal.pcbi.1006646

Na, D., Yoo, S. M., Chung, H., Park, H., Park, J. H., & Lee, S. Y. (2013). Metabolic engineering of Escherichia coli using synthetic small regulatory RNAs. *Nature Biotechnology*, *31*(2), 170–174. https://doi.org/10.1038/nbt.2461

Nakashima, N., T, T., & L, G. (2006). Paired termini stabilize antisense RNAs and enhance conditional gene silencing in Escherichia coli. *Nucleic Acids Research*, *34*(20). https://doi.org/10.1093/nar/gkl697

Natale, P., Brüser, T., & Driessen, A. J. M. (2008). Sec- and Tat-mediated protein secretion across the bacterial cytoplasmic membrane—Distinct translocases and mechanisms. *Biochimica et Biophysica Acta (BBA) - Biomembranes*, *1778*(9), 1735–1756. https://doi.org/10.1016/j.bbamem.2007.07.015

Nelson, D. E. (2012). The Chlamydial Cell envelope. In *Intracellular Pathogens 1: Chlamydiales Vol. 1* (1st ed., pp. 74–96). American Society for Microbiology Press.

Niehus, E., Cheng, E., & Tan, M. (2008). DNA supercoiling-dependent gene regulation in Chlamydia. *Journal of Bacteriology*, *190*(19), 6419–6427. https://doi.org/10.1128/JB.00431-08

Noh, M., Yoo, S. M., Kim, W. J., & Lee, S. Y. (2017). Gene Expression Knockdown by Modulating Synthetic Small RNA Expression in Escherichia coli. *Cell Systems*, *5*(4), 418-426.e4. https://doi.org/10.1016/j.cels.2017.08.016

Nowotny, M., & Yang, W. (2009). Structural and functional modules in RNA interference. *Current Opinion in Structural Biology*, *19*(3), 286–293. https://doi.org/10.1016/j.sbi.2009.04.006

Omsland, A., Sager, J., Nair, V., Sturdevant, D. E., & Hackstadt, T. (2012). Developmental stage-specific metabolic and transcriptional activity of Chlamydia trachomatis in an axenic medium. *Proceedings of the National Academy of Sciences*, *109*(48), 19781–19785. https://doi.org/10.1073/pnas.1212831109

O'Neill, C. E., Clarke, I. N., & Fisher, D. J. (2020). Chapter 11: Chlamydia Genetics. In *In Chlamydia Biology: From genome to disease* (pp. 241–262). Caister Academic Press, Norfolk, UK.

Opdyke, J. A., Fozo, E. M., Hemm, M. R., & Storz, G. (2011). RNase III participates in GadY-dependent cleavage of the gadX-gadW mRNA. *Journal of Molecular Biology*, *406*(1), 29–43. https://doi.org/10.1016/j.jmb.2010.12.009

Orillard, E., & Tan, M. (2016). Functional analysis of three topoisomerases that regulate DNA supercoiling levels in Chlamydia. *Molecular Microbiology*, *99*(3), 484–496. https://doi.org/10.1111/mmi.13241

Ouellette, S. P. (2018). Feasibility of a Conditional Knockout System for Chlamydia Based on CRISPR Interference. *Frontiers in Cellular and Infection Microbiology*, *8*. https://doi.org/10.3389/fcimb.2018.00059

Ouellette, S. P., Blay, E. A., Hatch, N. D., & Fisher-Marvin, L. A. (2021). CRISPR Interference To Inducibly Repress Gene Expression in Chlamydia trachomatis. *Infection and Immunity*. https://doi.org/10.1128/IAI.00108-21

Ouellette, S. P., Hatch, T. P., AbdelRahman, Y. M., Rose, L. A., Belland, R. J., & Byrne, G. I. (2006). Global transcriptional upregulation in the absence of increased translation in Chlamydia during IFNγ-mediated host cell tryptophan starvation. *Molecular Microbiology*, *62*(5), 1387–1401. https://doi.org/10.1111/j.1365-2958.2006.05465.x

Ouellette, S. P., Karimova, G., Subtil, A., & Ladant, D. (2012). Chlamydia co-opts the rod shape-determining proteins MreB and Pbp2 for cell division. *Molecular Microbiology*, *85*(1), 164–178. https://doi.org/10.1111/j.1365-2958.2012.08100.x

Pandey, S. P., Minesinger, B. K., Kumar, J., & Walker, G. C. (2011). A highly conserved protein of unknown function in Sinorhizobium meliloti affects sRNA regulation similar to Hfq. *Nucleic Acids Research*, *39*(11), 4691–4708. https://doi.org/10.1093/nar/gkr060

Pandey, S. P., Winkler, J. A., Li, H., Camacho, D. M., Collins, J. J., & Walker, G. C. (2014). Central role for RNase YbeY in Hfq-dependent and Hfq-independent

small-RNA regulation in bacteria. *BMC Genomics*, *15*, 121. https://doi.org/10.1186/1471-2164-15-121

Panzetta, M. E., Valdivia, R. H., & Saka, H. A. (2018). Chlamydia Persistence: A Survival Strategy to Evade Antimicrobial Effects in-vitro and in-vivo. *Frontiers in Microbiology*, *9*, 3101. https://doi.org/10.3389/fmicb.2018.03101

Papenfort, K., & Vanderpool, C. (2015). Target activation by regulatory RNAs in bacteria. *FEMS Microbiology Reviews*, *39*. https://doi.org/10.1093/femsre/fuv016

Park, J. S., Lee, W. C., Yeo, K. J., Ryu, K.-S., Kumarasiri, M., Hesek, D., Lee, M., Mobashery, S., Song, J. H., Kim, S. I., Lee, J. C., Cheong, C., Jeon, Y. H., & Kim, H.-Y. (2012). Mechanism of anchoring of OmpA protein to the cell wall peptidoglycan of the gram-negative bacterial outer membrane. *FASEB Journal: Official Publication of the Federation of American Societies for Experimental Biology*, *26*(1), 219–228. https://doi.org/10.1096/fj.11-188425

Parmeciano Di Noto, G., Molina, M. C., & Quiroga, C. (2019). Insights Into Non-coding RNAs as Novel Antimicrobial Drugs. *Frontiers in Genetics*, *10*. https://www.frontiersin.org/article/10.3389/fgene.2019.00057

Pazin, M. J., & Kadonaga, J. T. (1997). SWI2/SNF2 and Related Proteins: ATP-Driven Motors That Disrupt-Protein–DNA Interactions? *Cell*, *88*(6), 737–740. https://doi.org/10.1016/S0092-8674(00)81918-2

Pedersen, L. B., Birkelund, S., & Christiansen, G. (1996). Purification of recombinant Chlamydia trachomatis histone H1-like protein Hc2, and comparative functional analysis of Hc2 and Hc1. *Molecular Microbiology*, *20*(2), 295–311. https://doi.org/10.1111/j.1365-2958.1996.tb02618.x

Pfaffl, M. W. (2001). A new mathematical model for relative quantification in real-time RT-PCR. *Nucleic Acids Research*, *29*(9), e45. https://doi.org/10.1093/nar/29.9.e45

Pihan, G. A., Purohit, A., Wallace, J., Knecht, H., Woda, B., Quesenberry, P., & Doxsey, S. J. (1998). Centrosome defects and genetic instability in malignant tumors. *Cancer Research*, *58*(17), 3974–3985.

Pinidis, P., Tsikouras, P., Iatrakis, G., Zervoudis, S., Koukouli, Z., Bothou, A., Galazios, G., & Vladareanu, S. (2016). Human Papilloma Virus' Life Cycle and Carcinogenesis. *Mædica*, *11*(1), 48–54.

Pokorzynski, N. D., Brinkworth, A. J., & Carabeo, R. (2019). A bipartite iron-dependent transcriptional regulation of the tryptophan salvage pathway in Chlamydia trachomatis. *ELife*, *8*, e42295. https://doi.org/10.7554/eLife.42295

Pokorzynski, N. D., Thompson, C. C., & Carabeo, R. A. (2017). Ironing Out the Unconventional Mechanisms of Iron Acquisition and Gene Regulation in Chlamydia. *Frontiers in Cellular and Infection Microbiology*, *7*. https://www.frontiersin.org/article/10.3389/fcimb.2017.00394

Politi, N., Pasotti, L., Zucca, S., Casanova, M., Micoli, G., Cusella De Angelis, M. G., & Magni, P. (2014). Half-life measurements of chemical inducers for recombinant gene expression. *Journal of Biological Engineering*, *8*(1), 5. https://doi.org/10.1186/1754-1611-8-5

Prévost, K., Desnoyers, G., Jacques, J.-F., Lavoie, F., & Massé, E. (2011). Small RNA-induced mRNA degradation achieved through both translation block and activated cleavage. *Genes & Development*, *25*(4), 385–396. https://doi.org/10.1101/gad.2001711

Pulvermacher, S. C., Stauffer, L. T., & Stauffer, G. V. (2009). Role of the sRNA GcvB in regulation of cycA in Escherichia coli. *Microbiology (Reading, England)*, *155*(Pt 1), 106–114. https://doi.org/10.1099/mic.0.023598-0

Qi, L. S., Larson, M. H., Gilbert, L. A., Doudna, J. A., Weissman, J. S., Arkin, A. P., & Lim, W. A. (2013). Repurposing CRISPR as an RNA-Guided Platform for Sequence-Specific Control of Gene Expression. *Cell*, *152*(5), 1173–1183. https://doi.org/10.1016/j.cell.2013.02.022

Raden, M., Ali, S. M., Alkhnbashi, O. S., Busch, A., Costa, F., Davis, J. A., Eggenhofer, F., Gelhausen, R., Georg, J., Heyne, S., Hiller, M., Kundu, K., Kleinkauf, R., Lott, S. C., Mohamed, M. M., Mattheis, A., Miladi, M., Richter, A. S., Will, S., … Backofen, R. (2018). Freiburg RNA tools: A central online resource for RNA-focused research and teaching. *Nucleic Acids Research*, *46*(W1), W25–W29. https://doi.org/10.1093/nar/gky329

Rahnama, M., & Fields, K. A. (2018). Transformation of Chlamydia: Current approaches and impact on our understanding of chlamydial infection biology. *Microbes and Infection*, *20*(7–8), 445–450. https://doi.org/10.1016/j.micinf.2018.01.002

Raina, M., King, A., Bianco, C., & Vanderpool, C. K. (2018). Dual-function RNAs. *Microbiology Spectrum*, *6*(5), 10.1128/microbiolspec.RWR-0032–2018. https://doi.org/10.1128/microbiolspec.RWR-0032-2018

Ranjit, D. K., Liechti, G. W., & Maurelli, A. T. (2020). Chlamydial MreB Directs Cell Division and Peptidoglycan Synthesis in Escherichia coli in the Absence of FtsZ Activity. *MBio*, *11*(1), e03222-19. https://doi.org/10.1128/mBio.03222-19

Rice, J. B., & Vanderpool, C. K. (2011). The small RNA SgrS controls sugar-phosphate accumulation by regulating multiple PTS genes. *Nucleic Acids Research*, *39*(9), 3806–3819. https://doi.org/10.1093/nar/gkq1219

Rosario, C. J., Hanson, B. R., & Tan, M. (2014). The Transcriptional Repressor EUO Regulates Both Subsets of Chlamydia Late Genes. *Molecular Microbiology*, *94*(4), 888–897. https://doi.org/10.1111/mmi.12804

Rosario, C. J., & Tan, M. (2012). The early gene product EUO is a transcriptional repressor that selectively regulates promoters of Chlamydia late genes. *Molecular Microbiology*, *84*(6), 1097–1107. https://doi.org/10.1111/j.1365-2958.2012.08077.x

Rosario CJ, T. M. (2020). Chapter 10: Chlamydia gene regulation. In *In Chlamydia Biology: From genome to disease* (pp. 219–240). Caister Academic Press, Norfolk, UK.

Rosmarin, D. M., Carette, J. E., Olive, A. J., Starnbach, M. N., Brummelkamp, T. R., & Ploegh, H. L. (2012). Attachment of Chlamydia trachomatis L2 to host cells requires sulfation. *Proceedings of the National Academy of Sciences*, *109*(25), 10059–10064. https://doi.org/10.1073/pnas.1120244109

Ruijter, J. M., Ramakers, C., Hoogaars, W. M. H., Karlen, Y., Bakker, O., van den Hoff, M. J. B., & Moorman, A. F. M. (2009). Amplification efficiency: Linking baseline and bias in the analysis of quantitative PCR data. *Nucleic Acids Research*, *37*(6), e45. https://doi.org/10.1093/nar/gkp045

Said, N., Rieder, R., Hurwitz, R., Deckert, J., Urlaub, H., & Vogel, J. (2009). In vivo expression and purification of aptamer-tagged small RNA regulators. *Nucleic Acids Research*, *37*(20), e133. https://doi.org/10.1093/nar/gkp719

Saka, H. A., Thompson, J. W., Chen, Y.-S., Kumar, Y., Dubois, L. G., Moseley, M. A., & Valdivia, R. H. (2011). Quantitative proteomics reveals metabolic and pathogenic properties of Chlamydia trachomatis developmental forms. *Molecular Microbiology*, *82*(5), 1185–1203. https://doi.org/10.1111/j.1365-2958.2011.07877.x

Saliba, A.-E., C Santos, S., & Vogel, J. (2017). New RNA-seq approaches for the study of bacterial pathogens. *Current Opinion in Microbiology*, *35*, 78–87. https://doi.org/10.1016/j.mib.2017.01.001

Salisbury, J. L., Whitehead, C. M., Lingle, W. L., & Barrett, S. L. (1999). Centrosomes and cancer. *Biology of the Cell*, *91*(6), 451–460. https://doi.org/10.1111/j.1768-322X.1999.tb01100.x

Schaeffer, A. J., Nguyen, M., Liem, A., Lee, D., Montagna, C., Lambert, P. F., Ried, T., & Difilippantonio, M. J. (2004). E6 and E7 oncoproteins induce distinct patterns of chromosomal aneuploidy in skin tumors from transgenic mice. *Cancer Research*, *64*(2), 538–546. https://doi.org/10.1158/0008-5472.can-03-0124

Schmidt, K. N., Kuhns, S., Neuner, A., Hub, B., Zentgraf, H., & Pereira, G. (2012). Cep164 mediates vesicular docking to the mother centriole during early steps of ciliogenesis. *Journal of Cell Biology*, *199*(7), 1083–1101. https://doi.org/10.1083/jcb.201202126

Schoborg, R. V. (2011). Chlamydia persistence – a tool to dissect chlamydia–host interactions. *Microbes and Infection*, *13*(7), 649–662. https://doi.org/10.1016/j.micinf.2011.03.004

Schwarz, E., Freese, U. K., Gissmann, L., Mayer, W., Roggenbuck, B., Stremlau, A., & Hausen, H. zur. (1985). Structure and transcription of human papillomavirus sequences in cervical carcinoma cells. *Nature*, *314*(6006), 111–114. https://doi.org/10.1038/314111a0

Scidmore, M. A., & Hackstadt, T. (2001). Mammalian 14-3-3beta associates with the Chlamydia trachomatis inclusion membrane via its interaction with IncG. *Molecular Microbiology*, *39*(6), 1638–1650. https://doi.org/10.1046/j.1365-2958.2001.02355.x

Sedlyarova, N., Shamovsky, I., Bharati, B. K., Epshtein, V., Chen, J., Gottesman, S., Schroeder, R., & Nudler, E. (2016). SRNA-Mediated Control of Transcription Termination in E. coli. *Cell*, *167*(1), 111-121.e13. https://doi.org/10.1016/j.cell.2016.09.004

Seshasayee, A. S. N., Sivaraman, K., & Luscombe, N. M. (2011). An overview of prokaryotic transcription factors: A summary of function and occurrence in bacterial genomes. *Sub-Cellular Biochemistry*, *52*, 7–23. https://doi.org/10.1007/978-90-481-9069-0_2

Sharma, C. M., & Vogel, J. (2009a). Experimental approaches for the discovery and characterization of regulatory small RNA. *Current Opinion in Microbiology*, *12*(5), 536–546. https://doi.org/10.1016/j.mib.2009.07.006

Sharma, C. M., & Vogel, J. (2009b). Experimental approaches for the discovery and characterization of regulatory small RNA. *Current Opinion in Microbiology*, *12*(5), 536–546. https://doi.org/10.1016/j.mib.2009.07.006

Shaw, E. I., Dooley, C. A., Fischer, E. R., Scidmore, M. A., Fields, K. A., & Hackstadt, T. (2000). Three temporal classes of gene expression during the Chlamydia trachomatis developmental cycle. *Molecular Microbiology*, *37*(4), 913–925. https://doi.org/10.1046/j.1365-2958.2000.02057.x

Shaw, J. H., Key, C. E., Snider, T. A., Sah, P., Shaw, E. I., Fisher, D. J., & Lutter, E. I. (2018). Genetic Inactivation of Chlamydia trachomatis Inclusion Membrane Protein CT228 Alters MYPT1 Recruitment, Extrusion Production, and Longevity

of Infection. *Frontiers in Cellular and Infection Microbiology*, *8*, 415. https://doi.org/10.3389/fcimb.2018.00415

Sheehan, L. M., Budnick, J. A., Fyffe-Blair, J., King, K. A., Settlage, R. E., & Caswell, C. C. (2020). The Endoribonuclease RNase E Coordinates Expression of mRNAs and Small Regulatory RNAs and Is Critical for the Virulence of Brucella abortus. *Journal of Bacteriology*, *202*(20), e00240-20. https://doi.org/10.1128/JB.00240-20

Sheehan, L. M., & Caswell, C. C. (2017). A 6-Nucleotide Regulatory Motif within the AbcR Small RNAs of Brucella abortus Mediates Host-Pathogen Interactions. *MBio*, *8*(3), e00473-17. https://doi.org/10.1128/mBio.00473-17

Siegl, C., Prusty, B. K., Karunakaran, K., Wischhusen, J., & Rudel, T. (2014). Tumor Suppressor p53 Alters Host Cell Metabolism to Limit Chlamydia trachomatis Infection. *Cell Reports*, *9*(3), 918–929. https://doi.org/10.1016/j.celrep.2014.10.004

Sigalova, O. M., Chaplin, A. V., Bochkareva, O. O., Shelyakin, P. V., Filaretov, V. A., Akkuratov, E. E., Burskaia, V., & Gelfand, M. S. (2019). Chlamydia pan-genomic analysis reveals balance between host adaptation and selective pressure to genome reduction. *BMC Genomics*, *20*(1), 710. https://doi.org/10.1186/s12864-019-6059-5

Silva, J., Cerqueira, F., & Medeiros, R. (2014). Chlamydia trachomatis infection: Implications for HPV status and cervical cancer. *Archives of Gynecology and Obstetrics*, *289*(4), 715–723. https://doi.org/10.1007/s00404-013-3122-3

Skilton, R. J., Cutcliffe, L. T., Barlow, D., Wang, Y., Salim, O., Lambden, P. R., & Clarke, I. N. (2009). Penicillin Induced Persistence in Chlamydia trachomatis: High Quality Time Lapse Video Analysis of the Developmental Cycle. *PLoS ONE*, *4*(11), e7723. https://doi.org/10.1371/journal.pone.0007723

Skipp, P., Robinson, J., O'Connor, C. D., & Clarke, I. N. (2005). Shotgun proteomic analysis of Chlamydia trachomatis. *Proteomics*, *5*(6), 1558–1573. https://doi.org/10.1002/pmic.200401044

Smirnov, A., Wang, C., Drewry, L. L., & Vogel, J. (2017). Molecular mechanism of mRNA repression in trans by a ProQ-dependent small RNA. *The EMBO Journal*, *36*(8), 1029–1045. https://doi.org/10.15252/embj.201696127

Smith, J. S., Muñoz, N., Herrero, R., Eluf-Neto, J., Ngelangel, C., Franceschi, S., Bosch, F. X., Walboomers, J. M. M., & Peeling, R. W. (2002). Evidence for Chlamydia trachomatis as a Human Papillomavirus Cofactor in the Etiology of Invasive Cervical Cancer in Brazil and the Philippines. *The Journal of Infectious Diseases*, *185*(3), 324–331. https://doi.org/10.1086/338569

Soules, K. R., Dmitriev, A., LaBrie, S. D., Dimond, Z. E., May, B. H., Johnson, D. K., Zhang, Y., Battaile, K. P., Lovell, S., & Hefty, P. S. (2020). Structural and ligand binding analyses of the periplasmic sensor domain of RsbU in Chlamydia trachomatis support a role in TCA cycle regulation. *Molecular Microbiology*, *113*(1), 68–88. https://doi.org/10.1111/mmi.14401

Spardy, N., Covella, K., Cha, E., Hoskins, E. E., Wells, S. I., Duensing, A., & Duensing, S. (2009). Human Papillomavirus 16 E7 Oncoprotein Attenuates DNA Damage Checkpoint Control by Increasing the Proteolytic Turnover of Claspin. *Cancer Research*, *69*(17), 7022–7029.

Spurgeon, M. E., & Lambert, P. F. (2017). Human Papillomavirus and the Stroma: Bidirectional Crosstalk during the Virus Life Cycle and Carcinogenesis. *Viruses*, *9*(8). https://doi.org/10.3390/v9080219

Stamm, W. E. (1999). Chlamydia trachomatis infections: Progress and problems. *The Journal of Infectious Diseases*, *179 Suppl 2*, S380-383. https://doi.org/10.1086/513844

Stocks, M. E., Ogden, S., Haddad, D., Addiss, D. G., McGuire, C., & Freeman, M. C. (2014). Effect of water, sanitation, and hygiene on the prevention of trachoma: A systematic review and meta-analysis. *PLoS Medicine*, *11*(2), e1001605. https://doi.org/10.1371/journal.pmed.1001605

Storz, G., Vogel, J., & Wassarman, K. M. (2011). Regulation by Small RNAs in Bacteria: Expanding Frontiers. *Molecular Cell*, *43*(6), 880–891. https://doi.org/10.1016/j.molcel.2011.08.022

Storz, G., Wolf, Y. I., & Ramamurthi, K. S. (2014). Small Proteins Can No Longer Be Ignored. *Annual Review of Biochemistry*, *83*, 753–777. https://doi.org/10.1146/annurev-biochem-070611-102400

Su, H., Watkins, N. G., Zhang, Y. X., & Caldwell, H. D. (1990). Chlamydia trachomatis-host cell interactions: Role of the chlamydial major outer membrane protein as an adhesin. *Infection and Immunity*, *58*(4), 1017–1025.

Suchland, R. J., Sandoz, K. M., Jeffrey, B. M., Stamm, W. E., & Rockey, D. D. (2009). Horizontal transfer of tetracycline resistance among Chlamydia spp. In vitro. *Antimicrobial Agents and Chemotherapy*, *53*(11), 4604–4611. https://doi.org/10.1128/AAC.00477-09

Sun, G., Pal, S., Sarcon, A. K., Kim, S., Sugawara, E., Nikaido, H., Cocco, M. J., Peterson, E. M., & de la Maza, L. M. (2007). Structural and Functional Analyses of the Major Outer Membrane Protein of Chlamydia trachomatis. *Journal of Bacteriology*, *189*(17), 6222–6235. https://doi.org/10.1128/JB.00552-07

Sun, H. S., Sin, A. T.-W., Poirier, M. B., & Harrison, R. E. (2016). Chlamydia trachomatis Inclusion Disrupts Host Cell Cytokinesis to Enhance Its Growth in Multinuclear Cells. *Journal of Cellular Biochemistry*, *117*(1), 132–143. https://doi.org/10.1002/jcb.25258

Swanson, A. F., & Kuo, C. C. (1994). Binding of the glycan of the major outer membrane protein of Chlamydia trachomatis to HeLa cells. *Infection and Immunity*, *62*(1), 24–28. https://doi.org/10.1128/iai.62.1.24-28.1994

Tam, J. E., Davis, C. H., & Wyrick, P. B. (1994). Expression of recombinant DNA introduced into Chlamydia trachomatis by electroporation. *Canadian Journal of Microbiology*, *40*(7), 583–591. https://doi.org/10.1139/m94-093

Tang, Y., Wang, J., Lian, Y., Fan, C., Zhang, P., Wu, Y., Li, X., Xiong, F., Li, X., Li, G., Xiong, W., & Zeng, Z. (2017). Linking long non-coding RNAs and SWI/SNF complexes to chromatin remodeling in cancer. *Molecular Cancer*, *16*(1), 42. https://doi.org/10.1186/s12943-017-0612-0

Taylor, B. D., & Haggerty, C. L. (2011). Management of Chlamydia trachomatis genital tract infection: Screening and treatment challenges. *Infection and Drug Resistance*, *4*, 19–29. https://doi.org/10.2147/IDR.S12715

Tejada-Arranz, A., Crécy-Lagard, V. de, & Reuse, H. de. (2020). Bacterial RNA Degradosomes: Molecular Machines under Tight Control. *Trends in Biochemical Sciences*, *45*(1), 42–57. https://doi.org/10.1016/j.tibs.2019.10.002

Terns, M. P. (2018). CRISPR-Based Technologies: Impact of RNA-Targeting Systems. *Molecular Cell*, *72*(3), 404–412. https://doi.org/10.1016/j.molcel.2018.09.018

Thomas, J. T., & Laimins, L. A. (1998). Human papillomavirus oncoproteins E6 and E7 independently abrogate the mitotic spindle checkpoint. *Journal of Virology*, *72*(2), 1131–1137. https://doi.org/10.1128/JVI.72.2.1131-1137.1998

Thompson, C. C., Nicod, S. S., Malcolm, D. S., Grieshaber, S. S., & Carabeo, R. A. (2012). Cleavage of a putative metal permease in Chlamydia trachomatis yields an iron-dependent transcriptional repressor. *Proceedings of the National Academy of Sciences*, *109*(26), 10546–10551. https://doi.org/10.1073/pnas.1201398109

Toyoda, K., Manganelli, R., & Pátek, M. (2021). Editorial: Role of Sigma Factors of RNA Polymerase in Bacterial Physiology. *Frontiers in Microbiology*, *12*, 648. https://doi.org/10.3389/fmicb.2021.633740

Travers, A., & Muskhelishvili, G. (2005). DNA supercoiling—A global transcriptional regulator for enterobacterial growth? *Nature Reviews. Microbiology*, *3*(2), 157–169. https://doi.org/10.1038/nrmicro1088

Urban, J. H., & Vogel, J. (2007). Translational control and target recognition by Escherichia coli small RNAs in vivo. *Nucleic Acids Research*, *35*(3), 1018–1037. https://doi.org/10.1093/nar/gkl1040

Vanderpool, C. K., & Gottesman, S. (2004). Involvement of a novel transcriptional activator and small RNA in post-transcriptional regulation of the glucose phosphoenolpyruvate phosphotransferase system. *Molecular Microbiology*, *54*(4), 1076–1089. https://doi.org/10.1111/j.1365-2958.2004.04348.x

Vargas-Blanco, D. A., & Shell, S. S. (2020). Regulation of mRNA Stability During Bacterial Stress Responses. *Frontiers in Microbiology*, *11*. https://www.frontiersin.org/article/10.3389/fmicb.2020.02111

Vercruysse, M., Köhrer, C., Davies, B. W., Arnold, M. F. F., Mekalanos, J. J., RajBhandary, U. L., & Walker, G. C. (2014). The Highly Conserved Bacterial RNase YbeY Is Essential in Vibrio cholerae, Playing a Critical Role in Virulence, Stress Regulation, and RNA Processing. *PLOS Pathogens*, *10*(6), e1004175. https://doi.org/10.1371/journal.ppat.1004175

Vogel, J. (2020). An RNA biology perspective on species-specific programmable RNA antibiotics. *Molecular Microbiology*, *113*(3), 550–559. https://doi.org/10.1111/mmi.14476

Vogel, J., & Wagner, E. G. H. (2007). Target identification of small noncoding RNAs in bacteria. *Current Opinion in Microbiology*, *10*(3), 262–270. https://doi.org/10.1016/j.mib.2007.06.001

Wadler, C. S., & Vanderpool, C. K. (2007). A dual function for a bacterial small RNA: SgrS performs base pairing-dependent regulation and encodes a functional polypeptide. *Proceedings of the National Academy of Sciences of the United States of America*, *104*(51), 20454–20459. https://doi.org/10.1073/pnas.0708102104

Wagner, E. G. H., Altuvia, S., & Romby, P. (2002). Antisense RNAs in bacteria and their genetic elements. *Advances in Genetics*, *46*, 361–398. https://doi.org/10.1016/s0065-2660(02)46013-0

Wagner, E. G. H., & Romby, P. (2015). Small RNAs in bacteria and archaea: Who they are, what they do, and how they do it. *Advances in Genetics*, *90*, 133–208. https://doi.org/10.1016/bs.adgen.2015.05.001

Wallin, K.-L., Wiklund, F., Luostarinen, T., Angström, T., Anttila, T., Bergman, F., Hallmans, G., Ikäheimo, I., Koskela, P., Lehtinen, M., Stendahl, U., Paavonen, J., & Dillner, J. (2002). A population-based prospective study of Chlamydia trachomatis infection and cervical carcinoma. *International Journal of Cancer*, *101*(4), 371–374. https://doi.org/10.1002/ijc.10639

Wang, J., Rennie, W., Liu, C., Carmack, C. S., Prévost, K., Caron, M.-P., Massé, E., Ding, Y., & Wade, J. T. (2015). Identification of bacterial sRNA regulatory targets using ribosome profiling. *Nucleic Acids Research*, *43*(21), 10308–10320. https://doi.org/10.1093/nar/gkv1158

Wang, L., Miller, A., Rusch, S. L., & Kendall, D. A. (2004). Demonstration of a Specific Escherichia coli SecY–Signal Peptide Interaction. *Biochemistry*, *43*(41), 13185–13192. https://doi.org/10.1021/bi049485k

Wang, Y., Kahane, S., Cutcliffe, L. T., Skilton, R. J., Lambden, P. R., & Clarke, I. N. (2011). Development of a Transformation System for Chlamydia trachomatis: Restoration of Glycogen Biosynthesis by Acquisition of a Plasmid Shuttle Vector. *PLOS Pathogens*, *7*(9), e1002258. https://doi.org/10.1371/journal.ppat.1002258

Wang, Y., LaBrie, S. D., Carrell, S. J., Suchland, R. J., Dimond, Z. E., Kwong, F., Rockey, D. D., Hefty, P. S., & Hybiske, K. (2019). Development of Transposon Mutagenesis for Chlamydia muridarum. *Journal of Bacteriology*, *201*(23), e00366-19. https://doi.org/10.1128/JB.00366-19

Wassarman, K. M. (2007). 6S RNA: A small RNA regulator of transcription. *Current Opinion in Microbiology*, *10*(2), 164–168. https://doi.org/10.1016/j.mib.2007.03.008

Wassarman, K. M., Repoila, F., Rosenow, C., Storz, G., & Gottesman, S. (2001). Identification of novel small RNAs using comparative genomics and microarrays. *Genes & Development*, *15*(13), 1637–1651. https://doi.org/10.1101/gad.901001

Waters, L. S., & Storz, G. (2009). Regulatory RNAs in bacteria. *Cell*, *136*(4), 615–628. https://doi.org/10.1016/j.cell.2009.01.043

Weber, M. M., Bauler, L. D., Lam, J., & Hackstadt, T. (2015). Expression and Localization of Predicted Inclusion Membrane Proteins in Chlamydia trachomatis. *Infection and Immunity*, *83*(12), 4710–4718. https://doi.org/10.1128/IAI.01075-15

Weber, M. M., & Faris, R. (2019). Mutagenesis of Chlamydia trachomatis Using TargeTron. *Methods in Molecular Biology (Clifton, N.J.)*, *2042*, 165–184. https://doi.org/10.1007/978-1-4939-9694-0_12

Weber, M. M., Noriea, N. F., Bauler, L. D., Lam, J. L., Sager, J., Wesolowski, J., Paumet, F., & Hackstadt, T. (2016). A Functional Core of IncA Is Required for Chlamydia trachomatis Inclusion Fusion. *Journal of Bacteriology*. https://doi.org/10.1128/JB.00933-15

Wickstrum, J., Sammons, L. R., Restivo, K. N., & Hefty, P. S. (2013). Conditional Gene Expression in Chlamydia trachomatis Using the Tet System. *PLOS ONE*, *8*(10), e76743. https://doi.org/10.1371/journal.pone.0076743

Wong, Y. L., Anzola, J. V., Davis, R. L., Yoon, M., Motamedi, A., Kroll, A., Seo, C. P., Hsia, J. E., Kim, S. K., Mitchell, J. W., Mitchell, B. J., Desai, A., Gahman, T. C., Shiau, A. K., & Oegema, K. (2015). Reversible centriole depletion with an inhibitor of Polo-like kinase 4. *Science (New York, N.Y.)*, *348*(6239), 1155–1160. https://doi.org/10.1126/science.aaa5111

Wood, N. A., Blocker, A. M., Seleem, M. A., Conda-Sheridan, M., Fisher, D. J., & Ouellette, S. P. (n.d.). The ClpX and ClpP2 Orthologs of Chlamydia trachomatis Perform Discrete and Essential Functions in Organism Growth and Development. *MBio*, *11*(5), e02016-20. https://doi.org/10.1128/mBio.02016-20

Wright, P. R., Georg, J., Mann, M., Sorescu, D. A., Richter, A. S., Lott, S., Kleinkauf, R., Hess, W. R., & Backofen, R. (2014). CopraRNA and IntaRNA: Predicting small RNA targets, networks and interaction domains. *Nucleic Acids Research*, *42*(Web Server issue), W119-123. https://doi.org/10.1093/nar/gku359

Wurihan, W., Zou, Y., Weber, A. M., Weldon, K., Huang, Y., Bao, X., Zhu, C., Wu, X., Wang, Y., Lai, Z., & Fan, H. (n.d.). Identification of a GrgA-Euo-HrcA Transcriptional Regulatory Network in Chlamydia. *MSystems*, *6*(4), e00738-21. https://doi.org/10.1128/mSystems.00738-21

Wyrick, P. B. (2010). *Chlamydia trachomatis* Persistence In Vitro: An Overview. *The Journal of Infectious Diseases*, *201*(S2), 88–95. https://doi.org/10.1086/652394

Yadavalli, S. S., & Yuan, J. (2021). Bacterial Small Membrane Proteins: The Swiss Army Knife of Regulators at the Lipid Bilayer. *Journal of Bacteriology*. https://doi.org/10.1128/JB.00344-21

Yamamoto, K., Hirao, K., Oshima, T., Aiba, H., Utsumi, R., & Ishihama, A. (2005). Functional Characterization in Vitro of All Two-component Signal Transduction Systems from Escherichia coli*. *Journal of Biological Chemistry*, *280*(2), 1448–1456. https://doi.org/10.1074/jbc.M410104200

Yu, H. H. Y., Kibler, D., & Tan, M. (2006). In silico prediction and functional validation of sigma28-regulated genes in Chlamydia and Escherichia coli. *Journal of Bacteriology*, *188*(23), 8206–8212. https://doi.org/10.1128/JB.01082-06

Yu, H. H. Y., & Tan, M. (2003). Sigma28 RNA polymerase regulates hctB, a late developmental gene in Chlamydia. *Molecular Microbiology*, *50*(2), 577–584. https://doi.org/10.1046/j.1365-2958.2003.03708.x

Zhang, Y.-F., Han, K., Chandler, C. E., Tjaden, B., Ernst, R. K., & Lory, S. (2017). Probing the sRNA regulatory landscape of P. aeruginosa: Post-transcriptional control of determinants of pathogenicity and antibiotic susceptibility. *Molecular Microbiology*, *106*(6), 919–937. https://doi.org/10.1111/mmi.13857

Zhou, H., Kuang, J., Zhong, L., Kuo, W. L., Gray, J. W., Sahin, A., Brinkley, B. R., & Sen, S. (1998). Tumour amplified kinase STK15/BTAK induces centrosome amplification, aneuploidy and transformation. *Nature Genetics*, *20*(2), 189–193. https://doi.org/10.1038/2496

Zhu, H., Shen, Z., Luo, H., Zhang, W., & Zhu, X. (2016). Chlamydia Trachomatis Infection-Associated Risk of Cervical Cancer: A Meta-Analysis. *Medicine*, *95*(13), e3077. https://doi.org/10.1097/MD.0000000000003077